Aspects of B-Decays

DISSERTATION
zur Erlangung des Grades eines
Doktors der Naturwissenschaften

vorgelegt von
Dipl.-Phys. Sven Faller
geb. am 26.09.1977 in Aschaffenburg

eingereicht bei der
Natur- und Ingenieurwissenschaftlichen Fakultät
(Fakultät IV)
der Universität Siegen
Siegen 2011

Gutachter: Prof. Dr. Thomas Mannel
Zweitgutachter: Prof. Dr. Alexander Khodjamirian
Tag der mündlichen Prüfung: 4. März 2011

gedruckt auf alterungsbeständigem holz- und säurefreiem Papier

Abstract

B-meson decays are a good probe for testing the flavour sector of the standard model of particle physics. The standard model describes at present all experimental data satisfactorily, although some "tensions" exist, i.e. two to three sigma deviations from the predictions, in particular in B decays. The arguments against the standard model are thus purely theoretical. These tensions between experimental data and theoretical predictions provide an extension of the standard model by new physics contributions. Within the flavour sector main theoretical uncertainties are related to the hadronic matrix elements. For exclusive semileptonic $\bar{B} \to D^{(*)}\ell\bar{\nu}$ decays QCD sum rule techniques, which are suitable for studying hadronic matrix elements, however, with substantial, but estimable hadronic uncertainties, are used. The exploration of new physics effects in B-meson decays is done in an twofold way. In exclusive semileptonic $\bar{B} \to D^{(*)}\ell\bar{\nu}$ decays the effect of additional right-handed vector as well as left- and right-handed scalar and tensor hadronic current structures in the decay rates and the form factors are studied at the non-recoil point. As a second approach one used, the non-leptonic $B_s^0 \to J/\psi\phi$ and $B^0 \to J/\psi K_{S,L}$ decays. Discussing CP-violating effects in the time-dependent decay amplitudes by considering new physics phase in the $B^0 - \bar{B}^0$ mixing phase.

Zusammenfassung

Die Zerfälle der B-Mesonen eignen sich besonders gut den *Flavour* Bereich des Standardmodels der Teilchenphysik zu testen. Obwohl gewisse Spannungen, d.h. Abweichungen von zwei bis drei Standardabweichungen zwischen theoretischen Vorhersagen und experimentellen Daten, insbesondere in B Zerfällen, existieren, können bisher gewonnen experimentelle Daten durch das Standardmodell erklärt werden. Argumente einer Erweiterung des Standardmodels durch Beiträge *neuer Physik* sind deshalb von rein theoretischer Natur. Im Flavour Bereich sind die größten theoretischen Unsicherheiten mit der Bestimmung der hadronischen Matrixelemente verbunden. Zur Untersuchung dieser Matrixelemente im Allgemeinen und hier insbesondere in exklusiven semileptonischen $\bar{B} \to D^{(*)}\ell\bar{\nu}$ Zerfällen sind QCD Summenregel Methoden hervorragend geeignet, da sich die Größenordnung hadronischer Unsicherheiten abschätzen läßt. Die Suche nach Beiträgen neuer Physik in B-Mesonen zerfällen wird auf zweierlei Art und Weise durchgeführt. Zum einen in $\bar{B} \to D^{(*)}\ell\bar{\nu}$ Zerfällen, indem rechtshändige vektorielle, sowie skalare und tensorielle rechts- und linkshändige hadronische Ströme zugelassen werden. Die Beiträge neuer Physik in den Zerfallsraten und Formfaktoren werden am kinematischen Punkt maximalen Impulsübertrages diskutiert. Desweiteren werden Hinweise auf Beiträge neuer Physik in den nicht leptonischen Zerfällen $B_s^0 \to J/\psi\phi$ und $B^0 \to J/\psi K_{S,L}$ untersucht, indem in der $B^0 - \bar{B}^0$ Mischungsphase eine neue Physik Phase berücksichtig wird, welche zu CP verletzenden Effekten in den zeitabhängigen Zerfallsamplituden führt.

Contents

1

Introduction

The aesthetic beauty of Leonardo da Vinci's *Mona Lisa* (Musée du Louvre, Paris) or Michelangelo's *David* (Galleriea dell' Accademia, Florence, Italy) is not so much a question of colour, painting or material from that they are made, it is a question of symmetry: since ancient times, humans tried to mimic nature (φύσις) in art, architecture and science. Greek philosophers observed nature and found a proportionality realised in nature objects which they called *sectio divina* or "golden ratio", first geometrically defined by Euclide. A line with total length $(m + M)$ is divided such that the ratio of the *major* (M) and the *minor* (m) line elements is equal to the ratio of the total length and the major one, $\frac{m+M}{M} = \frac{M}{m} = (1 + \sqrt{5})/2$ [1, 2]. This is well-know, e.g. in solid-state physics well-known, because it is associated with the icosahedral (I_h) group, containing the symmetries of the icosahedron and dodecahedron [3]. Symmetry relations, particularly the golden ratio, influence arts until this day; in Fig. 1.1 four examples of the realisation of the golden ratio are shown. The example depicted in Fig. 1.1 (d) from the Swiss architect Le Corbusier is most impressive: He combined the golden ratio with the Fibonacci series in a *modulor* system as a scale representing the "human measurement". Famous buildings representing this system are the "Unité d'Habitation" at Marseille (France) or the National Museum of Western Art at Tokyo (Japan) [4].

The assumption of a geometrical basis of nature has inspired scientists developing more or less successful models for processes realised in nature, e.g. Kepler's Platonic model of the Solar system. In modern physics symmetries in a generalized sense are of particular importance; here a symmetry arises in nature, whenever a change in the variables of system the leaves the "essential physics", described by the action of the system, unchanged [5]. For field theories, in particular for quantum field theory, the

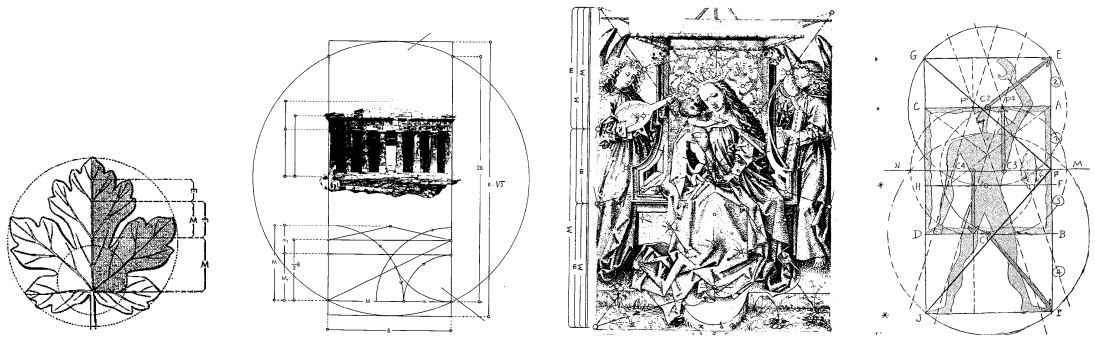

(a) Ranunculus (b) Parthenon, Greece (c) Albrecht Dürrer, "Madonna with Music-Making Angels" (d) Human

Figure 1.1.: Examples of the golden ratio; (a)–(c): realised in nature, and used in the art of the ancient world and the middle ages [2], and (d) in modern architecture [4].

Noether theorem [6] provides a general framework, which correlates a conservation law with a continuous symmetry transformation under which the Lagrangian of the system is invariant in form [7].

This has been central for the development of what is nowadays known as the standard model (SM) of particle physics [8–11]: one major step has been the insight, that the distinct symmetries space reflection (parity), charge conjugation and time reversal are each respected by the strong and electromagnetic interaction, but not by the the weak one. Furthermore, most importantly, only their combination based on symmetry principles described by a $\mathsf{G}_{\mathrm{SM}} = \mathsf{SU(3)}_C \otimes \mathsf{SU(2)}_L \otimes \mathsf{U(1)}_Y$ gauge group. Quarks and leptons are reside in representations of this gauge group, e.g. with respect to $\mathsf{SU(3)}_C$ the quarks in triplets and the leptons in singlets. The interactions are mediated by the corresponding gauge bosons. The gauge symmetry G_{SM} must be spontaneously broken, because neither mass terms for the gauge bosons nor for the leptons and quarks are gauge invariant. Within the standard model this is realised by the Higgs-mechanism [12–15]. Note that also this concept of symmetry-breaking is not restricted to physics, it is well-known, e.g. in biology [16].

On the one hand the standard model is experimentally well-tested, e.g. the electroweak theory as a quantum field theory at the level of 1% or better. On the other hand, obviously, the gravitational interaction is not included. Furthermore, explanations are needed for the origin of the particle masses and the baryon asymmetry of the universe, therefore the standard model is not a fundamental theory. Expecting results from the experiments ATLAS [17], CMS [18] and LHCb [19] at the LHC (CERN) a lot of

unanswered questions should be solved [20–22].

Extensions of the standard model are required, for which the term *new physics* (NP) is used in the literature. A systematic classification of new physics contributions in B-meson and D-meson decays is presented, e.g. in Ref. [23]. If one uses the concept of low-effective Hamiltonians, new physics may enter through the Wilson coefficients of the standard model operators that can receive new contributions through diagrams involving new heavy internal particles. These particles can be "integrated out" as the W boson and top quark in the standard model. Another way is that new physics enhance the operator basis, $\{\mathcal{Q}_i\} \to \{\mathcal{Q}_i^{\mathrm{SM}}, \mathcal{Q}_i^{\mathrm{NP}}\}$. Operators which are not present or strongly suppressed in the standard model may become important [24, 25].

The work presented here is dedicated to such extensions of the standard model quark flavour sector. The term flavour is used in order to describe the several copies of the same gauge group representations present in the standard model, namely for up-type and down-type quarks, charged leptons, and neutrinos. Flavour physics itself describes the non-trivial spectrum and interactions of this sector, and refers to the weak and Yukawa interactions [26, 27].

One prediction of the standard model flavour sector is a single CP-violating parameter, when ignoring an additional flavour diagonal CP-violating parameter, the strong CP phase, which is negligible, as experimental data constrain it to be smaller than $\mathcal{O}(10^{-10})$. CP-violating effects can be studied within B-meson decay channels in various ways. The amount of high precision data from the B-factories, BABAR at SLAC and Belle at KEK, established that the observed flavour and CP violation in nature is mainly driven by the Cabbibo-Kobayashi-Maskawa [28, 29] description [27]. This can be further tested by allowing new physics contributions to various clean observables which are calculated precisely within the standard model. However, those new physics contributions to these theoretically clean processes can not be bigger than $\mathcal{O}(30\%)$ of the standard model contributions [30, 31].

In order to study new physics effects it is essential to understand the flavour sector of the standard model. The main theoretical uncertainties are related to the strong interaction, i.e. to hadronic uncertainties. They can be studied by using non-perturbative methods such as QCD sum rule techniques or lattice QCD.

Following the above presented possibilities how new physics contributions can enter the effective Hamiltonians, there are two main strategies studying new physics effects: One can either build an explicit new physics model, which specifies the new matter fields and symmetries beyond the standard model one, or analyse the new physics

effects by using a generic effective-theory approach or by integrating out the new heavy fields [26]. The first strategy is more predictive then the second one, but more model dependent. The second strategy can be used e.g. for exclusive semileptonic B-meson decays. Integrating out the new degrees of freedom, the standard model Lagrangian can be treated as the renormalizable part of a more general local Lagrangian,

$$\mathcal{L}_{\text{eff}} = \mathcal{L}_{\text{SM}} + \sum \frac{1}{\Lambda_{\text{NP}}^{(D-4)}} \mathcal{C}_i^{(D)} \mathcal{Q}_i^{(D)},$$

where $\mathcal{C}_i$ are the Wilson coefficients and the operators with dimension $D > 4$ are suppressed by inverse powers of an effective new physics scale $\Lambda_{\text{NP}} > M_W$. Extensions of the standard model can be studied in a limited number of coefficients of the higher-dimensional operators. For nonleptonic B-meson transitions one can use CP-violating effects in order to search for relations or correlations that hold in the standard model but could be spoiled by new physic effects.

This thesis is organized as following. In Chap. 1 the standard model of particle physics is reviewed by having a closer look at the CP-violating effects in $B^0 - \bar{B}^0$ mixing. The theory of B-meson decays is discussed in Chap. 2, introducing heavy-quark effective theory as the working tool for the investigation of B-meson decay channels. In Chap. 4 exclusive semileptonic $\bar{B} \to D^{(*)}$ decays are analysed by using QCD sum rule techniques. However, QCD sum rules are not suitable for searching new physics effects. This is done for exclusive semileptonic $\bar{B} \to D^{(*)}$ transitions in Chap. 5 by taking an helicity-violating right-handed hadronic current into account. As a second approach in Chap. 6 new physics contributions in non-leptonic $b \to s$ decays are explored by analysing the CP-violating effects in the $B_s^0 \to J/\psi\phi$ and $B^0 \to J/\psi K$ time-dependent decay amplitudes. Finally, some concluding remarks are presented in Chap. 7.

2

Fundamentals

The fundamental framework of modern particle physics is the standard model of elementary particles (SM). It provides lot of facets which could not discussed here. Hence, this chapter is restricted on the basic facts of the standard model which are relevant for this work. Moreover, notations are introduced needed for the forthcoming chapters.

Exhaustively discussion about the standard model and related topics can be found in many textbooks, e.g. Refs.[5, 7, 32–34], or review articles, e.g. Refs. [20–22, 26, 35].

This chapter is organized in the following way: In Sec. 2.1 the standard model is briefly reviewed. In Sec. 2.1.1 the spinor representations of the leptons an quarks is introduced. The standard symmetry group $\mathsf{G}_{\mathrm{SM}} = \mathsf{SU}(3)_C \otimes \mathsf{SU}(2)_L \otimes \mathsf{U}(1)_Y$, including the electroweak theory, the quantum chromodynamics (QCD) and the concept of spontaneous symmetry breaking is subject of Sec. 2.1.2. One part of the general renormalizable standard model Lagrangian are Yukawa interactions which are the source of all flavour physics. They are generally flavour dependent and CPviolating. In Sec. 2.2 the CP violation within the standard model and especially in the $B - \bar{B}$-mixing is discussed.

2.1. Standard Model

The standard model of elementary particles [8–11] describes the interaction of the fundamental particles: leptons and quarks. There are three families of leptons and quarks which could independently represented by complex 2 component Weyl spinor fields. The families can be arranged in a $\mathsf{SU}(2)$ doublet of left-handed Weyl spinors,

$\psi_L \in \left(\frac{\mathbf{1}}{\mathbf{2}}, \mathbf{0}\right)$,

$$\begin{aligned} L &= \begin{bmatrix} \nu^i \\ e^i \end{bmatrix}_L = \Bigg[\underbrace{\begin{bmatrix} \nu^e \\ e \end{bmatrix}_L , \begin{bmatrix} \nu^\mu \\ \mu \end{bmatrix}_L , \begin{bmatrix} \nu^\tau \\ \tau \end{bmatrix}_L}_{\text{leptons}} \Bigg] , \\ q_L &= \begin{bmatrix} u^i \\ d^i \end{bmatrix}_L = \Bigg[\underbrace{\begin{bmatrix} u \\ d \end{bmatrix}_L , \begin{bmatrix} c \\ s \end{bmatrix}_L , \begin{bmatrix} t \\ b \end{bmatrix}_L}_{\text{quarks}} \Bigg] , \end{aligned} \tag{2.1}$$

and an SU(2) singlet of right-handed Weyl spinors, $\psi_R \in \left(\mathbf{0}, \frac{\mathbf{1}}{\mathbf{2}}\right)$,

$$R = \begin{cases} e^i_R = [e_R, \mu_R, \tau_R] \\ \nu^i_R = [\nu^e_R, \nu^\mu_R, \nu^\tau_R] \end{cases} \quad \text{and} \quad q_R = \begin{cases} u^i_R = [u_R, c_R, t_R] , \\ d^i_R = [d_R, s_R, b_R] \end{cases} . \tag{2.2}$$

Independent from handedness, the leptons can be placed into SU(3) singlets, and quarks into SU(3) triplets. Parity is not conserved from SU(2), because this group is chiral, but the non-chiral group SU(3) conserves parity. The vector boson gauge fields arise from the standard symmetry $\mathsf{U}(1)_Y \otimes \mathsf{SU}(2)_L \otimes \mathsf{SU}(3)_C$, which is a internal symmetry. Lepton and quark fields interact with each other via this $1 + 3 + 8 = 12$ gauge fields. In the following the spinor representations for leptons and quarks are discussed in more detail.

2.1.1. Spinor Representations

The observable physical space consists of one time and three space dimensions. Lorentz transformations in this space can be described by the Clifford algebras $\mathscr{C}\ell_3 \simeq \mathsf{Mat}(2, \mathbb{C})$, $\mathscr{C}\ell(3,1) \simeq \mathsf{Mat}(4, \mathbb{R})$ and $\mathscr{C}\ell(1,3) \simeq \mathsf{Mat}(2, \mathbb{H})$. In the latter, the entries of the real algebra of 2×2-matrices $\mathsf{Mat}(1, \mathbb{H})$ are quaternions. As mentioned before, the leptons and quarks are represented as Weyl spinors, but in physics the Dirac spinors are preferred. Chiral symmetry linked the two representations. Introductions into spinor representation can be found in any quantum mechanical book, see, e.g., Refs. [32, 33, 36]. In the following some fundamentals about spinor representations are presented.
The Lorentz transformations form the Lorentz group

$$\mathsf{O}(3,1) = \{\boldsymbol{\Lambda} \in \mathsf{Mat}(4, \mathbb{R}) | \boldsymbol{\Lambda}\boldsymbol{\eta}\boldsymbol{\Lambda}^T = \boldsymbol{\eta}\} ,$$

where $\boldsymbol{\Lambda}$ is a matrix, satisfying $\mathsf{det}\boldsymbol{\Lambda} = \pm 1$, and $\eta_{\mu\nu} = \mathsf{diag}(1, -1, -1, -1)$ is the usual Minkowski matrix. The positive determinant belongs to the special Lorentz

group $\mathsf{SO}(3,1) = \mathsf{O}(3,1) \cap \mathsf{SL}(4,\mathbb{R})$. The Lorentz transformations can be described within the Clifford algebras $\mathcal{C}\ell_3$, $\mathcal{C}\ell(3,1)$ and $\mathcal{C}\ell(1,3)$. Especially the Clifford algebra $\mathcal{C}\ell(1,3)$ is generated as a real algebra by the Dirac γ-matrices γ_i, $i = 0,1,2,3$, making this algebra particularly interesting in physics.
The matrix Λ can be written as

$$\boldsymbol{\Lambda} = \exp\left\{-\frac{i}{2}\omega_{\mu\nu}\boldsymbol{J}^{\mu\nu}\right\}, \tag{2.3}$$

where $\omega_{\mu\nu}$ is an asymmetric matrix corresponding to the six generators of the group, labelled as $J^{\mu\nu}$, with a pair of antisymmetric Lorentz indices. The associated Lie algebra $\mathfrak{so}(1,3)$ is represented by the commutator of these generators,

$$[J^{\mu\nu}, J^{\alpha\beta}] = i\left(\eta^{\nu\alpha}J^{\mu\beta} - \eta^{\mu\beta}J^{\nu\alpha} - \eta^{\nu\beta}J^{\mu\alpha} + \eta^{\mu\beta}J^{\nu\alpha}\right). \tag{2.4}$$

Splitting the generators $J^{\mu\nu}$ into generators of rotations, $J^i = \frac{1}{2}\epsilon_{ijk}J^{jk}$ and boosts, $K^i = J^{i0}$, the Lorentz group (2.4) becomes

$$[J^i, J^j] = i\epsilon^{ijk}J^k\,, \quad [J^i, K^i] = i\epsilon^{ijk}K^k\,, \quad [K^i, K^j] = -i\epsilon^{ijk}J^k\,. \tag{2.5}$$

Using the definitions $\theta^i = \frac{1}{2}\varepsilon^{ijk}\omega^{jk}$ and $\eta^i = \omega^{i0}$ the Lorentz transformation takes the simple form

$$\boldsymbol{\Lambda} = \exp\{-i\,\boldsymbol{\theta}\cdot\boldsymbol{J} + i\,\boldsymbol{\eta}\cdot\boldsymbol{K}\}\,. \tag{2.6}$$

The first relation in (2.5) represents the Lie algebras of $\mathsf{SU}(2)$ and $\mathsf{SO}(3)$. They are indistinguishable at the level of infinitesimal transformations. However, they differ at a global level, i.e. far from the identity. A rotation by 2π in $\mathsf{SO}(3)$ is the same as the identity. Contrastingly the group $\mathsf{SU}(2)$ is periodic only under rotations by 4π. Therefore considering $\mathsf{SU}(2)$ one includes the solution of (2.5) with half-integer spin, while for $\mathsf{SO}(3)$ one only used representations with integer spin. For $\mathsf{SU}(2)$ the spinoral representation is given by

$$\boldsymbol{J}^i = \frac{\sigma^i}{2}\,. \tag{2.7}$$

Here σ^i are the Pauli spin matrices,

$$\sigma_1 = \begin{bmatrix} 0 & 1 \\ 1 & 0 \end{bmatrix}, \quad \sigma_2 = \begin{bmatrix} 0 & -i \\ i & 0 \end{bmatrix}, \quad \sigma_3 = \begin{bmatrix} 1 & 0 \\ 0 & -1 \end{bmatrix}, \tag{2.8}$$

which satisfy the commutations and anticommutations rules

$$[\sigma_i, \sigma_j] = 2i\,\varepsilon_{ijk}\sigma_k \;, \qquad \{\sigma_i, \sigma_j\} = 2\delta_{ij}\,\mathbb{1}_2 \;, \tag{2.9}$$

where $\mathbb{1}_2$ is the 2×2 unity matrix. The Pauli matrices generate the real algebra $\mathsf{Mat}(2, \mathbb{C})$, being the matrix image of the Clifford algebra $\mathcal{C}\ell_3$. Using the Clifford algebra $\mathcal{C}\ell_3$ of $\mathbb{R}^3$ the universal covering group for the rotation group $\mathsf{SO}(3)$ of $\mathbb{R}^3$ can be constructed. The rotation of a vector $\vec{x} \in \mathbb{R}^3$ is given by $\vec{x}' = s\vec{x}s^{-1}$, where s is an element of the spin group $\mathsf{spin}(3)$. In the matrix formulation provided by the Pauli spin matrices, the spin group $\mathsf{spin}(3)$ has an isomorphic image, the special unitary group

$$\mathsf{SU(2)} = \{s \in \mathsf{Mat}(2, \mathbb{C}) | s^\dagger s = \mathbb{1}_2, \mathsf{det}\, s = 1\} \;. \tag{2.10}$$

Every element in $\mathsf{SO}(3)$ can be represented by a matrix in $\mathsf{SU(2)}$ [37–39].
Combining the generators of rotations $\boldsymbol{J}$ and of boosts $\boldsymbol{K}$ in a chiral way, $\boldsymbol{J}^\pm = \frac{1}{2}(\boldsymbol{J} \pm i\,\boldsymbol{K})$, Lorentz algebra can be represented by two half-integers (j_+, j_-) have dimension $(2j_- + 1)(2j_+ + 1)$. Using this the states have all possible spin values j in integer steps between $|j_+ - j_-|$ and $j_+ + j_-$. The representation for the left- and right-handed Weyl spiors are $(\frac{\mathbf{1}}{\mathbf{2}}, 0)$ and $(\mathbf{0}, \frac{\mathbf{1}}{\mathbf{2}})$, respectively, and their transformation law under Lorentz transformations using Eq. (2.6) and (2.7) is given by

$$\psi_L \longmapsto \psi'_L \equiv \Lambda_L \psi_L = \exp\left\{(-i\,\boldsymbol{\theta} - \boldsymbol{\eta}) \cdot \frac{\boldsymbol{\sigma}}{2}\right\} \psi_L \;, \tag{2.11}$$

$$\psi_R \longmapsto \psi'_R \equiv \Lambda_R \psi_R = \exp\left\{(-i\,\boldsymbol{\theta} + \boldsymbol{\eta}) \cdot \frac{\boldsymbol{\sigma}}{2}\right\} \psi_R \;. \tag{2.12}$$

In the chiral basis the Dirac field is defined as

$$\Psi \equiv \begin{bmatrix} \psi_L \\ \psi_R \end{bmatrix} \;. \tag{2.13}$$

The Pauli matrices (2.8) generate a basis for the four dimensional space-time, satisfying the commutator relation

$$\{\gamma^\mu, \gamma^\nu\} = 2\eta^{\mu\nu} \;, \tag{2.14}$$

where the Dirac γ-matrices in the chiral representation can be written as

$$\gamma_0 = \gamma^0 = \begin{bmatrix} \mathbb{1}_2 & 0 \\ 0 & -\mathbb{1}_2 \end{bmatrix} \;, \quad \gamma_k = -\gamma^k = \begin{bmatrix} 0 & -\sigma_k \\ \sigma_k & 0 \end{bmatrix} \quad \text{for} \quad k = 1, 2, 3 \;. \tag{2.15}$$

In Table 2.1 the 16 dimensional basis elements of this space are collected. The quadratic

form, associated with this algebra is

$$X = x^\mu \gamma_\mu \equiv \not{x} \ , \tag{2.16}$$

and by squaring

$$X^2 = (x^0)^2 - (x^1)^2 - (x^2)^2 - (x^3)^2 \ , \tag{2.17}$$

preserving the Minkowski norm of spacetime. Furthermore, one defines the pseudoscalar matrix $\gamma_5 \equiv i\,\gamma_0\gamma_1\gamma_2\gamma_3$ and the idempotent chiral projectors

$$P_{L/R} \equiv \frac{1}{2}\left(\mathbb{1}_4 \mp \gamma_5\right) \ . \tag{2.18}$$

Multiplication from the left with the chiral projectors a pair of Weyl spinors is projected from each Dirac spinor,

$$\psi_L = P_L \Psi \ , \quad \text{and} \quad \psi_R = P_R \Psi \ . \tag{2.19}$$

In terms of the 16 matrices, the general fermion bilinear is a combination of

$$\bar{\Psi} \Gamma \Psi \ , \quad \Gamma \in \{\mathbb{1}, \gamma^\mu, \gamma_5, \gamma_5\gamma^\mu, \sigma^{\mu\nu}\} \ , \tag{2.20}$$

where $\bar{\Psi} = \Psi^\dagger \gamma^0$ and $\sigma^{\mu\nu} = \frac{i}{2}[\gamma^\mu, \gamma^\nu]$. Due to their properties under Lorentz transformations the Γ's are scalar, vector, pseudoscalar, pseudovector and tensor operators, respectively. In terms of Dirac spinors, the Dirac equation is given by

$$\left(i\not{\partial} - m\right)\Psi = 0 \ , \tag{2.21}$$

from which the Dirac-Lagrangian is read off as

$$\mathcal{L}_D = \bar{\Psi}\left(i\not{\partial} - m\right)\Psi \ . \tag{2.22}$$

Table 2.1.: The basis elements for the 16 dimensional space $\mathbb{C}_4$.

$\mathbb{1}_4$	Scalar
$\gamma_i \ (i = 0, 1, 2, 3)$	Vectors
$\gamma_1\gamma_0,\ \gamma_2\gamma_0,\ \gamma_3\gamma_0,\ \gamma_1\gamma_2,\ \gamma_2\gamma_3,\ \gamma_3\gamma_1$	Bivectors
$\gamma_0\gamma_1\gamma_2,\ \gamma_0\gamma_2\gamma_3,\ \gamma_0\gamma_3\gamma_1,\ \gamma_1\gamma_2\gamma_3$	Trivectors
$\gamma_0\gamma_1\gamma_2\gamma_3$,	Pseudoscalar

Setting the mass term equal to zero the action yields the internal global symmetry

$$\psi_L \longmapsto \psi_L' = e^{i\theta_L}\psi_L \ , \qquad \psi_R \longmapsto \psi_R' = e^{i\theta_R}\psi_R \ , \tag{2.23}$$

where the spinors are rotated by two independent angles θ_L and θ_R. This transformation belongs to the $\mathsf{U}(1) \otimes \mathsf{U}(1)$ symmetry group. There are two special transformations, the first one is the vector $\mathsf{U}(1)$ for $\theta_L = \theta_R = \alpha$, and the other one is the chiral transformation or axial $\mathsf{U}(1)$ for $\theta_L = -\theta_R$, $\Psi \longmapsto \Psi' = e^{i\alpha}\Psi$ and $\Psi \longmapsto \Psi' = e^{i\beta\gamma^5}\Psi$, with the conserved vector current $j_V^\mu = \bar{\Psi}\gamma^\mu\Psi$ and the conserved axial current $j_A^\mu = \bar{\Psi}\gamma^\mu\gamma^5\Psi$, respectively. Note that the axial current is a pseudovector. When the mass term couples to Ψ_R and Ψ_L the Eq. (2.23) is a symmetry relation only for $\theta_L = \theta_R$. The axial $\mathsf{U}(1)$ is broken by the mass term, but the vector $\mathsf{U}(1)$ is preserved.

2.1.2. Standard Symmetry Group

The standard model of elementary particles based on the standard symmetry group $\mathsf{SU}(3)_C \otimes \mathsf{SU}(2)_L \otimes \mathsf{U}(1)_Y$, where the electroweak part of the theory is described by the $\mathsf{SU}(2)_L \otimes \mathsf{U}(1)_Y$ symmetry group and the gauge field theory that describes the strong interaction of coloured quarks and gluons is represented by the $\mathsf{SU}(3)_C$ symmetry group. Both theories are so-called Young-Mills Theories [40].
Every special unitary group $\mathsf{SU}(N)$ has $N^2 - 1$ generators T^a, which are hermitian and satisfy $\mathsf{Tr}[T^a] = 0$. The Lie algebra is given by the commutator relations

$$[T^a, T^b] = i f^{abc} T^c \ , \tag{2.24}$$

where f^{abc} are the structure constants of the $\mathsf{SU}(N)$, which are antisymmetric and real. The generators T^a can be written as a direct sum of a irreducible representations r. In this representation the trace of the product of two generators is $\mathsf{Tr}[T_r^a T_r^b] = D^{ab}$, where the matrix D^{ab} is positive definite if the generator matrices are Hermitian. The Young-Mills Lagrangian in the representation r is given by

$$\mathcal{L}_{\mathrm{YM}} = i\bar{\Psi}^\alpha \not{\partial} \Psi^\alpha - m\bar{\Psi}^\alpha\Psi^\alpha + g A_\mu^a \bar{\Psi}^\alpha \gamma^\mu (T_r^a)_{\alpha\beta}\Psi^\beta - \frac{1}{4}(F_{\mu\nu}^a)^2 \ , \tag{2.25}$$

or more compact

$$\mathcal{L}_{\mathrm{YM}} = \bar{\Psi}\left(i \not{D} - m\right)\Psi - \frac{1}{2}\mathsf{Tr}\left[F_{\mu\nu}F^{\mu\nu}\right] \ , \tag{2.26}$$

where $\alpha = 1, \ldots, \mathsf{dim}(r)$ and $F_{\mu\nu} = F^a_{\mu\nu} T^a$ is the field strength defined as

$$F^a_{\mu\nu} = \partial_\mu A^a_\nu - \partial_\nu A^a_\mu + g f^{abc} A^b_\mu A^c_\nu \,, \tag{2.27}$$

with the non-abelian gauge fields $A_\mu(x) = A^a_\mu(x) T^a$ and the scalar factor g. The covariant derivative on the field Ψ is

$$D_\mu \Psi = \left(\partial_\mu - i g A^a_\mu T^a_r\right) \Psi \,. \tag{2.28}$$

Quantum Electrodynamics

The interaction between charged spin-$\frac{1}{2}$-particles and photons is described by quantum electrodynamics (QED), based on the $\mathsf{U}(1)_{\mathrm{em}}$ gauge group, which has one generator, hence, there is one associated gauge field A_μ, which is the physical photon. The QED is described in a lot of textbooks, e.g. [7, 32, 33], here only the relations to the gauge symmetry groups are briefly noted. The Lagrangian (2.26) for QED is given by

$$\mathcal{L}_{\mathrm{QED}} = \bar{\Psi}(i \not{D} - m)\Psi - \frac{1}{4} F_{\mu\nu} F^{\mu\nu} \,, \tag{2.29}$$

where $D_\mu = \partial_\mu - i e A_\mu$ is the covariant derivative (2.28), $F_{\mu\nu} = \partial_\mu A_\nu - \partial_\nu A_\mu$ is the field strength, m is the fermion mass, and the scaling factor g is given by the electron charge e. The Lagrangian $\mathcal{L}_{\mathrm{QED}}$ is invariant under the local $\mathsf{U}(1)$ gauge transformations, where the spinors and fields transform like $\Psi(x) \longmapsto \Psi(x)' = e^{ie\alpha(x)}\Psi(x)$ and $A_\mu(x) \longmapsto A'_\mu(x) = A_\mu(x) - \partial_\mu \alpha(x)$, respectively. The existence of a local symmetry implies the existence of a global $\mathsf{U}(1)$ symmetry, with a constant parameter α, one finds for the spinors: $\Psi(x) \longmapsto \Psi(x)' = e^{ie\alpha}\Psi(x)$, and for the fields: $A_\mu(x) \longmapsto A'_\mu(x) = A_\mu(x)$. The associated Noether current is $\bar{\Psi}\gamma^\mu\Psi$, and the $\mathsf{U}(1)$ charge is conserved by the electromagnetic interaction. QED is invariant under charge $\boldsymbol{C}$ and parity $\boldsymbol{P}$ transformations, also under time reversal $\boldsymbol{T}$, therefore the $\boldsymbol{CPT}$-theorem[1] is fulfilled.

Electroweak Theory

The $\mathsf{SU}(2)_L \otimes \mathsf{U}(1)_Y$ part of the standard symmetry represents the electroweak theory. From $\mathsf{U}(1)$ there is one gauge field B_μ, and from $\mathsf{SU}(2)$ three gauge fields W^a_μ, $a = 1, 2, 3$. Using the spinor representation of the Pauli matrices (2.8) the generators of the

[1] The $\boldsymbol{CPT}$-theorem states that one cannot build a Lorentz-invariant quantum field theory with a Hermitian Hamiltonian that violates $\boldsymbol{CPT}$ [32].

SU(2) are given by $\tau^a = \frac{\sigma^a}{2}$. The Yang-Mills Lagrangian (2.26) for the $\mathsf{SU(2)}_L \otimes \mathsf{U(1)}_Y$ reads

$$\mathcal{L}_{\mathsf{SU(2)}\otimes\mathsf{U(1)}} = \mathcal{L}_{\text{gauge}} + \mathcal{L}_{\text{fermion}} + \mathcal{L}_{\Phi} + \mathcal{L}_{\text{Yuk}} \,, \tag{2.30}$$

where the Lagrangian of the gauge part is combined by the four gauge fields,

$$\mathcal{L}_{\text{gauge}} = -\frac{1}{4}\mathrm{W}^a_{\mu\nu}\mathrm{W}^{\mu\nu\ a} - \frac{1}{4}\mathrm{B}^a_{\mu\nu}\mathrm{B}^{\mu\nu\ a} \,, \tag{2.31}$$

where the field strength tensors follow from Eq. (2.27),

$$\mathrm{B}_{\mu\nu} = \partial_\mu \mathrm{B}_\nu - \partial_\mu \mathrm{B}_\nu \,, \tag{2.32}$$

$$\mathrm{W}^a_{\mu\nu} = \partial_\mu \mathrm{W}^a_\nu - \partial_\mu \mathrm{W}^a_\nu - g\epsilon_{abc}\mathrm{W}^b_\mu \mathrm{W}^c_\nu \,, \tag{2.33}$$

where g is the SU(2) gauge coupling. Moreover, the U(1) gauge field $\mathbf{B}$ is associated with the weak hypercharge $Y = Q + T^3$, where Q and T^3 are the electric charge operator and the third component of the weak SU(2) [35], respectively. Hence, the covariant derivative takes the form

$$D_\mu = \partial_\mu - i g \mathrm{W}^a_\mu \frac{\tau^a}{2} - i g' Y \mathrm{B}_\mu \,, \tag{2.34}$$

with g' as the U(1) gauge coupling. The three massive vector bosons are

$$\mathrm{W}^\pm_\mu = \frac{1}{\sqrt{2}}\left(\mathrm{W}^1_\mu - i\,\mathrm{W}^2_\mu\right) \,, \quad \mathrm{Z}^0_\mu = \frac{1}{\sqrt{g^2 + g'^2}}\left(g\mathrm{W}^3_\mu - g'\mathrm{B}_\mu\right) \tag{2.35}$$

and vector field, orthogonal to Z^0_μ, remains massless

$$A_\mu = \frac{1}{\sqrt{g^2 + g'^2}}\left(g' A^3_\mu + g\mathrm{B}_\mu\right) \,. \tag{2.36}$$

Using the Weyl spinor representations (2.19) the Lagrangian for the fermions is

$$\mathcal{L}_{\text{fermion}} = \bar{\psi}_L (i \not{D}) \psi_L + \bar{\psi}_R (i \not{D}) \psi_R \,, \tag{2.37}$$

where the covariant derivative is given by Eq. (2.34). Due to different quantum numbers the fermion fields are associated with different covariant derivatives.
The gauge invariance does not allow mass terms in the Lagrangian for gauge bosons or for chiral fermions, it must be broken spontaneously. Within the standard model this symmetry breaking this is described by the Higgs-mechanism [12–15]. The Lagrangian is modified such that it is still invariant under the same SU(2) ⊗ U(1) gauge

symmetry, but the lowest energy (vacuum) state is not. Introducing a complex Higgs scalar $\Phi \equiv \begin{bmatrix} \phi^+ \\ \phi^0 \end{bmatrix}$, which is a $\mathsf{SU(2)}_L$ doublet of scalar fields with $\mathsf{U(1)}$ charge $Y_\phi = 1$, a real mass parameter $\mu^2 < 0$, and a self coupling constant λ, the scalar Lagrangian can be written as

$$\mathcal{L}_\phi = (D^\mu \Phi)^\dagger (D_\mu \Phi) + \mu^2 (\Phi^\dagger \Phi) - \frac{\lambda}{4} (\Phi^\dagger \Phi)^2 \,. \tag{2.38}$$

The additional couplings for the fermions are called Yukawa couplings. With respect to the representations (2.1) and (2.2), they are given by

$$\mathcal{L}_{\text{Yuk}} = -\lambda^{ij}_{\text{lep}} \bar{L}^i \Phi e^j_R - \lambda^{ij}_u \bar{q}^i_L \tilde{\Phi} u^j_R - \lambda^{ij}_d \bar{q}^i_L \Phi d^j_R + \text{h.c.} \,, \tag{2.39}$$

where $\tilde{\Phi} = i\sigma_2 \phi^* = \begin{bmatrix} \phi^{0\dagger} \\ -\phi^- \end{bmatrix}$, and the term $\bar{q}_L \tilde{\Phi}$ transforms like a $\mathsf{SU(2)}$ singlet, which generates masses for up and down quarks with a single Higgs doublet. The Yukawa matrices $\boldsymbol{Y}_{\text{lep}}$, $\boldsymbol{Y}_u$ and $\boldsymbol{Y}_d$ are general, not necessarily symmetric or Hermitian, complex-valued matrices [32]. The various flavours of quarks and leptons are labelled by the indices i and j. In absence of right-handed neutrinos, $\nu^i_R \equiv 0$, one can not write Yukawa interactions for the neutrinos [41]. If $\mu^2 < 0$ the Higgs potential has a non-vanishing vacuum expectation value (VEV),

$$\langle 0 | \Phi_0 | 0 \rangle = \frac{1}{\sqrt{2}} \begin{bmatrix} 0 \\ v \end{bmatrix} \,, \tag{2.40}$$

where $v = \sqrt{\frac{\mu^2}{\lambda}}$. Therefore the generators of $\mathsf{SU(2)}_L \otimes \mathsf{U(1)}_Y$ are spontaneously broken. However, the vacuum carries no electric charge, so the $\mathsf{U(1)}_{\text{em}}$ is not broken. Thus, the electroweak $\mathsf{SU(2)}_L \otimes \mathsf{U(1)}_Y$ group is spontaneously broken to the $\mathsf{U(1)}_{\text{em}}$. The physical spectrum is given by

$$\Phi(x) = \exp\left\{ \frac{i \boldsymbol{\xi} \cdot \boldsymbol{\sigma}}{v} \right\} \begin{bmatrix} 0 \\ (v + H)/\sqrt{2} \end{bmatrix} \,, \tag{2.41}$$

where H is one physical Higgs boson and $\boldsymbol{\xi}(x)$ is a unphysical field. The masses to weak gauge bosons $W^\pm$ and Z^0 as well as to the fermions are generated at the same time by the Higgs mechanism. The flavour changing processes and the CP violation which are related to the Yukawa couplings are discussed in Sec. 2.2.1.

Table 2.2.: The eight Gell-Mann matrices, which generates the SU(2) gauge group, [42], their construction is similar to the Pauli spin matrices Eq. (2.8).

$$\lambda^1 = \begin{bmatrix} 0 & 1 & 0 \\ 1 & 0 & 0 \\ 0 & 0 & 0 \end{bmatrix} \quad \lambda^2 = \begin{bmatrix} 0 & -i & 0 \\ i & 0 & 0 \\ 0 & 0 & 0 \end{bmatrix} \quad \lambda^3 = \begin{bmatrix} 1 & 0 & 0 \\ 0 & -1 & 0 \\ 0 & 0 & 0 \end{bmatrix} \quad \lambda^4 = \begin{bmatrix} 0 & 0 & 1 \\ 0 & 0 & 0 \\ 1 & 0 & 0 \end{bmatrix}$$

$$\lambda^5 = \begin{bmatrix} 0 & 0 & -i \\ 0 & 0 & i \\ 0 & 0 & 0 \end{bmatrix} \lambda^6 = \begin{bmatrix} 0 & 0 & 0 \\ 0 & 0 & 1 \\ 0 & 1 & 0 \end{bmatrix} \quad \lambda^7 = \begin{bmatrix} 0 & 0 & 0 \\ 0 & 0 & -i \\ 0 & i & 0 \end{bmatrix} \quad \lambda^8 = \frac{1}{\sqrt{3}} \begin{bmatrix} 1 & 0 & 0 \\ 0 & 1 & 0 \\ 0 & 0 & -2 \end{bmatrix}$$

Quantum Chromodynamics

The last symmetry group of the standard model is the colour-SU(3) gauge group, which describes the colour symmetry of the strong interactions. The associated Lie group $\mathfrak{su}(3)$ which has 8 generators $T^a = \frac{1}{2}\lambda^a$, where the λ^i matrices can be represented by the Gell-Mann matrices, collected in Table 2.2. The matrices λ^a satisfy the commutator relation $[\lambda^a, \lambda^b] = 2if_{abc}\lambda^c$, and they are normalised by the condition $\mathrm{Tr}[\lambda^a\lambda^b] = 2\delta^{ab}$. Using the Young-Mills Lagrangian (2.26) the QCD Lagragian becomes

$$\mathcal{L}_{\mathrm{QCD}} = \sum_{r=1}^{F} \bar{\Psi}_{ri} \left(i \not{D}^i_j - m_r \delta^i_j \right) \Psi^j_r - \frac{1}{2}\mathrm{Tr}[G^a_{\mu\nu} G^{\mu\nu\ a}] \,, \tag{2.42}$$

where the quark fields are represented by an colour triplet Ψ_{if}, with the colour indices $i, j (= 1, 2, 3$ or red, blue, green) and the flavour indices $r = 1, 2, \ldots F$. For the field strength tensor (2.27) of the colour octet gauge bosons one gets

$$G^a_{\mu\nu} = \partial_\mu G^a_\mu - \partial_\nu G^a_\nu - i g_s f^{abc} G^b_\mu G^c_\nu \,, \tag{2.43}$$

with $G_\mu = \frac{1}{2} G^a_\mu \lambda^a$ and the covariant derviative

$$D^i_{\mu j} = \left(D_\mu\right)_{ij} = \partial_\mu \delta_{ij} + i g_s G^a_\mu T^a_{ij} \,. \tag{2.44}$$

The 8 gauge bosons are the massless gluons carrying the colour. However, they can not distinguish between the flavour of the quarks. If the quarks pattern bounding states for small quark masses m_r then the quark vector is part of fundamental representation of the unitarity $\mathrm{U}(F)$, and the corresponding bounding states are covered by a multiplet of irreducibel representations of $\mathrm{U}(F)$. These bounding states are the baryons and

Table 2.3.: Flavour quantum numbers for leptons, quarks and the Higgs doublet, where T is the weak isospin, T^3 is the third component of the weak isospin, Y is the hypercharge and Q the electric charge.

Field			T	T^3	Y	Q
$\begin{bmatrix} \nu^e \\ e \end{bmatrix}_L$	$\begin{bmatrix} \nu^\mu \\ \mu \end{bmatrix}_L$	$\begin{bmatrix} \nu^\tau \\ \tau \end{bmatrix}_L$	$\frac{1}{2}$	$\frac{1}{2}$ $-\frac{1}{2}$	$-\frac{1}{2}$	0 -1
e_R	μ_R	τ_R	0	0	-1	-1
$\begin{bmatrix} u \\ d \end{bmatrix}_L$	$\begin{bmatrix} c \\ s \end{bmatrix}_L$	$\begin{bmatrix} t \\ b \end{bmatrix}_L$	$\frac{1}{2}$	$\frac{1}{2}$ $-\frac{1}{2}$	$\frac{1}{6}$	$\frac{2}{3}$ $-\frac{1}{3}$
u_R	c_R	t_R	0	0	$\frac{2}{3}$	$\frac{2}{3}$
d_R	s_R	b_R	0	0	$-\frac{1}{3}$	$-\frac{1}{3}$
	$\begin{bmatrix} \phi^+ \\ \phi^0 \end{bmatrix}$		$\frac{1}{2}$	$\frac{1}{2}$ $-\frac{1}{2}$	$\frac{1}{2}$	1 0

the mesons. Their fundamental representations are $\boldsymbol{F} \times \boldsymbol{F} \times \boldsymbol{F}$ and $\boldsymbol{F} \times \boldsymbol{F}^*$ tensor products, respectively.
The quark masses break the $\mathsf{U}(F)$-symmetry of the QCD Lagrangian. The mass differences between hadrons within a special multiplet are predictable by perturbative methods. The flavour quantum numbers for the leptons and quarks are collected in Table 2.3.

Cabbibo-Kobayashi-Maskawa Matrix

The mass term in (2.39) for leptons and quarks after spontaneous symmetry breaking is described by

$$\mathcal{L}_M = G^{ij}_{\text{lep}} \bar{L}^i e^j_R - G^{ij}_u \bar{q}^i_L u^j_R - G^{ij}_d \bar{q}^i_L d^j_R + \text{h.c.}\,, \tag{2.45}$$

where the 6×6 mass eigenstate matrices $\boldsymbol{G}_{\text{lep,u,d}}$ could be diagonalized by unitary matrices $\boldsymbol{V}_L$ and $\boldsymbol{V}_R$ such that $\boldsymbol{V}_L \boldsymbol{G}_{\text{lep,u,d}} \boldsymbol{V}_R^\dagger = \boldsymbol{G}^{\text{diag}}$, where $\boldsymbol{G}^{\text{diag}}$ is diagonal and real. The interaction of the W-bosons to fermions is

$$\mathcal{L}_{W^\pm} = \frac{g}{\sqrt{2}} \mathcal{J}^{\mu+}_{\text{W}} \text{W}^+_\mu + \text{h.c.}\,, \tag{2.46}$$

where the weak current is given by

$$\mathcal{J}^{\mu+}_W = \bar{\nu}^i_L \gamma^\mu V^{ij}_{\text{lep}} e^j_L + \bar{u}^i_L \gamma^\mu V^{ij}_{\text{CKM}} d^j_L\,, \tag{2.47}$$

where $V_{\mathrm{CKM}} = V_L^{u\dagger} V_L^d$ is the 3×3 unitary Cabbibo-Kobayashi-Maskawa (CKM) matrix [28, 29],

$$V_{\mathrm{CKM}} = \begin{pmatrix} V_{ud} & V_{us} & V_{ub} \\ V_{cd} & V_{cs} & V_{cb} \\ V_{td} & V_{ts} & V_{tb} \end{pmatrix} , \tag{2.48}$$

and $V_{\mathrm{lep}} = V_L^{\nu\dagger} V_L^e$ the leptonic mixing matrix. For processes for which the neutrino masses are negligible one sets $V_{\mathrm{lep}} = \mathbb{1}$.

The 3×3 CKM matrix depends on three real angles and one complex phase. Due to the non-diagonal structure of the CKM matrix the $W^\pm$ gauge bosons couple quark states of different generations. This is in the standard model the only source of flavour changing interactions, because for the neutral currents the flavour changing processes also suppressed at tree level by the Glashow-Iliopoulos-Maiani (GIM) mechanism [11], which is discussed in more detail elsewhere, see, e.g., Refs. [7, 32, 34]

Some absolute values of CKM entries can be measured directly, namely by tree level processes. The latest values published by the particle data group (PDG) [43] are listed in Table 2.4. Two parametrizations of the CKM matrix have become standard: The first parametrization is given by

$$V = \begin{pmatrix} c_{12}c_{13} & s_{12}c_{13} & s_{13}e^{-i\delta} \\ -s_{13}c_{23} - c_{12}s_{23}s_{13}e^{i\delta} & c_{12}c_{23} - s_{12}s_{23}s_{13}e^{i\delta} & s_{23}c_{13} \\ s_{12}s_{23} - c_{12}c_{23}s_{13}e^{i\delta} & -c_{12}s_{23} - s_{12}c_{23}s_{13}e^{i\delta} & c_{23}c_{13} \end{pmatrix} , \tag{2.49}$$

Table 2.4.: CKM matrix entries from the particle data group [43].

V_{CKM}	description of the process	value	PDG update
$\lvert V_{ud}\rvert$	superallowed nuclear, neutron and pion decays	0.97425(22)	2009
$\lvert V_{us}\rvert$	semileptonic kaon and hyperon decays	0.2246 ± 0.0012	2009
$\lvert V_{cb}\rvert$	semileptonic inclusive and exclusive	0.0406 ± 0.0013	2010
$\lvert V_{ub}\rvert$	B-decays	0.00389 ± 0.00044	2010
$\lvert V_{cs}\rvert$	semileptonic D decays	1.04 ± 0.06	2008
$\lvert V_{td}/V_{ts}\rvert$	ratio of $B \to \rho\gamma$ and $K^*\gamma$ rates	0.21 ± 0.04	2008
$\lvert V_{tb}\rvert$	top-loop contributions to $\Gamma(Z \to b\bar{b})$	$0.77^{+0.18}_{-0.24}$	2008

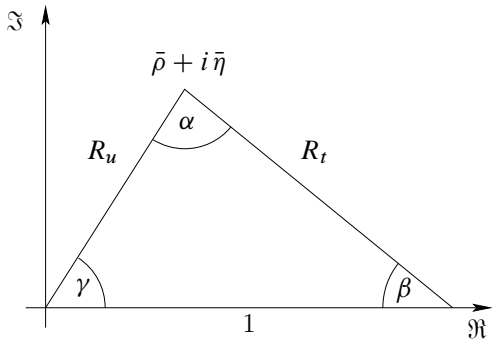

Figure 2.1: The unitarity triangle in the complex plane (Wolfenstein parametrization) arising from the condition $V_{ud}V_{ub}^* + V_{cd}V_{cb}^* + V_{td}V_{tb}^* = 0$.

where $s_{ij} = \sin\theta_{ij}$, $c_{ij} = \cos\theta_{ij}$, and δ is the KM [29] phase responsible for the CP-violating phenomena in flavour-changing processes within the standard model. The CP-violating effects are discussed in more detail in Sec. 2.1.2. The second one is the Wolfenstein parametrization [44–46], using the experimentally measured hierarchy $s_{13} \ll s_{23} \ll s_{12} \ll 1$, where

$$\begin{aligned} s_{12} &\equiv \frac{|V_{us}|}{\sqrt{|V_{ud}|^2 + |V_{us}|^2}} = \lambda\,, \quad s_{23} \equiv A\lambda^2 = \lambda\left|\frac{V_{cb}}{V_{us}}\right|\,, \\ s_{13}e^{i\delta} &\equiv V_{ub}^* = A\lambda^3(\rho + i\,\eta) = \frac{A\lambda^3(\bar{\rho} - i\,\bar{\eta})\sqrt{1 - A^2\lambda^4}}{\sqrt{1-\lambda^2}[1 - A^2\lambda^4(\bar{\rho} - i\,\bar{\eta})]}\,, \end{aligned} \tag{2.50}$$

preserving the phase-convention-independence of the expression $\bar{\rho} + i\,\bar{\eta} = -\frac{V_{ud}V_{ub}^*}{V_{cd}V_{cb}^*}$. Writing the CKM matrix in terms of λ, A, $\bar{\rho}$, and $\bar{\eta}$ it is unitary to all orders in λ. Using $\bar{\rho} = \rho(1 - \lambda^2/2 + \ldots)$ the CKM matrix up to order λ^4 can be written as

$$V_{\mathrm{CKM}} = \begin{pmatrix} 1 - \lambda^2/2 & \lambda & A\lambda^3(\rho - i\,\eta) \\ -\lambda & 1 - \lambda^2/2 & A\lambda^2 \\ A\lambda^3(1 - \rho - i\,\eta) & -A\lambda^2 & 1 \end{pmatrix} + \mathcal{O}(\lambda^4)\,. \tag{2.51}$$

The unitarity of the CKM matrix is expressed in the relations

$$\sum_i V_{ij}V_{ik}^* = \delta_{jk}\,, \tag{2.52}$$

$$\sum_j V_{ij}V_{kj}^* = \delta_{ik}\,, \tag{2.53}$$

which can be represented as a unitarity triangle (UT) in the complex $\bar{\rho} - \bar{\eta}$-plane depicted in Fig. 2.1. The sides of the unitary triangle are given by

$$R_u = \left|\frac{V_{ud}V_{ub}^*}{V_{cd}V_{cb}^*}\right| = \sqrt{\bar{\rho}^2 + \bar{\eta}^2}\,, \quad R_t = \left|\frac{V_{td}V_{tb}^*}{V_{cd}V_{cb}^*}\right| = \sqrt{(1-\bar{\rho})^2 + \bar{\eta}^2}\,, \tag{2.54}$$

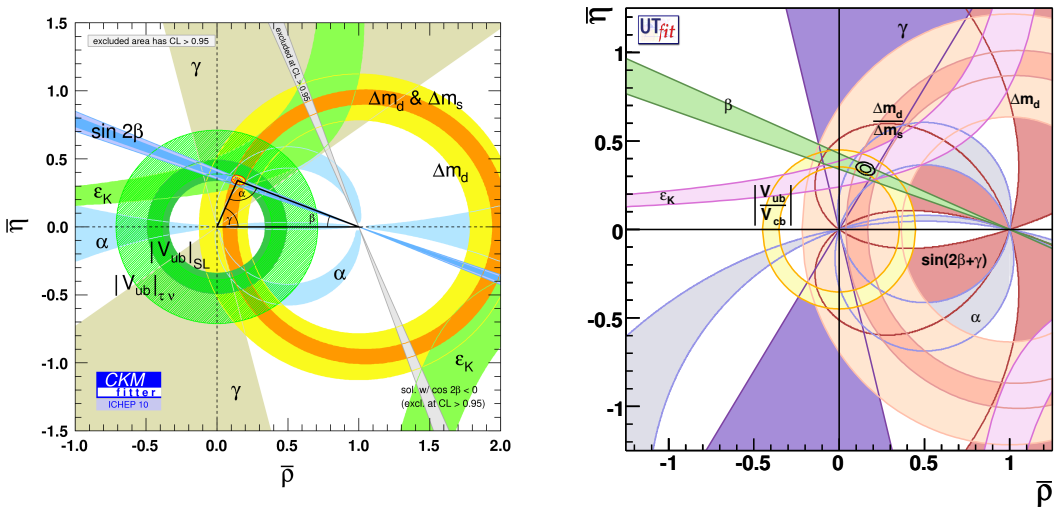

Figure 2.2.: Latest results for the CKM triangle from the CKMfitter (left panel) and the UTfitter (right panel) group.

and the three angels are

$$\alpha = \arg\left[-\frac{V_{td}V_{tb}^*}{V_{ud}V_{ub}^*}\right] \ , \ \beta = \arg\left[-\frac{V_{cd}V_{cb}^*}{V_{td}V_{tb}^*}\right] \ , \ \gamma = \arg\left[-\frac{V_{ud}V_{ub}^*}{V_{cd}V_{cb}^*}\right] \ , \tag{2.55}$$

where $\gamma \equiv \delta$ in the standard parametrization as explained above. By global fits the CKM matrix elements are determined very precisely. These non-trivial tests of the CKM mechanism use all available measurements and theory predictions for the hadronic matrix elements, and impose the standard model constraints. The latest results from CKMfitter [46] and UTfit [47] are presented in Fig. 2.2. The fit methods are different UTfit use a Bayesian approach [47], whereas CKMfitter use frequentist statistics [46, 48]. In Chap. 6 the CKMfitter methods are used for the new physics predictions.

Borders of the Standard Model

The standard model as described above is an $G_{SM} = SU(3) \otimes SU(2) \otimes U(1)$ gauge symmetry with the associated Lie algebra $\mathfrak{g}_{SM} = \mathfrak{su}(3)_C \oplus \mathfrak{su}(2)_T \oplus \mathfrak{u}(1)_Y$, where Y, T and C are the internal symmetries hypercharge, isospin and colour, respectively. It describes the elementary particles and forces approximately correct and it is well tested by experiments. However, there are some unanswered questions [20, 35], discussed in the following.

First of all gravitational forces is not implemented in the standard model. General relativity is not a quantum field theory. By now, there is no satisfying theory, how to generate a quantum theory from general relativity. Kaluza-Klein [49] and supergravity [50] theories are possible solutions, see, e.g. Ref. [35] and the references therein, but a stain clings on them, because they are not renormalizable. However, if the background is smooth-enough, the gravitational field can be quantised consistently [51, 52]. In the low-energy limit, general relativity can considered as an effective field theory, where renormalization is no longer an issue [53, 54].

Another problem is with the standard gauge group itself, called the *gauge problem*: Within the standard model there is no satisfying explanation for the three different gauge couplings. Moreover, there is no reason only the electroweak part is chiral, and the charged is quantised as multiples of $\frac{e}{3}$. Explanations by superstring theories or by an existence of magnetic monopoles are not satisfyingly yet.

As discussed above the masses of W, Z and the fermions are generated by the Higgs field, but for a consistent model, the mass of Higgs boson should not be too different from the W mass. Within the standard model there is no natural order of magnitude of the Higgs mass m_H. For a long time, the experimental lower limit was set up from LEP [55], $m_H \gtrsim 114.4$ GeV at the 95% confidence level.

However, in a recent paper [56] CDF and DØ Collaborations at the Tevatron reported a newly excluded range for the Higgs boson mass around $2m_W$. In nature there are two fundamental energy scales, the electroweak scale $\Lambda_W \sim 10^3$ GeV and the Plack scale $\Lambda_{\text{Planck}} = \sqrt{G_N} \sim 10^{18}$ GeV. At the Planck scale gravity becomes as strong as the gauge interactions [57]. In a unified scenario of strong, weak, and electromagnetic interaction, a natural scale is the unification scale $\Lambda_{\text{GUT}} \sim 10^{15} - 10^{16}$ GeV. The tree-level (bare) Higgs mass receives quadratically-divergent corrections from loop-diagrams, particularly from the top loop. Hence, bare Higgs masse becomes, $m_H^2 = (m_H)^2_{\text{bare}} + m_H^2(\Lambda^2)$, where Λ is a reference scale and must be of order $\Lambda \sim \mathcal{O}(1\text{ TeV})$, due to the well tested light Higgs mass by precision tests. In Fig. 2.3 the so-called blue band plot is depicted, where the blue band represents an estimate of the theoretical uncertainty due to missing higher order corrections The vertical band shows the 95% confidence level exclusion limit on the Higgs mass from the direct searches at LEP-II (up to 114 GeV) and the Tevatron (160 to 170 GeV) [55].

The discrepancy between the fundamental scales and the reference scale is called the hierachy problem [58, 59].

Further problems, which could not discussed at all, are the strong CP problem, the mechanism for small neutrino masses and the structure of dark energy and matter,

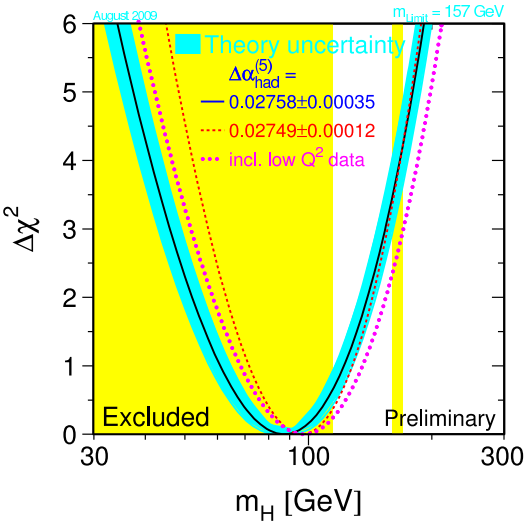

Figure 2.3: 2009 blue band plot as explained in the text.

which are discussed in more detail, e.g. in Refs. [35, 50, 55, 58].

2.2. *CP* Violation and B-Physics

In nature there are some fundamental symmetries, e.g. the space reflection or the time reversal. In quantum mechanics as well as in classical mechanics one finds from the invariance of the Lagrangians under these symmetry transformations conservation laws of the considered physical system. In quantum mechanics a special symmetry is the charge conjugation, and all quantum mechanical equations are invariant under the combination of charge conjugation, space reflection and time reversal called ***CPT***-theorem. However, in some special particle systems the combination of charge conjugation and space reflection is violated, this is called the CP violation.

In 1977 the b quark was experimentally verified by the discovery of the Υ resonances at Fermilab. One year later the DASP II and PLUTO collaborations verified, that the Υ resonances are bound states of b and $\bar{b}$. The resonances decay into B-mesons, e.g. $\Upsilon(4S) \rightarrow B^0\bar{B}^0$ or $\Upsilon(4S) \rightarrow B^+B^-$, which are bound states of an heavy $\bar{b}$ and a lighter quark $q \in \{u, d, s, c\}$ forming B^+, B^0, B_s or B_c and the charged conjugate states, respectively [60, 61]. In this section CP-violating effects are studied in B_q-meson systems, ($q \in \{d, s\}$), and it is organized as follows. In the first part CP violation in the standard model is briefly reviewed, and the CP-violating effects in $B^0 - \bar{B}^0$ mixing are studied in the second part of this section.

2.2.1. *CP* Violation

In physics and especially in particle physics, symmetries play a key rôle, because with continuous symmetry a conservation law is associated. In the following the space reflection (parity) $\boldsymbol{P} : \vec{r} \longmapsto -\vec{r}$, time reversal $\boldsymbol{T} : t \longmapsto -t$ and charge conjugation $\boldsymbol{C}$: particle $\longmapsto$ antiparticle and their application to B-physics are discussed. Within the standard model the three discrete symmetries are all conserved under the strong and electromagnetic interactions. Weak interaction preserves only the $\boldsymbol{CPT}$ symmetry; $\boldsymbol{P}$, $\boldsymbol{C}$, and $\boldsymbol{T}$ are violated separately. CP violation was first observed in the weak decay of the neutral kaon in 1964 [62] and in the B-meson system in 2001 by the B-factories BABAR at SLAC [63] and Belle at KEK [64].
The theory of CP violation has become textbook material and is discussed in more detail elsewhere, e.g. Refs. [65–68]. Here some aspects of CP violation are shortly reviewed. The action of the $\boldsymbol{P}$, $\boldsymbol{C}$ and $\boldsymbol{T}$ operations on a Dirac spinor are given by

$$\begin{aligned} \boldsymbol{P}\Psi(t,\vec{r})\boldsymbol{P}^{-1} &= \gamma^0\Psi(t,-\vec{r}) \;, \quad \boldsymbol{C}\Psi(t,\vec{r})\boldsymbol{C}^{-1} \;= i\gamma^0\gamma^2\bar{\Psi}(t,\vec{r})^{\mathrm{T}} \;, \\ \boldsymbol{T}\Psi(t,\vec{r})\boldsymbol{T}^{-1} &= \gamma^1\gamma^3\Psi(-t,\vec{r}) \;, \end{aligned} \tag{2.56}$$

and for the vector bosons associated with the $\mathsf{SU(2)}_L \otimes \mathsf{U(1)}_Y$ electroweak theory (2.46) are

$$\begin{aligned} \mathrm{W}^{\pm}_{\mu}(t,\vec{r}) &\overset{\boldsymbol{CP}}{\longmapsto} -\eta(\mu)\mathrm{W}^{\mp}_{\mu}(t,-\vec{r}) \;, \\ \mathrm{Z}^{0}_{\mu}(t,\vec{r}) &\overset{\boldsymbol{CP}}{\longmapsto} -\eta(\mu)\mathrm{Z}_{\mu}(t,-\vec{r}) \;, \\ A_{\mu}(t,\vec{r}) &\overset{\boldsymbol{CP}}{\longmapsto} -\eta(\mu)A_{\mu}(t,-\vec{r}) \;, \end{aligned} \tag{2.57}$$

where the CP-eigenvalues are given by

$$\eta(\mu) = \begin{cases} +1 \;, & \mu = 0 \;, \\ -1 \;, & \mu = 1,2,3 \;. \end{cases} \tag{2.58}$$

Using (2.56) and (2.57) together with the current transformations collected in Table 2.5 one gets

$$\begin{aligned} &\bar{u}_L\gamma^{\mu}V_{\mathrm{CKM}}d_L\mathrm{W}^{+}_{\mu} + \bar{d}_L V^{\dagger}_{\mathrm{CKM}}\gamma^{\mu}u_L\mathrm{W}^{-}_{\mu} \\ &\qquad \overset{CP}{\longmapsto} \bar{d}_L V^{\mathrm{T}}_{\mathrm{CKM}}\gamma^{\mu}u_L\mathrm{W}^{-}_{\mu} + \bar{u}_L\gamma^{\mu}V^{*}_{\mathrm{CKM}}d_L\mathrm{W}^{+}_{\mu} \;, \end{aligned} \tag{2.59}$$

hence the CP transformation of the CKM matrix is given by $V_{\mathrm{CKM}} \overset{CP}{\longmapsto} V^{*}_{\mathrm{CKM}}$. The transformation (2.59) yields that in the standard model the charged current is a source

for CP violation, due to fact that the CKM matrix is complex. The neutral current terms are CP invariant, hence, flavour changing neutral currents are forbidden in the standard model and the GIM mechanism is a direct consequence of the unitary mass-diagonalization matrices, together with the hypothesis of universal weak coupling [67]. For observable CP-violating effects further conditions are necessary summarised as [69–71]

$$(m_t^2 - m_c^2)(m_t^2 - m_u^2)(m_c^2 - m_u^2)(m_b^2 - m_s^2)(m_b^2 - m_d^2)(m_s^2 - m_d^2) \times J_{\text{CP}} \neq 0 \ , \quad (2.60)$$

where

$$J_{CP} = |\Im\{V_{i\alpha} V_{j\beta} V_{i\beta}^* V_{j\alpha}^*\}| \quad (i \neq j, \alpha \neq \beta) \ . \quad (2.61)$$

If any quarks of the same charge had the same mass in (2.60), the CP-violating phase of the CKM matrix could be transformed away by an unitary transformation of the quark fields. The Jarlskog parameter (2.61) measures the strength of the CP violation in the standard model, independent from the chosen quark-field parametrization. Using the parametrization (2.49) one gets for the Jarlskog parameter

$$J_{CP} = s_{12} s_{13} s_{23} c_{12} c_{23} c_{13}^2 \sin \delta_{13} \ . \quad (2.62)$$

The measurement of the CKM parameters implies a value for $J_C P$ of $\mathcal{O}(10^{-5})$, therefore in the standard model, the CP-violating effects could not be easily seen. In the next subsection the way how CP violation could be detected in the $B^0 - \bar{B}^0$ system is discussed.

2.2.2. $B^0 - \bar{B}^0$ Mixing and *CP* Violation

As mentioned in the previous subsection the observation of CP-violating effects in the standard model is very hard. In this subsection the CP violation in the neutral

Table 2.5.: Operations $\boldsymbol{P}$, $\boldsymbol{C}$ and $\boldsymbol{T}$ for the various quantities appear in the standard model gauge Lagrangian, [68].

Transformation of	Current Γ			
$\bar{\Psi}_i \Gamma \Psi_j$ under	scalar	pseudoscalar	vector	axial-vector
$\boldsymbol{P}$	$\bar{\Psi}_i \Psi_j$	$-i\bar{\Psi}_i \gamma_5 \Psi_j$	$\eta(\mu)\bar{\Psi}_i \gamma^\mu \Psi_j$	$-\eta(\mu)\bar{\Psi}_i \gamma^\mu \gamma_5 \Psi_j$
$\boldsymbol{C}$	$\bar{\Psi}_j \Psi_i$	$i\bar{\Psi}_j \gamma_5 \Psi_i$	$-\bar{\Psi}_j \gamma^\mu \Psi_i$	$\bar{\Psi}_j \gamma^\mu \gamma_5 \Psi_i$
CP	$\bar{\Psi}_j \Psi_i$	$-i\bar{\Psi}_j \gamma_5 \Psi_i$	$-\eta(\mu)\bar{\Psi}_j \gamma^\mu \Psi_i$	$-\eta(\mu)\bar{\Psi}_j \gamma^\mu \gamma_5 \Psi_i$

B-meson systems is shortly reviewed. The general formalism and the application to the neutral B-systems is discussed by several authors, see, e.g., Refs. [72–77] and the references within. Here some basic facts and notations which are useful for the next chapter are noted down.

The $B_q^0 - \bar{B}_q^0$ mixing is induced at lowest order through the box-diagrams shown in Fig. 2.4. The neutral B^0-meson and its antiparticle $\bar{B}^0$ yield a state vector, given by

$$\left|\psi_q(t)\right\rangle = a(t)\left|B_q^0\right\rangle + b(t)\left|\bar{B}_q^0\right\rangle \,, \tag{2.63}$$

whose time evolution is written as

$$i\frac{\partial}{\partial t}\phi(t) = \boldsymbol{\mathcal{H}}\phi(t)\,, \quad \phi(t) = \begin{pmatrix} a(t) \\ b(t) \end{pmatrix}, \quad \boldsymbol{\mathcal{H}} = \left[\boldsymbol{M} - \frac{i}{2}\boldsymbol{\Gamma}\right] \tag{2.64}$$

where the Wigner-Weisskopf approximation [78] is used. Here $\boldsymbol{M}$ and $\boldsymbol{\Gamma}$ are 2×2 matrices, with $\boldsymbol{M} = \boldsymbol{M}^\dagger$, $\boldsymbol{\Gamma} = \boldsymbol{\Gamma}^\dagger$. Due to guarantee the $\boldsymbol{CPT}$ invariance, one used the special form

$$\boldsymbol{M} = \begin{pmatrix} M_0^{(q)} & M_{12}^{(q)} \\ M_{12}^{*(q)} & M_0^{(q)} \end{pmatrix}, \quad \boldsymbol{\Gamma} = \begin{pmatrix} \Gamma_0^{(q)} & \Gamma_{12}^{(q)} \\ \Gamma_{12}^{*(q)} & \Gamma_0^{(q)} \end{pmatrix}, \tag{2.65}$$

for the matrices. The mass eigenstates[2] are

$$\begin{aligned} \left|B_L^{(q)}\right\rangle &= \frac{(1+\varepsilon)\left||B_q^0\right\rangle + (1-\varepsilon)\left|\bar{B}_q^0\right\rangle}{\sqrt{2(1+|\varepsilon|^2)}} \equiv p\left|B_q^0\right\rangle + q\left|\bar{B}_q^0\right\rangle \,, \\ \left|B_H^{(q)}\right\rangle &= \frac{(1+\varepsilon)\left|B_q^0\right\rangle - (1-\varepsilon)\left|\bar{B}_q^0\right\rangle}{\sqrt{2(1+|\varepsilon|^2)}} \equiv p\left|B_q^0\right\rangle - q\left|\bar{B}_q^0\right\rangle \,, \end{aligned} \tag{2.66}$$

where

$$\frac{p}{q} = \frac{1+\varepsilon}{1-\varepsilon} = \sqrt{\frac{M_{12}^{(q)} - \frac{i}{2}\Gamma_{12}^{(q)}}{M_{12}^{*(q)} - \frac{i}{2}\Gamma_{12}^{*(q)}}}\,. \tag{2.67}$$

[2] subscript L and H refer to "light" and "heavy"

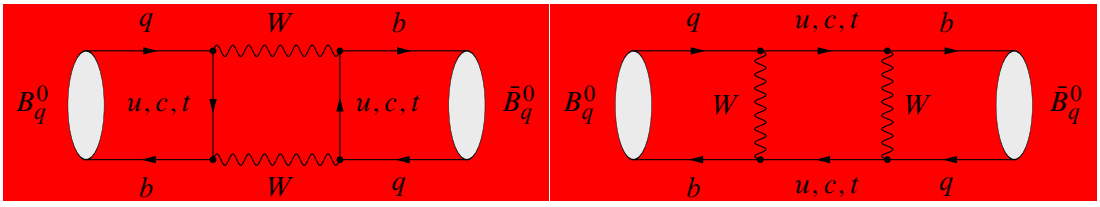

Figure 2.4.: Standard model box diagrams contributing to the $B_q^0 - \bar{B}_q^0$ mixing ($q \in \{d, s\}$).

Starting with an initially pure $\left|B_q^0(t=0)\right\rangle \equiv \left|B_q^0\right\rangle$ or $\left|\bar{B}_q^0(t=0)\right\rangle \equiv \left|\bar{B}_q^0\right\rangle$ state the time evolution is given by

$$\begin{aligned}\left|B_q^0(t)\right\rangle &= f_+^{(q)}(t)\left|B_q^0\right\rangle + \frac{q}{p} f_-^{(q)}(t)\left|\bar{B}_q^0\right\rangle \,, \\ \left|\bar{B}_q^0(t)\right\rangle &= \frac{p}{q} f_-^{(q)}(t)\left|B_q^0\right\rangle + \frac{q}{p} f_+^{(q)}(t)\left|\bar{B}_q^0\right\rangle \,.\end{aligned} \tag{2.68}$$

Here the functions $f_\pm^{(q)}$ are

$$f_\pm^{(q)}(t) = \frac{1}{2}\left[\exp\left\{-it\left(M_L^{(q)} - \frac{i\Gamma_L^{(q)}}{2}\right)\right\} \pm \exp\left\{-it\left(M_H^{(q)} - \frac{i\Gamma_H^{(q)}}{2}\right)\right\}\right] \,. \tag{2.69}$$

For later use, one introduces the following definitions for the differences of mass and width

$$\Delta M_q \equiv M_L^{(q)} - M_H^{(q)} = 2|M_{12}^{(q)}| > 0 \,, \tag{2.70}$$

$$\Delta\Gamma_q \equiv \Gamma_H^{(q)} - \Gamma_L^{(q)} = \frac{4\Re\{M_{12}^{(q)}\Gamma_{12}^{*(q)}\}}{\Delta M_q} \,, \tag{2.71}$$

while the average decay width is

$$\Gamma_q \equiv \frac{\Gamma_H^{(q)} + \Gamma_L^{(q)}}{2} = \Gamma_0^{(q)} \,. \tag{2.72}$$

The deviation of the quantity $|p/q|$ from one describes the CP-violating effects in the $B_q^0 - \bar{B}_q^0$ oscillations [75, 77]. The strength of the oscillations is given by the *mixing parameter* $x_q = \frac{\Delta M_q}{\Gamma_q}$. Another CP violation parameter is the measureable asymmetry

$$\mathcal{A}_{\mathrm{SL}}^{(q)}(t) = \frac{\Gamma(\bar{B}_q^0(t) \to \ell^+\nu_\ell X) - \Gamma(B_q^0(t) \to \ell^-\bar{\nu}_\ell X)}{\Gamma(\bar{B}_q^0(t) \to \ell^+\nu_\ell X) + \Gamma(B_q^0(t) \to \ell^-\bar{\nu}_\ell X)} = \frac{1 - |q/p|_q^4}{1 + |q/p|_q^4} \,. \tag{2.73}$$

The present ranges for the quantities (2.70) and (2.71), as well as for the CP-violating quantities x_q and $\mathcal{A}_{\mathrm{SL}}^{(q)}$ can be found in Ref. [79].
Finally, the B_q-decays ($q \in \{d, s\}$) into pure CP eigenstates are considered. If a pure B_q^0 and a pure $\bar{B}_q^0$ both decay into a nonleptonic final CP eigenstate $|f\rangle$,

$$\boldsymbol{CP}\,|f\rangle = \eta_f\,|f\rangle \,, \tag{2.74}$$

then the time evolution for these decays is given by [77, 80, 81]

$$|A_f(t)|^2 = \frac{|\mathcal{N}_f|^2}{2}\Big\{ R_L^f e^{-\Gamma_L^{(q)}t} + R_H^f e^{-\Gamma_H^{(q)}t} + 2e^{-\Gamma_q t}\left[A_D^f \cos(\Delta M_q t) + A_M^f \sin(\Delta M_q t)\right]\Big\} , \tag{2.75}$$

$$|\bar{A}_f(t)|^2 = \frac{|\mathcal{N}_f|^2}{2}\Big\{ R_L^f e^{-\Gamma_L^{(q)}t} + R_H^f e^{-\Gamma_H^{(q)}t} - 2e^{-\Gamma_q t}\left[A_D^f \cos(\Delta M_q t) + A_M^f \sin(\Delta M_q t)\right]\Big\} , \tag{2.76}$$

and the *unevolved* decay amplitudes can be written as

$$A_f = \mathcal{N}_f \left[1 - b_f e^{i\rho} e^{+i\gamma}\right] \equiv \mathcal{N}_f z , \tag{2.77}$$

$$\bar{A}_f = \mathcal{N}_f \left[1 - b_f e^{i\rho} e^{-i\gamma}\right] \equiv \eta_f \mathcal{N}_f \bar{z} , \tag{2.78}$$

where

$$\begin{aligned} R_L^f &\equiv \frac{1}{2}\left[|z|^2 + |\bar{z}|^2 + 2\eta_f \Re\left(e^{-i\phi_q} z^* \bar{z}\right)\right] \\ &= (1 + \eta_f \cos\phi_q) - 2b_f \cos\theta[\cos\gamma + \eta_f \cos(\phi_q + \gamma)] \\ &\quad + b_f^2[1 + \eta_f(\cos\phi_q + 2\gamma)] , \end{aligned} \tag{2.79}$$

$$\begin{aligned} R_H^f &\equiv \frac{1}{2}\left[|z|^2 + |\bar{z}|^2 - 2\eta_f \Re\left(e^{-i\phi_q} z^* \bar{z}\right)\right] \\ &= (1 - \eta_f \cos\phi_q) - 2b_f \cos\theta[\cos\gamma - \eta_f \cos(\phi_q + \gamma)] \\ &\quad + b_f^2[1 - \eta_f(\cos\phi_q + 2\gamma)] , \end{aligned} \tag{2.80}$$

$$A_D^f \equiv \frac{1}{2}\left(|z|^2 - |\bar{z}|^2\right) = 2b_f \sin\theta \sin\gamma , \tag{2.81}$$

$$\begin{aligned} A_M^f &\equiv -\eta_f \Im\left(e^{-i\phi_q} z^* \bar{z}\right) \\ &= \eta_f[\sin\phi_q - 2b_f \cos\theta \sin(\phi_q + \gamma) + b_f x^2 \sin(\phi_q + 2\gamma)] . \end{aligned} \tag{2.82}$$

Here $|\mathcal{N}_f|^2$ is the overall normalisation, γ denotes the UT angle (2.55), and ϕ_q the $B_q^0 - \bar{B}_q^0$ mixing phase,

$$\phi_q \equiv 2\arg(V_{tq}^* V_{tb}) = \begin{cases} 2\beta & (q = d) , \\ -2\delta\gamma & (q = s) , \end{cases} \tag{2.83}$$

where $2\delta\gamma \approx 0.03$ in the standard model, because of a Cabibbo-suppression of $\mathcal{O}(|\lambda|^2)$. Note that the subscripts "D" and "M" refer to direct and mixing-induced CP-violating effects, respectively. The quantities Eqs. (2.79)–(2.82) satisfy the relation

$$(A_D^f)^2 + (A_M^f)^2 = R_L^f R_H^f . \tag{2.84}$$

For the discussion of the CP-violating effects in the B_q systems, it is useful to define the time-dependent CP asymmetry

$$\begin{aligned}\mathcal{A}_{CP}(t;f) &\equiv \frac{|A_f(t)|^2 - |\bar{A}_f|^2}{|A_f(t)|^2 + |\bar{A}_f|^2} \\ &= 2e^{-\Gamma_q t}\left[\frac{\mathcal{A}_{CP}^{\mathrm{dir},f}\cos(\Delta M_q t) + \mathcal{A}_{CP}^{\mathrm{mix},f}\sin(\Delta M_q t)}{e^{-\Gamma_H^{(q)}t} + e^{-\Gamma_L^{(q)}} + \mathcal{A}^f_{\Delta\Gamma_q}(e^{-\Gamma_H^{(q)}t} - e^{-\Gamma_L^{(q)}t})}\right]\end{aligned} \tag{2.85}$$

with the observables

$$\mathcal{A}_{CP}^{\mathrm{dir},f} \equiv \frac{A_D}{N_f} = \frac{2b_f\sin\theta\sin\gamma}{N_f}\,, \tag{2.86}$$

$$\mathcal{A}_{CP}^{\mathrm{mix},f} \equiv \frac{A_M}{N_f} = \frac{+\eta_f}{N_f}\left[\sin\phi - 2b_f\cos\theta\sin(\phi_q+\gamma) + b_f^2\sin(\phi_q+2\gamma)\right]\,, \tag{2.87}$$

$$\begin{aligned}\mathcal{A}^f_{\Delta\Gamma_q} &\equiv \frac{R_H^f - R_L^f}{2N_f} \\ &= \frac{-\eta_f}{N_f}\left[\cos\phi_q - 2b_f\cos\theta\cos(\phi_q+\gamma) + b_f^2\cos(\phi_q+2\gamma)\right]\,,\end{aligned} \tag{2.88}$$

and the abbreviation

$$N_f \equiv \frac{1}{2}\left(R_H^f + R_L^f\right) = 1 - 2b_f\cos\theta\cos\gamma + b^2\,. \tag{2.89}$$

The *direct* $\mathcal{A}_{CP}^{\mathrm{dir}}$, *mixing-induced* $\mathcal{A}_{CP}^{\mathrm{mix}}$ and the observable $\mathcal{A}_{\Delta\Gamma_q}$ are not independent from each other, they satisfy the relation

$$(\mathcal{A}_{CP}^{\mathrm{dir}})^2 + (\mathcal{A}_{CP}^{\mathrm{mix}})^2 + (\mathcal{A}_{\Delta\Gamma_q})^2 = 1\,. \tag{2.90}$$

The index q was suppressed in the above formulae, because the time evolution of all kinds of neutral B-decays into final CP eigenstates are described by them. Finding physics beyond the standard model - *new physics* (NP) - is a major aim in modern elementary particle physics. In Chap. 6 the CP-violating asymmetries are used to find hints for it in the $B_s^0 - \bar{B}_s^0$ and $B_d^0 - \bar{B}_d^0$ mixing.
CP violation within the standard model is well understood, and provides suitable tools searching for new physics effects in CP-violating processes. In the next chapter the theory of B-meson decays are studied in more detail by using effective theory methods.

3

B-Meson Decays

B-meson decays play a key rôle in flavour physics, because a lot of fundamental problems of particle physics can be studied or even solved by understanding these decays more precisely. As mentioned at the end of the previous chapter, the B-mesons are build up of a heavy $\bar{b}$ quark and a light $q \in \{u, d, s, c\}$ quark or in charged conjugate case by b and a light $\bar{q} \in \{\bar{u}, \bar{d}, \bar{s}, \bar{c}\}$. Weak decays of B-mesons are distinguished in leptonic, semileptonic and non-leptonic transitions.
The chapter is organized as follows: In Sec. 3.1 non-leptonic B-meson decays are studied in an framework of an effective field theory, where the effective weak Hamiltonian for such decays is introduced. which is used in Sec. 3.2 for studying hadronic matrix elements. This brief review of B-meson decays is closed by discussing the heavy-quark effective theory (HQET) in Sec. 3.3, an effective field theory, providing symmetry relations and applications for a sophisticated study of $\bar{B} \to D^{(*)}$ transitions presented in the forthcoming chapters.

3.1. Effective Field Theory

Effective field theories have become powerful and fruitful tools in several fields of particle physics, dealing with widely-separated energy scales. They can be classified by their behaviour of the transition from the *fundamental* to the *effective* level. For instance within the weak decays of the B-mesons there are three energy scales. The first one is the weak energy scale, given by the mass of the W-boson, $M_W \sim 100$ GeV. Since the energy scale of the process is the one of the decaying meson, the second energy scale is the mass of the B-meson, $m_B \sim 5$ GeV, and the third energy scale comes from the meson itself, because the meson is a bound state of quarks, hence, the

strong interaction energy scale is taken into account, $\Lambda_{\mathrm{QCD}} \sim 0.2 - 1$ GeV. The search for physics beyond the standard model enforced another energy scale, $\Lambda_{\mathrm{NP}} >$ few TeV, with the consequence that the standard model as an effective field theory break down. For the B-meson decays, the four energy scales are widely separated from each other,

$$\Lambda_{\mathrm{QCD}} \ll m_B \ll M_W \ , \ \Lambda_{\mathrm{NP}} \ . \tag{3.1}$$

In order to construct the weak effective Hamiltonian the operator-product expansion formalism is introduced in Sec. 3.1.1, and in Sec. 3.1.2 the concept of renormalization-group improved theory is presented. The weak effective Hamiltonian is finally discussed in Sec. 3.1.2.

3.1.1. Operator-Product Expansion

The weak effective Hamiltonian can be constructed using the operator-product expansion (OPE) [82]. An introduction into the OPE formalism can be found in many textbooks, e.g. Refs. [5, 32, 34], or lecture notes [83, 84]. The presentation in this section follows Ref. [85].

The generic form of the weak Hamiltonian is given by

$$\mathcal{H}_{\mathrm{eff}} = \frac{G_F}{\sqrt{2}} \sum_i V^i_{\mathrm{CKM}} \mathcal{C}_i(\mu) \mathcal{Q}_i \ , \tag{3.2}$$

where $\mathcal{Q}_i$ are the local operators, which are relevant for the process, V^i_{CKM} are the Cabbibo-Kobayashi-Maskawa (CKM) factors and $\mathcal{C}_i$ are the Wilson coefficients, describing the strength with which a given operator enters the Hamiltonian. Note that the coupling constants $\mathcal{C}_i(\mu)$ depend on a scale μ, which can be chosen arbitrarily, but by a given decay amplitude it serves to separate the physics contributions into short-distance ones at scales higher than μ and long-distance ones at scales lower than μ. The Wilson coefficients $\mathcal{C}_i$ include the top quark and contributions from other heavy particles. Within the standard model this can be seen by evaluating the box and penguin diagrams with full W-, Z- and top, and, if extensions of the standard model are considered, new particles, exchanges and *properly* including short distance QCD effects, which govern the μ-dependence.

A formal approach is given by the path path integral formalism. The Lagrangian density containing the W-boson field and its interaction with charged currents can be

written as[1]

$$\mathcal{L}_W = -\frac{1}{2}\left(\partial_\mu \mathrm{W}^+_\nu - \partial_\nu \mathrm{W}^+_\mu\right)\left(\partial^\mu \mathrm{W}^{-\nu} - \partial^\nu \mathrm{W}^{-\mu}\right) + M_W^2 \mathrm{W}^+_\mu \mathrm{W}^{-\mu} + \mathcal{L}_{\mathrm{W}^\pm} \,, \quad (3.3)$$

where the Lagrangian $\mathcal{L}_{\mathrm{W}^\pm}$ is defined by Eq. (2.46) including the interaction with the quark fields. Without an overall normalising factor, the generating functional for the Green functions is

$$Z_W \sim \int [d\mathrm{W}^+][d\mathrm{W}^-] \, \exp\left\{ i \int d^4x \, \mathcal{L}_W \right\} \,. \quad (3.4)$$

Integrating out the W fields in this functional one gets the non-local action functional for the quark fields

$$\mathcal{S}_{cc} = -\frac{g^2}{8} \int d^4x \, d^4y \, \mathcal{J}^-_\mu(x) \, \Delta^{\mu\nu} \, \mathcal{J}^+_\nu(y) \,, \quad (3.5)$$

with the W propagator $\Delta^{\mu\nu}$. Performing an expansion of this action in powers of $1/M_W^2$ to all orders is equivalent to the full theory and leads to a series of local interaction operators. Up to $\mathcal{O}(1/M_4^2)$ the W propagator can be written as

$$\Delta^{\mu\nu} \approx \frac{g^{\mu\nu}}{M_W^2} \delta^{(4)}(x-y) + \mathcal{O}\left(\frac{1}{M_W^4}\right) \,, \quad (3.6)$$

inserting this into (3.5), the W-boson is removed as an explicit dynamical degree of freedom and one can read off the effective charged current interaction Lagrangian as

$$\mathcal{L}_{\mathrm{eff}} = -\frac{G_F}{\sqrt{2}} V^*_{ij} V_{i'j'} \left(\bar{d}^j_L u^i_L\right)\left(\bar{u}^{i'}_L d^{j'}_L\right) =: -\frac{G_F}{\sqrt{2}} \, V^*_{ij} V_{i'j'} \, \mathcal{Q}_2^{iji'j'} \,, \quad (3.7)$$

with the four-quark operator $\mathcal{Q}_2$. It is worthy of remark that this local four-fermion interaction terms are a modern version of the classical Fermi theory of weak interaction.

Short Distance QCD Effects

Now the strong interactions among the quarks have to be taken into account. Thanks to the asymptotic freedom of QCD, the short distance QCD corrections to weak decays can be calculated in the renormalisation-group (RG) improved perturbation theory. The weak effective Hamiltonian (3.2) is defined in such a way, that the hadronic amplitude takes the form

$$A(i \to f) = \langle f | \mathcal{H}_{\mathrm{eff}} | i \rangle = \frac{G_F}{\sqrt{2}} \sum_i \mathcal{C}_i(\mu) \, \langle f | \mathcal{Q}_i(\mu) | i \rangle \,. \quad (3.8)$$

[1] see Sec. 2.1.2 and 2.1.2 for more details

Both, the Wilson coefficients $\mathcal{C}_i(\mu)$ and the matrix elements $\langle Q_i(\mu)\rangle$ depend on the arbitrary scale μ, but the full amplitude can not depend on it. Therefore the μ-dependence of the Wilson coefficients have to cancel that one of the matrix elements. This problem can be solved by an factorization into a high- and low-energy part, or more precisely, by running the value of the scale μ, such that the coefficients $\mathcal{C}_i(\mu)$ contain the *short distance* effects above μ and the matrix elements $\langle Q_i(\mu)\rangle$ the *long distance* non-perturbative contributions below μ. In order to get the Wilson coefficients, one used the *matching* between the full and the effective theory: calculating the QCD corrections in the full theory, i.e. with the W exchange, and in the effective theory, where the W is *integrated out*, and expressed the QCD-corrected transition amplitude in terms of QCD-corrected matrix elements and Wilson coefficients. Including the QCD corrections the interaction (3.7) is generalized to

$$\mathcal{H}_{\text{eff}} \sim \mathcal{C}_1(\mu)\mathcal{C}_1(\mu)\mathcal{Q}_1^{iji'j'} + \mathcal{C}_2(\mu)\mathcal{Q}_2^{iji'j'}\,, \tag{3.9}$$

where a second current-current operator

$$\mathcal{Q}_1^{iji'j'} = \left(\bar{d}^j_{L,a}u^i_{L,b}\right)\left(\bar{u}^{i'}_{L,b}d^{j'}_{L,a}\right) \tag{3.10}$$

appeared through *operator mixing*: The renormalization of the operator $\mathcal{Q}_2$ is depicted in Fig. 3.1; in the first line of this figure the divergences of the full theory cancel. During this renormalization process enforced by non-factorizable QCD corrections new divergences appear canceled by counterterms for $\mathcal{Q}_1$ and $\mathcal{Q}_2$ being a consequence of the operator mixing. For operators with dimension greater than four, not all divergences can be canceled, and an additional *operator renormalization* has to be performed. Due to this mixing, the operator $\mathcal{Q}_2$ involves counterterms proportional to $\mathcal{Q}_1$ and vice versa, and their scale dependence is correlated. By an explicit calculation [83, 85] the Wilson coefficients are

$$\mathcal{C}_1 = -3\frac{\alpha_s}{4\pi}\ln\left(\frac{M_W^2}{\mu^2}\right) + \mathcal{O}(\alpha_s^2)\,, \quad \mathcal{C}_2 = 1 + \frac{3}{N}\frac{\alpha_s}{4\pi}\ln\left(\frac{M_W^2}{\mu^2}\right) + \mathcal{O}(\alpha_s^2)\,, \tag{3.11}$$

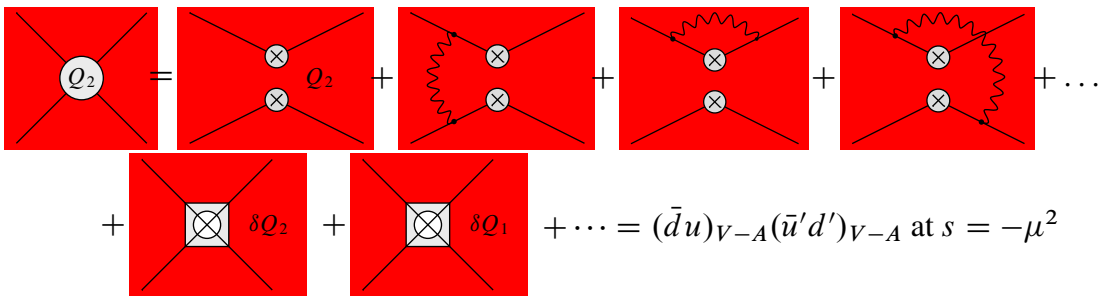

Figure 3.1.: Renormalization of the local operator $\mathcal{Q}_2$ as explained in the text, [86].

Table 3.1.: Operators for the non-leptonic B decays. For the electroweak penguin operators $e_{q'}$ denote the electrical quark charges.

Current-Current Operators	
$Q_1^{ij} = (\bar{i}_a j_b)_{V-A}(\bar{i}_b b_a)_{V-A}$	$Q_2^{ij} = (\bar{i}_a j_a)_{V-A}(\bar{i}_b b_b)_{V-A}$
QCD Penguin Operators	EW Penguin Operators
$Q_3^j = (\bar{j}_a b_a)_{V-A} \sum_{q'} (\bar{q}'_b q'_b)_{V-A}$	$Q_7^j = \frac{3}{2}(\bar{j}_a b_a)_{V-A} \sum_{q'} e_{q'} (\bar{q}'_b q'_b)_{V+A}$
$Q_4^j = (\bar{j}_a b_b)_{V-A} \sum_{q'} (\bar{q}'_b q'_a)_{V-A}$	$Q_8^j = \frac{3}{2}(\bar{j}_a b_b)_{V-A} \sum_{q'} e_{q'} (\bar{q}'_b q'_a)_{V+A}$
$Q_5^j = (\bar{j}_a b_a)_{V-A} \sum_{q'} (\bar{q}'_b q'_b)_{V+A}$	$Q_9^j = \frac{3}{2}(\bar{j}_a b_a)_{V-A} \sum_{q'} e_{q'} (\bar{q}'_b q'_b)_{V-A}$
$Q_6^j = (\bar{j}_a b_b)_{V-A} \sum_{q'} (\bar{q}'_b q'_a)_{V+A}$	$Q_{10}^j = \frac{3}{2}(\bar{j}_a b_b)_{V-A} \sum_{q'} e_{q'} (\bar{q}'_b q'_a)_{V-A}$

where the $\mathcal{C}_i(\mu)$ contain terms of $\ln(M_W/\mu)$, which become large for $\mu = \mathcal{O}(m_b)$. Moreover, the operator mixing is responsible for the fact, that the renormalization constant becomes a 2×2 matrix,

$$\mathcal{Q}_i^{(0)} = Z_{ij} \mathcal{Q}_j \ . \tag{3.12}$$

For non-leptonic B decays contributions from tree and penguin topologies appear. Hence, the operator basis is much larger than in the simple example (3.9). From the unitary of the CKM triangle (2.52) one gets

$$V_{uj}^* V_{ub} + V_{cj}^* V_{cb} + V_{tj}^* V_{tb} = 0 \quad (j \in \{d, s\}) \ , \tag{3.13}$$

integrating out the top quark and the W-boson, the effective Hamiltonian can be written as [24]

$$\mathcal{H}_{\text{eff}} \sim \sum_{i=u,c} V_{ij}^* V_{ib} \left[\sum_{k=1}^{2} \mathcal{C}_k(\mu) \mathcal{Q}_k^{ij} + \sum_{k=3}^{10} \mathcal{C}_k(\mu) \mathcal{Q}_k^{j} \right] \ , \tag{3.14}$$

with the quark-flavour label $i = \{u, c\}$. The operators $\mathcal{Q}_k^{ij}$ can be divided in three classes: current-current, QCD penguin and electroweak (EW) penguin operators which are listed in Table 3.1. If the renormalization scale is $\mu = \mathcal{O}(m_b)$, the Wilson coefficients for the current-current operators will be $\mathcal{C}_1(\mu) = \mathcal{O}(10^{-1})$, $\mathcal{C}_2(\mu) = \mathcal{O}(1)$, and those of the penguin operators $\mathcal{O}(10^{-2})$ [85].
In the case of a not “heavy" top quark, the contributions from the EW penguins could be neglected in comparison to that one of the QCD penguins. Interesting EW penguin effects could be expected since the Wilson Coefficient $\mathcal{C}_9$ increased strongly with the

top quark mass m_t, and the impact of such EW penguin effects can be studied in several B decay channels, e.g. $B \to K\phi$ which are affected significantly or $B \to \pi\phi$ and $B_s \to \pi^0\phi$ which are even dominated by EW penguin topologies [87, 88].
For all B decays caused by the same quark-level transition, applied by the low-energy effective Hamiltonians discussed here, the differences between the various exclusive modes arise from the hadronic matrix elements of the relevant four-quark operators for a given decay class. Before the factorization of the hadronic matrix elements is discussed in more detail, the renormalization-group improved perturbation theory is briefly reviewed in the next subsection.

3.1.2. Renormalization-Group improved Perturbation Theory

As discussed before, in order to get the amplitudes of weak decays, at first, the amplitude in the full theory at a suitable - in principle high - scale for the present problem have to be calculated. The calculation yields the operators at this scale, hence, one is able to write down the relevant OPE. In the next step the operators have to be renormalized and the anomalous dimensions have to be evaluated, therefore by matching the full theory into the effective theory, the Wilson coefficients can be found, and no divergences would appear. Logarithms of the form $\ln(M_W^2/\mu_W^2)$ are canceled by that ones of the form $\ln(\mu_W^2/s)$ in the matrix elements $\langle \mathcal{Q}_i(\mu) \rangle$, and the μ dependence disappear. In order to calculate the matrix elements, done at a low scale, the μ scale has to run down from the high scale M_W to the lower scale m_b. Since the high and low energy scale in general are widely separated, $M \gg \mu$, powers of $\alpha_s \ln(M/\mu)$ rather than powers of α_s come into account, and these large logarithms have to be resummed to all orders by solving renormalization-group equations [83]. Generally this problem is handled by the renormalization-group improved perturbation theory which is shortly discussed in this subsection. An exhaustive discussion can be found in Refs. [83–85, 89].
Treating $\alpha_s \ln(M/\mu)$ as an $\mathcal{O}(1)$ parameter and $\alpha_s \ll 1$ in the following. From order to order, starting with the leading order (LO), next-to-leading order (NLO) and so on, one has to sum up terms of the Wilson coefficients,

$$\alpha_s^n \left[\ln\left(\frac{M}{\mu}\right)\right]^n \text{ (LO)}\,, \quad \alpha_s^n \left[\ln\left(\frac{M}{\mu}\right)\right]^{n-1} \text{ (NLO)}\,, \ \ldots \tag{3.15}$$

This resummation can be done by using the renormalization-group. For the present problem, the operators $\{\mathcal{Q}_i(\mu)\}$, $i = 1, 2, \ldots, n$, perform a basis which closes under

renormalization. The scale μ itself is unphysical and the physical amplitudes are scale independent implying

$$\frac{d}{d\ln\mu}\sum_{i=1}^{n}\mathcal{C}_i(\mu)\,\langle\mathcal{Q}_i(\mu)\rangle = 0\,. \tag{3.16}$$

Expanding the logarithmic derivative of the operator matrix elements in terms of the same basis operators,

$$\frac{d}{d\ln\mu}\langle\mathcal{Q}_i(\mu)\rangle \equiv -\sum_{j=1}^{n}\gamma_{ij}(\mu)\langle\mathcal{Q}_i(\mu)\rangle\,, \tag{3.17}$$

with the "anomalous dimensions" $\boldsymbol{\gamma}$. Using Eqs. (3.16) and (3.17) and keeping in mind that the operators are linearly independent, the renormalization-group equation can be written as

$$\frac{d}{d\ln\mu}\mathcal{C}_i(\mu) - \sum_{i=1}^{n}\mathcal{C}_i(\mu)\gamma_{ij}(\mu) = 0\,. \tag{3.18}$$

Because of $\boldsymbol{\gamma}(\mu) = \boldsymbol{\gamma}(\alpha_s(\mu))$, the variables from $\ln\mu$ to $\alpha_s(\mu)$ changed and one ends up with

$$\frac{d}{d\alpha_s(\mu)}\vec{\mathcal{C}}(\mu) = \frac{\boldsymbol{\gamma}^T\left(\alpha_s(\mu)\right)}{\beta\left(\alpha_s(\mu)\right)}\,\vec{\mathcal{C}}(\mu)\,, \tag{3.19}$$

where $\beta = d\alpha_s(\mu)/d\ln\mu$ is the QCD β-function. A simple example is given in the case of a single Wilson coefficient, i.e. no mixing is present. One gets by expanding all terms to leading order

$$\begin{aligned}&\boldsymbol{\gamma}(\alpha_s) = \boldsymbol{\gamma}_0\frac{\alpha_s}{4\pi} + \mathcal{O}(\alpha_s)\,, \quad \beta(\alpha_s) = -2\alpha_s\left[\beta_0\frac{\alpha_s}{4\pi} + \mathcal{O}(\alpha_s^2)\right]\,,\\ &\mathcal{C}(M_W) = 1 + \mathcal{O}(\alpha_s)\,.\end{aligned} \tag{3.20}$$

Performing the calculation one finds for the Wilson coefficients [83]

$$\mathcal{C}(M_W) = 1 + \sum_{n=1}^{\infty} c_n\left(\frac{\alpha_s(M_W)}{4\pi}\right)^n\,, \tag{3.21}$$

yielding the structure of Eq. (3.15). For the operators $\mathcal{Q}_{1,2}$, which are discussed in the previous subsection, at first order in α_s the anomalous dimension is given by [85]

$$\boldsymbol{\gamma}(\alpha_s) = \frac{\alpha_s}{4\pi}\begin{pmatrix} -\frac{6}{N} & 6 \\ 6 & -\frac{6}{N}\end{pmatrix}\,. \tag{3.22}$$

With this preparation one is able to construct the weak effective Hamiltonian.

3.1.3. Weak Effective Hamiltonian

With the essential elements discussed in the previous parts, the standard model weak effective Hamiltonian (3.14) for $|\Delta B| = 1$, $\Delta C = \Delta U = 0$ transitions can be written as [88]

$$\mathcal{H}_{\text{eff}} = \mathcal{H}_{\text{eff}}(\Delta B = -1) + \mathcal{H}_{\text{eff}}(\Delta B = -1)^{\dagger} , \tag{3.23}$$

where

$$\mathcal{H}_{\text{eff}}(\Delta B = -1) = \frac{G_F}{\sqrt{2}} \left[\sum_{i=u,c} V_{iq}^* V_{ib} \left\{ \sum_{k=1}^{2} \mathcal{Q}_k^{iq} \mathcal{C}_k(\mu) + \sum_{k=3}^{10} \mathcal{Q}_k^{q} \mathcal{C}_k(\mu) \right\} \right] , \tag{3.24}$$

with the renormalization scale $\mu = \mathcal{O}(m_b)$, and the flavour labels $q \in \{d, s\}$ are associated with $b \to d$ and $b \to s$ transitions, respectively. The four-quark operators $\mathcal{Q}_k^{iq}$ in (3.24) are listed in Table 3.1. Going beyond the leading logarithm, one finds for the renormalization scheme independent Wilson coefficients at the scale $\mu = M_W$ [87],

$$\mathcal{C}_1(\mu) = \mathcal{O}(\alpha_s(\mu)) + \mathcal{O}(\alpha) , \quad \mathcal{C}_2(\mu) = 1 + \mathcal{O}(\alpha_s(\mu)) + \mathcal{O}(\alpha) , \tag{3.25}$$

$$\mathcal{C}_3(\mu) = -\frac{\alpha_s(\mu)}{4\pi} \left[\frac{E(x_t)}{6} - \frac{\alpha}{\alpha_s(\mu)} \frac{4B(x_t) + 4C(x_t)}{3\sin^2\theta_W} + \frac{1}{9} \log\left(\frac{\mu^2}{M_W^2} \right) - \frac{5}{27} \right] , \tag{3.26}$$

$$\mathcal{C}_4(\mu) = -\mathcal{C}_5(\mu) = \mathcal{C}_6(\mu) = \frac{\alpha_s}{4\pi} \left[\frac{E(x_t)}{2} + \frac{1}{3} \log\left(\frac{mu^2}{M_W^2} \right) - \frac{5}{9} \right] , \tag{3.27}$$

$$\mathcal{C}_7(\mu) = \frac{\alpha}{6\pi} \left[4C(x_t) + D(x_t) + \frac{4}{9} \ln\left(\frac{\mu^2}{M_W^2} \right) - \frac{20}{27} \right] \tag{3.28}$$

$$\mathcal{C}_8(\mu) = \mathcal{C}_{10}(\mu) = 0 , \tag{3.29}$$

$$\mathcal{C}_9(\mu) = \frac{\alpha}{6\pi} \left[4C(x_t) + D(x_t) + \frac{10B(x_t) - 4C(x_t)}{\sin^2\theta_W} + \frac{4}{9} \ln\left(\frac{\mu^2}{M_W^2} \right) - \frac{20}{27} \right] , \tag{3.30}$$

where $x_t = \frac{m_t^2}{M_W^2}$ and the Inami-Lim functions are [90]

$$B(x) = \frac{1}{4} \left[\frac{x}{1-x} + \frac{x \log x}{(x-1)^2} \right] , \tag{3.31}$$

$$C(x) = \frac{x}{8}\left[\frac{x-6}{x-1} + \frac{3x+2}{(x-1)^2}\log x\right] \tag{3.32}$$

$$D(x) = -\frac{4}{9}\log x - \frac{19x^3-25x^2}{36(x-1)^3} + \frac{x^2(5x^2-2x-6)}{18(x-1)^4}\log x\ , \tag{3.33}$$

$$E(x) = -\frac{2}{3}\log x + \frac{x(18-11x-x^2)}{12(1-x)^3} + \frac{x^2(15x-16x+4x^2)}{6(1-x)^4}\log x\ . \tag{3.34}$$

Since the calculation is performed at the scale $\mu = M_W$, with full W and Z propagators and internal top-quark exchanges, the functions (3.31)–(3.34) represent the contributions of box diagrams, Z penguins, photon penguins and gluon penguins, respectively [91]. The coefficients (3.25)–(3.30) depend on the top quark mass. For larges values of the top-quark, the magnitude of the electroweak penguin coefficient $\mathcal{C}_9(m_b)$ becomes comparable to the coefficients of the QCD penguin operators $\mathcal{Q}_3$ and $\mathcal{Q}_5$. In penguin-induced B-meson decays through the operator $\mathcal{Q}_9$ large electroweak penguin effects and a significant top quark mass dependence could arise, e.g. in $B^- \to K^-\Phi$ transition. However, the electroweak penguin effects are very small for the decay $B^- \to \pi^-\bar{K}^{0*}$, for comprehensive discussions of this topic see Refs. [84, 85, 87, 88].

Classification of the Decays

The non-leptonic decays of the B-mesons can be classified by their decay topologies: the decays are mediated by the transition $b \to q_1\bar{q}_2 d(s)$, $q_1, q_2 \in \{u, d, c, s\}$ at quark level. As discussed, one can distinguish between two topologies of decays, tree-diagram-like and penguin topologies. In Fig. 3.2 the leading order Feynman diagrams for non-leptonic B decays are shown.
The final states can be classified by their flavour content as following: if $q_1 \neq q_2 \in \{u, c\}$ only tree diagrams, whereas if $q_1 = q_2 \in \{u, c\}$ tree and penguin diagrams are contributing, and the contribution in the case $q_1 = q_2 \in \{d, s\}$ will come from penguin diagrams.
In the next part of this section, the matrix elements which appear in Eq. (3.8) will be discussed in more detail.

3.2. Hadronic Matrix Element

As discussed in Sec. 3.1.1 the effective weak Hamiltonian contain coefficients of the local operators $\mathcal{Q}_i$ which are renormalized by the strong-interaction corrections. Us-

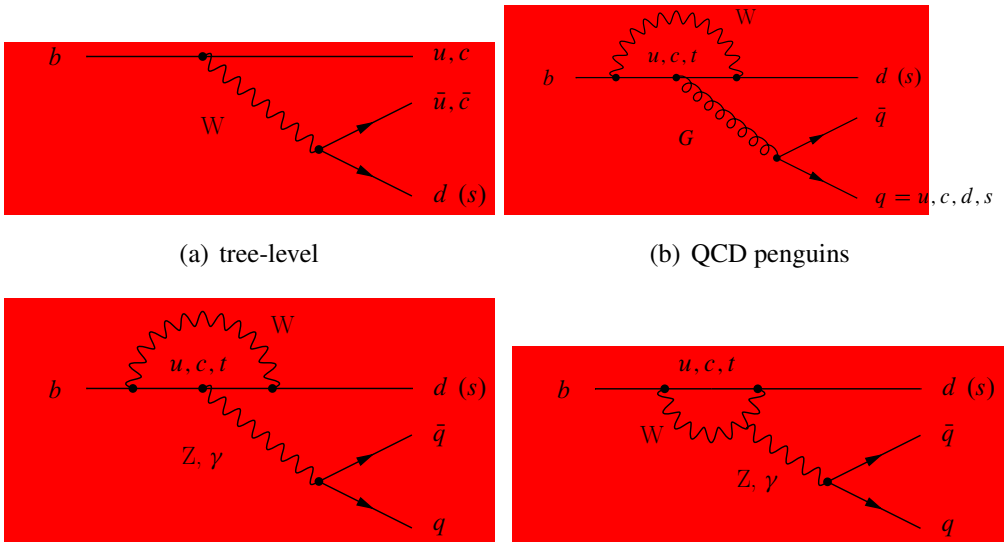

(a) tree-level

(b) QCD penguins

(c) electroweak penguins

Figure 3.2.: Leading order Feynman diagrams for non-leptonic B decays [24].

ing the concept of OPE the short and long distance physics can be *factorized*; the Wilson coefficients contain the short distance effects, depending on the large scale m_b, whereas the long distance physics is contained by the matrix elements of the operators. Within this work, $B \to D$ decays are issues at stake, the factorization of the $B \to D$ form factor leads to the *Isgur-Wise function*, which is a non-perturbative object, see. Sec. 3.3.2 for details.

The non-leptonic decay amplitudes are characterized by a two-meson final state, and factorization scheme has to reflect this physical property. Since working in the *heavy-quark* limit, these final states can be divided in a "light" meson and a "heavy" meson state. In the first case the mass remains finite, whereas in the second case the mass scales with m_b. However, the ratio m/m_b stays fixed [92, 93]. In this limit, the charm and the spectator quark form the final heavy mesons without difficulty, because if the charm quark is relatively heavy, its velocity will not be large. On the other hand, the light quark pair formed by the weak interaction vertex will be energetic and in a colour-singlet mode, leaving the interaction region without a strong interaction. This is Bjorken's colour transparency argument [94]. The described physical picture leads to an naïve factorization of the matrix element for the weak decays $\bar{B} \to M_1 M_2$, schematically written as [95–99]

$$\langle M_1 M_2 | (\bar{q}_1 q_2)(\bar{q}_3 b) | \bar{B} \rangle \xrightarrow{\text{fact}} \langle M_2 | (\bar{q}_1 q_2) | 0 \rangle \langle M_1 | (\bar{q}_3 b) | \bar{B} \rangle \sim f_{M_2} \cdot F^{\bar{B} \to M_1} , \tag{3.35}$$

with the decay constant f_{M_2} and the form factor $F^{\bar{B}\to M_1}$. This factorization provides in many cases correct order of magnitude of branching fractions, but it cannot predict e.g. direct CP asymmetries because of the assumption of no strong rescattering. Scale as well as renormalization scheme dependence is absent in the matrix element, because it is expressed in terms of observables. In order to solve these disadvantages the naïve factorization is superseded by *QCD factorization* [93, 100–102], providing a formalism to calculate the amplitudes at a leading order of a $\Lambda_{\mathrm{QCD}}/m_b$ expansion. For the decay $\bar{B} \to M_1 M_2$, where M_1 is either a heavy or a light meson and M_2 is light, in QCD factorization the transition amplitude is given by

$$A(\bar{B} \to M_1 M_2) = \text{“naïve factorization”} \times [1 + \mathcal{O}(\alpha_s) + \mathcal{O}(\Lambda_{\mathrm{QCD}}/m_b)] \,. \quad (3.36)$$

The $\mathcal{O}(\alpha_s)$ terms are systematically accessible, whereas the main limitation originates from the $\mathcal{O}(\Lambda_{\mathrm{QCD}}/m_B)$ terms [24], and the transition matrix of an operator $\mathcal{Q}_i$ in the weak effective Hamiltonian is in the case of M_1 and M_2 are both light,

$$\begin{aligned}\langle M_1 M_2|\mathcal{Q}_i|\bar{B}\rangle = &\sum_j F_j^{\bar{B}\to M_1}(m_2^2)\int_0^1 du\; T_{ij}^I(u)\Phi_{M_2}(u) + (M_1 \leftrightarrow M_2)\\ &+ \int_0^1 d\xi\; du\; dv\; T_i^{II}(\xi,u,v)\Phi_B(\xi)\Phi_{M_1}(v)\Phi_{M_2}(u)\,, \end{aligned} \quad (3.37)$$

and for M_1 is heavy and M_2 is light,

$$\langle M_1 M_2|\mathcal{Q}_i|\bar{B}\rangle = \sum_j F_j^{\bar{B}\to M_1}(m_2^2)\int_0^1 du\; T_{ij}^I(u)\Phi_{M_2}(u)\,. \quad (3.38)$$

Here $T_{ij}^i(u)$ and $T_i^{II}(\xi,u,v)$ are perturbatively calculable hard-scattering functions, $F_j^{\bar{B}\to M_{1,2}}$ is the $\bar{B} \to M_{1,2}$ form factor, and $\Phi_X(u)$ is the light-cone distribution amplitude (LCDA) for the quark-antiquark Fock state of meson X. Finally, ξ, u and v are longitudinal momentum fractions. Note that the Eqs. (3.37) and (3.38) hold true to leading order in $\Lambda_{\mathrm{QCD}}/m_b$, but to all orders at α_s. In Fig. 3.3 a graphical interpretation of these equations is depicted. Calculations of the hard-scattering kernels at NLO can be found in [93, 101, 102], and at NNLO in [103–109]. The kernel T_i^I starts at $\mathcal{O}(\alpha_s^0)$, and T_i^{II} at $\mathcal{O}(\alpha_s^1)$. At higher orders in α_s, T_i^I contains “non-factorizable” corrections from hard gluon exchange or light-quark loops. T_i^{II} contains hard “nonfactorizable” interactions involving the spectator quark.

In Fig. 3.4 the relevant contributions to these kernels at next-to-leading order are shown. For the B-meson transitions governed by Eq. (3.37) where the spectator quark

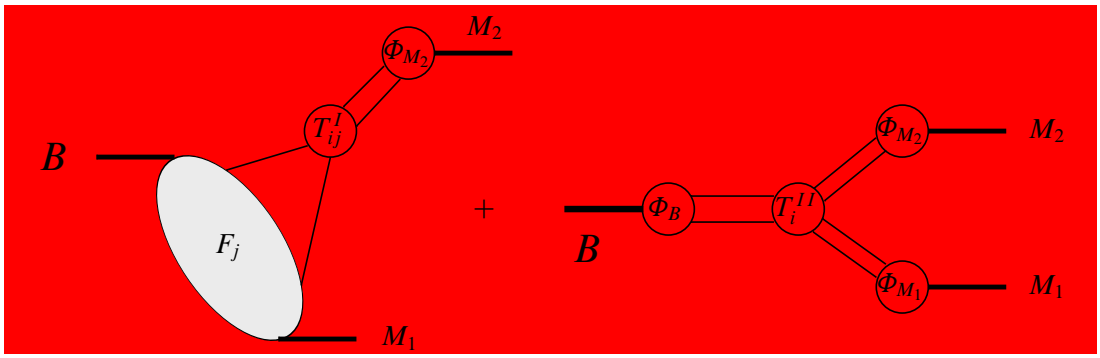

Figure 3.3.: Graphical representation of the factorization formulae (3.37) and (3.38), [93].

can only go to one of the light final-state mesons, the second form-factor term on the right side of Eq. (3.37) - second process in Fig. 3.3 - is power-suppressed. For the decays $\bar{B} \to M_1 M_2$, where M_1 is heavy and M_2 is light, described by Eq. (3.37), a simplification can achieved since the spectator quark goes to the heavy meson. The second term accounting for hard interactions with the spectator quark, is power-suppressed in the heavy-quark limit. Whereas if the spectator quark goes to the light meson factorization does not hold because the heavy meson is neither fast nor small. However, such amplitudes are power-suppressed in the heavy-quark limit [93].
QCD factorization is a powerful tool for the description of non-leptonic B transitions. However, the QCDF is from phenomenologically nature: in the transition am-

(a) "Non-factorizable" vertex corrections.

(b) Left panel: Diagram with a "penguin" contraction. Right panel: contribution from the chromodynamic dipol operator in the weak effective Hamiltonian.

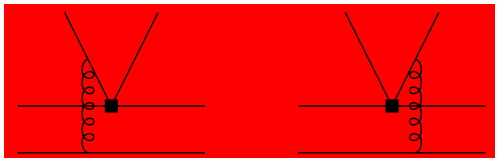

(c) "Non-factorizable" spectator interactions.

Figure 3.4.: $\mathcal{O}(\alpha_s)$ corrections to the kernels T_i^I - subfigures (a) and (b) - and T_i^{II} - subfigure (c) [93] as explained in the text.

plitudes non-perturbative quantities appear, which are simpler than the hadronic matrix elements. These quantities are either related to universal properties of a single mesons state, or describe the $B \to M_1 M_2$ transition matrix element of a local current, parametrized by a form factor. The quantities can be depicted from experimental data or by other theoretical techniques like lattice QCD or QCD sum rules. However, computation of the matrix element in lattice QCD, form factors and light-cone distribution amplitudes is very difficult and containing significant systematic errors at present. In Chap. 4 the QCD sum rule approach for $B \to D^{(*)}$ transitions is presented. Further details about QCD factorization in B transitions can be found in [93, 101, 102]. In order to discuss the $B \to D$ transitions in more detail, the non-perturbative parameters, light-cone distribution amplitudes (Sec. 3.2.1) and form factors (Sec. 3.2.2), are presented in the following part of this section.

3.2.1. Light-Cone Distribution Amplitudes

The light-cone distribution amplitudes appearing in the factorization formulae (3.37) and (3.38) are studied in this section in more detail. The definition of the LCDA's are defined as the ones in Refs. [110, 111]. Here only leading two particle twist (twist-2) and the twist-3 LCDA's are represented. Following Refs. [111, 112], the twist-2 and -3 light-cone distribution amplitudes for the pseudoscalar (P) mesons are

$$\begin{aligned}
\left\langle P\left(p'\right)\left|\bar{q}(y)\gamma_\mu\gamma_5 q'(y)\right|0\right\rangle\big|_{(x-y)^2=0} &= -if_P p'_\mu \int_0^1 du\, e^{i(\bar{u}p'\cdot x+up'\cdot y)}\Phi_P(u,\mu)\,, \\
\left\langle P\left(p'\right)\left|\bar{q}(y)i\gamma_5 q'(x)\right|0\right\rangle\big|_{(x-y)^2=0} &= f_P\mu_P \int_0^1 du\, e^{i(\bar{u}p'\cdot x+up'\cdot y)}\Phi_p(u,\mu)\,, \\
\left\langle P\left(p'\right)\left|\bar{q}(y)\sigma_{\mu\nu}\gamma_5 q'(x)\right|0\right\rangle\big|_{(x-y)^2=0} & \\
&= if_P\mu_P\left(p'_\mu z_\nu - p'_\nu z_\mu\right)\int_0^1 du\, e^{i(\bar{u}p'\cdot x+up'\cdot y)}\frac{\Phi(u,\mu)}{6}\,, \qquad (3.39)
\end{aligned}$$

with $\bar{u} \equiv 1-u$, $z \equiv y-x$, $\mu_p = m_P^2/(m_q+m_{q'})$, f_P is the decay constant, and μ is the renormalization scale of the light-cone operator. The leading-twist light-cone distribution amplitude is $\Phi_P(u,\mu)$, conventionally expanded in Gegenbauer polynomials,

$$\Phi_P(u,\mu) = 6u\bar{u}\left[1+\sum_{n=1}^{\infty}\alpha_n^P(\mu)C_n^{3/2}(u-\bar{u})\right]\,, \qquad (3.40)$$

where $\alpha_n^P(\mu)$ are the Gegenbauer moments and $C_n^{(3/2)}$ are the Gegenbauer polynomials; for a derivation of these equations, see, e.g. Ref. [113]. The coefficients $\alpha_n^P(\mu)$ are multiplicatively renormalizable. Neglecting three-particle contributions, the twist-3 two-particle amplitudes are

$$\Phi_p(u) = 1\,, \quad \frac{\Phi_\sigma'(u)}{6} = \bar{u} - u\,, \quad \frac{\Phi_\sigma(u)}{6} = u\bar{u}\,. \tag{3.41}$$

All distribution amplitudes (3.39) are normalized to 1, and can be combined to

$$\begin{aligned}\left\langle P\left(p'\right)\left|\bar{q}_\alpha(y)q'_\delta(x)\right|0\right\rangle =& \frac{if_P}{4}\int_0^1 du\, e^{i(\bar{u}p'\cdot x+up'\cdot y)}\Big\{\not{p}'\gamma_5\Phi_P(u,\mu)\\ &-\mu_P\gamma_5\left(\Phi_p(u,\mu)-\sigma_{\mu\nu}p'^\mu z^\nu\frac{\Phi_\sigma(u,\mu)}{6}\right)\Big\}_{\delta\alpha}\,.\end{aligned} \tag{3.42}$$

The asymptotic distribution amplitude is defined as the limit, in which renormalization scale is sent to infinity, one finds

$$\phi_X(u,\mu) \overset{\mu\to\infty}{=} 6u\bar{u}\,, \quad X\in\{P,p,\sigma\}\,. \tag{3.43}$$

For light vector mesons (V) one has to regard the polarization tensor, being separated in longitudinal ($\|$) and transverse ($\perp$) projections [114],

$$\varepsilon^*_{\|\mu} \equiv \frac{\boldsymbol{\varepsilon}^*\cdot z}{P'\cdot z}\left(P'_\mu - \frac{m_V^2}{P'\cdot z}z_\mu\right)\,, \quad \varepsilon^*_{\perp\mu} = \varepsilon^*_\mu - \varepsilon^*_{\|\mu}\,, \tag{3.44}$$

Here P' is the meson momentum with $P'^2 = m_V^2$. With the light-like vector $p'_\mu = P'_\mu - m_V^2 z_\mu/(2P'\cdot z)$ the twist-2 and -3 chiral-even light-cone distribution amplitudes are

$$\begin{aligned}&\left\langle V(P',\boldsymbol{\varepsilon}^*)\left|\bar{q}(y)\gamma_\mu q'(x)\right|0\right\rangle\\ &\quad= -if_V m_V\int_0^1 du\, e^{i(\bar{u}p'\cdot x+up'\cdot y)}\left\{p'_\mu\frac{\boldsymbol{\varepsilon}^*\cdot z}{p'\cdot z}\Phi_\|(u,\mu)+\varepsilon^*_{\perp\mu}g_\perp^{(v)}(u,\mu)\right\}\,,\\ &\left\langle V(P',\boldsymbol{\varepsilon}^*)\left|\bar{q}(y)\gamma_\mu\gamma_5 q'(x)\right|0\right\rangle\\ &\quad= if_V m_V\epsilon_{\mu\nu\rho\sigma}\varepsilon^{*\nu}p'^\rho z^\sigma\int_0^1 du\, e^{i(\bar{u}p'\cdot x+up'\cdot y)}\frac{g_\perp^{(a)}(u,\mu)}{4}\,,\end{aligned} \tag{3.45}$$

with the vector meson decay constant f_V. The chiral-odd light-cone distribution amplitudes are given by

$$\begin{aligned}
&\left\langle V(P',\boldsymbol{\varepsilon}^*)\middle|\bar{q}(y)\sigma_{\mu\nu}q'(x)\middle|0\right\rangle = -f_\perp \int_0^1 du\; e^{i(\bar{u}p'\cdot x + up'\cdot y)} \\
&\quad\times\left\{\left(\varepsilon^*_{\perp\mu}p'_\nu - \varepsilon^*_{\perp\nu}p'_\mu\right)\Phi_\perp(u,\mu) + \frac{m_V^2\,\boldsymbol{\varepsilon}^*\cdot z}{(p'\cdot z)^2}\left(p'_\mu z_\nu - p'_\nu z_\mu\right)h_\parallel^{(t)}(u,\mu)\right\}, \\
&\left\langle V(P',\boldsymbol{\varepsilon}^*)\middle|\bar{q}(y)q'(x)\middle|0\right\rangle = -f_\perp m_V^2\,\boldsymbol{\varepsilon}^*\cdot z\int_0^1 du\; e^{i(\bar{u}p'\cdot x + up'\cdot y)}\frac{h_\parallel^{(s)}(u,\mu)}{2}\,,
\end{aligned} \tag{3.46}$$

where $f_\perp$ is the - scale-dependent - transverse decay constant [114]. As in the case of the pseudoscalar mesons one combined (3.45) and (3.46), yielding

$$\begin{aligned}
&\left\langle V(P',\boldsymbol{\varepsilon}^*)\middle|\bar{q}_\alpha(y)q'_\delta(x)\middle|0\right\rangle \\
&\qquad= -\frac{i}{4}\int_0^1 du\; e^{i(\bar{u}p'\cdot x + up'\cdot y)}\left\{f_V m_V\left(p'_\mu\frac{\boldsymbol{\varepsilon}^*\cdot z}{p'\cdot z}\Phi_\parallel(u,\mu) + \not{\varepsilon}^*_\perp g_\perp^{(v)}(u,\mu)\right.\right. \\
&\qquad\quad\left. + \epsilon_{\mu\nu\rho\sigma}\varepsilon^{*\mu}p'^\rho z^\sigma\gamma^\mu\gamma_5\frac{g_\perp^{(a)}(u,\mu)}{4}\right) + f_\perp\left(\not{\varepsilon}^*_\perp\not{p}'\Phi_\perp(u,\mu)\right. \\
&\qquad\quad\left.\left. - i\,\frac{m_V^2\,\varepsilon\cdot z}{(p'\cdot z)^2}\sigma_{\mu\nu}p'^\mu z^\nu h_\parallel^{(t)}(u,\mu) - i m_V^2\,\boldsymbol{\varepsilon}^*\cdot z\frac{h_\parallel^{(s)}(u,\mu)}{2}\right)\right\}_{\delta\alpha}.
\end{aligned} \tag{3.47}$$

Finally, by the Wandzura-Wilczek-type relations the twist-3 distribution amplitudes are related to the twist-2 ones [114], for the chiral-even amplitudes these relations are

$$\begin{aligned}
g_\perp^{(v)}(u,\mu) &= \frac{1}{2}\left[\int_0^u dv\;\frac{\Phi_\parallel(u,\mu)}{\bar{v}} + \int_u^1 dv\;\frac{\Phi_\parallel(u,\mu)}{v}\right] + \dots\,, \\
g_\perp^{(a)}(u,\mu) &= 2\left[\bar{u}\int_0^u dv\;\frac{\Phi_\parallel(u,\mu)}{\bar{v}} + \int_u^1 dv\;\frac{\Phi_\parallel(u,\mu)}{v}\right] + \dots\,,
\end{aligned} \tag{3.48}$$

and the chiral-odd ones are

$$\begin{aligned}
h_\parallel^{(t)}(u,\mu) &= (2u-1)\left[\int_0^u dv\;\frac{\Phi_\perp(u,\mu)}{\bar{v}} - \int_u^1 dv\;\frac{\Phi_\perp(u,\mu)}{v}\right] + \dots\,, \\
h_\parallel^{(s)}(u,\mu) &= 2\left[\bar{u}\int_0^u dv\;\frac{\Phi_\perp(u,\mu)}{\bar{v}} + u\int_u^1 dv\;\frac{\Phi_\perp(v,\mu)}{v}\right] + \dots\,.
\end{aligned} \tag{3.49}$$

Formally the twist-3 light-cone distribution amplitudes contribute at $\mathcal{O}(1/m_b)$.
In non-leptonic B decays the light-cone distribution amplitudes arise in the calculation of the hadronic matrix elements in QCDF. The quark and antiquark pair of the outgoing (light) meson with momentum p' have the assigned momenta up' and $\bar{u}\,p'$, respectively. Calculation of the on-shell amplitude in momentum space one finds a term of the form

$$\bar{u}_{\alpha a}\left(up'\right)\Gamma(u,\dots)_{\alpha\beta,ab,\dots}v_{\beta b}\left(\bar{u}\,p'\right)\ . \tag{3.50}$$

For pseudoscalar and, with modifications, for vector mesons, this term between the vacuum and mesons state has to be replaced by

$$\frac{if_P}{4N_C}\int_0^1 du\ \Phi_P(u)(\not{p}'\gamma_5)_{\beta\alpha}\Gamma(u,\dots)_{\alpha\beta,aa,\dots}\ , \tag{3.51}$$

where N_C refers to the numbers of colours, and it is a manifestation of factorization, requiring a strict separation of short- and long-distance distributions [86, 93].
More aspects about light-cone distribution amplitudes can be found in the literature, see, e.g. Refs. [111, 114]. Here the light-cone distribution amplitudes of B-mesons are discussed in more detail. The third term of the factorization formula (3.37) is the hard spectator interaction term, only within this term, the B-mesons light-cone distribution amplitude appears. The spectator quark in the B-meson is not energetic in the B-meson rest frame, its assigned momentum l is of order Λ_{QCD}. At $\mathcal{O}(\alpha_s)$ the hard spectator interaction amplitude depends only on $p'\cdot l$ at leading order in $1/m_b$, where p' is the momentum of the light meson, picking up the the spectator quark.
The B-meson is described at leading-power in $1/m_b$ by two scalar wave functions [115]. In the case of negligible transverse momentum $l_\perp$ of the spectator quarks, one finds for the most general decomposition of the B-meson leading-power light-cone distribution amplitude,

$$\begin{aligned}&\langle 0|\bar{q}_\alpha(z)[\dots]b_\beta(0)|\bar{B}_d(p)\rangle\big|_{z_+=z_\perp=0}\\ &\quad=-\frac{if_B}{4}[(\not{p}+m_b)\gamma_5]_{\beta\gamma}\int_0^1 d\xi\ e^{-i\xi p_+z_-}\left[\Phi_{B_1}(\xi)+\not{n}_-\Phi_{B_2}(\xi)\right]_{\gamma\alpha}\ .\end{aligned} \tag{3.52}$$

Here $n_\pm^\mu=(1,0,0,\mp1)$ are the two light-cone vectors with the properties $n_\pm^2=0$ and $n_+\cdot n_-=2$, and the subscripts $(+,-,\perp)$ refer to the light-cone decomposition of any vector a^μ such that $a^\mu=\frac{1}{2}(a_+n_-^\mu+a_-n_+^\mu)+a_\perp^\mu$, where $a_\pm=a\cdot n_\pm$. The matrix

element has to be gauge invariant, therefore the exponential has to be path-ordered, this is denoted by the dots in Eq. (3.52). In a hard spectator scattering interaction at leading order the hard spectator scattering contribution depends only on the light-cone distribution amplitude Φ_{B_1}. This dependence can be expressed by the hadronic parameter $\lambda_B = \mathcal{O}(\Lambda_{\mathrm{QCD}})$, which is defined as [100]

$$\int_0^1 d\xi \, \frac{\Phi_B(\xi)}{\xi} \equiv \frac{m_B}{\lambda_B} \, . \tag{3.53}$$

As mentioned before in the QCD sum rule approach light-cone distribution amplitudes play an important rôle. The discussion of all aspects of B-meson light-cone distribution amplitudes is beyond the scope of this work. Here, only the ones for $B \to D^{(*)}$ transitions are relevant, presented in App. A. For an exhaustive discussion of B-meson light-cone distribution amplitudes see, e.g., Refs. [93, 100, 101, 116].

3.2.2. Form Factors

In this section the definitions for the decay constants and form factors, which appear in the factorization formulae (3.37) and (3.38), are given.
For pseudoscalar mesons (P) with 4-momentum p' the decay constant f_P is defined as

$$\left\langle P\left(p'\right) \left| \bar{q}\gamma_\mu\gamma_5 \right| 0 \right\rangle \equiv -if_P\, p'_\mu \, , \tag{3.54}$$

and for vector mesons (V), the longitudinal ($f_V^{\parallel}$) and transverse ($f_V^{\perp}$) decay constants are

$$\left\langle V\left(p', \boldsymbol{\varepsilon}^*\right) \left| \bar{q}\gamma_\mu q' \right| 0 \right\rangle \equiv -if_V^{\parallel} m_V \varepsilon^*_\mu \, , \tag{3.55}$$

$$\left\langle V\left(p', \boldsymbol{\varepsilon}^*\right) \left| \bar{q}\sigma_{\mu\nu} q' \right| 0 \right\rangle \equiv -if_V^{\perp} \left(p'_\mu \varepsilon^*_\nu - p'_\nu \varepsilon^*_\mu\right) \, , \tag{3.56}$$

respectively. Using the identity $\partial_\mu(\bar{q}\gamma^\mu\gamma_5 q') = i(m_q + m_{q'})\bar{q}\gamma_5 q'$, derived by applying the Dirac equation (2.21) for the quark fields, one finds for the pseudoscalar current

$$\left\langle P\left(p'\right) \left| \bar{q}\gamma_5 q' \right| 0 \right\rangle = \frac{if_P m_P^2}{m_q + m_{q'}} \, . \tag{3.57}$$

The scalar matrix element is $\langle V\left(p', \boldsymbol{\varepsilon}^*\right) |\bar{q}q'|0\rangle \equiv 0$, because it depends only on $p'\cdot\boldsymbol{\varepsilon}^*$, with respect to Eq. (3.44). The origin of the form factors is the decomposition of the matrix elements

$$\langle M\left(p'\right) |\bar{q}\Gamma b| \bar{B}(p)\rangle \, , \tag{3.58}$$

with $M \in \{P, V\}$ and Γ can be any irreducible Dirac matrix[2]. For $\bar{B} \to P$ decays the form factors are defined by the following Lorentz decompositions of bilinear quark (2.20) current matrix elements [112, 117]

$$\begin{aligned}\left\langle P\left(p'\right)|\bar{q}\gamma^{\mu}b|\,\bar{B}(p)\right\rangle =& F_{+}^{\bar{B}\to P}\left(q^2\right)\left[\left(p+p'\right)^{\mu}-\frac{m_B^2-m_P^2}{q^2}q^{\mu}\right]\\ &+F_0^{\bar{B}\to P}\left(q^2\right)\frac{m_B^2-m_P^2}{q^2}q_{\mu}\,,\end{aligned} \tag{3.59}$$

with the momentum transfer $q^{\mu} = (p - p')^{\mu}$. The $F_{+}^{\bar{B}\to P}(q^2)$ term vanish when it is contracted with the momentum transfer. As before, using the Dirac equation (2.21) one gets the identity $\partial_{\mu}(\bar{q}\gamma^{\mu}b) = i(m_q - m_b)\bar{q}b$, implying for the scalar current

$$\left\langle P\left(p'\right)|\bar{q}b|\,\bar{B}(p)\right\rangle = F_0^{\bar{B}\to P}\left(q^2\right)\frac{m_B^2-m_P^2}{m_b-m_q}\,. \tag{3.60}$$

The pole at $q^2 = 0$ is spurious, because it is eliminated by the coincidence $F_{+}^{\bar{B}\to P}(0) \equiv F_0^{\bar{B}\to P}(0)$ of the form factors.

For the $\bar{B} \to V$ transitions the form factors for the vector and axial vector current are defined as

$$\left\langle V\left(p',\boldsymbol{\varepsilon}^*\right)\middle|\bar{q}\gamma^{\mu}b\middle|\bar{B}(p)\right\rangle \equiv \frac{2iF_0^{\bar{B}\to V}}{m_B+m_V}\epsilon^{\mu\nu\alpha\beta}\varepsilon_{\nu}^*p'_{\alpha}p_{\beta}\,, \tag{3.61}$$

$$\begin{aligned}&\left\langle V\left(p',\boldsymbol{\varepsilon}^*\right)\middle|\bar{q}\gamma^{\mu}\gamma_5 b\middle|\bar{B}(p)\right\rangle\\ &\quad\equiv 2m_V F_0^{\bar{B}\to V}\left(q^2\right)\frac{\boldsymbol{\varepsilon}^*\cdot q}{q^2}q^{\mu}+(m_B+m_V)F_1^{\bar{B}\to V}\left(q^2\right)\left[\varepsilon^{*\mu}-\frac{\boldsymbol{\varepsilon}^*\cdot q}{q^2}q^{\mu}\right]\\ &\qquad-F_2^{\bar{B}\to V}\left(q^2\right)\frac{\boldsymbol{\varepsilon}^*\cdot q}{m_B+m_V}\left[p^{\mu}+p'^{\mu}-\frac{m_B^2-m_V^2}{q^2}q^{\mu}\right]\,,\end{aligned} \tag{3.62}$$

respectively, where the sign convention $\epsilon^{0123} = -1$ is used. Here, the form factors are noted in the general form $F_j^{\bar{B}\to M}$, because of the universality of the Lorentz decompositions. In Sec. 3.3.2, where the $B \to D^{(*)}$ decays are discussed in more detail, the common notation in literature for the form factors is used. In this work, the focus lies on the $\bar{B} \to M$ transitions, for completeness, the $B \to VV$ transitions are discussed, e.g., in Refs. [118–120].

For further studies of weak decay form factors one needs some implications from the heavy-quark effective theory, which is recapitulated in the next section.

[2] see Sec. 2.1.1 for details.

3.3. Heavy-Quark Effective Theory

An essential ingredients for the understanding of weak decay form factors is the heavy-quark effective theory. In this section the basic formalism, and its application for $B \to M$, $M \in \{P, V\}$, decays is reviewed. Heavy-quark effective theory itself is a kind of an effective field theory. The basic idea is, that in hadronic systems containing a single heavy-quark Q with mass $m_Q \gg \Lambda_{\mathrm{QCD}}$, additional symmetries appear, which are not present in the full QCD Lagrangian (2.42). This heavy quark is at leading approximation considered as a static source of the gluon field with a typical size of order $\Lambda_{\mathrm{QCD}}^{-1}$. HQET provide techniques to include $1/m$ corrections systematically in perturbation theory, and the additional symmetries can be used to obtain relations among heavy hadron form factors, but such simplified problems are unsolvable in QCD. Lattice simulations or sum rule approaches have to be used to obtain quantitative results.
The heavy-quark effective theory is a well-established theory [121–127]. For further reading, there are many reviews [92, 128, 129], lecture notes [130–132], and textbook material [34, 89, 133, 134], about heavy-quark effective theory and heavy-quark symmetries available.

3.3.1. Heavy-Quark Symmetry

The additional symmetries which appear, and not present in full QCD, are the heavy-flavour symmetry (HFS), and in the heavy-quark limit, $m \to \infty$, the spin symmetry. Generally, in the full as well as in the effective theory, the infrared or long distance behaviour is the same [128].
Within the standard model the quark contribution to the QCD Lagrangian (2.42) can be separated into two pieces; one from the light quarks $q \in \{u, d, s\}$ and one from the heavy quarks $Q \in \{c, b, t\}$, where every part is associated with a distinct symmetry. The light-quark sector has an approximate $\mathsf{SU(3)}_L \otimes \mathsf{SU(3)}_R$ chiral symmetry which is spontaneously broken to the usual vector $\mathsf{SU(3)}$. The eight (pseudo)Goldstone bosons, pions, kaons, and η, reflect this breaking of the chiral symmetry, because their masses are generated by the current quark masses. Figure 3.5 presents diagrammatically the quark flavour symmetry in the standard model. Note that the Lorentz invariance and the presence of chiral symmetry of full QCD ensuring that no mass renormalization can occur in the massless limit. For discussion about the chiral symmetry and heavy-quark symmetries, see, e.g. Refs. [136–138]
In lowest order the heavy quark can be treated as a static source of colour - or strong in-

teraction - localized at the origin, and, since the light degrees of freedom are concerned, the interaction is independent of m_Q, for $m_Q \gg \Lambda_{\rm QCD}$. This is the heavy-flavour symmetry, which is an approximative symmetry, with the corresponding heavy-flavour group $\mathsf{SU}(N_{\rm hf})_{\rm hf}$, where $N_{\rm hf}$ is the number of heavy flavours. For example, the $\bar{B}$ and D mesons, where the bottom and charm quarks are the heavy ones, they can be related by an $b \leftrightarrow c$ heavy-flavour $\mathsf{SU(2)}$ symmetry even though m_b and m_c are very different, because the heavy-quark masses are not present in the static Lagrangian.

Considering an heavy-light QCD bound state, the interactions of the light degrees of freedom with the heavy quarks depend on the heavy quark's four-velocity v^μ. The effective theory is formulated that the mass of the heavy quark is taken to infinity in such a way that its four-velocity v^μ is fixed.

Following Ref. [124] the heavy quark field Q (Dirac spinor), could be transformed into $h_v(x) = e^{im_Q v\cdot x} Q(x)$, and the field $h_v(x)$ is constrained to satisfy $\not{v} h_v(x) = h_v(x)$. The QCD Lagrangian (2.42) becomes $\mathcal{L}_v = \bar{h}_v(x) i \not{D} h_v(x)$, where the covariant derivative is given by Eq. (2.44). By using the positive-energy projection operator $\mathcal{P}_+ = (\mathbb{1} + \not{v})/2$, defined by $\mathcal{P}_\pm = (\mathbb{1} \pm \not{v})/2$, $\mathcal{P}_\pm^2 = \mathcal{P}_\pm$, and $\mathcal{P}_\pm \mathcal{P}_\mp = 0$, the effective Lagrangian becomes

$$\mathcal{L}_{\rm eff} = \bar{h}_v \, i v \cdot D \, h_v \, . \tag{3.63}$$

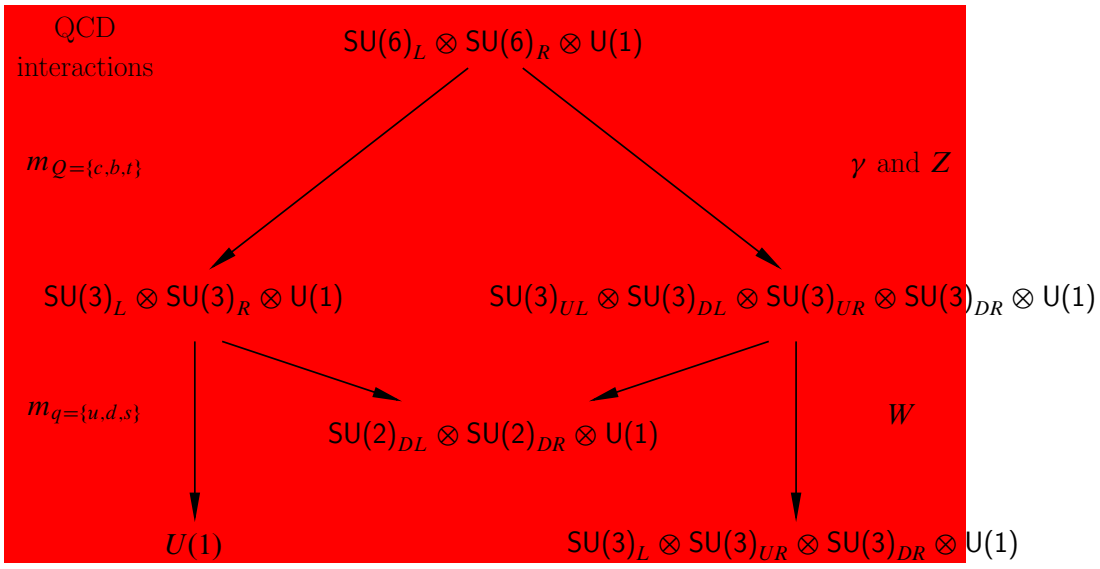

Figure 3.5.: Quark flavour symmetry: the symmetry group of the QCD interactions acting on six massless quarks is broken by the heavy-quark masses m_Q and separately by the γ and Z, with an common subgroup, [135].

In an heavy-light QCD bound state the heavy quarks carry most of momentum and energy, being split into an large part $m_Q v$ and a residual part $k = \mathcal{O}(\Lambda_{\rm QCD})$,

$$p_Q = m_Q v + k = m_Q \left(v + \frac{k}{m_Q} \right) . \tag{3.64}$$

In momentum space the derivative acting on h_v produces the residual momentum k, because the heavy part ($m_Q v$) canceled out. All Green's functions in the full theory are produced at leading order in $1/m_Q$ and $\alpha_s(m_Q)$ by the effective Lagrangian. However, since the quark field Q contains a component H_v satisfying $\not{v} H_v = -H_v$, corresponding to the "small" components of the full spinor Q, the effective Lagrangian is only an approximation of the corresponding part of the QCD Lagrangian (2.42), and leads to corrections of $\mathcal{O}(1/m_Q)$ to the effective Lagrangian. Note that h_v (H_v) annihilates (creates) a heavy quark with velocity v; and in the case of an on-shell heavy quark, the field H_v is absent.

The second symmetry appearing in the limit $m_Q \gg \Lambda_{\rm QCD}$ is the spin symmetry. If the effective Lagrangian (3.63) contains no Dirac γ-matrices, heavy quark interactions with gluons leave its spin unchanged, and an SU(2) symmetry group exists under which the effective Lagrangian is invariant. In Hilbert space, the generators of the spin SU(3) can be chosen as $\boldsymbol{S}^k = \gamma_5 \gamma^0 \gamma^k$, using the chiral representation of the Dirac γ-matrices (2.15). Working in a general frame, with three unit vectors ε_i^μ, $\varepsilon_i^2 = -1$, which are orthogonal to v^μ, one introduces a triplet of quark (antiquark) spin operators $\boldsymbol{S}^+(v, \boldsymbol{\varepsilon})$ ($\boldsymbol{S}^-(v, \boldsymbol{\varepsilon})$), which satisfy the commutator relations,

$$\left[\boldsymbol{S}^\pm(v, \boldsymbol{\varepsilon}), h_v^\pm \right] = \begin{cases} \gamma_5 \not{v} \not{\boldsymbol{\varepsilon}} h_v^+ \\ -\gamma_5 \not{v} \not{\boldsymbol{\varepsilon}}^* h_v^- \end{cases} , \quad \left[\boldsymbol{S}^\pm(v, \boldsymbol{\varepsilon}), h_v^\mp \right] = 0 , \tag{3.65}$$

and $\boldsymbol{S}^+(v, \boldsymbol{\varepsilon})$ and $\boldsymbol{S}^-(v, \boldsymbol{\varepsilon})$ commute with each other, these are the usual SU(2) $\otimes$ SU(2) commutation relations. Here, the field h_v^+ (h_v^-) annihilates (creates) heavy quark (antiquark) states, and the relation to h_v is given by $h_v^\pm = \mathcal{P}_\pm h_v$. Splitting the field h_v into the new fields $h_v^\pm$, the heavy part of the QCD Lagrangian (3.63) can be written as

$$\mathcal{L}_v = \bar{h}_v^+ \, i v \cdot D \, h_v^+ + \bar{h}_v^- \, i v \cdot D \, h_v^- , \tag{3.66}$$

where the mass of the heavy quark does not appear explicitly, hence, it is invariant under rotations in the flavour space.
For $N_{\rm hf}$ heavy quarks the spin symmetries can be extended to a SU($2N_{\rm hf}$) $\otimes$ SU($2N_{\rm hf}$) symmetry, this is the heavy-quark spin-flavour symmetry [92, 121, 122, 124].

The spin symmetry acts on a heavy-light mesons with mass M such that the mass is of order of that of the heavy quark, $M = m_Q[1 + \mathcal{O}(\Lambda_{\mathrm{QCD}})]$. The system is moving with an "infinite" momentum $P^\mu = M v^\mu$, and the present heavy-quark states in the wavefunction originate from the v^μ part of the theory. By the operators $\boldsymbol{S}^+(v, \boldsymbol{\varepsilon})$ the symmetry is generated, and all hadron states appear in multiplets of spin SU(2). Note that the spin operators $\boldsymbol{S}^+(v, \boldsymbol{\varepsilon})$ do not commute with the total angular momentum, generally they connect states of different spins [129].
Applications of heavy quark symmetry are exhaustively discussed in the literature; e.g. generally Refs. [139, 140], for mesons Refs. [126, 141] and for baryons Refs. [142, 143]. Spectroscopic implications of the heavy-quark spin symmetry are discussed, e.g., in Refs. [92, 144]. In the next subsection hadronic matrix elements and form factors resulting naturally by the heavy-quark symmetries are reported.

3.3.2. Transition Matrix Elements and Covariant Trace Formalism

Setting up the heavy-quark symmetry approach, the transition matrix elements and the covariant trace formalism can be introduced. It is out of the scope of this work to give a general deduction of the hadronic matrix elements, this can be found, e.g., in Ref. [140]. Here, the focus lies on the ones for $B \to D^{(*)}$ decays, which are defined by

$$\begin{aligned}
&\left\langle D\left(p'\right)\left|V_\mu\right|\bar{B}(p'+q)\right\rangle \\
&\quad \equiv 2p'_\mu f_{BD}^+(q^2) + q_\mu\left[f_{BD}^+\left(q^2\right) + f_{BD}^-\left(q^2\right)\right] , \qquad (3.67)\\
&\left\langle D^*\left(p', \boldsymbol{\varepsilon}\right)\left|(V-A)_\mu\right|\bar{B}(p'+q)\right\rangle \\
&\quad \equiv -i\,\varepsilon_\mu^*\left(m_B + m_D^*\right) A_1^{BD^*}\left(q^2\right) + i\left(2p'+q\right)_\mu (\boldsymbol{\varepsilon}^* q)\,\frac{A_2^{BD^*}(q^2)}{m_B + m_D^*} \\
&\qquad + i\,q_\mu\,(\boldsymbol{\varepsilon}^* q)\,\frac{2m_D^*}{q^2}\left[A_3^{BD^*}\left(q^2\right) - A_0^{BD^*}\left(q^2\right)\right] \\
&\qquad + \epsilon_{\mu\nu\rho\sigma}\varepsilon^{*\nu} q^\rho p'^\sigma \frac{2V^{BD^*}(q^2)}{m_B + m_D^*} , \qquad (3.68)
\end{aligned}$$

where $V_\mu = \bar{c}\gamma_\mu b$ and $A_\mu = \bar{c}\gamma_\mu\gamma_5 b$ are the vector and axial vector currents, respectively, and the Lorentz scalar form factors are functions of the momentum transfer squared $q^2 = (p - p')^2$. Some of the form factors are in the heavy-quark limit not independent from each other. Instead of q^2 it is common to use the variable w, being defined as

$$w \equiv v \cdot v' = \frac{m_B^2 + m_{D^{(*)}}^2 - q^2}{2m_B m_{D^{(*)}}} , \qquad (3.69)$$

where $v_\mu = (p' + q)_\mu / m_B$ and $v'_\mu = p'_\mu / m_{D^{(*)}}$ are the four-velocities of B and $D^{(*)}$. Heavy-quark effective theory provide methods to find relations between the form factors at maximum momentum transfer squared, $q^2 = q^2_{\text{max}} = (m_B - m_{D^{(*)}})^2$. At this kinematic point, the $D^{(*)}$ meson is not able to recoil in the rest frame of the decaying B-meson, and it is called "zero-recoil".

By using the *covariant trace formalism*, formulated in Refs. [126, 142, 145] and generalized to excited states in Ref. [140] the relations between the form factors could be calculated in an elegant manner. The main idea is to use the covariant tensor representation of the states with definite transformation properties under the Lorentz group and the heavy-quark spin-flavour symmetry.

The heavy quark in the meson can be represented by the spinor $\mathfrak{u}_Q(v,s)$, satisfying $\not{v}\mathfrak{u}_Q(v,s) = \mathfrak{u}_Q(v,s)$. In the following only the case $j^P = \frac{1}{2}^-$ is discussed, for a discussion with higher spins see Ref. [140]. Quarks and antiquarks have opposite intrinsic parity, and the corresponding physical states are ground-state pseudoscalar ($J^P = 0^-$) and vector ($J^P = 1^-$) mesons. Under Lorentz transformation the light degrees of freedom as a whole transform as an antiquark moving with velocity v. The antiquark is described by a antifermion spinor $\bar{\mathfrak{v}}_{\bar{q}}(v,s') = \mathfrak{v}^\dagger_{\bar{q}}\gamma^0$, $\bar{\mathfrak{v}}_{\bar{q}}(v,s')\not{v} = -\bar{\mathfrak{v}}_{\bar{q}}(v,s')$, representing the light degrees of freedom with $j = \frac{1}{2}$. The two spinors can be combined representing the ground-state mesons wave function, $\Psi = \mathfrak{u}_Q \bar{\mathfrak{v}}_{\bar{q}}$, which transforms under a connected Lorentz transformation $\boldsymbol{\Lambda}$ as $\Psi \longmapsto D(\boldsymbol{\Lambda})\Psi D^{-1}(\boldsymbol{\Lambda})$, whereas under a heavy-quark spin rotation $\tilde{\boldsymbol{\Lambda}}$ as $\Psi \longmapsto D(\tilde{\boldsymbol{\Lambda}})\Psi$. Working in a rest frame, where the quantization axis is the 3-direction and the spinor rest frame basis is $\mathfrak{u}^{(r)}_Q = \begin{pmatrix} \chi^r \\ 0 \\ 0 \end{pmatrix}$, and $\mathfrak{v}^{(r)}_{\bar{q}} = \begin{pmatrix} 0 \\ 0 \\ \chi^r \end{pmatrix}$, with $\chi^1 = \binom{1}{0}$, and $\chi^2 = \binom{0}{1}$, the pseudoscalar state in the rest frame becomes

$$P(v) = \frac{1}{\sqrt{2}}\left(\mathfrak{u}^{(1)}_Q \bar{\mathfrak{v}}^{(1)}_{\bar{q}} + \mathfrak{u}^{(2)}_Q \bar{\mathfrak{v}}^{(2)}_{\bar{q}}\right) = -\frac{1}{\sqrt{2}}\frac{\mathbb{1} + \gamma^0}{2}\gamma_5 \,, \tag{3.70}$$

and for the three vector states,

$$V(\boldsymbol{\varepsilon}_+) = \mathfrak{u}^{(1)}_Q \mathfrak{v}^{(2)}_{\bar{q}} = \frac{1}{\sqrt{2}}\frac{\mathbb{1} + \gamma^0}{2}\not{\boldsymbol{\varepsilon}}_+ \,, \tag{3.71}$$

$$V(\boldsymbol{\varepsilon}_-) = \mathfrak{u}^{(2)}_Q \mathfrak{v}^{(1)}_{\bar{q}} = \frac{1}{\sqrt{2}}\frac{\mathbb{1} + \gamma^0}{2}\not{\boldsymbol{\varepsilon}}_- \,, \tag{3.72}$$

$$V(\boldsymbol{\varepsilon}_3) = \frac{1}{\sqrt{2}}\left(\mathfrak{u}^{(1)}_Q \mathfrak{v}^{(1)}_{\bar{q}} + \mathfrak{u}^{(2)}_Q \mathfrak{v}^{(2)}_{\bar{q}}\right) = \frac{1}{\sqrt{2}}\frac{\mathbb{1} + \gamma^0}{2}\not{\boldsymbol{\varepsilon}}_3 \,, \tag{3.73}$$

where the two transverse polarisation vectors $\boldsymbol{\varepsilon}_\pm$ and the longitudinal polarization vector $\boldsymbol{\varepsilon}_3$ are defined as

$$\varepsilon_\pm^\mu = \frac{1}{2}(0, 1, \pm i, 0) \ , \quad \varepsilon_3^\mu = (0, 0, 0, 1) \ . \tag{3.74}$$

In the rest frame the matrix representation of the components $\boldsymbol{\Sigma}^i$ of the general spin operator $\boldsymbol{\Sigma}$ is $\boldsymbol{\Sigma}^k = \frac{1}{2}\gamma_5\gamma^0\gamma^k$, and acts on the meson wave function as $\boldsymbol{\Sigma}^k\Psi = [\boldsymbol{\Sigma}^k, \Psi]$. Using this representation, the pseudoscalar meson has spin zero, and the vector mesons (3.71), (3.72), and (3.73), have spin 1, -1, and 0, respectively. The heavy-quark spinor operators $\boldsymbol{S}^k$ have the same matrix representation as $\boldsymbol{\Sigma}$, however, acting only on the heavy-quark spinor Ψ, $\boldsymbol{S}^k\Psi = S^k\Psi$, one gets

$$S^3 P = \frac{1}{2}V(\boldsymbol{\varepsilon}_3) \ , \quad S^3 V(\boldsymbol{\varepsilon}_3) = \frac{1}{2}P \ , \quad S^3 V(\boldsymbol{\varepsilon}_\pm) = \pm\frac{1}{2}V(\boldsymbol{\varepsilon}_\pm) \ . \tag{3.75}$$

By replacing γ^0 with $\not{v}$ the tensor wave functions (3.70)–(3.73) can be generalized in a Lorentz covariant way. Note that the polarization vector of a vector meson with velocity v' satisfies $\boldsymbol{\varepsilon} \cdot v' = 0$ and $\boldsymbol{\varepsilon} \cdot \boldsymbol{\varepsilon}^* = -1$, as well as

$$\sum_{\text{pol.}} = \varepsilon^\mu \varepsilon^{*\nu} = v'^\mu v'^\nu - g^{\mu\nu} \ . \tag{3.76}$$

It is convenient to introduce a combined meson wave functional $\mathfrak{M}(v)$ that represents $P(v)$ and $V(v, \boldsymbol{\varepsilon})$ by

$$\mathfrak{M}(v) = \sqrt{m_M}\mathcal{P}_+ \begin{cases} -\gamma_5 & \text{pseudoscalar meson,} \\ \not{\boldsymbol{\varepsilon}} & \text{vector meson ,} \end{cases} \tag{3.77}$$

satisfying $\not{v}\mathfrak{M}(v) = \mathfrak{M}(v)$, as expected. The amplitude for transition between two heavy mesons, e.g. $\bar{B} \to D^{(*)}$, must be proportional to $\mathfrak{M}'(v')\Gamma\mathfrak{M}(v)$, which is a Dirac matrix with two indices representing the light degrees of freedom. In order to ensure the SU(2) invariance these indices must contract those of a matrix Ξ. This matrix contains all long-distance dynamics, and heavy-quark symmetry implies that it is independent from spins and masses of the heavy quarks as well as of the Dirac structure of the current. However, it is a function of the mesons velocity and of the renormalization scale μ. Because of Lorentz covariance and parity Ξ transform as a scalar with even parity. A decomposition could be chosen as

$$\Xi(v, v', \mu) = \Xi_1 + \Xi_2\not{v} + \Xi_3\not{v}' + \Xi_4\not{v}\not{v}' \ , \tag{3.78}$$

where $\xi_i(w = v \cdot v', \mu)$ are Lorentz scalar functions. The hadronic matrix element can be written as

$$\left\langle \mathfrak{M}'(v') \left| h^{(c)}_{v'} \Gamma h^{(b)}_{v} \right| \mathfrak{M}(v) \right\rangle = \mathsf{Tr}\left\{ \Xi(w,\mu) \bar{\mathfrak{M}}'(v') \Gamma \mathfrak{M}(v) \right\} , \tag{3.79}$$

where $\bar{\mathfrak{M}} = \gamma^0 \mathfrak{M}^\dagger \gamma^0$. The combination $\xi(w,\mu) \equiv \Xi_1 - \Xi_2 - \Xi_3 + \Xi_4$ under the trace has the same effect as Ξ, therefore [126]

$$\left\langle \mathfrak{M}'(v') \left| h^{(c)}_{v'} \Gamma h^{(b)}_{v} \right| \mathfrak{M}(v) \right\rangle \equiv -\xi(w,\mu) \mathsf{Tr}\left\{ \bar{\mathfrak{M}}'(v') \Gamma \mathfrak{M}(v) \right\} . \tag{3.80}$$

In the heavy-quark limit the form factors in Eqs. (3.67) and (3.68) reduce to a universal single form factor $\xi(w,\mu)$, coincides with the Isgur-Wise function [121, 122, 146, 147]. It is, from a group theoretical point of view, a reduced matrix element, being universal for the whole spin-flavour symmetry multiplet. According to the Wigner-Eckhard theorem [148, 149] the trace in (3.80) is the Clebsch-Gordon coefficient beeing determined by the current operator and the states of the multiplet [128]. By using flavour symmetry one finds that the current between B-meson states is given by Eq. (3.80), and since the current $\Gamma = \gamma^0$ generates this symmetry, the normalization condition for the Isgur-Wise function is given by

$$\xi(w = 1) \equiv 1 . \tag{3.81}$$

The behaviour of the Isgur-Wise function near maximum recoil and zero-recoil is investigated with respect to $\bar{B} \to D^{(*)}$ transitions in Chap. 4 and 5, respectively.
Note finally that for non-zero angular momentum the calculation of the covariant representation similar to (3.70)–(3.73) is straightforward by using the properties of spin$(n + \frac{1}{2})$ Rarita-Schwinger tensor spinors [150]; for details of this calculation see Ref. [140].
For exclusive $\bar{B} \to D^{(*)} \ell \bar{\nu}$ decays, heavy-quark symmetry provides relations between the form factors parametrizing these decays; treating charm and top quark as heavy static quarks, a single heavy form factor describe these decays, which allows a model-independent determination of the CKM matrix element V_{cb}, which is shown in Sec. 3.3.4. In order to refine the theoretical understanding of the heavy-quark symmetry in the next subsection the renormalization effects at next-to-leading order as well as the first-order power corrections in perturbation theory are discussed.

3.3.3. Renormalization and Power Counting

The Isgur-Wise function $\xi(w,\mu)$ as defined above depends on the mesons velocity as well as on the renormalization scale μ. The μ-dependence is necessary in order to

cancel the scale dependence of the Wilson coefficients, multiplying the renormalized current operators in the short distance expansion. An exhaustively discussion of of matching an renormalization for the flavour-changing vector $V_\mu = \bar{q}\gamma_\mu Q$ and axial vector $A_\mu = \bar{q}\gamma_\mu\gamma_5 Q$ currents can be found in Ref. [92].
In QCD the vector current $V_\mu = \bar{Q}_j\gamma_\mu Q_i$ is a partly conserved current, and renormalization is obsolete [151], and hence the matrix elements are free of ultraviolet divergences. However, in the matrix element large logarithms of the type $\log(m_Q^2/\mu^2)$ can appear which diverge in the heavy-quark limit, and the vector current requires renormalization [152, 153]. In the heavy-quark limit the matrix elements are μ-dependent separating the regions of short- and long-distance physics. The short-distance correction can be perturbatively calculated since $\Lambda_{\rm QCD} \ll \mu \ll m_Q$, because the effective coupling in region between μ and m_Q is small. As discussed in Sec. 3.1.1 the matrix element can be expanded as $\langle V_{ij}^\mu\rangle_{\rm QCD} = \mathcal{C}_{ji}(\mu)\langle V_{ji}^\mu(\mu)\rangle_{\rm HQET} + \mathcal{O}(1/m_Q) + \mathcal{O}(\alpha_s)$. An explicit calculation for the Wilson coefficient $\mathcal{C}_{cb}$ of the vector current $V^\mu = \bar{c}\gamma^\mu b$ yields [126, 154]

$$\mathcal{C}_{cb}(\mu) = \left(\frac{\alpha_s(m_b)}{\alpha_s(m_c)}\right)^{\frac{6}{25}} \left(\frac{\alpha_s(m_c)}{\alpha_s(\mu)}\right)^{\frac{8(wr(w)-1)}{27}} , \tag{3.82}$$

with

$$r(w) = \frac{\log(w+\sqrt{w^2-1})}{\sqrt{w^2-1}} . \tag{3.83}$$

For the axial current A_μ the result is identically. The μ-dependence of the Wilson coefficients has to be canceled against that one of the Isgur-Wise function. A renormalization-group invariant Isgur-Wise function can be defined as

$$\xi_{\rm ren}(w) = \xi(w,\mu)\mathcal{C}_{cb}(\mu) , \tag{3.84}$$

which comply with the normalization condition $\xi_{\rm ren}(1) = 1$ at zero-recoil.

Renormalization-group corrections as discussed above are effects at leading order in the $1/m_Q$ expansion. The formalism of $1/m_Q$ expansion has become textbook material and can be found, e.g. in Refs. [89, 133, 134]. The basic idea is to take the "small" components H_v into account and parametrize them like the "large" components h_v, therefore the quark field Q can be written as $Q = e^{im_Q v\cdot x}[h_v + H_v]$. Defining a decomposition of the covariant derivative into a "longitudinal" and a "transverse" part,

$$D_\mu = v_\mu\,(v\cdot D) + D_\mu^\perp , \quad D_\mu^\perp = \left(g_{\mu\nu} - v_\mu v_\nu\right) D^\nu , \quad \left\{\not{D}^\perp, \not{v}\right\} = 0 , \tag{3.85}$$

the QCD Lagrangian (2.42) for heavy quarks takes the form

$$\mathcal{L}_Q = i\bar{h}_v\, iv\cdot D h_v - \bar{H}_v(iv\cdot D + 2m_Q)H_v + \bar{h}_v\, i\not{D}^\perp H_v + \bar{H}_v\, i\not{D}^\perp h_v\ . \quad (3.86)$$

In this Lagrangian the heavy degrees of freedom are represented by the field H_v. They can be eliminated by using the QCD equations of motion, and one gets

$$H_v = \frac{1}{iv\cdot D + 2m_Q - i\epsilon}\, i\not{D}^\perp h_v\ , \quad (3.87)$$

reflecting that the small component field $H_v = \mathcal{O}(1/m_Q)$, whose corresponding effective Lagrangian reads

$$\mathcal{L}_{\text{eff}} = \bar{h}_v\, iv\cdot D\, h_v + \bar{h}_v\, i\not{D}^\perp \frac{1}{iv\cdot D + 2m_Q - i\epsilon} i\not{D}^\perp\, h_v\ . \quad (3.88)$$

This non-local effective Lagrangian is the correct generalization of (3.63) for large but finite heavy-quark masses. Here, for the deduction of the effective Lagrangian a "classical" way by using the equations of motion is used. A more sophisticated way can be found in Ref. [155]. The Lagrangian can be derived by using the generating functional of QCD Green's function containing the heavy-quark fields.
An expansion of the effective Lagrangian at order Λ_{QCD}/m_Q yields [123, 127]

$$\mathcal{L}_{\text{eff}} = \bar{h}_v\, iv\cdot D\, h_v + \frac{1}{2m_Q}\bar{h}_v\left(iD^\perp\right)^2 h_v + \frac{g}{4m_Q}\bar{h}_v\sigma_{\alpha\beta}G^{\alpha\beta}h_v + \mathcal{O}\left(\frac{1}{m_Q^2}\right)\ , \quad (3.89)$$

where $G^{\alpha\beta}$ is the gluon field strength tensor (2.43). At order $1/m_Q$ two new operator appear, identified in the rest frame as

$$\mathcal{Q}_{\text{kin}} = \frac{1}{2m_Q}\bar{h}_v\left(iD^\perp\right)^2 h_v \longrightarrow -\frac{1}{2m_Q}\bar{h}_v\,(i\boldsymbol{D})^2\, h_v\ ,$$
$$\mathcal{Q}_{\text{mag}} = \frac{g}{4m_Q}\bar{h}_v\sigma_{\alpha\beta}G^{\alpha\beta}h_v \longrightarrow -\frac{g}{m_Q}\bar{h}_v\boldsymbol{S}\cdot\boldsymbol{B}_c h_v\ ,$$

where $\boldsymbol{S}^k = \frac{1}{2}\gamma_5\gamma^0\gamma^k$ is the spin operator, and $B_c^i = \epsilon^{ijk}G^{jk}$ are the components of the colour-magnetic gluon field. The first operator $\mathcal{Q}_{\text{kin}}$ is the gauge covariant extension of the kinetic energy, which arise from the off-shell residual motion of the heavy quark. The interaction of the heavy-quark with the gluon field is described by the second operator $\mathcal{Q}_{\text{mag}}$; it is a nonabelian analog of the Pauli term, and a relativistic effect scaling like $1/m_Q$. This is the origin of the heavy-quark spin symmetry.
Higher order power corrections to $b\to c$ transitions and its impact for B decays have been studied by several authors in the last years, see., e.g., Refs. [156, 157] and the references therein.

3.3.4. Semi-leptonic Decay Rates

Closing this chapter about fundamentals of B-meson decays, the impact of the form factors defined in Eqs. (3.67) and (3.68) for $\bar{B} \to M$ decay rates, and, in particular, for the semileptonic $\bar{B} \to D^{(*)}\ell\bar{\nu}$, decay rates are discussed. In exclusive $\bar{B} \to D^*\ell\bar{\nu}$ transitions the decay rates can be characterized by four variables, three angles and the momentum transfer squared q^2. The kinematics of these decays is well analysed within the standard model [158, 159], and the B-factories provide high precision data for analysis, used in the chapters 4–6 for comparison with theoretical predictions. Here, the derivation of the decay rates for the exclusive processes $\bar{B} \to M\ell\bar{\nu}$, $M \in \{D, D^*\}$, for light leptons, $\ell \in \{e, \mu\}$, is briefly reviewed. For light leptons, a vanishing lepton mass $m_\ell = 0$, can be assumed. In the rest frame of the $\bar{B}$-meson, the decay rate is defined by

$$d\Gamma(\bar{B} \to M\ell\bar{\nu}) = \frac{1}{2m_B} \left|\mathcal{A}\left(\bar{B} \to M\ell\bar{\nu}\right)\right|^2 d\Pi_3 \,, \tag{3.90}$$

with

$$d\Pi_3 = (2\pi)^4 \delta^{(4)}\left(p - (p_\ell + p_{\bar{\nu}}) - p'\right) \prod_f \frac{d^4 p_f}{(2\pi)^3 2E_f} \,, \tag{3.91}$$

where $f \in \{M, \ell, \bar{\nu}\}$ denotes the final states momenta, and the amplitude is given by

$$A\left(\bar{B} \to M\ell\bar{\nu}\right) = \frac{G_F}{\sqrt{2}} V_{Qq} L^\mu W_\mu \,, \tag{3.92}$$

with the CKM matrix element V_{Qq}, corresponding to the $Q \to q$ transitions. The quark-level diagram is depicted in Fig. 3.6 (a). The virtual W-boson carries the four-momentum $q = p_\ell + p_{\bar{\nu}}$. In the standard model framework the leptonic current and the hadronic matrix element are given by

$$L^\mu = \bar{\ell}\gamma^\mu(\mathbb{1} - \gamma_5)\nu \,, \quad W^\mu = \left\langle M\left(p'\right) \left| \mathcal{J}^\mu_{\text{had}}(0) \right| \bar{B}(p) \right\rangle \,, \tag{3.93}$$

respectively. As discussed above, the matrix element of the hadronic current is constructed from Lorentz-invariant form factors. Using $\mathcal{J}^\mu_{\text{had}} = V^\mu - A^\mu$, one achieved the form factors defined in Eqs. (3.67) and (3.68). For $\bar{B} \to D^{(*)}$ transitions the form factors become

$$\frac{\langle D(p')|\bar{c}\gamma_\mu b|\bar{B}(p)\rangle}{\sqrt{m_B m_D}} = (v + v')_\mu h_+(w) + (v - v')_\mu h_-(w) \,, \tag{3.94}$$

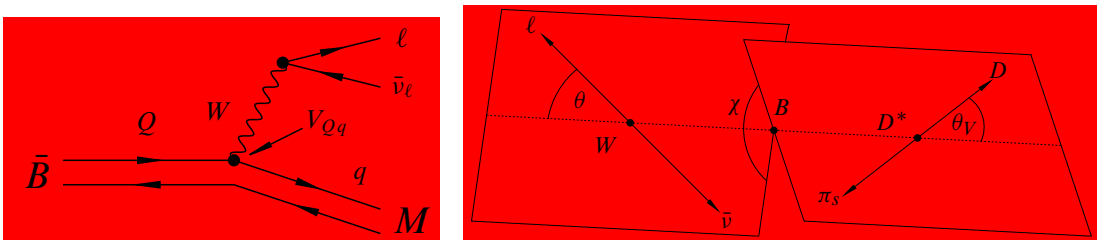

(a) Quark-level diagram for the weak decay of a heavy quark Q into a lighter quark q and a virtual W, which decays into a lepton its corresponding neutrino.

(b) Definition of the decay angles θ, θ_V, and χ, for the $\bar{B}^0 \to D^{*+}[\to D^0\pi^+]\ell\bar{\nu}$ decay, mediated by a weak virtual intermediate vector boson W [160].

Figure 3.6.: Semileptonic weak decay of a B-meson.

$$\frac{\langle D^*(p',\boldsymbol{\varepsilon})|\bar{c}\gamma_\mu b|\bar{B}(p)\rangle}{\sqrt{m_B m_D}} = \epsilon_{\mu\nu\alpha\beta}\varepsilon^{*\nu}v^\alpha v'^\beta h_V(w)\ , \tag{3.95}$$

$$\begin{aligned}\frac{\langle D^*(p',\boldsymbol{\varepsilon})|\bar{c}\gamma_\mu\gamma_5 b|\bar{B}(p)\rangle}{\sqrt{m_B m_D}} &= i\,\varepsilon^*_\mu(1+w)h_{A_1}(w) \\ &\quad - i\left[h_{A_2}(w)v_\mu + h_{A_3}(w)v'_\mu\right](\boldsymbol{\varepsilon}^*\cdot v)\ ,\end{aligned} \tag{3.96}$$

From a direct calculation, done in Ref. [159], the decay rate for the first transition, $\bar{B} \to D\ell\bar{\nu}$, depends on the form factors $h_+(w)$ and $h_-(w)$, and is given by

$$\frac{d\Gamma(\bar{B}\to D\ell\bar{\nu})}{dw} = G_0(w)|V_{cb}|^2\frac{w-1}{w+1}(1+r)^2\left|h_+(w) - \frac{1-r}{1+r}h_-(w)\right|^2\ , \tag{3.97}$$

with

$$r_{(*)} \equiv \frac{m_{D^{(*)}}}{m_B}\ , \tag{3.98}$$

and

$$G_0^{(*)}(w) \equiv \frac{G_F^2 m_B^5}{48\pi^3}r_{(*)}^3\sqrt{w^2-1}(w+1)^2\ . \tag{3.99}$$

For the variable w there are two boundaries in the semileptonic region, maximum recoil $q^2 = 0$ and zero-recoil $q^2 = (m_B - m_{D^{(*)}})^2$ corresponding to $w_{\max} \simeq 1.589$ or $w^*_{\max} \simeq 1.503$, and $w = 1$, respectively.

For the second decay, $\bar{B} \to D^*\ell\bar{\nu}$, it is convenient to introduce invariant helicity amplitudes $H_\pm(w)$ and $H_0(w)$, corresponding to the transverse and longitudinal polarizations. In the B-meson rest frame the D^*-meson and the virtual W-boson go back to back and they are forced to have the same helicity. For this decay, the definition of

the angles are shown in Fig. 3.6 (b), where the angle θ is defined as the angle between the D^*-meson and the lepton in the rest frame of the virtual W-boson. The differential decay rate can be expressed in terms of the helicity functions[3] and is given by

$$\frac{d\Gamma(\bar{B} \to D^* \ell \bar{\nu})}{dw} = G_0^*(w)(1-r_*)^2 \, |V_{cb}|^2 \, |h_{A_1}(w)|^2 \sum_{i=\pm,0} |H_i(w)|^2 \ , \tag{3.100}$$

where the helicity functions are

$$\begin{aligned} |H_\pm(w)|^2 &= \frac{r_*^2 - 2wr_* + 1}{(1-r_*)^2} \left(1 \mp \sqrt{\frac{w-1}{w+1}} R_1(w) \right)^2 \ , \\ |H_0(w))^2 &= \left[1 + \frac{w-1}{1-r_*} \big(1 - R_2(w) \big) \right]^2 \ , \end{aligned} \tag{3.101}$$

with the ratios

$$R_1 = \left[1 - \frac{q^2}{(m_B + m_{D^*})^2} \right] \frac{V(q^2)}{A_1(q^2)} = \frac{h_V(w)}{h_{A_1}(w)} \ , \tag{3.102}$$

$$R_2 = \left[1 - \frac{q^2}{(m_B + m_{D^*})^2} \right] \frac{A_2(q^2)}{A_1(q^2)} = \frac{h_{A_3}(w) + r_* h_{A_2}(w)}{h_{A_1}(w)} \ . \tag{3.103}$$

At zero-recoil the helicity functions are normalized to unity, $|H_i(1)|^2 = 1$, and at maximum recoil only virtual W-bosons with longitudinal polarization contribute, hence, the transverse polarisation functions vanish, $|H_\pm(w_{\max})|^2 = 0$.
Using Luke's theorem [161] in the limit $v = v'$ there are no terms of order $1/m_Q$ in the hadronic matrix elements (3.67) and (3.68). A power correction up to second order of the form factors h_+ and h_{A_1} yields

$$h_+(1) = \eta_V + \mathcal{O}(1/m_Q^2) \ , \quad h_{A_1}(1) = \eta_A + (1/m_Q^2) \ , \tag{3.104}$$

these are the only two form factors protected by Luke's theorem, whereas the other ones are multiplied with kinematical factors which vanish for $w = 1$. The $1/m_Q$ corrections for the form factors h_-, h_V, h_{A_2}, and h_{A_3} do not vanish at zero-recoil, and the kinematical suppression of these form factors do not bar a contribution to the decay rate. In the $\bar{B} \to D \ell \bar{\nu}$ transition the angular momentum is conserved, therefore, in order to match the helicity of the lepton pair the two pseudoscalar mesons have to be in a relative p-wave configuration. In the decay rate (3.97) a factor $(w^2 - 1)$ appears,

[3] Note that in Refs. [158, 159] the helicity functions are functions of the momentum transfer squared q^2,whereas here the H_i are considered as functions of w.

because the amplitude in the B-meson rest frame is proportional to the four-velocity of the D-meson. Form factors which are kinematically suppressed can now contribute, which is reflected by the proportionality

$$\frac{d\Gamma(\bar{B} \to M\ell\bar{\nu})}{dw} \sim (w^2-1)^{3/2} \left| h_+(w) - \frac{1-r}{1+r} h_-(w) \right|^2 , \tag{3.105}$$

of the decay rate (3.97). The form factor h_+ as well as h_- contribute to the decay rate, and consequently the decay rate receives corrections of $\mathcal{O}(1/m_Q)$ at zero-recoil. The situation is rather different for the $\bar{B} \to D^*\ell\bar{\nu}$ decay, because the D^*-meson has spin one, the decay can proceed in an s-wave configuration, and there is no helicity suppression near zero-recoil [162], where the decay rate (3.100) becomes proportional to $\sqrt{w^2-1}|h_{A_1}|^2$, because this is the only form factor protected by Luke's theorem. Hence, this decay is suitable for a precision measurement of the CKM element V_{cb}, [92], explicitly, at $w = 1$, the decay rate becomes

$$\lim_{w\to 1} \frac{1}{\sqrt{w^2-1}} \frac{d\Gamma(\bar{B} \to D^*\ell\bar{\nu})}{dw} = \frac{G_F^2 m_B^5}{4\pi^3} (1-r_*)^2 r_*^3 |V_{cb}|^2 |h_{A_1}(1)|^2 , \tag{3.106}$$

where the $1/m_Q$ expansion of $h_{A_1}(1)$ is given by Eq. (3.104), and the latest result from lattice QCD [163, 164] is given by

$$h_{A_1}(1) = 0.9077 \pm 0.0051 \pm 0.0158 , \tag{3.107}$$

where the systematic errors are added in quadrature. The presented decay rates are achieved within the standard model by a left-handed hadronic current. In Chap. 5 the search for new physics effects is performed by allowing an additional helicity violating right-handed hadronic current. Furthermore, scalar and tensor currents are taken into account. The exclusive semileptonic $\bar{B} \to D^{(*)}\ell\bar{\nu}$ decay rates are then more sensitive on wrong helicity admixtures than the ones from inclusive decays.

After this briefly review of B-meson decays in the next chapters some applications are presented. For an investigation of the hadronic matrix elements in Chap. 4 the QCD sum rules for $\bar{B} \to D^{(*)}$ form factors are presented. B-meson decays are a suitable source for exploring new physics effects in different ways. In Chap. 5 such effects are studied in exclusive semileptonic B-meson decays by taking a helicity violating right-handed hadronic current into account. New physics effects as a sources for new CP violation are studied in $B^0 - \bar{B}^0$ mixing in Chap. 6.

4

B-Decays with QCD Sum Rules

QCD sum rules have become a quite powerfull tool for the calculation of hadron phenomenology. The method itself was developed by Shifman, Vainshtein and Zakharov (SVZ) [165] in 1979. As studied in Sec. 3.1.1, with the operator-product expansion short- and long-distance quark-gluon interactions can be seperated. The general idea of SVZ is to devolve this procedure to correlators of certain currents at small euclidean distances. Non-perturbative corrections are related to a non-trivial vacuum structure and are included into an vacuum expectation value of local quark-gluon operators. Sum rules can therefore be obtained by using dispersion relations relating current correlators to spectral densities. Due to quark-hadron duality, the spectral densities can be interpreted in terms of physical intermediate states [92]. However, quark-hadron duality and the approximations in the operator-product expansion of the correlator functions are responsible for the limited applicability of QCD sum rules and their predictions have to be treated carefully. In this chapter a short aspect of QCD sum rules within the investigation of exclusive $\bar{B} \to D^{(*)}\ell\bar{\nu}$ decays is described. For a comprehensive presentation of the QCD sum rule approach see, e.g., Refs. [116, 166, 167] and the references therein.

The plan of the chapter is following. In the first section the basic formalism is briefly reviewed by discussing the correlation function, construction of light-cone sum rules, and the impact of heavy-quark effective theory on the $B \to D^*$ form factors. Section 4.2 presents a numerical analysis of the achieved form factor sum rules, and the fit results are compared with recent experimental data. In Sec. 4.3 the results of this chapter are summarized.

4.1. QCD Sum Rule Formalism

In order to study the application of QCD sum rules on exclusive $\bar{B} \to D^{(*)}\ell\bar{\nu}$ transitions, the basic concepts behind light-cone sum rules are set up. The presented introduction follows Refs. [167–169], and the explicit relations for the $\bar{B} \to D^{(*)}\ell\bar{\nu}$ decays are taken from Ref. [170].
Light-cone sum rules can be interpreted as an hybrid of the original method developed by Shifman, Vainshtein and Zakharov with methods from hard exclusive decays. The SVZ sum rules start with a vacuum-to-vacuum correlation function, whereas, in the light-cone sum rule approach the correlation function is a time-ordered (T-)product of two quark currents sandwiched between vacuum and an on-shell state [171], where it can be a light hadron or a photon. In Refs. [92, 172] the SVZ approach is discussed in the heavy-quark symmetry framework. Light-cone sum rules can be used for reliable calculations of heavy-to-light transition form factors in QCD. Hadronic input in semileptonic $B \to M\ell\nu_\ell$, $B \to M\ell\bar{\ell}$, $M \in \{P, V\}$, and radiative $B \to V\gamma$ decays is parametrized by the $B \to M$ form factors with pseudoscalar $P = \pi, K, D$ and vector $V = \rho, K^*, D^*$ particles, while the same form factors fix factorizable amplitudes in non-leptonic charmless B decays.

4.1.1. Correlation Function

For $\bar{B} \to D^{(*)}\ell\bar{\nu}$ transitions a special designed correlation function for the two quark currents sandwiched between the vacuum and the on-shell $\bar{B}$-meson state is used, written as [168]

$$F_{ab}^{(B)}(p', q) = i \int d^4x \, e^{ip'\cdot x} \left\langle O \left| T \left\{ \bar{q}_2(x) \Gamma_a q_1(x), \bar{q}_1(0) \Gamma_b b(0) \right\} \right| \bar{B}(p) \right\rangle \ , \quad (4.1)$$

where $\bar{q}_1 \Gamma_b b$ is one of the light-heavy transition currents and $\bar{q}_2 \Gamma_a q_1$ is the interpolating current for a pseudoscalar or a vector meson, where the valence quarks $q_{1,2}$ determine the flavour content. For the $\bar{B} \to D^{(*)}\ell\bar{\nu}$ transitions the current $\Gamma_a = m_c i\gamma_5$ ($\Gamma_a = \gamma_v$) interpolates the pseudoscalar (vector) D- (D^*-)meson, hence, the correlation function (4.1) becomes

$$\begin{aligned} &F_{a\mu}^{(B)}(p', q) \\ &\quad = i \int d^4x \, e^{ip'\cdot x} \left\langle O \left| T \left\{ \bar{d}(x) \Gamma_a c(x), \bar{c}(0) \gamma_\mu (\mathbb{1} - \gamma_5) b(0) \right\} \right| \bar{B}(p) \right\rangle \ . \end{aligned} \quad (4.2)$$

Note that in the isospin-symmetry limit $\bar{B}_d \to D^{(*)+}$ decays are equivalent to $\bar{B}_u \to D^{(*)0}$. In order to construct light-cone sum rules, one has to ensure that the operator-product expansion is applicable for the correlation functions (4.1) and (4.2). The argumentation for the proof of the general correlation function (4.1), which is given in Ref. [169], can be carried over to the correlation function (4.2), where instead of the virtual light quark now the charm-quark propagates in the correlation function. Working in the B-meson rest frame, where its momentum $p = p_B$ is defined by Eq. (3.64), and, in first approximation, $m_B = m_b + \bar{\Lambda}$ ($k_0 \sim \bar{\Lambda}$), the b- and c-quark fields are redefined by their effective fields, $b(x) = h_v(x)e^{-im_b v\cdot x} + \mathcal{O}(1/m_b)$ and $h'_v(x) = c(x)e^{-im_c v\cdot x}$, respectively. The external four-momenta are redefined: $p' = m_c v + \tilde{p}$, $q' = -m_c v + \tilde{q}$, where the parts proportional to the four-velocity v are separated: $q = (m_b - m_c)v + \tilde{q}$, and $\tilde{q} + \tilde{p} = k$. These redefinitions do not imply that the heavy-quark effective-theory is used for the virtual c-quark field, on the contrary it is done to decouple the c-quark mass scale. Using relativistic normalization of states, $|B(p)\rangle = |B_v\rangle$, and applying heavy-quark effective theory the correlation function (4.2) becomes at leading order, $F^{(b)}_{a\mu}(p', q) = \tilde{F}^{(B_v)}_{a\mu}(p', \tilde{q}) + \mathcal{O}(1/m_b)$. Inserting the redefinitions one ends up with the correlation function in the heavy-quark limit

$$\tilde{F}(\tilde{p},\tilde{q}) \;\; = i \int d^4x \; e^{i\tilde{p}\cdot x} \left\langle 0 \left| T\left\{ \bar{d}(x)\Gamma_a h'_v(x), \bar{h}'_v \gamma_\mu (\mathbb{1} - \gamma_5) h_v(0) \right\} \right| \bar{B}_v \right\rangle . \quad (4.3)$$

This correlation function depends neither explicitly on the b-quark nor on the c-quark mass and furthermore, it contains only scales associated with either effective or light-quark degrees of freedom. Since both rescaled four-momenta are assumed to be space-like and sufficiently large - P^2, $|\tilde{q}|^2 \gg \Lambda^2_{\rm QCD}$, $\bar{\Lambda}^2$ - and furthermore, the difference between the virtualities is also assumed to be large - $\zeta = \frac{2\tilde{p}\cdot k}{P^2} \sim \frac{|\tilde{q}|^2 - P^2}{P^2} \sim 1$ - the region of small $x^2 \leq 1/P^2$ dominates in the integral in Eq. (4.3). Large P^2 and $\zeta \sim 1$ ensure the validity of light-cone operator-product expansion, because the external momenta squared p'^2 and q^2 are far below the hadronic thresholds in the currents $\bar{d}\,\Gamma_a c$ and $\bar{c}\gamma_\mu(\mathbb{1} - \gamma_5)b$, respectively.

Note that the operator-product expansion can only be used far from the zero-recoil point: In the rest frame, where $\tilde{p}_0 = \zeta P^2/2\bar{\Lambda}$, the initial external momenta are

$$\begin{aligned} q^2 &= (m_b - m_c)^2 - \zeta(1+\zeta)(m_b - m_c)\frac{P^2}{\bar{\Lambda}} - P^2(1+\zeta) \,, \\ p^2 &= m_c^2 - \zeta m_c \frac{P^2}{\bar{\Lambda}} - P^2 \,. \end{aligned} \quad (4.4)$$

Here the first relation becomes at the zero-recoil $q^2 = (m_B - m_{D^{(*)}})^2 \sim (m_b - m_c)^2$. As an important consequence of this statement, the light-cone sum rule can be applied

only at the maximum recoil, $q^2 \sim 0$. The solution of the second relation at $q^2 = 0$ yields $P^2 \sim \bar{\Lambda}(m_b - m_c) \ll m_b^2$, however, in this case, the components of the external momenta are of order of the heavy mass scale.

In the second equation of (4.4) a scale $\chi \sim P^2/\bar{\Lambda} \gg \bar{\Lambda}, \Lambda_{\rm QCD}$ is present, being large in terms of $\Lambda_{\rm QCD}$, but generally independent of the heavy quark mass. An interval $\sim m_c \chi$ in the charm meson channel shifted the external momentum squared p^2 below the threshold $m^2_{D^{(*)}} \sim m_c^2$. A quite similar situation can be found by the derivation of light-cone sum rules for $B \to \pi$ form factors with pion distribution amplitudes, see, e.g., Refs. [173, 174].

Because of the light-cone dominance of the correlation function the quark field q_1 and q_2 can be contracted and the free propagator $S_{q_1}(x,0) = -i\,\langle 0|T\{q_1(x)q_1(0)\}|0\rangle$ can be used. Here, one is interested in the leading-order contributions of two- and three particle B-meson distribution amplitudes, depicted in Fig. 4.1 (left and middle panel). Near the light-cone, including the gluon part [175], the c-quark propagator yields

$$S_c(x,0) = \int \frac{d^4p'}{(2\pi)^4}\, e^{-ip'\cdot x} \times \left\{ \frac{\not{p}' + m_c}{p'^2 - m_c^2} + \int_0^1 d\alpha\; G_{\mu\nu}(\alpha x) \left[\frac{\alpha x^\mu \gamma^\nu}{p'^2 - m_c^2} - \frac{(\not{p}' + m_c)\sigma^{\mu\nu}}{2(p'^2 - m_c^2)^2} \right] \right\} . \quad (4.5)$$

$\mathcal{O}(\alpha_s)$ radiative corrections, caused by hard-gluon exchanges between the quark-antiquark lines, Fig. 4.1 (right panel), are neglected. The correlation functions and their implications on the light-cone sum rules are studied in the next subsection.

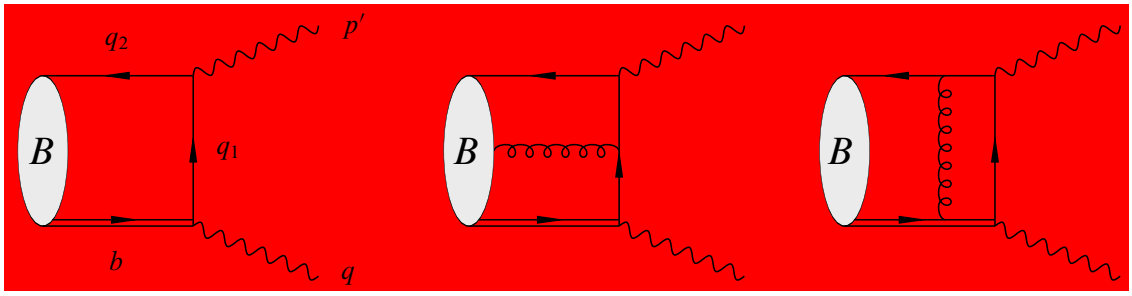

Figure 4.1.: Contributions of two-particle (left panel) and three-particle (middle panel) B-meson DA's to the correlation function. In the case of $\bar{B} \to D^{(*)}$, q_1 (q_2) is the $c(d)$-quark. Right panel: one of $\mathcal{O}(\alpha_s)$ diagrams.

4.1.2. Light-Cone Sum Rule

As discussed above the correlation functions for $\bar{B} \to D^{(*)}$ transitions satisfy conditions for an operator-product expansion. Therefore light-cone sum rules can be constructed. Following the standard procedure [165]; the OPE-result for the correlation function has to be matched to the hadronic representation via quark-hadron duality and a Borel transformation has to be performed.
Using the hadronic dispersion relation the general correlation function (4.1) as well as the modified one (4.3) can be related to the form factors in the channel of the charmed meson, one gets

$$F_{a\mu}^{(B)} = \frac{\langle 0|\bar{d}\,\Gamma_a c|D^{(*)}(p')\rangle\langle D^{(*)}(p')|\bar{c}\gamma_\mu(\mathbb{1}-\gamma_5)b|\bar{B}(p'+q)\rangle}{m_{D^{(*)}}^2 - p^2} + \text{excited and continuum states}\,, \tag{4.6}$$

where the $D^{(*)}$-meson pole are explicitly shown. The decay constants on the r.h.s of (4.6) are given by

$$\left\langle 0\left|\bar{d} m_c i\gamma_5 c\right|D\left(p'\right)\right\rangle = m_D^2 f_D\,, \quad \left\langle 0\left|\bar{d}\gamma_\nu c\right|D^*\left(p',\boldsymbol{\varepsilon}\right)\right\rangle = \varepsilon_\nu m_D^* f_D^*\,, \tag{4.7}$$

and the hadronic matrix elements for $\bar{B} \to D^{(*)}$ are noted in Eqs. (3.67) and (3.68). Now, in order to achieve a sum rule for each form factor or combination of form factors, the correlation function has to be equated to the hadronic representation, where from independent Lorentz structures the sum rules can be read off. In the correlation function for the $B \to D$ form factors the coefficients at p'_μ and q_μ are taken to obtain the sum rules for the form factors f_{BD}^+ and $f_{BD}^+ + f_{BD}^-$, respectively. In the case of $B \to D^*$ the kinematical structures $\epsilon_{\mu\nu\rho\sigma}q^\sigma p'^\sigma$, $g_{\mu\nu}$ and $p'_\mu q_\nu$ are taken for the form factors V^{BD^*}, $A_1^{BD^*}$ and $A_2^{BD^*}$, respectively. For the combined form factor $A_3^{BD^*} - A_0^{BD^*}$, one multiplies the invariant amplitude with $q_\mu p'_\nu$ and subtracts the sum rule for $A_2^{BD^*}$, where the relation $2m_D^* A_3^{BD^*}(q^2) = (m_B + m_{BD^*})A_1^{BD^*}(q^2) - (m_B - m_{BD^*})A_2^{BD^*}(q^2)$ is taken into account.

A central rôle in the calculation of these kind of light-cone sum rules play the B-meson distribution amplitudes. General aspects about distribution amplitudes are discussed in Sec. 3.2.1. The two- and three-particle B-meson distribution amplitudes are presented in App. A as well as sum rules for $\bar{B} \to D^{(*)}$ form factors. It is beyond the scope of this work to discuss all details of the light-cone distribution amplitudes, exhaustive discussions about their properties and model-dependence can be found, e.g., in Refs. [115, 116, 168, 176].

4.1.3. Implications from Heavy-Quark Effective Theory

B-meson distribution amplitudes are usually defined in the framework of heavy-quark effective theory. Comparing the $\bar{B} \to D^{(*)}$ form factors, Eqs. (3.94)–(3.96), with the ones given in Eqs. (3.67) and (3.68) one finds the following relations,

$$h_{\pm}(w) = \frac{1}{2\sqrt{r}} \left[(1 \pm r) f_{BD}^{+}\left(q^2\right) + (1 \mp r) f_{BD}^{-}\left(q^2\right) \right] , \tag{4.8}$$

$$h_V(w) = \frac{2\sqrt{r_*}}{1 + r_*} V^{BD^*}\left(q^2\right) , \tag{4.9}$$

$$h_{A_1}(w) = \frac{1 + r_*}{\sqrt{r}_*(1 + w)} A_1^{BD^*}\left(q^2\right) , \tag{4.10}$$

$$r_* h_{A_2}(w) + h_{A_3}(w) = \frac{2\sqrt{r}_*}{1 + r_*} A_2^{BD^*}\left(q^2\right) , \tag{4.11}$$

$$r_* h_{A_2}(w) - h_{A_3}(w) = \frac{4 r_* \sqrt{r}_* [A_3^{BD^*}(q^2) - A_0^{BD^*}(q^2)}{1 + r_*^2 - 2 r_* w} \tag{4.12}$$

where $r_{(*)}$ is defined as in Eq. (3.98). Note that the h_i form factors represent linear combinations of the initial form factors, and for their definitions no heavy-quark limit is involved. The form factors, which are derived from the sum rules, have to obey the heavy-quark symmetry relations in the heavy-quark limit, $m_c, m_b(m_B) \to \infty$. For this consistency check, some redefinitions have to be performed which are described in Sec. 4.2.3. In the heavy-quark limit, the form factors $h_+(w)$, $h_V(w)$, $h_{A_1}(w)$, and $h_{A_3}(w)$, reduce to the universal Isgur-Wise function, whereas the form factors $h_-(w)$ and $h_{A_2}(w)$ vanish; the sum rule for the Isgur-Wise function at tree-level is given by

$$\xi(w) = \int_0^{\beta_0/w} d\rho \, \exp\left\{ \frac{\bar{\Lambda} - \rho w}{\tau} \right\} \left[\frac{1}{2w} \phi_-^B(\rho) + \left(1 + \frac{1}{2w}\right) \phi_+^B(\rho) \right] . \tag{4.13}$$

Note that there is a difference of $\mathcal{O}(1/m_c)$ corrections between the form factors $h_i(w)$ obtained from sum rules with finite m_c and m_b and the ones in the heavy-quark limit. Three-particle distributions are suppressed with at least one power of the heavy-quark mass and give no contribution to (4.13). The sum rule (4.13) relates the Isgur-Wise function to the B-meson distribution amplitudes only near the maximum recoil, in the region, where the light-cone expansion of the initial sum rules are reliable.

4.2. Numerical Analysis

Within this section the B-meson distribution amplitudes and the form factor sum rules for exclusive semileptonic $\bar{B} \to D^{(*)}\ell\bar{\nu}$ transitions are analysed numerically following [170]. The explicit expression for the DA's and the LCSR are collected in App. A. For the B-meson distribution amplitudes the numerical values for the input parameters are listed in Table 4.1. They are the the same as the ones used in Ref. [169]. The decay constant f_B and the inverse moment λ_B, whose evolution is neglected, are taken from two-point sum rules with $\mathcal{O}(\alpha_s)$ accuracy. Three-particle distribution amplitudes are characterized by the parameter $\lambda_E^2 = \frac{3}{2}\lambda_B^2$.

The masses of the mesons are same as in Ref. [43]. Note that for the charm-quark the $\overline{\text{MS}}$ mass is used because, since it is highly virtual in the correlation function, the $\overline{\text{MS}}$ mass scheme is in general a natural choice. For the decay constants of the charmed mesons f_D and f_{D^*} the intervals from two-point sum rules are used [178–182].

The Borel mass squared M^2 in light-cone sum rules for charmed mesons lies in the range $3 - 6$ GeV^2 while the effective threshold is fixed at $s_0^{D^{(*)}} = 6.0(8.0)$ GeV^2. In this range for the Borel mass the light-cone sum rules are stable and the contributions of the three-particle distribution amplitudes are numerically suppressed. Note that the Borel mass M originates from the Borel transformation of the dispersion relation and the threshold $s_0^{D^{(*)}}$ from the quark-hadron duality approximation; for details, see. Refs. [116, 167].

Predictions from light-cone sum rules can only be trusted near the maximum recoil $w_{\text{max}}^{(*)}$ ($q^2 = 0$), where the light-cone operator-expansion is applicable, as explained in Sec. 4.1.2. Furthermore, the upper limits $\omega_0(q^2, s_0^{D^{(*)}})$ in the sum rule integrals are small, hence, the influence of the B-meson distribution amplitudes at large w - especially from the "radiative tail" [183] which is not taken into account - on the sum rules is weak. The behaviour of the sum rules is mainly affected by the inverse moment λ_B.

Table 4.1.: Input parameters for the numerical analysis.

Parameter		Ref.	Parameter		Ref.
m_B	$= 5.279$ GeV	[43]	f_B	$= 180 \pm 30$ MeV	[169]
m_D	$= 1.869$ GeV	[43]	f_D	$= 200 \pm 20$ MeV	
m_{D^*}	$= 2.01$ GeV	[43]	f_{D^*}	$= 270 \pm 30$ MeV	
$\bar{m}_c(\bar{m}_c)$	$= 1.25 \pm 20$ MeV	[43]	$\lambda_B(1\text{ GeV})$	$= 460 \pm 110$ MeV	[177]

In the following subsections the exclusive semileptonic $\bar{B} \to D\ell\bar{\nu}$ and $\bar{B} \to D^*\ell\bar{\nu}$ decays are numerically analysed explicitly. The predictions are compared with the latest experimental data.

4.2.1. Semileptonic $\bar{B} \to D^*\ell\bar{\nu}$ Decay

The exclusive semileptonic $B \to D^*$ decay is suitable for the calculation of the CKM matrix element $|V_{cb}|$, because at zero-recoil $w = 1$, the differential decay rate (3.106) depends besides a kinematical factor only on the CKM matrix element $|V_{cb}|$ and the form factor $h_{A_1}(1)$. In the whole semileptonic region, $1 < w < w^*_{\text{max}}$, the differential decay rate (3.100) can be written in the form

$$\frac{d\Gamma(\bar{B} \to D^*\ell\bar{\nu})}{dw} = G_0^*(w)(1-r_*)^2 g(w)\,|V_{cb}|^2\,|\mathcal{F}(w)|^2 \ , \tag{4.14}$$

where

$$|\mathcal{F}(w)|^2 \equiv \frac{|h_{A_1}|^2}{g(w)} \sum_{i=\pm,0} |H_i(w)|^2 \ , \tag{4.15}$$

and $g(w) = 1 + 4w(1 - 2wr_* + r_*^2)/[(1+w)(1-r_*)^2]$. The helicity functions $H_i(w)$, given by Eqs. (3.101), depend on the form factor ratios $R_1(w)$ and $R_2(w)$ defined by Eqs. (3.102) and (3.103), respectively. For phenomenological studies one uses a parametrization suggested by Caprini, Lellouch and Neubert (CLN) [184] which has the form of power expansions in the variable $z = \frac{\sqrt{w+1}-\sqrt{2}}{\sqrt{w+1}+\sqrt{2}}$,

$$h_{A_1}(w) = h_{A_1}(1)\left[1 - 8\rho_*^2 z + \left(53\rho_*^2 - 15\right)z^2 - \left(231\rho_*^2 - 91\right)z^3\right] \ , \tag{4.16}$$

$$R_1(w) = R_1(1) - 0.12(w-1) + 0.05(w-1)^2 \ , \tag{4.17}$$

$$R_2(w) = R_2(1) + 0.11(w-1) - 0.06(w-1)^2 \ . \tag{4.18}$$

The functions are fitted using data from BABAR [185], Belle [186], and the rescaled ones by the Heavy Flavor Averaging Group (HFAG) [79]. For $|V_{cb}|$ the latest exclusive value [43]

$$|V_{cb}| = (38.7 \pm 1.1) \times 10^{-3} \ , \tag{4.19}$$

is taken into account during the fit. In Table 4.2 the fit parameters and the results for $h_{A_1}(w)$ at the kinematical point $w = w^*_{\text{max}}$ are presented. For these fits the rescaled values from HFAG for $|V_{cb}|\,\mathcal{F}(1)$ and the slope parameter ρ_*^2 are used. Note that

Table 4.2.: Parameters and results for the $h_{A_1}(w)$ fits at $w = 1$ and $w = w^*_{\text{max}}$.

HFAG [79]			
Parameter	BABAR (global)	Belle	Average
$\lvert V_{cb}\rvert\,\mathcal{F}(1)$	$35.7 \pm 0.2 \pm 1.2$	$34.3 \pm 0.2 \pm 1.0$	36.04 ± 0.52
ρ^2_*	$1.20 \pm 0.02 \pm 0.07$	$1.29 \pm 0.04 \pm 0.03$	1.24 ± 0.04
total correlation	0.73	0.14	0.23
$h_{A_1}(1)$	0.92 ± 0.04	0.89 ± 0.04	0.93 ± 0.03
$h_{A_1}(w^*_{\text{max}})$	0.54 ± 0.08	0.49 ± 0.05	0.53 ± 0.02

they are different from the ones published by BABAR [185] and Belle [186], because the values from the experiments are rescaled to common $R_1 = 1.410 \pm 0.049$ and $R_2 = 0.844 \pm 0.027$ by the HFAG.
The results for $\mathcal{F}(1) = h_{A_1}(1)$ are consistent with the most recent result obtained in unquenched lattice QCD, $h_{A_1}(1) = 0.921 \pm 0.013 \pm 0.020$ [187]. Statistical and systematical errors are added in quadrature and the total correlations are taken into account. Note that for the fits only the global BABAR, Belle, and the HFAG average for $\lvert V_{cb}\rvert\,\mathcal{F}(1)$ and ρ^2_* are applied. Using the sum rule for $A_1^{BD^*}(q^2 = 0)$ and relation (4.10) one gets

$$\left[h_{A_1}(w^*_{\text{max}})\right]_{\text{LCSR}} = 0.65 \pm 0.12 \pm [0.11]_{f_B} \pm [0.07]_{f_{D^*}} \,, \tag{4.20}$$

where the errors are estimated by varying m_c, λ_B, and the Borel parameter M. The sum rule prediction (4.20) is somewhat larger than the extracted form factors from experimental data, but still consistent within uncertainties, depicted in Fig. 4.2 (a). For the slope parameter ρ^2_* one obtains comparing the sum rule predictions at $w = 1.3$ and w^*_{max} with the CLN-parametrization

$$\left[\rho^2_*\right]_{\text{LCSR}} = 0.81 \pm 0.22 \,. \tag{4.21}$$

The form factor ratios $R_1(w)$ and $R_2(w)$ from the combination of sum rules are given by

$$\left[R_1(w^*_{\text{max}})\right]_{\text{LCSR}} = 1.32 \pm 0.04 \,, \quad \left[R_2(w^*_{\text{max}})\right]_{\text{LCSR}} = 0.91 \pm 0.17 \,. \tag{4.22}$$

For the fits to the experimental data the reported ratios from BABAR [188] and Belle [189] as well as the HFAG average are used. The fit results are collected in Table

Table 4.3.: Parameters and fit results for $R_1(w)$ and $R_2(w)$ at the kinematical points $w = 1$ and $w = w^*_{\text{max}}$.

Parameter	BABAR [188]	Belle [189]	HFAG [79]
$R_1(1)$	$1.429 \pm 0.061 \pm 0.044$	$1.401 \pm 0.034 \pm 0.018$	1.410 ± 0.049
$R_2(1)$	$0.827 \pm 0.038 \pm 0.022$	$0.864 \pm 0.024 \pm 0.008$	0.844 ± 0.027
$R_1(w^*_{\text{max}})$	1.38 ± 0.22	1.35 ± 0.13	1.36 ± 0.05
$R_2(w^*_{\text{max}})$	0.87 ± 0.15	0.90 ± 0.09	0.88 ± 0.03

4.3, and compared with the ligh-cone sum rule prediction shown in Fig. 4.2 (b). Note that possible correlations are neglected for the fits. The sum rule ratios are in good agreement with the experimental data.

4.2.2. Semileptonic $\bar{B} \to D\ell\bar{\nu}$ Decay

The decay rate (3.97) for the semileptonic $\bar{B} \to D\ell\nu_\ell$ can be written in the form

$$\frac{d\Gamma(\bar{B} \to D\ell\bar{\nu})}{dw} = G_0(w)\frac{w-1}{w+1}(1+r)^2 \, |V_{cb}|^2 \, |\mathcal{G}(w)|^2 \ , \tag{4.23}$$

with the combination of the form factors $h_+(w)$ and $h_-(w)$ within a single function

$$\mathcal{G}(w) = h_+(w) - \frac{1-r}{1+r}h_-(w) \ . \tag{4.24}$$

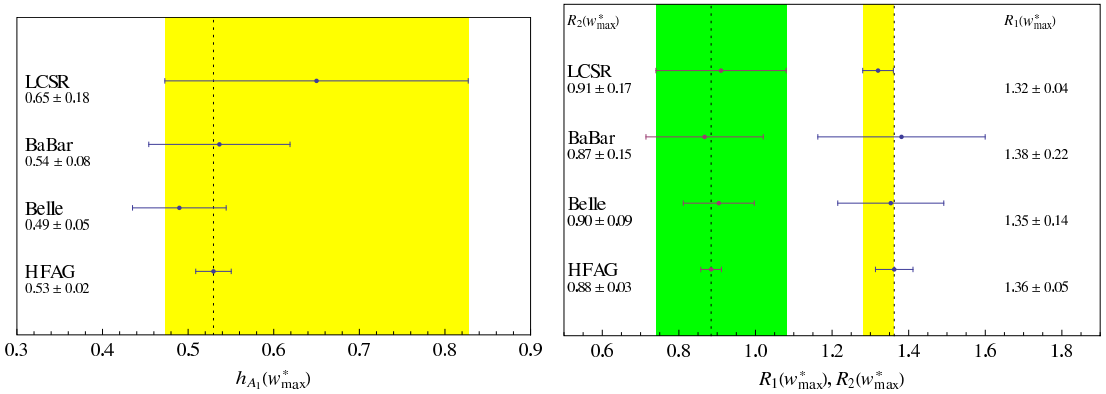

(a) $h_{A_1}(w^*_{\text{max}})$ fit results

(b) $R_1(w^*_{\text{max}})$ and $R_2(w^*_{\text{max}})$ fit results

Figure 4.2.: Comparison of the $\bar{B} \to D^*$ fit results at the kinematical point $w = w^*_{\text{max}}$ using the CLN parametrizations (4.16)–(4.18).

Table 4.4.: Parameters and fit results for $\mathcal{G}(1)$ and $\mathcal{G}(w_{\max})$ as explained in the text.

HFAG [79]			
Parameter	BABAR (tagged)	BABAR (global)	Average
$\lvert V_{cb}\rvert\,\mathcal{G}(1)$	$42.3 \pm 1.90 \pm 1.0$	$43.1 \pm 0.8 \pm 2.1$	$42.3 \pm 1.90 \pm 1.0$
ρ^2	$1.20 \pm 0.09 \pm 0.04$	$1.20 \pm 0.04 \pm 0.06$	$1.18 \pm 0.04 \pm 0.04$
total correlation	0.7	0.63	0.88
$\mathcal{G}(1)$	1.09 ± 0.06	1.11 ± 0.07	1.09 ± 0.05
$\mathcal{G}(w_{\max})$	0.59 ± 0.05	0.60 ± 0.05	0.59 ± 0.04

For this function the CLN-parametrization [184] is given by

$$\mathcal{G}(w) = \mathcal{G}(1)\left[1 - 8\rho^2 z + \left(51\rho^2 - 10\right) z^2 - \left(252\rho^2 - 84\right) z^3\right] \ . \tag{4.25}$$

The fit results for the kinematical points $w = 1$, $w = w_{\max}$, and the latest value for exclusive $|V_{cb}|$ (4.19), based on the BABAR data and the HFAG average for $|V_{cb}|\mathcal{G}(1)$ and the slope parameter ρ^2 are presented in Table 4.4. Using the sum rules for $f^+_{BD}(0)$ and $[f^+_{BD}(0) + f^-_{BD}(0)]$, relation (4.8) and the CLN-parametrization (4.25) one gets

$$[\mathcal{G}\,(w_{\max})]_{\text{LCSR}} = 0.61 \pm 0.11 \pm [0.10]_{f_B} \pm [0.07]_{f_D} \ , \tag{4.26}$$

$$\left[\rho^2\right]_{\text{LCSR}} = 1.15 \pm 0.15 \ , \tag{4.27}$$

which are in reasonable agreement with the experimental fits, shown in Fig. 4.3. Here, instead of the reported data from BABAR[190, 191] the rescaled ones from HFAG are used and again possible correlations are neglected.

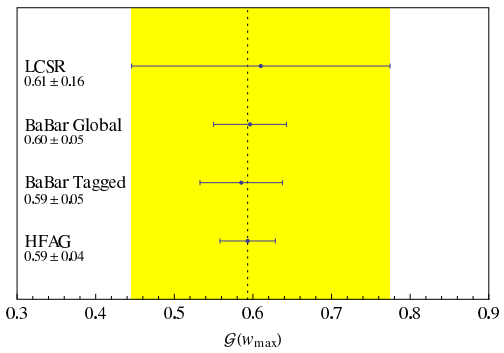

Figure 4.3: Comparison of $\mathcal{G}(w_{\max})$ fit results using the CLN parametrization (4.25).

4.2.3. Heavy-Quark Symmetry Limit

In the heavy-quark symmetry limit the form factors $h_+(w)$, $h_V(w)$, and $h_{A_1}(w)$, and $h_{A_3}(w)$ become a single function $\xi(w)$, the Isgur-Wise function, whereas the form factors $h_-(w)$ and $h_{A_2}(w)$ vanish. For the Isgur-Wise function the limiting sum rule is given by Eq. (4.13). In order to compare the sum rule predictions with the heavy-quark symmetry relations one has to rescale the masses and decay constants of heavy mesons,

$$m_B = m_Q + \bar{\Lambda} \,, \qquad m_{D^{(*)}} = \kappa m_Q + \bar{\Lambda} \,, \tag{4.28}$$

$$f_B = \frac{\hat{f}}{\sqrt{m_Q}} \,, \qquad f_{D^{(*)}} = \frac{\hat{f}}{\sqrt{\kappa m_Q}} \,, \tag{4.29}$$

furthermore, the threshold and Borel parameter have to be redefined.

$$s_0^{D^{(*)}} = (\kappa m_Q)^2 + 2\,\kappa m_Q\,\beta_0 \,, \qquad M^2 = 2\,\kappa m_Q \,, \tag{4.30}$$

with the ratio $\kappa = m_c/m_b$, and $m_b \to m_Q$. Using these rescalings and redefinitions, and the same input parameters as for the finite-mass sum rules, one gets for the Isgur-Wise function at maximum recoil, $\xi(w_{\rm max}) = 0.72$, which is of the same order as the three-point sum rule predictions [92]. With finite charm-quark mass neither $h_+(w_{\rm max}) = 0.56$, nor $h_{A_1}(w^*_{\rm max})$ confirmed the heavy-quark symmetry relations at maximum recoil. However the evolution of the form factor $h_{A_1}(w)$ from its central value (4.20) at finite m_c to the heavy quark limit depicted in Fig. 4.4 shows that light-cone sum rule for $h_{A_1}(w^*_{\rm max})$ tends to $\xi(w^*_{\rm max}) = 0.73$ for $m_c = \kappa m_Q$ at $m_Q \to \infty$. Note that $R_{1,2}(w_{\rm max}) \neq 1$ determines the symmetry violation for the remaining $B \to D^*$ form factors.

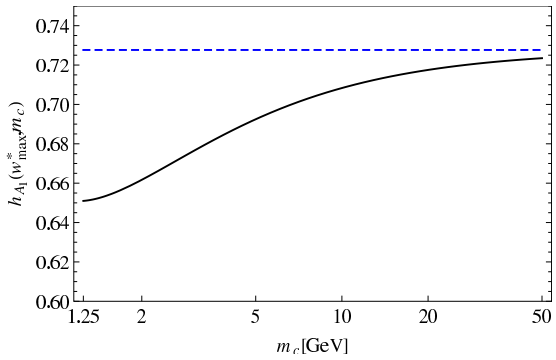

Figure 4.4: Form factor $h_{A_1}(w^*_{\rm max})$ dependence on the charm-quark mass m_c (*solid*). Heavy-quark limit (*dashed*), at central values of the input parameters, at maximum recoil $w^*_{\rm max}$ [170].

4.3. Conclusions

The new light-cone sum rules implementing B-meson distribution amplitudes, developed by Khodjamirian *et al.* [169] are used at finite charm-quark mass to obtain sum rules for the form factors of exclusive semileptonic $\bar{B} \to D^{(*)}\ell\bar{\nu}$ transitions. However the predictions can be trusted only at large recoils $w \sim w_{\max}$ because light-cone sum rules are only valid in this kinematic regime. Obtaining the sum rules at the finite c-quark mass allows to investigate the deviations from heavy-quark effective theory. The quark-hadron duality in the charmed meson channel used here is better understood and presumably introduces smaller systematic uncertainty than the duality ansatz in double dispersion relations used for three-point sum rules. Moreover, the achieved sum rules and the ones in Ref. [169] can be combined in order to calculate the ratios of $B \to \pi, \rho$ and $B \to D^{(*)}$ form factors, employing the same approach and input to extract the ratio $|V_{ub}|/|V_{cb}|$.
The accuracy of the investigation could be improved by a better knowledge of the B-meson distribution amplitudes, decay constants, and calculating gluon radiative corrections to the correlation function, including the renormalization of the B-meson distribution amplitudes.

QCD light-cone sum rule predictions are restricted to the kinematical region of large-recoil, together with limiting factors discussed above, they are not suitable for search of new physics effects in exclusive $\bar{B} \to D^{(*)}$ decays. The form factors presented so far have been calculated using a standard-model-like $(V-A)$ left-handed hadronic current structure. In the next chapter an investigation of $\bar{B} \to D^{(*)}$ transitions are discussed by taking a helicity violating right-handed hadronic current into account. However, in this exploration the kinematical region is restricted near zero-recoil $w \to 1$.

5

New Physics in $B \to D^{(*)}\ell\bar{\nu}_\ell$ Decays

Within the previous chapters exclusive $\bar{B} \to D^{(*)}$ transitions are studied standard-model-like. The hadronic current $\mathcal{J}^\mu_{\text{had}}$ is treated as a combination of vector ($V_\mu = \gamma_\mu$) and axial vector ($A_\mu = \gamma_\mu\gamma_5$) currents, reflecting the $(V-A)$ charged current structure in weak interaction physics. Parity violation is implemented in the standard model by associating left- and right-handed leptons and quarks (2.1) with different weak quantum numbers, but there is a lack of knowledge about the underlying symmetry breaking mechanism in weak interactions with respect to parity transformations. However, measurements in the leptonic sector confirm parity violation, e.g. by the measurement of the Michel parameters of muon decay. Limits on right-handed admixture in weak $b \to c$ transitions are recently tested by analysing BABAR data: exclusive $\bar{B} \to D^{(*)}\ell\bar{\nu}$ decays are much more sensitive on helicity violating admixtures than inclusive decays [192]. However, in the hadronic sector uncertainties present in the hadronic matrix elements of the quark currents restrict the extraction of different helicity structures in the charged current.

As discussed in Sec. 2.1.1, the Dirac γ-matrices are assigned with the Clifford algebra $\mathcal{C}\ell(1,3)$ of the Minkowski space-time. Combinations of the 16 dimensional basis elements of these algebra, represented by the γ-matrices, $\mathbb{1}$, γ_5, $\sigma_{\mu\nu}$, and $\sigma_{\mu\nu}\gamma_5$ can physically interpreted as scalar (S), pseudoscalar (P), tensor (T) and pseudotensor (PT) current, respectively. From these currents additional hadronic matrix elements can be constructed. In Ref. [193] the behaviour of these form factors in the heavy-quark symmetry limit is studied.

Here the $\bar{B} \to D^{(*)}$ decay amplitudes are investigated by implementing right-handed admixture in the hadronic current analogously as presented in [194]. The used $\bar{B} \to D^{(*)}\ell\bar{\nu}$ kinematic variables are defined in Chap. 3.

The outline of this chapter is as follows: In the first part of this chapter the exclusive semileptonic $\bar{B} \to D^{(*)}\ell\bar{\nu}$ hadronic form factors and decay rates including helicity violating parameters are discussed. Furthermore, the QCD short-distance radiative corrections for the additional Dirac structures in the hadronic currents are numerically analysed. Finally, bounds on right-handed admixtures are presented by using recent data for $\bar{B} \to D^{(*)}$ decays from the B-factories published by the Heavy Flavor Averaging Group (HFAG).

5.1. Form Factors and Decay Rates

For an analysis of the helicity violating admixture in exclusive semileptonic $\bar{B} \to D^{(*)}$ transitions the hadronic current is modified and lead to differential decay rates containing helicity violating coefficients, reflecting the right-handed admixture.
First, the form factors parametrizing the scalar, pseudoscalar, tensor and pseudotensor current hadronic matrix elements - usually suppressed in the standard model - are discussed by applying heavy-quark effective theory. With these additional form factors and the right-handed admixture in the hadronic current the $\bar{B} \to D^{(*)}\ell\bar{\nu}$ decay rates are calculated.

5.1.1. Scalar, Pseudo-Scalar, Tensor and Pseudo-Tensor Form Factors

For the vector and the axial vector current the form factors for $b \to c$ transition matrix elements are given by Eqs. (3.94)–(3.94). The decomposition of the matrix elements (3.58), where $\Gamma = \mathbb{1}, \gamma_5, \sigma_{\mu\nu}, \sigma_{\mu\nu}\gamma_5$ are the scalar, pseudoscalar, tensor and pseudotensor current, respectively, yield

$$\frac{\left\langle D\left(p'\right)\left|\bar{c}b\right|\bar{B}(p)\right\rangle}{\sqrt{m_B m_D}} = h_S(w)\,, \tag{5.1}$$

$$\frac{\left\langle D\left(p'\right)\left|\bar{c}\sigma_{\mu\nu}b\right|\bar{B}(p)\right\rangle}{\sqrt{m_B m_D}} = i\left(v'_\mu v_\nu - v'_\nu v_\mu\right) h_T(w)\,, \tag{5.2}$$

$$\frac{\left\langle D^*\left(p',\boldsymbol{\varepsilon}\right)\left|\bar{c}\gamma_5 b\right|\bar{B}(p)\right\rangle}{\sqrt{m_B m_{D^*}}} = \left(\boldsymbol{\varepsilon}^*\cdot v\right) h_P(w)\,, \tag{5.3}$$

$$\begin{aligned}\frac{\left\langle D^*\left(p',\boldsymbol{\varepsilon}\right)\left|\bar{c}\sigma_{\mu\nu}b\right|\bar{B}(p)\right\rangle}{\sqrt{m_B m_{D^*}}} &= -\epsilon_{\mu\nu\alpha\beta}\left[\varepsilon^{*\alpha}\left(v+v'\right)^\beta h_{T_+}(w)\right.\\ &\left.+\,\varepsilon^{*\beta}\left(v'-v\right)^\alpha h_{T_-}(w) + v'^\alpha v^\beta\left(\boldsymbol{\varepsilon}^*\cdot v\right) h_{T'}(w)\right]\,,\end{aligned} \tag{5.4}$$

$$\frac{\left\langle D^*(p',\boldsymbol{\varepsilon})\left|\bar{c}\sigma_{\mu\nu}\gamma_5 b\right|\bar{B}(p)\right\rangle}{\sqrt{m_B m_{D^*}}} = \left(v_\mu\varepsilon_\nu^* - v_\nu\varepsilon_\mu^*\right)h_{PT_1}(w) + \left(v'_\mu\varepsilon_\nu^* - v'_\nu\varepsilon'_\mu\right)h_{PT_1}(w) + (\boldsymbol{\varepsilon}\cdot v)\left(v_\mu v'_\nu - v_\nu v'_\mu\right)h_{PT_3}(w)\,. \tag{5.5}$$

Associating the bottom and charm flavour with an SU(4), the heavy-quark spin-flavour symmetry is SU(4) ⊗ SU(4). In this symmetry limit the form factors become a single scalar function,

$$\frac{h_S(w)}{1+w} = h_T(w) = h_P(w) = h_{T_+}(w) = h_{PT_1}(w) = h_{PT_2}(w) = \xi(w)\,, \tag{5.6}$$

where the function $\xi(w)$ is normalized at zero-recoil, $\xi(1) = 1$. The form factors $h_{T_-}(w)$ and $h_{T'}(w)$ vanish in this symmetry limit. Applying the Ademollo-Gatto theorem[1] [195] one finds that the form factors (5.6) get second-order power corrections

$$h_S(1) = 2\left[1+\mathcal{O}\left(k^2/m_Q^2\right)\right]\,,\quad h_P(1) = 1+\mathcal{O}\left(\sqrt{k^2}/m_Q\right)\,,$$
$$h_T(1) = 1+\mathcal{O}\left(\sqrt{k^2}/m_Q\right)\,,\quad h_{T_+}(1) = 1+\mathcal{O}\left(k^2/m_Q^2\right)\,,$$

whereas the power corrections of the form factors $h_{T_-}(1)$ and $h_{T'}(1)$ are of order $\sqrt{k^2}/m_Q$. Here, k_μ is the scale of soft-gluon momenta, not integrated out in the effective Lagrangian [193].
With these set of hadronic form factors the $\bar{B}\to D^{(*)}$ decay rates are calculated, done in the next subsection involving a helicity violating right-handed hadronic current.

5.1.2. New-Physics Decay Rates

Within the standard model the semileptonic $\bar{B}\to D^{(*)}$ decay rates in Sec. 3.3.4 are deduced from the $(V-A)$ hadronic current structure. Effects from energy scales higher than the standard model one can be included since the standard model itself is considered as an effective field theory. If these effects act on a high scale $\Lambda_{\rm NP}$ in this framework, any effect from this scale will be suppressed by inverse powers of $\Lambda_{\rm NP}$. Expanding the Lagrangian at the weak scale in inverse powers of $\Lambda_{\rm NP}$ yields

$$\mathcal{L} = \mathcal{L}_0 + \frac{1}{\Lambda_{\rm NP}}\mathcal{L}_1 + \frac{1}{\Lambda_{\rm NP}^2}\mathcal{L}_2 + \dots\,, \tag{5.7}$$

[1] The Ademollo-Gatto theorem states in its original form that matrix elements of a charge operator can deviate from their symmetry values only to second order in symmetry breaking. Luke's theorem [161] used in Sec. 3.3.4 is a renormalization-free reminiscent of it.

where in leading order $\mathcal{L}_0$ is the 4-dimensional standard model Lagrangian $\mathcal{L}_{\rm SM}$. The higher order (dimensional) Lagrangians have to be invariant under $\mathsf{SU(2)}_L \otimes \mathsf{U(1)}_Y$ symmetry. For quarks there is no 5-dimensional $\mathsf{SU(2)}_L \otimes \mathsf{U(1)}_Y$ invariant operator, therefore, in the expansion (5.7) the next-to-leading order involve only 6- or higher-dimensional operators. Hence, the number of operators is limited and can be found, e.g. in Ref. [196]. Including only operators up to dimension 6, and integrating out the W-boson, the generalized hadronic $b \to c$ current is given by [197]

$$\begin{aligned}\mathcal{J}_{\text{had},\mu} =& \mathfrak{e}_L \bar{c}\, \gamma_\mu P_L\, b + \mathfrak{e}_R \bar{c}\, \gamma_\mu P_R\, b + \mathfrak{g}_L \bar{c}\, \frac{i\overleftrightarrow{D}_\mu}{m_b} P_L\, b + \mathfrak{g}_R \bar{c}\, \frac{i\overleftrightarrow{D}_\mu}{m_b} P_R\, b \\ &+ \mathfrak{d}_L\, \frac{i\partial^\nu}{m_b} \left(\bar{c}\, i\sigma_{\mu\nu} P_L\, b\right) + \mathfrak{d}_R\, \frac{i\partial^\nu}{m_b} \left(\bar{c}\, i\sigma_{\mu\nu} P_R\, b\right) \,, \end{aligned} \tag{5.8}$$

where P_R (P_L) denotes the projector of positive (negative) chiral duality (2.18), D_μ is the QCD covariant derivative, the curly coefficients denote coupling constants for the different Dirac structures, and the left-right derivative is defined as $\bar{\psi}\overleftrightarrow{\partial}\psi = \bar{\psi}(\partial\psi) - (\partial\bar{\psi})\psi$.

Gauge invariance for the scalar operator, entering as a derivative in the current, is protected by the $\bar{c} i \overleftrightarrow{D}_\mu b$ operator structure. For the tensor contribution $\bar{c} i\sigma_{\mu\nu} b$ the only possible gauge invariant operator is $i\partial^\nu(\bar{c} i\sigma_{\mu\nu} b)$ [157].

Considering the b quark with four-velocity v, as well as the c quark with four-velocity v' as heavy quarks, the associated heavy-quark fields are h_v^b and $h_{v'}^c$, respectively. In the heavy-quark limit the current (5.8) becomes

$$\begin{aligned}\mathcal{J}^{\rm HQ}_{\text{had},\mu} =& \mathfrak{e}_L \bar{h}^c_{v'} \gamma_\mu P_L h^b_v + \mathfrak{e}_R \bar{h}^c_{v'} \gamma_\mu P_R h^b_v + \mathfrak{g}_L t_{+\mu} \bar{h}^c_{v'} P_L h^b_v + \mathfrak{g}_R t_{+\mu} \bar{h}^c_{v'} P_R h^b_v \\ &+ \mathfrak{d}_L t^\nu_- \left(\bar{h}^c_{v'} i\sigma_{\mu\nu} P_L h^b_v\right) + \mathfrak{d}_L t^\nu_- \left(\bar{h}^c_{v'} i\sigma_{\mu\nu} h^b_v\right) \,, \end{aligned} \tag{5.9}$$

where $t_{\pm\mu} = (m_b v_\mu \pm m_c v'_\mu)$. Using the leptonic tensor $L^{\mu\nu} = 2(p_\ell^\mu p_{\bar{\nu}}^\nu + p_\ell^\mu p_{\bar{\nu}}^\nu - g^{\mu\nu} p_\ell \cdot p_{\bar{\nu}} - i\epsilon^{\alpha\nu\beta\mu} p_{\ell\alpha} p_{\bar{\nu}\beta})$, where the momenta of the lepton ℓ and its antineutrino are p_ℓ and $p_{\bar{\nu}}$, respectively, the decay rate could be derived in the standard way.

For $\bar{B} \to D\ell\bar{\nu}$ transition the function $|\mathcal{G}(w)|^2$, Eq. (4.24), in the semileptonic decay rate (4.23) with helicity violating contributions yields

$$\left|\mathcal{G}^{\rm NP}(w)\right|^2 = \left[c_+ - \frac{m_B d_+ \left(r^2 - 2rw + 1\right) - 2m_B r g_+ (w+1)}{1+r}\right]^2 \left|\hat{\xi}(w)\right|^2 , \tag{5.10}$$

where the notation $c_\pm = (\mathfrak{e}_L \pm \mathfrak{e}_R)$, $d_\pm = (\mathfrak{d}_L \pm \mathfrak{d}_R)$ and $g_\pm = (\mathfrak{g}_L \pm \mathfrak{g}_R)$ is used. The helicity functions (3.101) for $\bar{B} \to D^* \ell \bar{\nu}$ decay with right-handed admixture are

$$\begin{aligned}
|H_\perp(w)|^2 &= \left|H_+^{\rm NP}(w)\right|^2 + \left|H_-^{\rm NP}(w)\right|^2 \\
&= 2\frac{1-2wr_*+r_*^2}{(1-r_*)^2}\Big\{[c_- + d_- m_B(r_*-1)]^2 \\
&\quad + \frac{w-1}{w+1}[c_+ + d_+ m_B(r_*+1)]^2\Big\}\,, \\
\left|H_\parallel(w)\right|^2 &= \left|H_0^{\rm NP}\right|^2 \\
&= \left[c_- - \frac{2g_- m_B r_*(w-1) + d_- m_B(1-2r_* w + r_*^2)}{1-r_*}\right]^2 .
\end{aligned} \tag{5.11}$$

In the enhanced current (5.8) the term proportional to $\mathfrak{e}_L$ contains the standard model contribution. Setting $c_\pm \equiv 1$ in the Eqs. (5.10) and (5.11) one finds

$$\left|\mathcal{G}^{\rm NP}(w)\right|^2 = \left|\mathcal{F}^{\rm NP}(w)\right|^2 = \left|\hat{\xi}(w)\right|^2\,, \tag{5.12}$$

which is consistent with the standard model prediction in the heavy-quark limit [198]. In this limit the hadronic factors coincides with the Isgur-Wise function $\xi(w)$. The normalization of the function $|\hat{\xi}(w)|$ is determined by Luke's theorem up to second-order power corrections, $\hat{\xi}(1) = 1 + \mathcal{O}(1/m^2)$.

The standard model is contained in the coefficient $\mathfrak{e}_L = 1 + \mathcal{O}(\phi^2_{\rm VEV}/\Lambda^2_{\rm NP})$, where $\phi^2_{\rm VEV}$ is the vacuum expectation value from spontaneous symmetry breaking. All other coefficients are associated with new physics effects. Within an effective field approach these coefficients are of second-order in $\phi^2_{\rm VEV}/\Lambda^2_{\rm NP}$. In particular, $\mathfrak{e}_R = \mathcal{O}(\phi^2_{\rm VEV}/\Lambda^2_{\rm NP})$, and all helicity changing contributions are expected additively suppressed by a small Yukawa coupling [197, 199]. Neglecting $d_\pm$ and $g_\pm$ the authors of Ref. [192] claimed for the ratio $\mathfrak{e}_R/\mathfrak{e}_L$ for exclusive semileptonic $b \to c$ transition $0.05^{+0.33}_{-0.50}$ and for the inclusive decay 0.01 ± 0.03. Hence, this could not explain the tension between $|V_{cb}|_{\rm excl}$ and $|V_{cb}|_{\rm incl}$ [43], however, new physics contributions are not excluded.

Calculating the decay rates with the hadronic form factors Eqs. (5.1)–(5.5), results presented in App. B, the hadronic form factors are associated with the coupling constants, $c_\pm$, $d_\pm$, and $g_\pm$, where the coefficients $d_\pm$ and $g_\pm$ assumed to be small, which is used in Sec. 5.3 for an estimate on the ratio c_+/c_-.

5.2. New Physics Contributions in Heavy-Quark Symmetry

Allowing new physics contributions in the exclusive semileptonic $\bar{B} \to D^{(*)}\ell\bar{\nu}$ decay rates additional coefficients are present which are discussed in the previous section. The measured decay rates contain standard model as well as new physics contributions. From the experimental data the hadronic form factors $|V_{cb}|\,\mathcal{F}(1)$ and $|V_{cb}|\,\mathcal{G}(1)$ for $B \to D$ and $B \to D^*$ transitions, respectively, are extracted by using the Caprini, Lellouche and Neubert parametrizations [184] for them; these parametrizations are discussed in Sec. 4.2. The parametrizations contain a slope parameter determining the behaviour of the Isgur-Wise function near zero-recoil. New physics contributions originated from the heavy-quark current (5.9) appear in this slope parameter. This is subject of discussion in the first part of this section. Finally, the radiative corrections including the Dirac structure for scalar, pseudoscalar, tensor, and pseudotensor appearing in the enhanced hadronic current (5.8) are presented, and numerically analysed.

5.2.1. Slope Parameter

Experimentally measured $\bar{B} \to D^{(*)}\ell\bar{\nu}$ decay rates contain standard model as well as possible new physics contributions. Following Ref. [200] the standard model contributions are extracted from the decay rates. For simplification one defines, $M(w) = |V_{cb}|^2|\mathcal{G}(w)|^2$ and $M^*(w) = |V_{cb}|^2|\mathcal{F}(w)|^2$ for $B \to D$ and $B \to D^*$ decays, respectively. In the heavy quark limit, $M(w)$ and $M^*(w)$ become simultaneously $|V_{cb}|^2|\xi(w)|^2$. At zero-recoil the Isgur-Wise function is normalized $\xi(1) = 1$ and the CKM-matrix element $|V_{cb}|$ can be extracted model independently. The behaviour of the Isgur-Wise function close to zero-recoil is determined by the slope parameter $\rho^2 > 0$, defined by $\xi(1)' = -\rho^2$, where the expansion around zero-recoil is given by

$$\xi(w) = \xi(1)\left[1 - \rho^2(w-1) + \mathcal{O}\left((w-1)^2\right)\right] . \tag{5.13}$$

In the standard model one finds for the slope

$$\begin{aligned}\rho^2 &= \frac{1}{2M(1)}\frac{\partial M(w)}{\partial w}\bigg|_{w=1} = \frac{1}{2M_\perp^*(1)}\frac{\partial M_\perp^*(w)}{\partial w}\bigg|_{w=1} \\ &= \frac{1}{2M_\parallel^*(1)}\frac{\partial M_\parallel^*(w)}{\partial w}\bigg|_{w=1} = \frac{1}{2M^*(1)}\frac{\partial M^*(w)}{\partial w}\bigg|_{w=1} ,\end{aligned} \tag{5.14}$$

where $M_\perp^*(w)$ and $M_\parallel^*(w)$ refer to the the transverse ($\perp$) and longitudinal ($\parallel$) mode of the $\bar{B} \to D^*\ell\bar{\nu}$ decay, respectively. Since right-handed admixture is allowed, these

relations do not hold. At zero-recoil one obtained from Eq. (5.10) and the helicity functions Eqs. (5.11),

$$M(1) = |V_{cb}|^2 \, |\xi(1)|^2 \left[c_- - \frac{(1-r)^2 m_B d_+ - 4 m_B r g_+}{1+r} \right] , \tag{5.15}$$

$$M^*(1) = |V_{cb}|^2 \, |\xi(1)|^2 \, [c_- - (1-r_*) m_B d_-]^2 = \frac{3}{2} M_\perp^*(1) = 3 M_\parallel^* , \tag{5.16}$$

and the slopes become in the symmetry limit,

$$\begin{aligned} \rho^2_{\mathrm{HQL}} + \rho^2_{\mathrm{NP}} &= \frac{-1}{2|\mathcal{G}^{\mathrm{NP}}_{\mathrm{HQL}}(1)|^2} \frac{\partial |\mathcal{G}^{\mathrm{NP}}_{\mathrm{HQL}}(w)|^2}{\partial w}\bigg|_{w=1} , \quad (B \to D) , \\ \rho^2_{\mathrm{HQL}} + \rho^2_{*\mathrm{NP}} &= \frac{-1}{2|\mathcal{F}^{\mathrm{NP}}_{\mathrm{HQL}}(1)|} \frac{\partial |\mathcal{F}^{\mathrm{NP}}_{\mathrm{HQL}}(w)|^2}{\partial w}\bigg|_{w=1} , \quad (B \to D^*) , \end{aligned} \tag{5.17}$$

where the new physics containing slopes are given by

$$\rho^2_{\mathrm{NP}} = \frac{2 r m_B (d_+ + g_+)}{m_B d_+ (r-1)^2 - (r+1) c_+ - 4 r m_B g_+} , \tag{5.18}$$

$$\begin{aligned} \rho^2_{*\mathrm{NP}} = \frac{1}{6} \Bigg\{ 1 - \left(\frac{c_+ + m_B (r_*+1) d_+}{c_- + m_B (r_*-1) d_-} \right)^2 \\ + \frac{4 m_B r_* (d_- - g_-)}{(r_*-1)[c_- + m_B (r_*-1) m_B]} \Bigg\} . \end{aligned} \tag{5.19}$$

For the transverse and longitudinal decay modes the corresponding slopes are collected in App. B. The presented formulae provide analysis methods for new physics contributions, one of them is discussed in Sec. 5.3.

5.2.2. Radiative Corrections

Luke's theorem protect some of the form factors at zero-recoil, however, from the kinematic suppressed form factors at zero-recoil there are corrections of order $1/m_Q$ and radiative corrections which are neglected in the previous discussions. For the $(V-A)$ standard-model-like current-structure the radiative corrections are well studied and have become textbook material, see, e.g., Refs. [34, 85, 133, 201].

Radiative corrections for the scalar, pseudoscalar, tensor, and pseudotensor currents are calculated and exhaustively discussed in Refs. [157, 200]. These corrections can be calculated in QCD, using the dimensional regularization scheme [202]. For the subtraction of divergences the modified minimal subtraction scheme $\overline{\mathrm{MS}}$ [203] is used. In this scheme the space-time is analytically continued to dimension $D = 4 - 2\epsilon$, with

infinitesimal ϵ. Divergences are eliminated by renormalization of fields and parameters in the QCD-Lagrangian (2.42), generally

$$\begin{aligned} G^a_{0\mu} &= \sqrt{Z_3} G^a_\mu \,, & q_0 &= \sqrt{Z_q} q \,, \\ g_{s0} &= Z_g g_s \mu^\epsilon \,, & m_{q0} &= Z_m m_q \,, \end{aligned} \tag{5.20}$$

where the subscript "0" refers to unrenormalized (bare) quantities, Z_i are the renormalization constants, G^a_μ is the gluon field, and μ is an arbitrary mass scale, making the QCD coupling constant g_s dimensionless in $D = 4-2\epsilon$ dimensions. Inserting the renormalized fields and parameters in the QCD-Lagrangian (2.42) the quark kinetic term becomes $\mathcal{L} = \bar{q}(i\not{\partial} - m_q)q + (Z_q - 1)\bar{q} i\not{\partial} q - (Z_q Z_m - 1) m_q \bar{q} q$, $q \in \{b, c\}$, for $b \to c$ transitions. The bare quantities are μ-independent, hence, the renormalization group equations are given by [204],

$$\begin{aligned} \frac{d g_s(\mu)}{d \ln \mu} &= -\epsilon g - g \frac{1}{Z_g} \frac{d Z_g}{d \ln \mu} \equiv -\epsilon g_s + \beta(g_s) \,, \\ \frac{d m_q(\mu)}{d \ln \mu} &= -\frac{1}{Z_m} \frac{d Z_m}{d \ln \mu} m_q(\mu) \,, \end{aligned} \tag{5.21}$$

where the first equation defines the β function. Introducing the shorthand $\alpha_s = g_s^2/(4\pi)$ one finds $d\alpha_s(\mu)/d\ln\mu = -2\beta_0 \alpha_s^2/(4\pi) - 2\beta_1 \alpha_s^3/(4\pi)^2$ with the coefficients $\beta_0 = (11 N_C - 2N_f)/3$, $\beta_1 = (34/3) N_C^2 - (10/3) N_C N_f - 2 C_F N_f$, and $C_F = (N_C^2 - 1)/(2N_C)$, where N_C and N_f are the numbers of colours and flavours, respectively. At one-loop order the the quark self-energy part $\Sigma_{ij}(q)$ is depicted in Fig. 5.1. Adopting the on-shell renormalization condition for the determination of the quark-field Z_q,

$$\left. \frac{\partial \Sigma_{ij}(q)}{\partial \not{q}} \right|_{\not{q} = m_q} = 0 \,, \tag{5.22}$$

yielding two conditions for the pole one finds for the renormalization constants

$$Z_q = 1 - C_F \frac{\alpha_s}{4\pi} \frac{1}{\epsilon} \,, \qquad Z_m = 1 - 3 C_F \frac{\alpha_s}{4\pi} \frac{1}{\epsilon} \,, \tag{5.23}$$

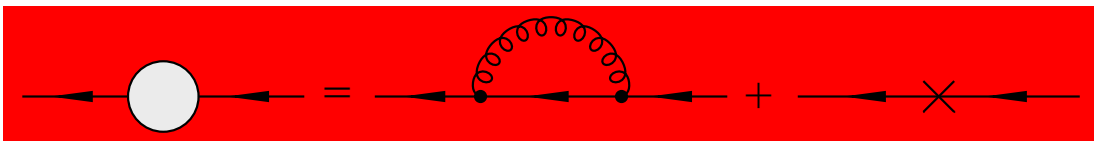

Figure 5.1.: Contributions to the quark self-energy part in QCD at one-loop order. The last term on the right-hand side represents the one-loop counter term.

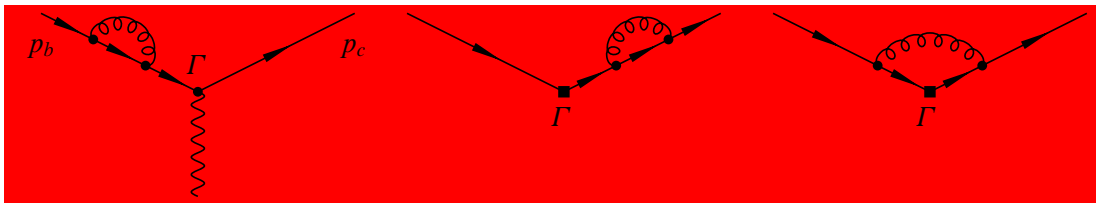

(a) One-loop diagrams for the renormalization of the different currents.

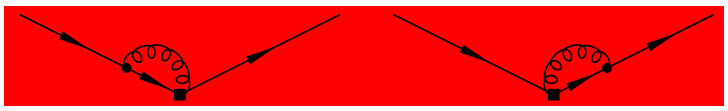

(b) Additional diagrams for the scalar and pseudoscalar vertex correction. Left-panel (right-panel): The gluon is absorbed form the bottom (charm)-quark.

Figure 5.2.: Renormalization diagrams at one-loop order. Incoming bottom-quark with momentum $p_b = m_b v$ and outgoing charm-quark with momentum $p_c = m_c v$ have the same velocity v.

where ϵ is defined in the $\overline{\text{MS}}$ scheme. The correction of the wave function is defined by Eq. (5.22). The calculation of the vertex corrections shown in Fig. 5.2 is straightforward. Since the current (5.8) is used, scalar, pseudoscalar, vector, axial vector, and tensor operators, listed in Table 5.1, contribute to the vertex correction. In the case of scalar and pseudoscalar currents at order α_s a quark-quark-gluon-boson vertex from the covariant derivative being of order g_s appears, and hence this vertex is neglected at tree-level. However, rendering the scalar and pseudoscalar one-loop corrections gauge invariant the vertex is calculated up to order α_s. Note that the vertex can be read off from the Lagrangian $\bar{\psi}_{L/R} m_b \bar{c} g_s G^a_\mu T^a P_{L/R} b$ and is given by $\bar{\psi}_{L/R} m_b g_{\mu\nu} T^a P_{L/R}$, where the index μ is the couplings to the W-boson in the leptonic current and the

Table 5.1.: Contribution to the vertex correction from the different operators.

Operator	Vertex correction $i\Gamma$
$\mathcal{Q}_S = p_b^\mu + p_c^\mu$	$(m_b + m_c)\gamma^\mu + \frac{\alpha_s}{4\pi}\frac{C_F(m_b+m_c)\gamma^\mu}{2(m_b^2-m_c^2)}\Big[-3(m_b^2-m_c^2)\frac{1}{\epsilon} - 3\log\frac{m_c^2}{m_b^2} m_c m_b$ $+\left(6\log\frac{m_b^2}{\mu^2} - 3\log\frac{m_c^2}{\mu^2} - 13\right)m_b^2 - \left(6\log\frac{m_c^2}{\mu^2} - 3\log\frac{m_b^2}{\mu^2} - 13\right)m_c^2\Big]$
$\mathcal{Q}_V = \gamma_\mu$	$\gamma^\mu + \frac{\alpha_s}{4\pi} C_F \gamma^\mu \left[-6 - 3\frac{m_b+m_c}{m_b-m_c}\log\frac{m_c}{m_b}\right]$
$\mathcal{Q}_A = \gamma_\mu\gamma_5$	$\gamma^\mu\gamma^5 + \frac{\alpha_s}{4\pi} C_F \gamma^\mu\gamma^5 \left[-8 - 3\frac{m_b+m_c}{m_b-m_c}\log\frac{m_c}{m_b}\right]$
$\mathcal{Q}_P = \gamma_5$	$\frac{\alpha_s}{4\pi}\frac{C_F\gamma^\mu\gamma^5}{2}\left[\frac{3(m_b-m_c)}{\epsilon} + \left(-3\log\frac{m_b^2}{\mu^2} + 7\right)m_b + \left(3\log\frac{m_c^2}{\mu^2} - 7\right)m_c\right]$
$\mathcal{Q}_T = (p_{bv} - p_{cv})(-i\sigma^{\mu\nu})$	0

index ν is associated with the outgoing gluon.
The explicit calculations of the Feynman diagrams Fig. 5.2 at zero-recoil can be found in Ref. [157] and should not be repeated here. Note that for the calculation the naïve dimensional regularization scheme with anticommuting γ_5 [205] is used. The vertex corrections $i\Gamma$ for the different operators are listed in Tab. 5.1. In the heavy-quark limit at zero-recoil, the corrections η_Γ to the form factors are computed from the finite parts of the vertex corrections $i\Gamma$. For $\Gamma \in \{S, P, V, A, T\}$, one finds for the short-distance radiative corrections

$$\eta_S = 1 + \frac{\alpha_s}{8\pi}\frac{C_F}{m_b^2 - m_c^2}\left[-3\log\frac{m_c^2}{m_b^2}m_c m_b + \left(6\log\frac{m_b^2}{\mu^2} - 3\log\frac{m_c^2}{\mu^2} - 13\right)m_b^2 - \left(-3\log\frac{m_b^2}{\mu^2} + 6\log\frac{m_c^2}{\mu^2} - 13\right)m_c^2\right], \tag{5.24}$$

$$\eta_P = \frac{\alpha_s}{4\pi}\frac{C_F}{2(m_b + m_c)}\left[\left(-3\log\frac{m_b^2}{\mu^2} + 7\right)m_b + \left(3\log\frac{m_c^2}{\mu^2} - 7\right)m_c\right], \tag{5.25}$$

$$\eta_V = 1 + C_F\frac{\alpha_s}{4\pi}\left[-6 - 3\frac{m_b + m_c}{m_b - m_c}\log\frac{m_c}{m_b}\right], \tag{5.26}$$

$$\eta_A = 1 + C_F\frac{\alpha_s}{4\pi}\left[-8 - 3\frac{m_b + m_c}{m_b - m_c}\log\frac{m_c}{m_b}\right], \tag{5.27}$$

$$\eta_T = 0\,. \tag{5.28}$$

The vector (5.26) and axial-vector (5.27) corrections are in agreement with radiative corrections calculated in the heavy-quark limit, e.g. presented in Ref. [133].
For a numerical analysis one used the quark masses $m_b = 4.8$ GeV and $m_c = 1.44$ GeV, and for the coefficient $C_F = \frac{4}{3}$. The coupling constant in the $\overline{\text{MS}}$ renormalization scheme is taken at the renormalization scale at the geometric mean mass $\mu = \sqrt{m_b m_c}$. Adopting $\alpha_s(\sqrt{m_b m_c}) = 0.24$ [206], one finds for the vector and axial vector short-distance radiative corrections at one-loop order

$$\eta_V \approx 1.02\,, \qquad \eta_A \approx 0.967\,. \tag{5.29}$$

The latest results from lattice QCD [163, 164] yield

$$\mathcal{G}(1) = 1.074 \pm 0.018 \pm 0.016\,, \qquad \mathcal{F}(1) = 0.9077 \pm 0.0051 \pm 0.0158\,, \tag{5.30}$$

where for $\mathcal{F}(1)$ the systematic errors are added in quadrature. Up-to two-loop order the QCD corrections are given by $\eta_V = 1.022 \pm 0.004$ and $\eta_A = 0.960 \pm 0.007$ [207]. The uncertainty for η_A at zero-recoil is dominated by the error in the $1/m_Q^2$ corrections [92, 207, 208].

The coefficient functions for scalar, pseudoscalar and tensor currents are analogously defined as the ones for vector and axial-vector currents. In order to get dimensonless factors η_S and η_T, the $m_b + m_c$ and $m_b - m_c$ structures are excluded, respectively. Since the anomalous dimension does not vanish for scalar and pseudoscalar cases, one used $\mu = m_b(m_c)$ and $\alpha_s(m_b(m_c)) = 0.22(0.30)$ as an indicator for the error. From the Eqs. (5.24) and (5.25) one gets $\eta_S \approx 1.03^{+0.06}_{-0.04}$ and $\eta_P \approx 0.002^{+0.023}_{-0.030}$. The sign of the corrections as well as the handedness of the scalar current can not be judged from this analysis [200].

New physics contributions are discussed in this section originated from the right-handed current structures (5.8). These contributions appear in the hadronic form factors describing the exclusive semileptonic $\bar{B} \to D^{(*)}\ell\bar{\nu}$ transitions. In the heavy-quark limit these form factors become a solely function, the Isgur-Wise function, being determined near zero-recoil by the slope parameter as discussed above. The form factors $\mathcal{G}(w)$ and $\mathcal{F}(w)$ as well as the slopes are affected by new physics parameters. The achieved formulae (5.10) and (5.11) for the form factors and the slopes (5.17) can be used for analysing these new physics effects. Note that (5.17) present the contributions to the form factors separated into transversal and longitudinal $\bar{B} \to D^*\ell\bar{\nu}$ decay modes. For those form factors which are not vanish at zero-recoil, due to Luke's theorem, the leading corrections are of order $1/m_Q^2$, while for the vanishing form factors the corrections are in general linear in $1/m_q$, $q \in \{b, c\}$. Beside these corrections there are QCD short-distance radiative corrections. For the new Dirac structures appearing in the $b \to c$ current (5.8) these corrections are calculated at zero-recoil by using relations from heavy-quark effective theory [157, 200].
Information about the helicity violating right-handed admixtures are contained in the functions $\mathcal{G}(w)$ and $\mathcal{F}(w)$.
The $h_i(w)$ form factors seem to be more suitable for such an investigation, hence, in the next section bounds on the right-handed admixtures are investigated by using the these form factors.

5.3. Analysis of Right-handed Admixtures

The B-factories have collected high precision data for exclusive semileptonic $\bar{B} \to D^{(*)}\ell\bar{\nu}$ decays since a couple of years. The values for $|V_{cb}|\,\mathcal{F}(1)$ and $|V_{cb}|\,\mathcal{G}(1)$, and the corresponding slope parameters at zero-recoil reported by them are rescaled on common values for $R_1(1)$ and $R_2(1)$ as explained in Sec. 4.2 and listed by the HFAG

[79]. The latest experimental results are depicted in Fig. 5.3. Using the hadronic current (5.8) with right-handed current structures new physics contributions appear in the form factors $\mathcal{G}(w)$ and $\mathcal{F}(w)$ for exclusive semileptonic $\bar{B} \to D\ell\bar{\nu}$ and $\bar{B} \to D^*\ell\bar{\nu}$ transitions, respectively. The form factors including such contributions are presented in App. B. In the following bounds on right-handed admixture are extracted by restricting on vector and axial-vector currents, and assuming the Caprini, Lellouch and Neubert parametrization for the Isgur-Wise function.

Expanding $\mathcal{G}(w)$ and $\mathcal{F}(w)$ around the kinematic point $w = 1$ and comparing the result with the parametrization of the Isgur-Wise function (5.13) one finds for the slope

$$\rho^2 = \frac{-1}{2|\hat{\xi}(1)|^2} \frac{\partial |\hat{\xi}(w)|^2}{\partial w}\bigg|_{w=1} , \tag{5.31}$$

where for the both form factors the common notation $\hat{\xi}(w)$ is used. The slope for $B \to D$ transition at the kinematical point $w = 1$ is given by

$$\rho^2 = -\frac{h'_+(1) - \frac{1-r}{1+r}h'_-(1)}{h_+(1) - \frac{1-r}{1+r}h_-(1)} \quad \xrightarrow{\text{HQL}} \quad -\frac{\xi'(1)}{\xi(1)} , \tag{5.32}$$

since the derivative $h'_-(1)$ vanish in the symmetry limit. The slope ρ^2 is independent from left and right coefficients; hence, one sets $\rho^2 \equiv \rho^2_{\text{SM}}$. For $B \to D^*$ transitions the

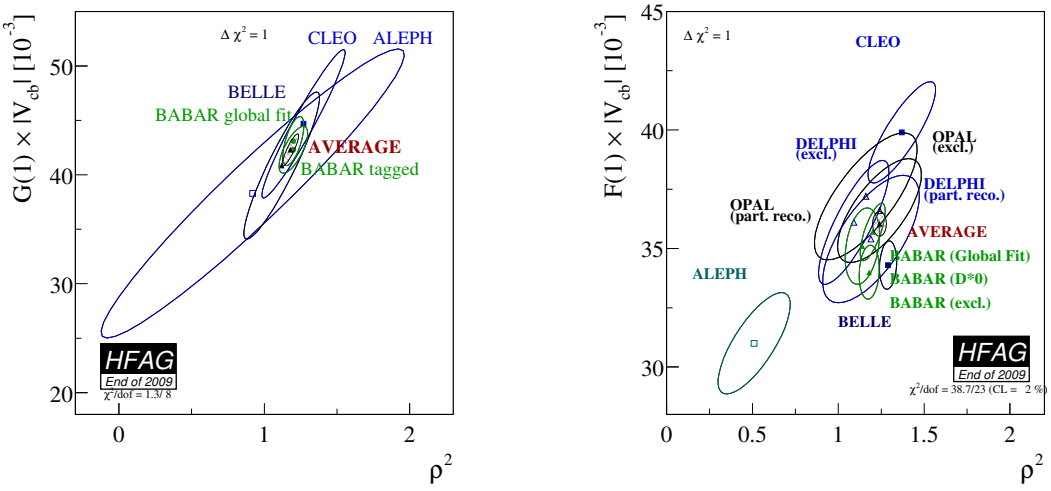

Figure 5.3.: Latest results for $|V_{cb}|\,\mathcal{G}(1)$ and $|V_{cb}|\,\mathcal{F}(1)$ from exclusive semileptonic $B \to D$ and $B \to D^*$ decays published by the HFAG.

slope can be calculated by using Eqs. (B.4) and (B.5), and the standard model slope can be separated from the new physics one. Therefore, the ratio c_+/c_- is given by

$$\left(\frac{c_+}{c_-}\right)^2 = 1 - 6\frac{\rho_*^2 - \rho^2}{R_1^2(1)} \,, \tag{5.33}$$

which measures the strength of the right-handed admixture. Using the latest HFAG averages for ρ^2 and ρ_*^2 one achieved as an estimate for the right-handed admixture $c_+/c_- = 0.90 \pm 0.09$, where correlations between the errors are not taken into account and $R_1(1) = 1.41 \pm 0.049$, which is used from HFAG for rescaling, as explained in Sec. 4.2.

For zero-recoil the $B \to D$ transition is dominated by the vector current, and the $B \to D^*$ transition by the axial-vector current. In this limit one finds from Eqs. (B.2) and (B.6), $M(1) = c_+^2 |V_{cb}|^2 |\mathcal{G}(1)|^2$ and $M^*(1) = c_-^2 |\mathcal{F}(1)|^2$, respectively.

Another constraint can directly derived from the experimental data. Assuming that the experimental results, $|V_{cb}|\,\mathcal{G}(1) = (42.3 \pm 1.48) \times 10^{-3}$ and $|V_{cb}|\,\mathcal{F}(1) = (36.04 \pm 0.52) \times 10^{-3}$ contain right-handed admixtures one finds for the ratio

$$\frac{c_+}{c_-} = 0.99 \pm 0.05 \,, \tag{5.34}$$

where for $\mathcal{G}(1)$ and $\mathcal{F}(1)$ the latest lattice QCD data (5.30) are used[2]. Both ratios are in agreement with the standard model prediction $(c_+/c_-)_{\rm SM} \equiv 1$.

5.4. Conclusions

Within the leptonic sector there are stringent limits on the non-standard contributions from various sources, e.g. the measurement of the μ and τ decay parameters. The admixture of right-handed contributions for charged leptons is below 1%. A mass limit of right-handed W-bosons is given by electroweak fits, $m_{W_R} > 715$ GeV, which yields a right-handed admixture in the charged currents of $\epsilon_R < 1.3\%$ [43]. Non-standard couplings in inclusive semileptonic $\bar{B} \to X_c \ell \bar{\nu}$ transitions are studied, e.g. in Refs.[192, 194, 197], using higher dimension operators. New physics effects in the charged hadronic currents are originated from the dimension six operators, while the leptonic current does not contains any right-handed admixtures.

Adopting the charged current (5.8) suggested in Ref. [197] additional hadronic form factors, namely scalar, pseudoscalar, tensor, and pseudotensor ones, have to be regarded. In the heavy-quark limit the form factors reduce to the universal Isgur-Wise

[2]The errors of the lattice values are added in quadrature. Correlations between the values are neglected.

function, normalized at zero-recoil $\xi(1) = 1$. Its well-established parametrization stems from Caprini, Lellouch and Neubert [184]. Using this parametrization, the behaviour of the Isgur-Wise function near zero-recoil is determined by the slope ρ^2 (ρ_*^2) for $B \to D$ ($B \to D^*$) transitions.
QCD short-distance radiative corrections as well as non-perturbative $1/m_Q^2$ corrections are well studied for the standard-model-like $(V - A)$ hadronic current structure. For the additional appearing Dirac structures in the hadronic current (5.8) the perturbative QCD short-distance radiative corrections at one-loop order are calculated, which lead to sizeable effects.
The received new physics contributions containing slopes and form factors at zero-recoil are compared with precision data from the B-factories. As an bound for right-handed admixtures one finds for the ratio $c_+/c_- = 0.90 \pm 0.09$, and, taking lattice QCD data into account, 0.99 ± 0.05. The results are in reasonable agreement with the standard model prediction for this ratio $(c_+/c_-)_{\rm SM} \equiv 1$.
However, the analysis does not exclude right-handed admixtures in exclusive semileptonic $\bar{B} \to D^{(*)}$ transitions. Due to the high precision data from the B-factories a future more sophisticated analysis is expected to decrease the bounds for helicity violating admixture more precisely as the naïve numerical analysis, which has been done in this chapter.
In the next chapter the search for new physics contributions in B-meson decays is enhanced taking nonleptonic B-meson decays, explicitly $B_s^0 \to J/\psi\phi$ and $B^0 \to J/\psi K_{S,L}$ decays, into account, where new physics contributions are manifested in CP-violating effects in the time-dependent angular distribution of the corresponding decay products.

6

New Physics in $b \to s$ Decays

Symmetries and their breaking play an important rôle for the new physics search. For semileptonic B-meson decays the heavy-quark spin symmetry is an adequate tool for such search as discussed in Chap. 5. Furthermore these decays allow precise determinations of the Cabbibo-Kobayashi-Maskawa (CKM) matrix elements $|V_{cb}|$ and $|V_{ub}|$, while from nonleptonic decays such high precision could not achieved.

Precise measurements of the angles α, β and γ of the unitary angle (UT) are a main task in particle physics. B-meson systems provide within the standard model (SM) several suitable decay channels for precise predictions for CP violation [209] depicted in Fig. 6.1 for some prominent decay channels which are differently sensitive to the angles of the unitarity triangle.

In a recent paper [210] CP violation in nonleptonic B-decays are discussed using

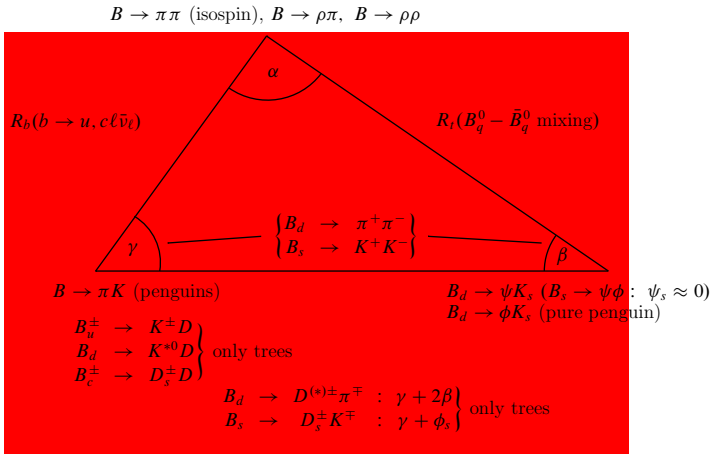

Figure 6.1.: Overview of prominent B-meson decays for exploring of CP violation [24].

flavour symmetries, where for non-standard contributions in nonleptonic $b \to s$ transitions U-spin[1] breaking is taken into account. Flavour symmetries and their application to B-decays [211–216] as well as the extraction of CP-violating parameters by using flavour-symmetry methods are discussed in the literature, see, e.g. Refs. [217–220].

This chapter is denoted to the CP-violating effects in the time-dependent angular distribution of the $B_s^0 \to J/\psi[\to \ell^+\ell^-]\phi[\to K^+K^-]$ decay products, expected to be small in the standard model. In $B_s^0 - \bar{B}_s^0$ mixing CP-violating new physics contributions are assumed to be a preferred mechanism to accommodate a measurement of nonvashing CP-asymmetries [221].

CP violation can also be studied in $B_d^0 - \bar{B}_d^0$ mixing, where the "golden modes" $B^0 \to J/\psi K_{S,L}$ are considered to be clean probes for this phenomenon [72–74, 222–224]. The exploration of CP-violating effects in B-meson decays is done by the CDF and DØ Collaborations at Tevatron [225] and is a main target of the LHCb [19] experiment at CERN.

The discussion presented here has been published in Refs. [226, 227]. In Sec. 6.1 the $B_s^0 \to J/\psi\phi$ analysis and the exploration of the impact of the penguin effects on the measurement of ϕ_s is discussed, taking into account the strategy to include hadronic penguin contributions by using the $B_s^0 \to J/\psi \bar{K}^{*0}$ channel. These strategies are converted to the golden modes $B^0 \to J/\psi K_{S,L}$ in Sec. 6.2. A detailed discussion of the SU(3)-breaking effects and internal consistence checks offered by the observables of B-meson decays into two vector mesons are presented in Sec. 6.3. Conclusions of these discussions are given in Sec. 6.4.

6.1. $B \to J/\psi\phi$

In order to explore CP-violating effects in B_s-meson decays the key channel is $B_s^0 \to J/\psi\phi$, which is the counterpart of the "gold-plated" decay $B_d^0 \to J/\psi K_s$, to measure the angle β in the unitary triangle [72–74].

In this section the CP-violating observables in the $B_s^0 \to J/\psi\phi$ channel are studied, discussing CP violation in the angular distributions (Sec. 6.1.1) and in the decay amplitude (Sec. 6.1.2), where the $B_s^0 \to J/\psi \bar{K}^{*0}$ decay as a control channel is introduced. The time-dependent observables are briefly reviewed in Sec. 6.1.3. These

[1] U-spin is an SU(2) subgroup of flavour SU(3), under which the pair of down- and strange-quarks is a doublet, similar to (u, d) in isospin.

observables get an impact of penguin contributions (Sec. 6.1.4), which could be controlled by hadronic parameter provided by the $B_s^0 \to J/\psi \bar{K}^{*0}$ channel (Sec. 6.1.5).

6.1.1. Structure of Angular Distribution

$B_s^0 \to J/\psi[\to \ell^+\ell^-]\phi[\to K^+K^-]$ decay mediated by the quark transition $b \to \bar{s}c\bar{c}$ is the key channel for this investigation. In the final state there are two vector mesons, leading to an admixture of CP-odd and CP-even eigenstates. These can be disentangled by using the angular distribution of the decay products. To this aim linear polarization states of vector mesons are introduced, which are longitudinal (0) or transverse to the direction of motion. The transverse polarization states may be parallel ($\|$) or perpendicular ($\perp$) to one another [228]. Generally, the time-dependent angular distributions can be written as [229]

$$f\,(\Theta,\Phi,\Psi;t) = \sum_k g^{(k)}\,(\Theta,\Phi,\Psi)\,b^{(k)}(t)\,, \tag{6.1}$$

$$\bar{f}\,(\Theta,\Phi,\Psi;t) = \sum_k \bar{\mathcal{O}}^{(k)}(t)\bar{g}^{(k)}\left(\bar{\Theta},\bar{\Phi},\bar{\Psi}\right)\,, \tag{6.2}$$

for $B_s^0 \to J/\psi\phi$ and its CP conjugate decay $\bar{B}_s^0 \to J/\psi\phi$, respectively. Here $g^{(k)}(\Theta,\Phi,\Psi)$ describes the decay kinematics, and the time-dependent coefficients $b^{(k)}(t)$ are $|A_{f\in\{0,\|,\perp\}}(t)|^2$, $\Re\{A_0^*(t)A_\|(t)\}$, and $\Im\{A_{f\in\{0,\|\}}A_\perp(t)\}$, with linear polarization amplitudes $A_f = \langle (J/\psi\phi)_f|\mathcal{H}_{\text{eff}}|B_s^0(t)\rangle$, where $\mathcal{H}_{\text{eff}}$ is the low-energy effective Hamiltonian. Note that $A_\perp(t)$ describes a CP-odd final-state configuration, and $A_0(t)$ and $A_\perp(t)$ correspond to CP-even final-state ones. Assuming for both decays the meson content of the $J/\psi\phi$ state to be the same, the decay kinematics are described by the same angles $\Theta \equiv \bar{\Theta}$, $\Phi \equiv \bar{\Phi}$ and $\Psi \equiv \bar{\Psi}$. Hence, the effects of CP transformations relating $B_s^0 \to (J/\psi\phi)_f$ to $\bar{B}_s^0 \to (J/\psi\phi)_f$ are taken into through CP eigenvalues of the final state configuration $(J/\psi\phi)_f$, then the functions $g^{(k)}\,(\Theta,\Phi,\Psi)$ and $\bar{g}^{(k)}\left(\bar{\Theta},\bar{\Phi},\bar{\Psi}\right)$ in Eqs. (6.1) and (6.2) are equal. The explicit forms of these quantities are presented in Ref. [229].

6.1.2. Decay Amplitudes

As discussed in Sec. 3.1.3, colour-suppressed tree-diagram-like and penguin topologies contribute to the $B_s^0 \to J/\psi\phi$ decay within the standard model, which is depicted in Fig. 6.2. The decay amplitude for a given final-state configuration $f \in \{0,\|,\perp\}$

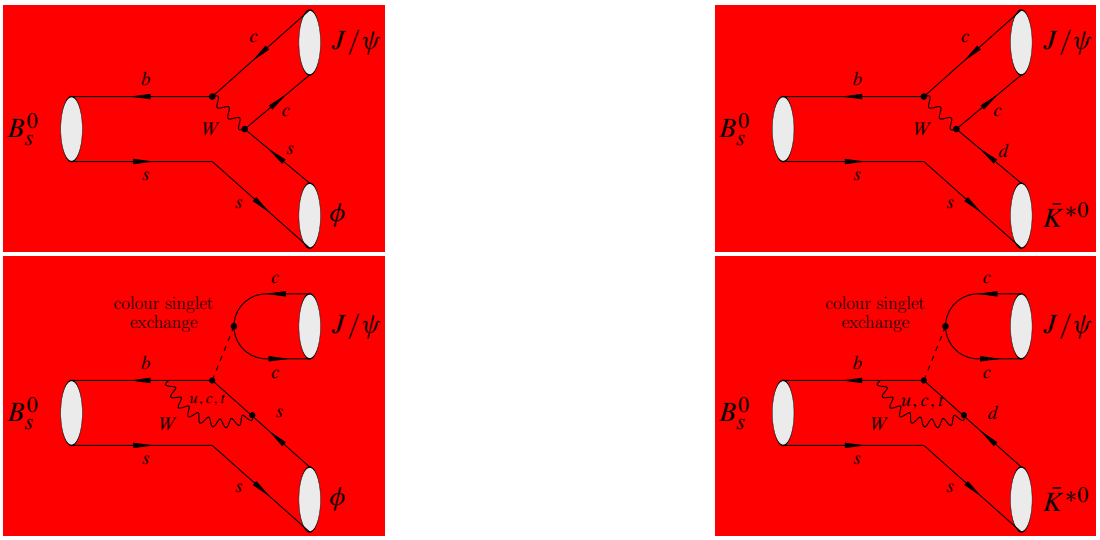

Figure 6.2.: $B_s^0 \to J/\psi\phi$ (left panel) and $B_s^0 \to J/\psi \bar{K}^{*0}$ (right panel) decay topologies in the standard model.

can be written as

$$A\left(B_s^0 \to (J/\psi\phi)_f\right) = \lambda_c^{(s)}\left[A_T^{(c)f} + A_P^{(c)f}\right] + \lambda_u^{(s)} A_P^{(u)f} + \lambda_t^{(s)} A_P^{(t)f} \,, \tag{6.3}$$

where the $\lambda_j^{(s)} \equiv V_{js}V_{jb}^*$ are CKM factors, while $A_T^{(c)f}$ and $A_P^{(j)f}$ denote CP-conserving strong amplitudes related to tree-diagram-like and penguin topologies (with internal $j \in \{u,c,t\}$ quarks), respectively. These amplitudes can be expressed in terms of linear combinations of perturbatively calculable Wilson coefficient functions and non-perturbative hadronic matrix elements of the corresponding four-quark operators using the appropriate low-energy effective Hamiltonian. The $\lambda_t^{(s)}$ factor can be eliminated by the CKM unitarity relation (2.52), one gets

$$A\left(B_s^0 \to (J/\psi\phi)_f\right) = \left(1 - \frac{\lambda^2}{2}\right)\mathcal{R}_f\left[1 + \epsilon a_f e^{i\theta_f} e^{i\gamma}\right] \,, \tag{6.4}$$

where

$$\mathcal{R}_f \equiv \lambda^2 A\left[A_T^{(c)f} + A_P^{(c)f} - A_P^{(t)f}\right] \,, \tag{6.5}$$

and

$$a_f e^{i\theta_f} \equiv R_b\left[\frac{A_P^{(u)f} - A_P^{(t)f}}{A_T^{(c)f} + A_P^{(c)f} - A_P^{(t)f}}\right] \tag{6.6}$$

Table 6.1.: CKM parameter used in Ref. [226, 227] and latest values from CKMfitter reported at ICHEP 2010.

Parameter	Refs. [226, 227]	CKMfitter [46]
$\lambda = \lvert V_{us}\rvert$	0.22521 ± 0.00083	0.22543 ± 0.00077
$A = \lvert V_{cb}\rvert/\lambda^2$	0.809 ± 0.026	$0.812^{+0.013}_{-0.027}$

are CP-conserving hadronic parameters, while $\lambda \equiv |V_{us}|$, $A = |V_{cb}|/\lambda^2$, $R_b = (1-\lambda^2/2)|V_{ub}|/(\lambda|V_{cb}|)$ and $\epsilon = \lambda^2/(1-\lambda^2)$ are CKM parameters [43], see Sec. 2.1.2 for details. For the following discussions the values from Ref. [226, 227] are used, explicitly $\lambda = 0.22521 \pm 0.00083$, $A = 0.809 \pm 0.026$, $R_b = 0.423^{+0.015}_{-0.022} \pm 0.029$ and $\epsilon = 0.053$. Note that the values for λ and A have slightly changed as shown in Table 6.1. This, however, does not change the presented analysis crucial. Considering CP-conjugate processes the UT angle γ flips its sign,

$$A\left(\bar{B}_s^0 \to (J/\psi\phi)_f\right) = \eta_f \left(1 - \frac{\lambda^2}{2}\right) \mathcal{A}_f \left[1 + \epsilon a_f e^{i\theta_f} e^{-i\gamma}\right] , \tag{6.7}$$

where η_f is the CP eigenvalue of the final-state configuration $(J/\psi\phi)_f$ defined in Eq. (2.74).

For the control channel $B_s^0 \to J/\psi \bar{K}^{*0}$, originated in $\bar{b} \to \bar{d}c\bar{c}$ transitions the CKM factors are different. The decay amplitude for this channel becomes

$$A\left(B_s^0 \to J/\psi(\bar{K}^{*0})_f\right) = \lambda \mathcal{A}'_f \left[1 - a'_f e^{i\theta'_f} e^{i\gamma}\right] , \tag{6.8}$$

where $\mathcal{A}'_f$ and $a'_f e^{i\theta'_f}$ are the counterparts of (6.5) and (6.6), respectively. This channel offers a sensitive probe for the parameter $a'_f e^{i\theta_f}$, because this parameter does not enter (6.8) in a doubly Cabibbo-suppressed way as $a_f e^{i\theta_f}$ does in (6.4). Applying SU(3) flavour symmetry of strong interactions and assuming, that penguin annihilation (PA) and exchange (E) topologies[2], contributing to $B_s^0 \to (J/\psi\phi)_f$ but without counterpart in $B_s^0 \to J/\psi \bar{K}^{*0}$, can be neglected, one obtains $|\mathcal{A}_f| = |\mathcal{A}'_f|$ as well as $a_f = a'_f$ and $\theta_f = \theta'_f$. The uncertainties associated with procedure are discussed in Sec. 6.3.

[2]These topologies can be explored with the help of $B_d^0 \to (J/\psi\phi)_f$ transitions, which amplitudes are proportional to $(PA + E)_f$. The Belle Collaboration recently reported an upper limit 9.4×10^{-7} for the branching ratio at the 90% confidence level for this decay channel [230].

6.1.3. Time-dependent Observables

For $B_q^0 - \bar{B}_q^0$ mixing ($q \in \{d, s\}$) the time-dependent observables in the standard model are presented in Sec. 2.2.2, setting $b_f = -\epsilon a_f$ in the following. Neglecting the doubly Cabbibo-suppressed part, one defines $\Gamma[f,t] \equiv \left|A_f(t)\right|^2 + \left|\bar{A}_f(t)\right|^2$, where $|A_f(t)|^2$ and $|\bar{A}_f(t)|^2$ are given by the Eqs. (2.75) and (2.76), respectively, and finds

$$\Gamma[f,t] = 2|\mathcal{N}_f|^2 \left[\left(1 + \eta_f \cos\phi_s\right) e^{-\Gamma_L^{(s)} t} + \left(1 - \eta_f \cos\phi_s\right) e^{-\Gamma_H^{(s)} t}\right] , \tag{6.9}$$

$$\left|A_f(t)\right|^2 - \left|\bar{A}_f(t)\right|^2 = 2\eta_f |\mathcal{N}_f|^2 e^{-\Gamma_s t} \sin\left(\Delta M_s t\right) , \tag{6.10}$$

where ϕ_s is the CP-violating $B_s^0 - \bar{B}_s^0$ mixing phase (2.83), and $\mathcal{N}_f \equiv (1 - \lambda^2/2)\mathcal{A}_f$. The CP-violating rate difference (6.10) required "tagging" whether initially - i. e. at the time $t = 0$ - a B_s^0 or $\bar{B}_s^0$ meson is present. For the extraction of the phase ϕ_s one uses the ratio of this "tagged" and "untagged" rate (6.9), where the overall normalization $|\mathcal{N}_f|$ cancels. The time-dependence of the other observables is discussed, e.g. in Ref. [231].

In the standard model the phase ϕ_s is fixed in terms of the Wolfenstein parameters; latest CKM fits [47] yield $\phi_s^{\rm SM} = -2\lambda^2\eta = -(0.0366 \pm 0.0015)$. However, new physics effects could enhance this value. $B_s^0 - \bar{B}_s^0$ mixing is a strongly suppressed flavour-changing neutral-current process in the standard model, it is on the other side a sensitive probe for new physics effects in the TeV regime. Since new particles contribute, the off-diagonal elements of the mixing matrix is modified as $M_{12}^s = M_{12}^{s,\rm SM}(1 + \kappa_s e^{i\sigma_s})$, where κ_s measures the relative strength of the new physics contributions and σ_s is the new physics phase [24, 221]. The B_s mixing parameters then read

$$\Delta M_s \equiv \Delta M_s^{\rm SM} \left|1 + \kappa_s e^{i\sigma_s}\right| , \tag{6.11}$$

$$\phi_s \equiv \phi_s^{\rm SM} + \phi_s^{\rm NP} = -2\lambda^2\eta + \arg\left(1 + \kappa_s e^{i\sigma_s}\right) . \tag{6.12}$$

The phase ϕ_s and the ratio $\rho_s \equiv \Delta M_s / \Delta M_s^{\rm SM}$ can be depicted as contours in the $\sigma_s - \kappa_s$ plane, setting the parameter space for new physics contributions to $B_s^0 - \bar{B}_s^0$ mixing [221]. For ΔM_s one finds from the experiments

$$\Delta M_s = \begin{cases} (18.56 \pm 0.87)\text{ps}^{-1} & \text{(DØ Collaboration [232])} , \\ (17.77 \pm 0.10 \pm 0.07)\text{ps}^{-1} & \text{(CDF Collaboration [233])} . \end{cases} \tag{6.13}$$

In order to determine the parameter ρ_s from these measurements, the standard model value of ΔM_s is required, involving a hadronic parameter $f_{B_s}^2 \hat{B}_{B_s}$ being determined

by means of lattice QCD techniques and introduces the corresponding uncertainties in the analysis. Using $\Delta M_s^{\mathrm{SM}} = 20.3(3.0)(0.8)\ \mathrm{ps}^{-1}$ from the HPQCD Collaboration [234, 235] one finds $\rho_s = 0.88 \pm 0.13$, where the errors have been naïvely added in quadrature. Data from CDF and DØ Collaborations [236] for ϕ_s, listed by the Heavy Flavor Averaging Group (HFAG) [79] yield a twofold solution,

$$\phi_s = \left(-44^{+17}_{-21}\right)^\circ \vee \left(-135^{+21}_{-17}\right)^\circ . \tag{6.14}$$

Following Ref. [221] the $\sigma_s - \kappa_s$ plane is depicted in Fig. 6.3 (left panel). The overlap of the ΔM_s (central hill-like region) and ϕ_s (two branches) constraints result in the two shaded allowed regions. These results are under the condition that the doubly Cabbibo-suppressed parameters $a_f e^{i\theta_f}$, describing the penguin to tree contributions, can be neglected. However, expecting precise data from LHCb the standard model effects must be controlled.

6.1.4. Penguin Contributions

In order to search for new physics effects, the standard model contributions must be well understood. The "untagged" observables R_L^f and R_H^f are defined in Sec. 2.2.2 in the Eqs. (2.79) and (2.80), respectively. At the time $t = 0$, Eq. (6.9) becomes

$$\Gamma[f, t = 0] = 2\left|\mathcal{N}_f\right|^2 \left[1 + 2\epsilon a_f \cos\theta_f \cos\gamma + \epsilon^2 a_f^2\right] . \tag{6.15}$$

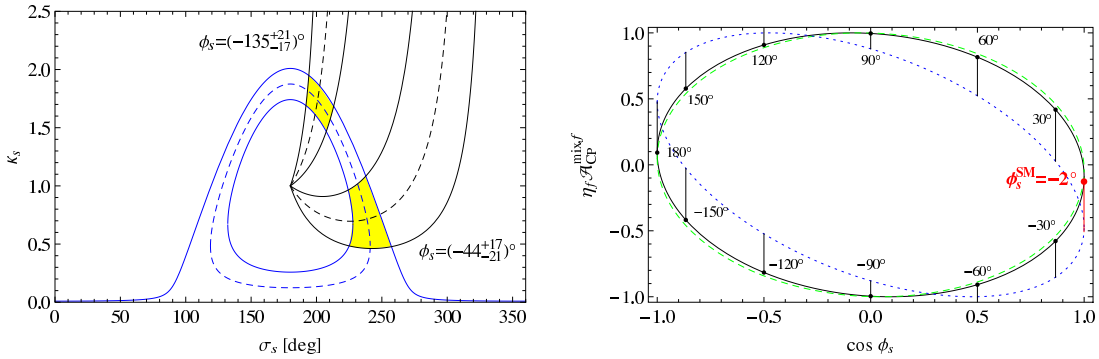

Figure 6.3.: Left panel: $\sigma_s - \kappa_s$ plane of the new physcis parameters for $B_s^0 - \bar{B}_s^0$ mixing. Right panel: Impact of the penguin parameter a_f on the mixing-induced CP-asymmetry $\eta_f \hat{A}_M^f$ for $\theta_f = 180°$, $\gamma = 65°$, and $a_f = 0.5, 1, 5$, with a dashed, solid and dotted line, respectively, as a function of the $B_s^0 - \bar{B}_s^0$ mixing angle $\cos\phi_s$ [227].

Furthermore, the CP-violating observables are given by the Eqs. (2.86)–(2.88). In Fig. 6.3 (right panel) the impact of the penguin parameter a_f is illustrated. The CP-conserving parameter $a_f e^{i\theta_f}$ is defined in such a way that $\theta_f = 180°$ in the standard model. Penguin effects for this strong phase are maximal in the mixing-induced CP-asymmetry $\mathcal{A}_{CP}^{\text{mix},f}$ since only $\cos\theta_f$ enters. However, the direct CP-asymmetries $\mathcal{A}_{CP}^{\text{dir},f}$ vanish, because they are proportional to $\sin\theta_f$.
The value for the penguin parameter a_f is unknown, but one can estimate some bounds; e.g. for $\phi_s \sim -44°$, as in (6.14), a_f is in the (unrealistic) range $2.5 - 5$. However, there are large uncertainties in a_f, hence, values as large as $0.5-1$ can not be excluded. Since the phase ϕ_s is assumed to be small, these hadronic standard model contributions lead to a significant uncertainty in $B_s^0 - \bar{B}_s^0$ mixing phase extraction [227].
This effect can be explored by using the mixing- and direct-induced CP-asymmetries. From Eqs. (2.86) and (2.87) one finds

$$\frac{\eta_f \mathcal{A}_{CP}^{\text{mix},f}}{\sqrt{1-(\mathcal{A}_{CP}^{\text{dir},f})^2}} = \sin\left(\phi_s + \Delta\phi_s^f\right) , \tag{6.16}$$

where

$$\begin{aligned} \sin\Delta\phi_s^f &= \frac{2\epsilon a_f \cos\theta_f \sin\gamma + \epsilon^2 a_f^2 \sin 2\gamma}{N_f\sqrt{1-(\mathcal{A}_{CP}^{\text{dir},f})^2}} , \\ \cos\Delta\phi_s^f &= \frac{1 + 2\epsilon a_f \cos\theta_f \cos\gamma + \epsilon^2 a_f^2 \cos 2\gamma}{N_f\sqrt{1-(\mathcal{A}_{CP}^{\text{dir},f})^2}} . \end{aligned} \tag{6.17}$$

Note that the shift $\Delta\phi_s^f$ of the $B_s^0 - \bar{B}_s^0$ mixing phase is independent from the value of ϕ_s itself. In the left panel of Fig. 6.4 the dependence of $\Delta\phi_s^f$, and in the right panel the dependence of the direct CP-asymmetries $\mathcal{A}_{CP}^{\text{dir},f}$, on the parameter a_f for various values of θ_f are depicted. For a penguin contribution $a_f \sim 0.4$ the shift $\Delta\phi_s^f$ is of the same size as ϕ_s^{SM} and a value of $a_f \sim 1$ induces a shift of order $-5°$. Furthermore the direct CP-asymmetries are in the range of $-0.05 \lesssim \mathcal{A}_{CP}^{\text{dir},f} \lesssim +0.005$ for $a_f \lesssim 1$ and values of $|\theta_f - 180|$ as large as $40°$. In the next subsection a controlling mechanism of the penguin effects by means of the angular distributions of the $B_s^0 \to J/\psi[\to \ell^+\ell^-]\bar{K}^{*0}[\to \pi^+K^-]$ and its CP conjugate is discussed.

6.1.5. Controlling the Observables

As a control channel for the penguin effects the flavour-specific decay $B_s^0 \to J/\psi[\to \ell^+\ell^-]\bar{K}^{*0}[\to \pi^+K^-]$ and its CP conjugate can be used. In the time-dependent angu-

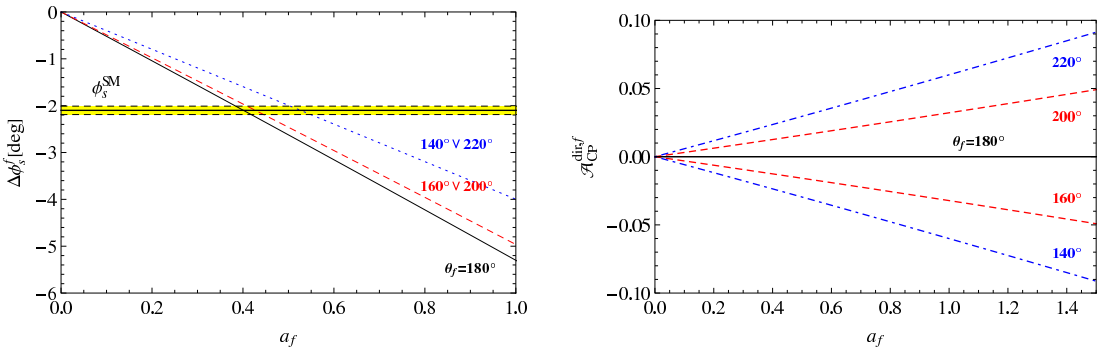

Figure 6.4.: Dependence of $\Delta\phi_s^f$ (left panel) and $\mathcal{A}_{CP}^{\mathrm{dir},f}$ (right panel) on a_f for various values of θ_f [227].

lar distributions there are no CP-violating effects between mixing and decay. Hence, the A_M^f observables (2.82) have no counterpart and they are independent from the $B_s^0 - \bar{B}_s^0$ mixing phase. The penguin parameter a_f' and the the strong phase θ_f' are determined by the untagged observables, as well as by direct CP asymmetries. In App. C the time-dependent observables are listed.

For discussing the untagged case one introduces the relation

$$H_f \equiv \frac{1}{\epsilon}\left|\frac{\mathfrak{A}_f}{\mathfrak{A}_f'}\right|^2 \frac{\Gamma[f,t=0]'}{\Gamma[f,t=0]} = \frac{1-2a_f'\cos\theta_f'\cos\gamma + a_f'^2}{1+2\epsilon a_f\cos\theta_f\cos\gamma+\epsilon^2 a_f^2}\,, \tag{6.18}$$

with $\Gamma[f,t=0]'$ being the $B_s^0 \to J/\psi\bar{K}^{*0}$ counterpart of (6.9). Using the SU(3) flavour symmetry to obtain $|\mathfrak{A}_f| = |\mathfrak{A}_f'|$, H_f can be extracted from untagged observables. Furthermore the SU(3) flavour-symmetry provides

$$a_f = a_f'\,, \quad \theta_f = \theta_f'\,, \tag{6.19}$$

hence, defining $U_{H_f} \equiv \frac{1+\epsilon H_f}{1-\epsilon^2 H_f}\cos\theta_f'\cos\gamma$ and $V_{H_f} \equiv (1-H_f)/(1-\epsilon^2 H_f)$, the penguin parameter a_f' is determined as a function of θ_f',

$$a_f' = U_{H_f} \pm \sqrt{U_{H_f}^2 - V_{H_f}}\,. \tag{6.20}$$

The SU(3) flavour-symmetry assumption $|\mathfrak{A}_f| = |\mathfrak{A}_f'|$ leads to the main uncertainty of H_f. The impact of (6.19) can be neglected because of the ϵ terms present in Eq. (6.18).

At the time $t = 0$ the direct direct CP asymmetry $\mathcal{A}_{CP}^{\mathrm{dir},f'} = (2a_f'\sin\theta_f'\sin\gamma)/(1 - 2a_f'\cos\theta_f'\cos\gamma + a_f'^2)$ is of the same form as (2.85). Using the replacements $U_{H_f} \to$

$U_{\mathcal{A}_{CP}^{\mathrm{dir},f'}} \equiv \cos\theta'_f \cos\gamma + (\sin\theta'_f \sin\gamma)/\mathcal{A}_{CP}^{\mathrm{dir},f}$ and $V_{H_f} \to V_{\mathcal{A}_{CP}^{\mathrm{dir},f'}} \equiv 1$, a_f can be determined as a function of θ'_f in analogy to (6.20). Theoretical uncertainties are related to the SU(3)-breaking effects as discussed above and studied in more detail in Sec. 6.3.

6.2. The Golden Modes $B^0 \to J/\psi K_{S,L}$

The B-decay channel $B \to J/\psi K$ is the so-called "golden mode", because the decay amplitude $A(\bar{B} \to J/\psi \bar{K})$ is dominated by a single weak phase. Hence, the time-dependent CP-asymmetry in this decay is completely determined by the $B^0 - \bar{B}^0$ mixing amplitude, involving the CKM angle β [72–74]. In the weak effective Hamiltonian (3.24) the effects from terms proportional to $V_{ub}V_{us}^*$ are small, because of the Cabbibo-suppression of $|V_{ub}V_{us}^*|$ with respect to $|V_{cb}V_{cs}^*|$, where the ratio becomes, $|V_{ub}V_{us}^*|/|V_{cb}V_{cs}^*| \sim \lambda^2 \ll 1$, and penguin suppression: first of all the current-current operators $\mathcal{Q}_{1,2}^{(u)}$ do not contain charm quarks, hence, the hadronic matrix elements $\langle J/\psi K|\mathcal{Q}_{1,2}^{(u)}|B\rangle$ are suppressed. Secondly the Wilson coefficients of the loop-induced penguin operators can be neglected compared to the tree ones. Finally the ones from electroweak penguin operators are even smaller.
Analogously to the previous section in Sec. 6.2.1 the time-dependent CP-asymmetries in the golden modes $B^0 \to J/\psi K_{S,L}$ are explored, introducing $\bar{B}^0 \to J/\psi\pi^0$ as the control channel for these decays. In Sec. 6.2.2 the strategy of the extraction of the new physics contributions is discussed.

6.2.1. Observables in $B \to J/\psi K$ Decays

The CP violation in the $B_d^0 - \bar{B}_q^0$ system is discussed in Sec. 2.2.2, and the discussion of the CP observables for $B^0 \to J/\psi K^0$ follow the lines given in the previous section. The time-dependent rate asymmetries (2.85) can be written as $\mathcal{A}_{CP}(t; f) = C(f)\cos(\Delta M_d t) - S(f)\sin(\Delta M_d t)$, where $C(f)$ and $S(f)$ are the direct and mixing-induced CP violation, respectively. In the standard model, neglecting doubly Cabbibo-suppressed contributions, one gets

$$C(J/\psi K_{S,L}) \approx 0\,, \quad S(J/\psi K_{S,L}) \approx -\eta_{S,L}\sin 2\beta\,, \tag{6.21}$$

where the CP eigenvalue η_S (η_L) is -1 ($+1$) [72–74, 222–224]. Assuming these correlations are correct, the latest values obtained from the measured $S(J/\psi K_{S,L})$

from BABAR[237] and Belle [238], averaged by the HFAG [79] yield $(\sin 2\beta)_{J/\psi K^0} = 0.655 \pm 0.0244$. Note that in the following $2\beta = \phi_d$ is used.
Analogously to $B_s^0 \to J/\psi\phi$ the decay amplitude for $B^0 \to J/\psi K_{S,L}$ is given by Eq. (6.4), where $\mathcal{R}_f$ and $a_f e^{i\theta}$ are defined as in Eqs. (6.5) and (6.6), respectively. Using the replacements $\eta_f \mathcal{A}_{CP}^{\text{mix},f} \to -\eta_{S,L} S(J/\psi K_{S,L})$ and $\mathcal{A}_{CP}^{\text{dir},f} \to -C(J/\psi K_{S,L})$, the Eq. (6.16) reads

$$\frac{-\eta_{S,L} S(J/\psi K_{S,L})}{\sqrt{1 - C(J/\psi K_{S,L})^2}} = \sin\left(\phi_d + \Delta\phi_d\right) \ . \tag{6.22}$$

The latest, over the final states $J/\psi K_S$ and $J/\psi K_L$ averaged value for the direct CP violation yields $C(J/\psi K^0) = -0.003 \pm 0.020$ [79]. Hence, the deviation of the denominator in (6.22) from one can be neglected.

Following the strategy of the previous section, one introduces the $SU(3)$ counterpart of $B_d^0 \to J/\psi K^0$. As $B_s \to J/\psi \bar{K}^0$ is not measured so far, one uses $\bar{B}^0 \to J/\psi\pi^0$. The two decays are related to each other via SU(3) in the approximation that isospin symmetry holds and the emission-annihilation parameter EA_2 can be neglected. This can be checked by using the $B \to \bar{D}^0\phi$ decay proceeding only via this diagram [239], which is done in Ref. [240]. In the standard model, the amplitude for the $\bar{B}^0 \to J/\psi\pi^0$ decay can be written as

$$A\left(\bar{B}^0 \to J/\psi\pi^0\right) = \frac{1}{\sqrt{2}}\lambda\mathcal{R}'\left[1 - a' e^{i\theta'} e^{i\gamma}\right] \ , \tag{6.23}$$

where the factor $\sqrt{2}$ refers to the π^0 wavefunction. Recent measurements from BABAR [241] and Belle [242] yield the averages [79]

$$C(J/\psi\pi^0) = -0.10 \pm 0.13 \ , \qquad S(J/\psi\pi^0) = -0.93 \pm 0.15 \ . \tag{6.24}$$

The penguin parameter a' can again be determined as a function of θ'. The counterpart of (6.20) is given by

$$a' = U_{\mathcal{O}} \pm \sqrt{U_{\mathcal{O}}^2 - V_{\mathcal{O}}} \ , \quad \mathcal{O} \in \{C, S\} \ , \tag{6.25}$$

with

$$\begin{aligned} U_C &\equiv \cos\theta' + \frac{\sin\theta' \sin\gamma}{C(J/\psi\pi^0)} \ , \quad V_C \equiv 1 \ , \\ U_S &\equiv \left[\frac{\sin(\phi_d + \gamma) + S(J/\psi\pi^0)\cos\gamma}{\sin(\phi_d + 2\gamma) + S(J/\psi\pi^0)}\right]\cos\theta' \ , \\ V_S &= \frac{\sin\phi_d + S(J/\psi\pi^0)}{\sin(\phi_d + 2\gamma) + S(J/\psi\pi^0)} \ . \end{aligned} \tag{6.26}$$

The hadronic parameters a' and θ' are fixed in the standard model by the intersection of the $C(J/\psi\pi^0)$ and $S(J/\psi\pi^0)$ contours; in order to have a constraint in the $a' - \theta'$ plane from $S(J/\psi\pi^0)$, $S(J/\psi K^0)$ has to be taken into account in order to fix the new physics phase. Another constraint is given by $C(J/\psi K^0)$, being of the form (6.25) with the replacements $a' \to \epsilon a$ and $\theta' \to 180° + \theta$. Note that since the expressions (6.25) and (6.26) follow from the standard model structure of the $\bar{B}^0 \to J/\psi\pi^0$ transition, they are exactly valid.
As argued before penguin annihilation and exchange topologies, contributing to $\bar{B}^0 \to J/\psi\pi^0$ but without counterpart in $B_d^0 \to J/\psi K^0$ and expected to be small, are neglected. In the SU(3) symmetry limit, one obtains (6.19). Using these relations together with Eq. (6.22) the shift $\Delta\phi_d$ can be determined from the data. The relations (6.19) are associated with SU(3)-breaking corrections, because of non-factorizable effects. The impact of SU(3)-breaking effects on the shift $\Delta\phi_d$ is discussed in Sec. 6.3.3.

From the CP-averaged branching ratios there is another constraint. The counterpart of the observable (6.18) becomes

$$\begin{aligned} H &\equiv \frac{2}{\epsilon}\left[\frac{\mathrm{BR}(\bar{B}^0 \to J/\psi\pi^0)}{\mathrm{BR}(B_d^0 \to J/\psi K^0)}\right]\left|\frac{\mathcal{A}}{\mathcal{A}'}\right|^2 \frac{\Phi_{J/\psi K^0}}{\Phi_{J/\psi\pi^0}} \\ &= \frac{1 - 2a'\cos\theta' + a'^2}{1 + 2\epsilon a\cos\theta\cos\gamma + \epsilon^2 a^2}\,, \end{aligned} \tag{6.27}$$

with the phase-space factors $\Phi_{J/\psi P} \equiv \Phi(M_{J/\psi}/M_{B^0}, M_P/M_{B^0})$, $P \in \{K^0, \pi^0\}$ [81]. H is extracted from data, assuming that the SU(3)-breaking corrections to $|\mathcal{A}/\mathcal{A}'|$ are factorizable, i. e. given by the ratio of two form factors, evaluated at $q^2 = M_{J/\psi}^2$. Using QCD light-cone sum rules methods [173], the latest results for the form factors at $q^2 = 0$ yield $f_{B\to K}^+(0)/f_{B\to\pi}^+(0) = 1.38^{+0.11}_{-0.11}$ [174, 243]. Using a naïve Becirevic-Kaidalov (BK) parametrization [244], the extrapolation to $q^2 = M_{J/\psi}^2$ is given by

$$f_+(q^2) = f^+(0)\left[\frac{M_B^2 M_*^2}{(M_*^2 - q^2)(M_B^2 - \alpha q^2)}\right]\,, \tag{6.28}$$

where M_*^2 denotes the mass of the ground state vector meson in the relevant channel, and the contribution of the hadronic continuum for $q^2 > M_*^2$ is modeled by the pole at M^2/α. Using $B \to \pi$ lattice data, the BK parameter α has been fitted to be $\alpha_\pi = 0.53 \pm 0.006$. However, the value α for the $B \to K$ form factor is unknown. Assuming the main SU(3)-breaking effect is due to the shift of the continuous part of the spectral

Table 6.2.: Branching fractions of neutral B-modes in units of 10^{-4} and results for H defined by (6.27).

	Refs. [227]	HFAG 2010 [79]
$\mathrm{BR}(B_d^0 \to J/\psi K^0)$	8.63 ± 0.35	8.63 ± 0.35
$\mathrm{BR}(\bar{B}^0 \to J/\psi \pi^0)$	0.20 ± 0.02	0.174 ± 0.015
H	$1.53 \pm 0.16_{\mathrm{BR}} \pm 0.27_{\mathrm{FF}}$	$1.33 \pm 0.13_{\mathrm{BR}} \pm 0.24_{\mathrm{FF}}$

function from $B \to \pi$ to the $B \to K$ threshold, one gets $\alpha_K = 0.49 \pm 0.05$, and further the extrapolation to $q^2 = M_{J/\psi}^2$ yield $f_{B\to K}^+(M_{J/\psi}^2)/f_{B\to\pi}^+(M_{J/\psi}^2) = 1.34 \pm 0.12$. Using the values for the branching fractions reported by the HFAG [79] one can calculate (6.27). The value reported in Ref. [227] for H changed slightly, because the ones for $\bar{B}^0 \to J/\psi\pi^0$ changed; the values for (6.27) are listed in Table 6.2, where the errors induced by the branching ratios and the form-factor ratio are separated.
Following Ref. [81], the Eq. (6.19) provides a probe for SU(3)-breaking effects, which can be expressed as

$$C(J/\psi K^0) = -\epsilon H C(J/\psi\pi^0)\,. \tag{6.29}$$

However, the values of H in Tab. 6.2 yield $C(J/\psi K^0) = 0.01 \pm 0.01$, being consistent with the latest value for $C(J/\psi K^0)$, but too small for a sophisticated test.
Using Eq. (6.25) with $\mathcal{O} = H$, one finds

$$U_H = \left(\frac{1+\epsilon H}{1-\epsilon^2 H}\right)\cos\theta'\cos\gamma\,, \quad V_H = \frac{1-H}{1-\epsilon^2 H}\,, \tag{6.30}$$

determining the parameter a' as a function of the strong angle θ'. In this case one has to deal with SU(3)-breaking effects, entering implicitly through the determination of H.

6.2.2. New Physics Contributions

Assuming that new physics effects in the $B^0 - \bar{B}^0$ mixing phase ϕ_d provide CP-violating, one defined the mixing phase as

$$\phi_d = 2\beta + \phi_d^{\mathrm{NP}}\,, \tag{6.31}$$

where ϕ_d^{NP} is the new physics component. Neglecting a new physics impact on the $B^0 \to J/\psi K^0$ amplitude, the relations (6.31) remain valid, with the replacement

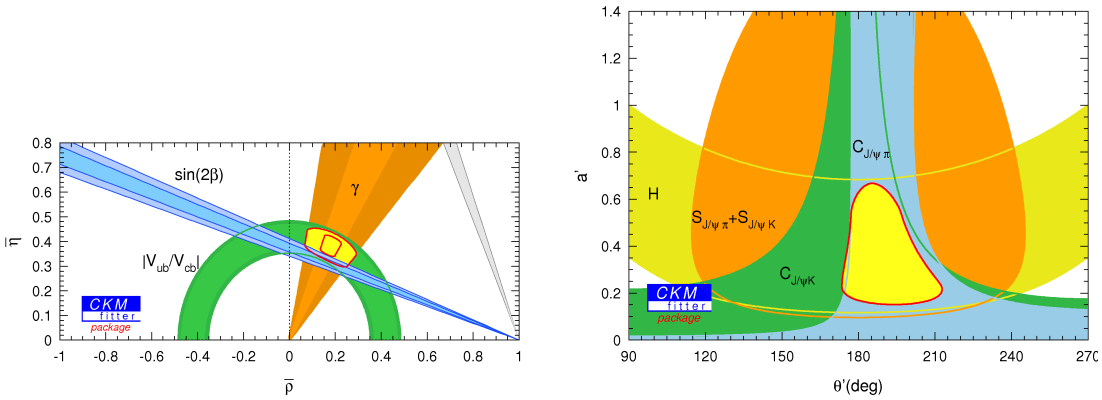

Figure 6.5.: Left panel: constraints in the $\bar{\rho} - \bar{\eta}$ plane at 1σ and 2σ ranges; right panel: 1σ ranges in the $\theta' - a'$ plane [227]. The fit procedure is exhaustively discussed in Ref. [240].

$2\beta \to \phi_d$. Including data for CP violation in $B^0 \to J/\psi K^*$ decays [79], the UT angle β can be fixed unambiguously. In Fig. 6.5 (left panel) the situation in the $\bar{\rho} - \bar{\eta}$ plane is depicted created with the CKMFITTER software [48], where generalized Wolfenstein parameters are used [44, 45], and the circle coming from the UT side R_b. From the fit the "true" value of β can be determined through R_b and tree-level extractions of γ; one gets $\beta_{\text{true}} = (24.9^{+1.0}_{-1.5} \pm 1.9)°$, which is independent of the error of the UT angle γ for a central value around 65°, and yields

$$(\phi_d)_{J/\psi K^0} - 2\beta_{\text{true}} = -\left(8.7^{+2.6}_{-3.6} \pm 3.8\right)^\circ \ . \tag{6.32}$$

Using the observables defined in the previous subsection, new physics contribution can be extracted from a fit to recent data. In Fig. 6.5 (right panel) the fit in the $\theta' - a'$ plane with 1σ ranges are shown. As expected from Eq. (6.22) $S(J/\psi\pi^0)$ is $\theta' \in [90°, 270°]$. Furthermore, $S(J/\psi K^0)$ fixes the new physics phase essentially to $(\phi_d)_{J/\psi K^0} - 2\beta_{\text{true}}$, as here new physics is an $\mathcal{O}(1)$ effect, while the additional standard model contribution is suppressed by ϵ. The negative central value of the direct CP asymmetry $C(J/\psi\pi^0)$ prefers $\theta' > 180°$, and its intersection with the H band falls into the $S(J/\psi\pi^0, J/\psi K^0)$ as well as in the $C(J/\psi K_{S,L})$ region, which yields $a' \in [0.15, 0.67]$ and $\theta' \in [174°, 213°]$ at the 1σ level. These four constraints give finally an unambiguous solution for these parameters [227].

The corresponding fit in the $\theta - \Delta\phi_d$ plane is depicted in Fig. 6.6 (left panel) with the help of Eqs. (6.17) and (6.19). The resulting shift $\Delta\phi_d$ is negative; the global fit yields $\Delta\phi_d \in [-3.9°, -0.8°]$, affected by the constraints from H and $C(J/\psi\pi^0)$, corresponding to $\phi_d = (42.4^{+3.4}_{-1.7})°$. Hence, the negative sign of the standard model

Table 6.3.: Fit results for the two scenarios discussed in the text.

Scenario	$S(J/\psi\pi^0)$	$\Delta\phi_d$	a'	θ'
(a)	-0.98 ± 0.03	$[-3.1°, -1.8°]$	~ 0.42	$\sim 191°$
(b)	-0.85 ± 0.03	$[-1.2°, -0.8°]$	~ 0.18	$\sim 201°$

correction $\Delta\phi_d$ softens tension in the fit of the UT. The range for $\phi_d^{\rm NP}$ from the fit is given by $-13.8° \leq \phi_d \leq 1.1°$, including the standard model value $\phi_d^{\rm NP} = 0°$.

Expecting high precision data from LHCb or a future Super-B factory which will constrain the hadronic parameters, two benchmark scenarios are discussed, shown in Fig. 6.6 (right panel), assuming a reduction of the experimental uncertainties of the CP asymmetries of $B_d^0 \to J/\psi K^0$ by a factor of 2, and errors of the branching ratios and γ that are five times smaller. Both scenarios agree with $C(J/\psi\pi^0) = -0.10 \pm 0.03$, but differ in $S(J/\psi\pi^0)$. The fit results for the two scenarios are listed in Table 6.3. In the high-S scenario (a) the range for $\Delta\phi_d$ is determined from lower value of S and H, assuming $H = 1.53 \pm 0.03 \pm 0.27$. In contrast in the low-S scenario (b) the range is determined by S and C alone, whilst H would only be used to rule out the second solution.

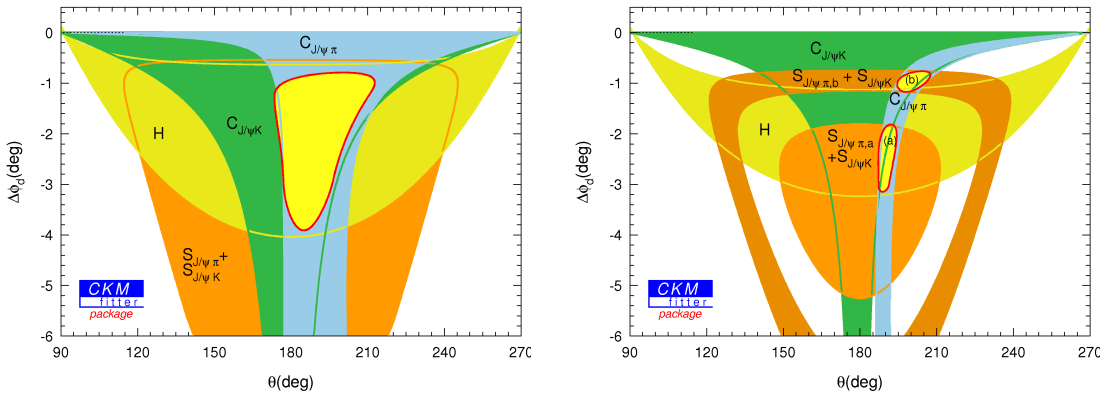

Figure 6.6.: Left panel: $\Delta\phi_d$ for the constraints shown in right panel in Fig. 6.5. Right panel: Fit for a future benchmark scenarios, as discussed in the text [227].

6.3. SU(3) Breaking Effects

Theoretical uncertainties are originated in SU(3) breaking effects in (6.19) and $\mathcal{A} = \mathcal{A}'$. In order to distinguish standard model effects from new physics ones, the understanding of SU(3) breaking is essential. In the following section the SU(3) breaking effects in the considered decays is discussed in more detail.
In Sec. 6.3.1 the $\omega - \phi$ mixing is discussed preparing the use of QCD sum rule predictions for the $B \to \bar{K}^{*0}$ form factors in Sec. 6.3.2 for the SU(3)-breaking effects to the ratio $|\mathcal{A}/\mathcal{A}'|$. The SU(3) breaking to (6.19) is studied in Sec. 6.3.3 by introducing a breaking factor ξ. Finally, in Sec. 6.3.4 some internal consistence checks of SU(3) symmetry in B-decays are presented.
For investigations of new physics effects in nonleptonic $b \to s$ transitions by using U-spin breaking see Refs. [210, 240].

6.3.1. $\omega - \phi$ Mixing

In the case of $B_s^0 \to J/\psi\phi$ transitions one deals with vector meson final states. The ϕ-meson ϕ-meson state is in good approximation an $s\bar{s}$ state, and hence a superposition of SU(3) eigenstates.
The SU(3) nonet contains three neutral, nonstrange states. Assuming isospin as a good symmetry, one of these states is the ρ-meson with the quark decomposition $\rho^0 = (u\bar{u} - d\bar{d})/\sqrt{2}$, and the other two states are isosinglets, explicitly $\phi^0 = (u\bar{u} + d\bar{d} + s\bar{s})/\sqrt{3}$, being an SU(3) singlet, and $\phi_8 = (u\bar{u} + d\bar{d} - 2s\bar{s})/4$, which belongs to the SU(3) octet. Since isospin is assumed to be unbroken, the amplitudes for processes involving the members of the octet are related to one another, while the singlet remains separate.
However, as mentioned before, the physical ϕ state is in good approximation a pure $s\bar{s}$ state. Hence, it can be considered as a superposition of the singlet ϕ^0 and the octet ϕ_8. The isoscalar ω-meson decomposed as $\omega = (u\bar{u} + d\bar{d})/\sqrt{2}$ is the corresponding orthogonal state. Following the discussion in Ref. [245], the mixing between ω and ϕ is negligibly small and hence these are the (strong) mass eigenstates.
SU(3) symmetry is applied as follows: one assumes the matrix elements of $\phi = s\bar{s}$ are related to the corresponding matrix elements of members of the octet, i. e. that the form factors of the $B_s^0 \to \phi$ decay are the same as the ones for the $B_s^0 \to \bar{K}^{*0}$ transition. Note that this assumption goes beyond SU(3)-symmetry-assumptions since octet and singlet components are related to each other. Due to a lack of detailed information on the quality of such an assumption one relies e.g. on QCD sum rule estimates, indicating

that the strong dynamics in the $\phi = (s\bar{s})_{S=1}$ state are very similar to $\bar{K}^{*0} = (d\bar{s})_{S=1}$, see. Sec. 6.3.2. Note that penguin annihilation and exchange topologies are neglected, an assumption which can be probed through the $B_d^0 \to J/\psi\phi$ decay.

6.3.2. SU(3)-Breaking in the Exctraction of H_f

For nonleptonic decays it is very difficult to get a reliable estimate of the SU(3) breaking effects. From the corresponding processes with pseudoscalar final states it is known that the decays with J/ψ in the final state are dominated by non-factorizable contributions; in the considered decays the factorization of the penguin contributions is not clear. However, considering $B_s \to \pi\pi, \pi K, KK$ decays, sizable non-factorizable effects are encountered, whereas the data do not indicate large SU(3)-breaking effects [246]. In particular, a calculation of the relevant form-factor ratio by means of QCD sum rule techniques [247] for the counterpart of the H_f quantities for $B_s^0 \to K^+K^-$, $B_d^0 \to \pi^+\pi^-$ system yields good agreement with the current data that would be spoiled by large non-factorizable, SU(3)-breaking effects. This empirical behaviour is in the following used for an estimate of the SU(3)-breaking effects for the extraction of the H_f from the data by using the QCD sum rule form factor predictions for $B_s \to \bar{K}^{*0}$.

For the SU(3)-breaking corrections to the amplitude ratio $|\mathcal{A}_f/\mathcal{A}'_f|$, one applied the formulae presented in Ref. [229]. At the time $t = 0$ the linear polarization amplitudes of the $B_s^0 \to J/\psi\phi$ channel is given by $A_0(0) = -xa - (x^2-1)b$, $A_\parallel(0) = \sqrt{2}a$, and $A_\perp(0) = \sqrt{2(x^2-1)}c$, with $x \equiv p_{J/\psi} \cdot p_\phi/(m_{J/\psi}m_\phi)$. Neglecting the doubly Cabbibo-suppressed penguin corrections, because one is interested in the overall amplitudes A_f, the "factorized" contributions can be written as $a_{\rm fact} = \frac{G_F}{\sqrt{2}}\lambda_c^{(s)}[\mathcal{C}_1^{\rm eff}(\mu) + \mathcal{C}_5^{\rm eff}(\mu)]A_1^{\rm eff}$, $b_{\rm fact} = \frac{G_F}{\sqrt{2}}\lambda_c^{(s)}[\mathcal{C}_1^{\rm eff}(\mu) + \mathcal{C}_5^{\rm eff}(\mu)]B_1^{\rm eff}$, and $c_{\rm fact} = \frac{G_F}{\sqrt{2}}\lambda_c^{(s)}[\mathcal{C}_1^{\rm eff}(\mu) + \mathcal{C}_5^{\rm eff}(\mu)]C_1^{\rm eff}$, with the effective Wilson coefficients $\mathcal{C}_i^{\rm eff}(\mu)$. The relations between the form factors $A_{1,2}^{B_s\phi}(q^2)$ and $V^{B_s\phi}(q^2)$ of the quark-current matrix elements of the $B_s \to \phi$ decay, q denoting the momentum transferred by the quark current, and the "factorized" contributions are given by

$$\begin{aligned}
A_1^{\rm fac} &= -f_{J/\psi}m_{J/\psi}\left(m_{B_s}+m_\phi\right)A_1^{B_s\phi}\left(m_{J/\psi}^2\right)\,,\\
B_1^{\rm fac} &= 2\frac{f_{J/\psi}m_{J/\psi}^2 m_\phi}{m_{B_s}+m_\phi}A_2^{B_s\phi}\left(m_{J/\psi}^2\right)\,,\\
C_1^{\rm fac} &= 2\frac{f_{J/\psi}m_{J/\psi}^2 m_\phi}{m_{B_s}+m_\phi}V^{B_s\phi}\left(m_{J/\psi}^2\right)\,.
\end{aligned} \tag{6.33}$$

In the case of the $B_s^0 \to J/\psi \bar{K}^{*0}$ channel, the corresponding $B_s \to \bar{K}^{*0}$ decay form factors are needed, and ϕ has to replaced by $\bar{K}^{*0}$ in the above formulae. These form factors are analysed in Ref. [173]. Light-cone sum rules allow an estimate of the values at $q^2 = 0$. For the form factor values at $q^2 > 0$, e.g. $q^2 = m_{J/\psi}^2$, they are extrapolated by using the functional forms suggested in Ref. [173], assuming an uncertainty of 15%, being an ad hoc assumption. The results are collected in Table 6.4 and yielding the SU(3)-breaking ratios

$$\begin{aligned} &\frac{A_1^{B_s\bar{K}^*}(m_{J/\psi}^2)}{A_1^{B_s\phi}(m_{J/\psi}^2)} = 0.78 \pm 0.17\,, \qquad \frac{A_2^{B_s\bar{K}^*}(m_{J/\psi}^2)}{A_2^{B_s\phi}(m_{J/\psi}^2)} = 0.84 \pm 0.18\,, \\ &\frac{V^{B_s\bar{K}^*}(m_{J/\psi}^2)}{V^{B_s\phi}(m_{J/\psi}^2)} = 0.76 \pm 0.16 \end{aligned} \tag{6.34}$$

Using the linear polarization amplitudes, one gets

$$\left|\frac{\mathfrak{A}_0'}{\mathfrak{A}_0}\right|^2 = 0.42 \pm 0.27\,, \quad \left|\frac{\mathfrak{A}_\parallel'}{\mathfrak{A}_\parallel}\right|^2 = 0.70 \pm 0.29\,, \quad \left|\frac{\mathfrak{A}_\perp'}{\mathfrak{A}_\perp}\right|^2 = 0.38 \pm 0.16\,, \tag{6.35}$$

allowing the extraction of the H_f from the untagged rates with the help of (6.18). Note that this discussion is analogous to the one in Sec. 6.2.1.

6.3.3. SU(3)-Breaking in $a_f' = a_f$ and $\theta_f' = \theta_f$

The equality of $a_f = a_f'$ and $\theta_f = \theta_f$ as noted in Eq. (6.19) is supported by SU(3) flavour-symmetry of the strong interaction. However, sizable non-factorizable effects could induce SU(3)-breaking corrections. In this subsection their impact on (6.19) is discussed. Using the $B_s^0 \to J/\psi \bar{K}^{*0}$ observables (see Sec. 6.1.5), a_f' and θ' can extracted from the data. Their $B_s^0 \to J/\psi\phi$ counterparts a_f and θ_f enter in H_f in combination with the tiny parameter ϵ, hence, this determination is unaffected by

Table 6.4.: $B_s \to V$ form factors at $q^2 = m_{J/\psi}^2$ extrapolated from the results of Ref. [173] and assuming an uncertainty of 15%.

	$V = \phi$	$V = \bar{K}^*$
$A_1^{B_sV}(m_{J/\psi}^2)$	0.42 ± 0.06	0.33 ± 0.05
$A_2^{B_sV}(m_{J/\psi}^2)$	0.38 ± 0.06	0.32 ± 0.05
$V^{B_sV}(m_{J/\psi}^2)$	0.82 ± 0.12	0.62 ± 0.09

corrections to (6.19). Consequently the main corrections enter through the value of H_f by the SU(3)-breaking corrections to the amplitude ratios $|\mathcal{A}_f/\mathcal{A}'_f|$, as discussed in Sec. 6.3.2.

Calculating the shifts $\Delta\phi_s^f$ and $\Delta\phi_d$ the relations (6.19) are used. However, as discussed in the previous sections, sizable non-factorizable effect could induce SU(3)-breaking corrections. But the relation $\tan\phi_d$ from (6.17) is independent from direct CP asymmetries and can be used as an inference for the SU(3)-breaking impact on the determination of $\Delta\phi_s^f$ and $\Delta\phi_d$. Since one neglects terms $\mathcal{O}(\epsilon^2)$, the dependence on $a\cos\theta$ is linearly, hence, corrections to $a = a'$ propagate linearly as well, while in general SU(3)-breaking effects in the strong phase lead to an asymmetric uncertainty for $\Delta\phi_s^f$ and $\Delta\phi_d$.
Moreover, the impact of SU(3)-breaking corrections could be explored in the analysis of $\bar{B}^0 \to J/\psi\pi^0$ data by introducing a symmetry-breaking factor ξ in the left-hand side of (6.19), $a = \xi a'$, and uncorrelating the strong phases θ and θ' of the $B_d^0 \to J/\psi K^0$ and $\bar{B}^0 \to J/\psi\pi^0$ decays, respectively. Allowing for $\xi \in [0.5, 1.5]$ and $\theta, \theta' \in [90°, 270°]$ in the fit, and using a 50% increased error for the form-factor ratio in view of non-factorizable contributions to $|\mathcal{R}/\mathcal{R}'|$, the global fit yields $\Delta\phi_d \in [-6.7°, 0.0°]$, and $\phi_d^{\rm NP} \in [-14.9°, 4.0°]$, determined now mostly by $C(J/\psi K_{S,L})$ and H [227]. In the case $\xi = 1$ and $\theta = \theta'$ one finds $\Delta\phi_d \in [-3.9°, -0.8°]$. A similar situation is expected for $\Delta\phi_s^f$ [226]. Hence, even allowing such large SU(3)-breaking corrections, the picture is not significantly changed. Note that these analysis include doubly Cabbibo-suppressed standard model contributions, being crucial in order to eventually detect or exclude such new physics effects.

6.3.4. Internal Consistency Checks of SU(3)

The B-meson decays into two vector mesons offer more observables, because of the angular distribution of their decay products, than in the case of $B \to PP$ or $B \to PV$ decays, where P and V denote generically pseudoscalar and vector mesons, respectively. This comments supported internal consistence checks of the SU(3) flavour-symmetry.

As a first consistence check, the different values of the $B_s^0 - \bar{B}_s^0$ mixing phase ϕ_s originated from the three polarization states $f \in \{0, \|, \perp\}$, which should agree with another are used. Hence, more quantitative tests of SU(3)-breaking can be performed. The strategy of the consistence check is as follows. Choosing one of the three linear

polarization states to extract ϕ_s from Eq. (6.22), taking the shift $\Delta\phi_s^f$ through the penguin effects into account. Using the $B_s^0 \to J/\psi\phi$ observables $\mathcal{A}_{CP}^{\text{mix},f'}$ and $\mathcal{A}_{CP}^{\text{dir},f'}$ of the remaining two polarization states; knowing ϕ_s the corresponding shifts $\Delta\phi_s^f$ can be extracted from (6.22), and the values of the $\Delta\phi_s^f$ can converted into contours in the $\theta_f - a_f$ plane by using $\tan\Delta\phi_s^f$ from (6.17). Performing in Eq. (6.20) the replacements

$$\begin{aligned} U_{H_f} \to U_{\Delta\phi_s^f} &\equiv \left(\frac{\sin\gamma - \cos\gamma\tan\Delta\phi_s^f}{\cos 2\gamma\tan\Delta\phi_s^f - \sin 2\gamma}\right)\cos\theta_f\,, \\ V_{H_f} \to V_{\Delta\phi_s^f} &\equiv \frac{\tan\Delta\phi_s^f}{\cos 2\gamma\tan\Delta\phi_s^f - \sin 2\gamma}\,, \end{aligned} \tag{6.36}$$

as well as $a_f' \to \epsilon a_f$. Additionally one replaced $\theta_f' \to 180° + \theta_f$ and $\mathcal{A}_{CP}^{\text{dir},f'} \to \mathcal{A}_{CP}^{\text{dir},f}$ in $U_{\mathcal{A}_{CP}^{\text{dir},f'}}$, hence, the direct CP-asymmetry in $B_s^0 \to J/\psi\phi$ can be converted into a contour in the $\theta_f - a_f$ plane as well. Note that these constructions are valid exactly. In Fig. 6.7 this strategy is depicted by considering a simple numerical example. Assuming $\gamma = 65°$ and the hadronic parameters are given by $a_f = 0.4 \pm 0.1$ and $\theta_f = (220 \pm 10)°$, yielding $\mathcal{A}_{CP}^{\text{dir},f} = 0.025 \pm 0.008$ and $\Delta\phi_s^f = (-1.7 \pm 0.5)°$. The internal consistence check of SU(3) flavour-symmetry can then performed by using the values of the hadronic $B_s^0 \to J/\psi\phi$ hadronic parameters a_f and θ_f, comparing them with the values of a_f' and θ_f' following from the $B_s^0 \to J/\psi\bar{K}^{*0}$ strategy proposed in Sec. 6.1.5.

Another consistence check is offered by the relation $\mathcal{A}_{CP}^{\text{dir},f} = -\epsilon H_f \mathcal{A}_{CP}^{\text{dir},f'}$, relying on Eq. (6.19). Note that the practical usefulness of these consistence checks is restricted depending on the values of the observables hopefully measured by LHCb or a future Super-B factory.

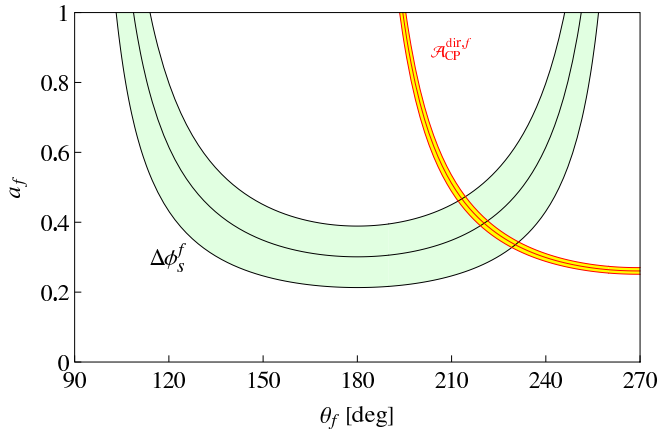

Figure 6.7: Numerical example for the extraction a_f and θ_f from $\Delta\phi_s^f$ and the direct CP-asymmetry $\mathcal{A}_{CP}^{\text{dir},f}$, as described in the text.

6.4. Conclusions

The CP-violating effects in the time-dependent angular distributions of $B_s^0 \to J/\psi[\to \ell^+\ell^-]\phi[\to K^+K^-]$ are expected to be small in the standard model, limiting the theoretical accuracy of the benchmark for new physics search. Hadronic effects, which are due to doubly Cabbibo-suppressed penguin contributions usually neglected could induce mixing-induced CP-violating effects as large as $\mathcal{O}(-10\%)$ [227]. These penguin contributions, which cannot be calculated reliably from QCD, have to be controlled, hence, such CP-violating effects, being misinterpreted as CP-violating new physics contributions to $B_s^0 - \bar{B}_s^0$ mixing.

For the analysis of the CP-violating effects in the golden $B^0 \to J/\psi K_{S,L}$ channel by using analogically strategies as for $B_s^0 \to J/\psi\phi$ final conclusion can not be done, because of the large experimental errors. The performed analysis does not rule out new physics effects in the amplitude as an explanation for the observed shift. In a recent paper [248], it is argued that the sub-leading effects in the standard model being $\mathcal{O}(10^{-3})$. Following their line of argumentation, large standard model effects can be excluded, and new physics contribution in the amplitude are sufficient to explain the data and their behaviour under SU(3) transformations is standard-model-like [240].

The expected accuracy of LHCb and a possible future upgrade of this experiment encouraged controlling of the sub-leading effects in $B_q^0 - \bar{B}_q^0$ mixing, $q \in \{s, d\}$, in order to distinguish new physics contributions from standard model ones.

7

Concluding Remarks

B-meson decays are quite suitable for testing the flavour sector of the standard model in different ways. Here, exclusive semileptonic B-meson transitions are studied using QCD sum rules techniques and symmetry relations provided by the heavy-quark expansion theory. New physics effects are explored in exclusive semileptonic as well as in nonleptonic B-meson decays.

For exploring the hadron phenomenology, QCD sum rules have become a powerful tool. In Chap. 5 the light-cone sum rules have been used for the semileptonic $\bar{B} \to D^{(*)}\ell\bar{\nu}$ transitions. The achieved results for the form factors are in agreement with experimental data and results from lattice QCD calculations. However, their predictions have to be treated carefully, due to hadron duality and approximations in the operator-product expansion of the correlator functions.

The exploration of the $B \to D^{(*)}$ transitions with QCD sum rules is done in an standard-model-like way, explicitly using the $(V - A)$ left-handed hadronic current structure. However, this can be done only at the other end of the phase space compared to the heavy-quark limit.

For leptonic currents the $(V - A)$ current structure is experimentally well-tested. For hadronic currents the situation is less clear; constraints on right-handed admixtures are strong, but they are not excluded. Moreover, beside the vector and axial vector currents the Dirac structure of space-time provide scalar, pseudoscalar, tensor and pseudotensor currents, usually suppressed in the standard model. Taking right-handed admixtures and these additional current structures into account, new physics contributions appear in the exclusive semileptonic $\bar{B} \to D^{(*)}\ell\bar{\nu}$ decay rates as discussed in Chap. 6. At zero-recoil the non-vanishing form factors become a single function, the Isgur-Wise function, in which these new physics contributions also appear. A com-

mon parametrisation of the Isgur-Wise function is suggested by Caprini, Lellouch and Neubert, wherein its behaviour is described by a slope parameter. Neglecting scalar, pseudoscalar, tensor and pseudotensor contributions, the form factor as well as the slope parameter predictions at zero-recoil compared with experimental data yield constraints on right-handed admixtures. The presented formulae make in the future more sophisticated analysis of the experimental data possible.

In Chap. 6 the new physics search is extended to nonleptonic B-meson decays, namely $b \to s$ decays. An understanding of standard model contributions to such decays is essential, because the hadronic matrix elements for such decays are poorly known. There are two possibilities dealing with this problem. One can use amplitude relations to eliminate the hadronic matrix elements, or interference effects between $B^0 - \bar{B}^0$ mixing and decay processes. Because such effects may induce mixing-induced CP violation, and if the decay is governed by a single CKM amplitude the hadronic matrix elements will be canceled in the corresponding CP asymmetries. The most important example is the "golden mode" $B_d^0 \to J/\psi K_S$.

New physics contributions are studied using CP-violating effects in the time-dependent decay amplitudes of $B_s^0 \to J/\psi\phi$ decays, where the $B_s^0 - \bar{B}_s^0$ mixing phase ϕ_s is associated with new physics contributions. Since SU(3) flavour symmetry is approximately valid, one used the $B_s^0 \to J/\psi \bar{K}^{*0}$ decay as an control channel. The hadronic effects usually neglected in the standard model could induce mixing-induced CP-violating effects as large as -10%. The strategies are converted to $B \to J/\psi K$, explicitly the $B_d^0 - \bar{B}_d^0$ mixing phase ϕ_d also influenced by a new physics phase, with $B \to J/\psi\pi^0$ as the flavour symmetry counterpart. The resulting new physics phase is compatible with zero. Large penguin contributions are able to explain the data in both decays and leading to shifts in $\sin 2\beta$ up to a few percent. In a recent paper [248] it is argued that this this too large for being a standard model effect. However, the presented analysis confirms that a new physics contribution in the amplitude is sufficient to explain the data and shifts in $\sin 2\beta$ can be explained by standard model effects. Expecting precision data from the LHCb experiment encouraged further studies of sub-leading effects in $B_s^0 - \bar{B}_s^0$ as well in $B_d^0 - \bar{B}_d^0$ mixing in order to distinguish between standard model and new physics contributions in the data.

Moreover, there are good reasons that the experiments at the LHC, which have been started taking first data in 2009, will stimulate flavour physics in the TeV energy regime. The expected high precision data from LHCb or an future Super B-factory hopefully provide answers to open questions within the standard model and especially in the flavour physics sector.

Danksagung

Mein Dank gilt all denen, die mir die Anfertigung dieser Dissertation ermöglicht und die mich während meiner Promotionszeit mit Rat und Tat unterstütz haben.

Bedanken möchte ich mich ganz herzlich bei meinem Doktorvater Prof. Dr. Thomas Mannel für die Betreuung dieser Arbeit, für die interessanten Themen die ich im Rahmen meines Promotionsstudiums bearbeiten durfte, für die vielen konstruktiven Diskussionen, für meinen fünfmonatigen Forschungsaufenthalt am CERN und für die sehr angenehme Arbeitsatmosphäre.
Besonders bedanken möchte ich mich bei Herrn Prof. Dr. Alexander Khodjamirian für die Übernahme des Koreferats dieser Arbeit.
Herrn Dr. Robert Fleischer möchte ich danken für die Betreuung während meines Forschungsaufenthalts am CERN.
Ganz besonders bedanken möchte ich mich bei Herrn Dr. Thorsten Feldmann, der mir während der Anfertigung meiner Diplomarbeit und meiner ersten Puplikation, sowie in der Anfangsphase meiner Promotionszeit jederzeit mit wissenschaftlichem Rat zur Seite stand.
Ich danken allen Mitgliedern der Theoretischen Physik 1 für das exzellente Arbeitsklima während meiner Promotionszeit.

Danken möchte ich Dr. Nils Offen, M.Sc. Sascha Turzyk und ganz besonders Dr. Martin Jung für das Korrekturlesen des Manuskripts und wertvollen Hinweisen zu dessen Verbesserung.

Bedanken möchte ich mich bei meinen Kommilitonen Kai Grybel, André Krabbenhöft, Delia und Peter Kaufmann für die schöne Studienzeit in Siegen.

Ganz besonders danke ich meinen Eltern und meiner Familie, die mich während meiner Studien- und Promotionszeit immer und uneingeschränkt unterstützt haben.

A

QCD Sum Rules for $B \to D^{(*)}\ell\nu_\ell$

In this appendix the results for the QCD sum rules for the $\bar{B} \to D^{(*)}\ell\bar{\nu}$ transitions [170] dervied from the new light-cone sum rules [169] are presented.

A.1. B-Meson Distribution Amplitudes

For the two-particle B-meson distribution amplitudes are given by

$$\begin{aligned}\left\langle 0\left|\bar{q}_{2\alpha}(x)[x,0]h_{v\beta}\right|\bar{B}_v\right\rangle &= -\frac{if_B m_B}{4}\int_0^\infty d\omega\, e^{-i\omega v\cdot x} \\ &\times\left[(1+\not{v})\left\{\phi_+^B(\omega)-\frac{\phi_+^B(\omega)-\phi_-^B(\omega)}{2v\cdot x}\not{x}\right\}\gamma_5\right]_{\beta\alpha}, \end{aligned} \tag{A.1}$$

where the distribution amplitudes $\phi_+^B(\omega)$ and $\phi_-^B(\omega)$ are normalized, $\int_0^\infty d\omega\,\phi_\pm^B(\omega) = 1$, and the variable $\omega > 0$ is the plus component of the spectator-quark momentum of the B-meson.

The three-particle B-meson distribution amplitudes are defined as in Ref. [176],

$$\begin{aligned}\left\langle 0\left|\bar{q}_{2\alpha}(x)G_{\lambda\rho}(u,x)h_{v\beta}\right|\bar{B}^0(v)\right\rangle &= \frac{if_B m_B}{4}\int_0^\infty d\omega\int_0^\infty d\xi\, e^{-i(\omega+u\xi)v\cdot x} \\ &\times\left[(1+\not{v})\left\{\left(v_\lambda\gamma_\rho - v_\rho\gamma_\lambda\right)\left(\Psi_A(\omega,\xi)-\Psi_V(\omega,\xi)\right) - i\sigma_{\lambda\rho}\Psi_V(\omega,\xi)\right.\right. \\ &\left.\left.-\left(\frac{x_\lambda v_\rho - x_\rho v_\lambda}{v\cdot x}\right)X_A(\omega,\xi)+\left(\frac{x_\lambda\gamma_\rho - x_\rho\gamma_\lambda}{v\cdot x}\right)Y_A(\omega;\xi)\right\}\gamma_5\right]_{\beta\alpha}, \end{aligned} \tag{A.2}$$

where the path-ordered gauge factors are omitted, and the distribution amplitudes Ψ_V, Ψ_A, X_A, and Y_A, depend on the variables $\omega, \xi > 0$, which are the plus compoments of th light-quark and gluon momenta in the B-meson, respectively.
For the numerical analysis one uses expontential models, for the two-particle distribution amplitudes [115],

$$\phi_+^B(\omega) = \frac{\omega}{\omega_0^2} e^{-\frac{\omega}{\omega_0}}, \quad \omega_-^B(\omega) = \frac{1}{\omega_0} e^{-\frac{\omega}{\omega_0}}, \tag{A.3}$$

where the inverse moment λ_B is defined as $\lambda_B^{-1} = \int_0^\infty \frac{d\omega}{\omega} \phi_+^B(\omega)$ is equal to ω_0, as well as for the three-particle distribution amplitudes [169],

$$\begin{aligned}
\Psi_A(\omega,\xi) &= \Psi_V(\omega,\xi) = \frac{\lambda_E^2}{6\omega_0^4}\xi^2 e^{-(\omega+\xi)/\omega_0}, \\
X_A(\omega;\xi) &= \frac{\lambda_E^2}{6\omega_0^4}\xi(2w-\xi) e^{-(\omega+\xi)/\omega_0}, \\
Y_A(\omega,\xi) &= -\frac{\lambda_E^2}{6\omega_0^4}\xi(7\omega_0 - 13\omega + 3\xi) e^{-(\omega+\xi)/\omega_0}.
\end{aligned} \tag{A.4}$$

A.2. Form factors

In this section the sum rules for the $\bar{B} \to D^{(*)}$ decays are presented, which are taken from [170]. The form factors for the both decays, $B \to D$ and $B \to D^*$ are listed seperately. Whereas the contributions to the three-particle distribution amplitudes are collected in Sec. A.2.3.

A.2.1. $B \to D$ Decay

The sum rules for $B \to D$ form factors are

$$\begin{aligned}
&f_{BD}^+(q^2) \\
&= \frac{f_B m_B m_c}{2 f_D m_D^2} \left\{ \int_0^{\omega_0(q^2, s_0^D)} d\omega \, \exp\left\{ \frac{-s(\omega,q^2) + m_D^2}{M^2} \right\} \right. \\
&\quad \times \left[\frac{m_c(\varpi + m_c)}{\varpi^2 + m_c^2 - q^2} \phi_-^B(\omega) + (\varpi + m_c) \left(\frac{1}{\varpi} - \frac{m_c}{\varpi^2 + m_c^2 - q^2} \right) \phi_+^B(\omega) \right. \\
&\quad \left. - \left(\frac{1}{\varpi} + \frac{m_c(\varpi^2 + 2m_c\varpi - m_c^2 + q^2)}{(\varpi^2 + m_c^2 - q^2)^2} \right) \bar{\Phi}_\pm^B(\omega) \right] \\
&\quad \left. + \Delta f_{BD}^+(q^2, s_0^D, M^2) \right\}, \qquad \text{(A.5)} \\
&f_{BD}^+(q^2) + f_{BD}^-(q^2)
\end{aligned}$$

$$
\begin{aligned}
&= -\frac{f_B m_B m_c}{f_D m_D^2}\left\{\int_0^{\omega_0(q^2,s_0^D)} d\omega\ \exp\left\{\frac{-s(\omega,q^2)+m_D^2}{M^2}\right\}\right.\\
&\times\left[\frac{m_c(\omega-m_c)}{\varpi^2+m_c^2-q^2}\phi_-^B(\omega)+(\omega-m_c)\left(\frac{1}{\varpi}-\frac{m_c}{\varpi^2+m_c^2-q^2}\right)\phi_+^B(\omega)\right.\\
&+\left.\left(\frac{1}{\varpi^2}-\frac{m_c(m_B^2-\omega^2-2m_c\varpi+m_c^2-q^2)}{(\varpi^2+m_c^2-q^2)^2}\right)\bar{\Phi}_\pm^B(\omega)\right]\\
&+\left.\Delta f_{BD}^{\pm}\left(q^2,s_0^D,M^2\right)\right\}, \qquad \text{(A.6)}
\end{aligned}
$$

where $\varpi \equiv m_B - \omega$,

$$
\bar{\Phi}_\pm^B(\omega) = \int_0^\omega d\tau\ \left(\phi_+^B - \phi_-^B(\tau)\right)\ , \qquad \text{(A.7)}
$$

and

$$
s\left(\omega,q^2\right) = m_B\omega + \frac{m_c^2 m_B - q^2\omega}{\varpi}\ . \qquad \text{(A.8)}
$$

In the charmed meson channel the threshold $s_0^{D^{(*)}}$ transforms into the upper limit of the ω-integration,

$$
\begin{aligned}
&\omega_0\left(q^2,s_0^{D^{(*)}}\right)\\
&\quad=\frac{m_B^2-q^2+s_0^{D^{(*)}}-\sqrt{4(m_c^2-s_0^{D^{(*)}})m_B^2+(m_B^2-q^2+s_0^{D^{(*)}})^2}}{2m_B}\ . \qquad \text{(A.9)}
\end{aligned}
$$

In the sum rules (A.5) and (A.6), Δf_{BD}^+ and Δf_{BD}^- denote the contributions of the three-particle distributions amplitudes calculated form Fig. 4.1(middle panel), which are listed in Sec. A.2.3.

A.2.2. $B \to D^*$ Decay

The form factors for the $B \to D^*$ transition can be reproduced from the sum rules for the heavy-light $B \to K^*$ form factors in Ref. [169] by replacing $m_s \to m_c$,

$$
\begin{aligned}
V^{BD^*}\left(q^2\right) =& \frac{f_B m_B}{2 f_{D^*} m_{D^*}}(m_B+m_{D^*})\left\{\int_0^{\omega_0(q^2,s_0^{D^*})} d\omega\ \exp\left\{\frac{-s(\omega,q^2)+m_{D^*}^2}{M^2}\right\}\right.\\
&\times\left[\frac{m_c}{\varpi^2+m_c^2-q^2}\phi_-^B(\omega)+\left(\frac{1}{\varpi}-\frac{m_c}{\varpi^2+m_c^2-q^2}\right)\phi_+^B(\omega)\right.\\
&-\left.\left.\frac{2m_c\varpi}{\left(\varpi^2+m_c^2-q^2\right)^2}\bar{\Phi}_\pm^B(\omega)\right]+\Delta V^{BD^*}\left(q^2,s_0^{D^*},M^2\right)\right\}, \qquad \text{(A.10)}
\end{aligned}
$$

$$A_1^{BD^*}\left(q^2\right) = \frac{f_B m_B^3}{2 f_{D^*} m_{D^*}(m_B + m_{D^*})}\Bigg\{ \int\limits_0^{\omega_0(q^2, s_0^{D^*})} d\omega \ \exp\left\{\frac{-s(\omega, q^2) + m_{D^*}^2}{M^2}\right\}$$
$$\times \Bigg[\frac{(\varpi + m_c)^2 - q^2}{\varpi^2}\left\{\frac{m_c \varpi}{\varpi^2 + m_c^2 - q^2}\bar{\phi}_-^B(\omega) + \left(1 - \frac{m_c \varpi}{\varpi^2 + m_c^2 - q^2}\right)\phi_+^B(\omega)\right\}$$
$$- \frac{4\varpi m_c^2}{\left(\varpi^2 + m_c^2 - q^2\right)^2}\bar{\Phi}_\pm^B(\omega)\Bigg] + \Delta A_1^{BD^*}\left(q^2, s_0^{D^*}, M^2\right)\Bigg\}, \tag{A.11}$$

$$A_2^{BD^*}(q^2) = \frac{f_B}{2 f_{D^{(*)}} m_{D^*}}(m_B + m_{D^*})\Bigg\{ \int\limits_0^{\omega_0(q^2, s_0^{D^*})} d\omega \ \exp\left\{\frac{-s(\omega, q^2) + m_{D^*}^2}{M^2}\right\}$$
$$\times \Bigg[\frac{(m_c m_B - 2\varpi\omega)}{\varpi^2 + m_c^2 - q^2}\phi_-^B(\omega) + \left(1 - \frac{\omega}{\varpi} - \frac{(m_c m_B - 2\omega\varpi)}{\varpi^2 + m_c^2 - q^2}\right)\phi_+^B(\omega)$$
$$- 2\left(\frac{\varpi(m_c m_B - 2\omega\varpi)}{\left(\varpi^2 + m_c^2 - q^2\right)^2} + \frac{(\omega - \varpi)}{\varpi^2 + m_c^2 - q^2}\right)\bar{\Phi}_\pm^B(\omega)\Bigg] + \Delta A_2^{BD^*}\left(q^2, s_0^{D^*}, M^2\right)\Bigg\}, \tag{A.12}$$

and a new sum rule for the remaining combination $\bar{B} \to D^*$ form factors,

$$A_3^{BD^*}\left(q^2\right) - A_0^{BD^*}\left(q^2\right) = \frac{f_B\, q^2}{4 f_{D^*} m_{D^*}^2}\Bigg\{ \int\limits_0^{\omega 0(q^2, s_0^{D^*})} d\omega \exp\left\{\frac{-s(\omega, q^2) + m_{D^*}^2}{M^2}\right\}$$
$$\times \Bigg[-\frac{m_c m_B - 2\omega(m_B + \omega)}{\varpi^2 + m_c^2 - q^2}\phi_-^B(\omega) + \left(\frac{m_c m_B - 2\omega\varpi - 4\omega^2}{\varpi^2 + m_c^2 - q^2} - \frac{2\omega + m_B}{\varpi}\right)\phi_+^B(\omega)$$
$$- \frac{2}{\varpi^2 + m_c^2 - q^2}\left(m_B + 2\omega + \frac{\varpi(2\omega\varpi + 4\omega^2 - m_c m_B)}{\varpi^2 + m_c^2 - q^2}\right)\bar{\Phi}_\pm^B(\omega)\Bigg]$$
$$+ \Delta A_{3-0}^{BD^*}(q^2, s_0^{D^*}, M^2)\Bigg\}, \tag{A.13}$$

As before, n (A.10)-(A.13), ΔV^{BD^*}, $\Delta A_1^{BD^*}$, $\Delta A_2^{BD^*}$, $\Delta A_{3-0}^{BD^*}$ denote the contributions of the B-meson three-particle DA's.

A.2.3. Contributions of three-particle DA's to LCSR

For the three-particle distributions amplitudes to the light-cone sum rules, expresed in a generic form, one find

$$\Delta F\left(q^2, s_0^{D^{(*)}}, M^2\right) = \int\limits_0^{\omega_0(q^2, s_0^{D^{(*)}})/m_B} d\sigma \ \exp\left\{\frac{-s(\sigma m_B, q^2) + m_{D^{(*)}}^2}{M^2}\right\}$$

$$\times \left(-I_1^{(F)}(\sigma) + \frac{I_2^{(F)}(\sigma)}{M^2} - \frac{I_3^{(F)}(\sigma)}{2M^4} \right)$$
$$+ \frac{e^{(-s_0^{D^{(*)}} + m_{D^{(*)}}^2)/M^2}}{m_B^2} \left\{ \eta(\sigma) \left[I_2^{(F)}(\sigma) \right.\right.$$
$$\left.\left. - \frac{1}{2} \left(\frac{1}{M^2} + \frac{1}{m_B^2} \frac{d\eta(\sigma)}{d\sigma} \right) I_3^{(F)}(\sigma) - \frac{\eta(\sigma)}{2m_B^2} \frac{d I_3^{(F)}(\sigma)}{d\sigma} \right] \right\} \Bigg|_{\sigma=\omega_0/m_B} , \tag{A.14}$$

where

$$\Delta F = \left\{ \Delta f_{BD}^+, \Delta f_{BD}^\pm, \frac{\Delta V^{BD^*}}{m_B}, \frac{\Delta A_1^{BD^*}}{m_B}, \frac{\Delta A_2^{BD^*}}{m_B}, \frac{\Delta A_{3-0}^{BD^*}}{m_B} \right\} , \tag{A.15}$$

and the following notation is used,

$$\eta(\sigma) = \left(1 + \frac{m_c^2 - q^2}{\bar{\sigma}^2 m_B^2} \right)^{-1} . \tag{A.16}$$

The integrals over the three-particle DA's multiplying the inverse powers of the Borel parameter $1/M^{2(n-1)}$ with $n = 1, 2, 3$ are defined as:

$$I_n^{(F)}(\sigma) = \frac{1}{\bar{\sigma}^n} \int_0^{\sigma m_B} d\omega \int_{\sigma m_B - \omega}^{\infty} \frac{d\xi}{\xi} \Big[C_n^{(F,\Psi A)}(\sigma, u, q^2) \Psi_A(\omega, \xi)$$
$$+ C_n^{(F,\Psi V)}(\sigma, u, q^2) \Psi_V(\omega, \xi)$$
$$+ C_n^{(F,XA)}(\sigma, u, q^2) \overline{X}_A(\omega, \xi)$$
$$\left. + C_n^{(F,YA)}(\sigma, u, q^2) \overline{Y}_A(\omega, \xi) \right] \Big|_{u=(\sigma m_B - \omega)/\xi} \tag{A.17}$$

where:

$$\overline{X}_A(\omega, \xi) = \int_0^\omega d\tau \; X_A(\tau, \xi) , \quad \overline{Y}_A(\omega, \xi) = \int_0^\omega d\tau \; Y_A(\tau, \xi) . \tag{A.18}$$

The nonvanishing coefficients entering Eq. (A.17) are:

$$C_1^{(f_{BD}^+, \Psi A)} = -2 \frac{1-u}{m_B \bar{\sigma}} ,$$
$$C_2^{(f_{BD}^+, \Psi A)} = m_B \bar{\sigma}(4u-1) + 3m_c - 2 \frac{m_c^2 - q^2}{m_B \bar{\sigma}} (1-u) ,$$
$$C_1^{(f_{BD}^+, \Psi V)} = \frac{2(1-u)}{m_B \bar{\sigma}} ,$$

$$
\begin{aligned}
C_2^{(f_{BD}^+,\Psi V)} &= m_B\bar{\sigma}(2u+1) + 3m_c + 2\frac{m_c^2-q^2}{m_B\bar{\sigma}}(1-u)\,,\\
C_2^{(f_{BD}^+,XA)} &= 1-2u-\frac{2m_c}{m_B\bar{\sigma}}\,,\\
C_3^{(f_{BD}^+,XA)} &= 2\Bigg(m_cm_B\bar{\sigma} + m_B^2\bar{\sigma}^2(1-2u) - \frac{m_c(m_c^2-q^2)}{m_B\bar{\sigma}}\\
&\qquad - \left(m_c^2+q^2\right)(1-2u)\Bigg)\,,\\
C_3^{(f_{BD}^+,YA)} &= -12m_c\left(m_B\bar{\sigma} - m_c(1-2u)\right)\,,
\end{aligned}
$$

$$
\begin{aligned}
C_1^{(f_{BD}^\pm,\Psi_A)} &= -2\frac{1-u}{m_B\bar{\sigma}}\,,\\
C_2^{(f_{BD}^\pm,\Psi_A)} &= -\left(m_B[1+(1-4u)\bar{\sigma}+2u] - 3m_c + 2\frac{m_c^2-q^2}{m_B\bar{\sigma}}(1-u)\right)\,,\\
C_1^{(f_{BD}^\pm,\Psi_V)} &= 2\frac{1-u}{m_B\bar{\sigma}}\,,\\
C_2^{(f_{BD}^\pm,\Psi_V)} &= m_B[1+(1+2u)\bar{\sigma}-4u] + 3m_c + 2\frac{m_c^2-q^2}{m_B\bar{\sigma}}(1-u)\,,\\
C_2^{(f_{BD}^\pm,X_A)} &= -\frac{m_B(1+\sigma)(1-2u)+2m_c}{m_B\bar{\sigma}}\,,\\
C_3^{(f_{BD}^\pm,X_A)} &= -2\Bigg(m_B^2\sigma\bar{\sigma}(1-2u) + m_cm_B(1+\sigma)\\
&\qquad + \frac{\left[m_c^2(1+\bar{\sigma})-q^2\sigma\right]}{\bar{\sigma}}(1-2u) + \frac{m_c(m_c^2-q^2)}{m_B\bar{\sigma}}\Bigg)\,,\\
C_3^{(f_{BD}^\pm,Y_A)} &= 12m_c\left(m_B\sigma + m_c(1-2u)\right)\,,
\end{aligned}
$$

$$
\begin{aligned}
C_2^{(V^{BD^*},\Psi_A)} &= -\frac{1-2u}{m_B}\,,\\
C_2^{(V^{BD^*},\Psi_V)} &= -\frac{1}{m_B}\,,\\
C_2^{(V^{BD^*},X_A)} &= 2\frac{1-2u}{m_B^2\bar{\sigma}}\,,\\
C_3^{(V^{BD^*},X_A)} &= 2\left(\bar{\sigma}(1-2u) + 2\frac{m_c}{m_B} + \frac{m_c^2-q^2}{m_B^2\bar{\sigma}}(1-2u)\right)\,,\\
C_3^{(V^{BD^*},Y_A)} &= -4\frac{m_c}{m_B}\,,
\end{aligned}
$$

$$
\begin{aligned}
C_1^{(A_1^{BD^*},\Psi_A)} &= -\frac{1-2u}{m_B^2\bar{\sigma}}\,, \\
C_2^{(A_1^{BD^*},\Psi_A)} &= -\bar{\sigma}(1-2u) + 2\frac{m_c}{m_B} - \frac{m_c^2-q^2}{m_B^2\bar{\sigma}}(1-2u)\,, \\
C_1^{(A_1^{BD^*},\Psi_V)} &= -\frac{1}{m_B^2\bar{\sigma}}\,, \\
C_2^{(A_1^{BD^*},\Psi_V)} &= -\left(\bar{\sigma} + 2\frac{m_c}{m_B} + \frac{m_c^2-q^2}{m_B^2\bar{\sigma}}\right)\,, \\
C_1^{(A_1^{BD^*},X_A)} &= 2\frac{1-2u}{m_B^3\bar{\sigma}^2}\,, \\
C_2^{(A_1^{BD^*},X_A)} &= \frac{2}{m_B}\left(1 + 2\frac{m_c^2-q^2}{m_B^2\bar{\sigma}^2}\right)(1-2u)\,, \\
C_3^{(A_1^{BD^*},X_A)} &= 2\Big(m_B\bar{\sigma}^2 - 2\frac{m_c^2+q^2}{m_B} + \frac{(m_c^2-q^2)^2}{m_B^3\bar{\sigma}^2}\Big)(1-2u)\,, \\
C_2^{(A_1^{BD^*},Y_A)} &= -\frac{4}{m_B}\left(1-2u+\frac{m_c}{m_B\bar{\sigma}}\right)\,, \\
C_3^{(A_1^{BD^*},Y_A)} &= -4m_c\left(\bar{\sigma} - 2\frac{m_c}{m_B}(1-2u) + \frac{m_c^2-q^2}{m_B^2\bar{\sigma}}\right)\,,
\end{aligned}
$$

$$
\begin{aligned}
C_2^{(A_2^{BD^*},\Psi_A)} &= -\left(1+2u+2\sigma(1-2u) - \frac{4m_c}{m_B}\right)\,, \\
C_2^{(A_2^{BD^*},\Psi_V)} &= -\left(1+2\sigma-4u+\frac{4m_c}{m_B}\right)\,, \\
C_2^{(A_2^{BD^*},X_A)} &= -\frac{2\sigma}{m_B\bar{\sigma}}(1-2u)\,, \\
C_3^{(A_2^{BD^*},X_A)} &= 2\Bigg(m_B\bar{\sigma}(2\bar{\sigma}-1)(1-2u) - 2m_c \\
&\qquad - \frac{[m_c^2(2\bar{\sigma}+1) + q^2(2\bar{\sigma}-1)]}{m_B\bar{\sigma}}(1-2u)\Bigg)\,, \\
C_3^{(A_2^{BD^*},YA)} &= 4\left(2m_B\sigma\bar{\sigma}(1-2u) - m_c(1-4\sigma)\right)\,,
\end{aligned}
$$

$$
\begin{aligned}
C_2^{(A_3^{BD^*}-A_0^{BD^*},\Psi_A)} &= 2(1-2u)\bar{\sigma} - 1 + 6u + \frac{4m_c}{m_B}\,, \\
C_2^{(A_3^{BD^*}-A_0^{BD^*},\Psi_V)} &= 2\bar{\sigma} - 1 - 4u - \frac{4m_c}{m_B}\,, \\
C_2^{(A_3^{BD^*}-A_0^{BD^*},X_A)} &= -\frac{2(2u-1)\,(\bar{\sigma}-3)}{\bar{\sigma}m_B}\,,
\end{aligned}
$$

$$
\begin{aligned}
C_3^{(A_3^{BD^*}-A_0^{BD^*},X_A)} &= 2\Bigg(m_B\bar{\sigma}(2\bar{\sigma}-3)(1-2u) + 2m_c \\
&\qquad - \frac{m_c^2(2\bar{\sigma}+3) + q^2(2\bar{\sigma}-3)}{\bar{\sigma} m_B}(1-2u)\Bigg) , \\
C_3^{(A_3^{BD^*}-A_0^{BD^*},Y_A)} &= 4\Bigg(2m_B\left[\bar{\sigma}(\sigma+2)-2\right](1-2u) \\
&\qquad + m_c\,(1+4\sigma)\Bigg) ,
\end{aligned}
$$

B

Exclusive Semi-leptonic B Decays with New Physics

In the following the exclusive semileptonic $\bar{B} \to D^* \ell \bar{\nu}$ decay rates including new physics contributions and taking scalar, tensor and pseudotensor currents into account as explained in Chap. 5. The collected formulae are taken from [200].

B.1. Decay Rates with Full Form Factors

In Sec. 5.1.1 scalar-, pseudosclar- and tensor-current form factors in $\bar{B} \to D^{(*)} \ell \bar{\nu}$ decay are presented. In the heavy-quark limit not all form factors disappear, some are protected by Luke's theorem [193]. In this section the decay rates for $B \to D^*$ and $B \to D^*$ transitions are presented with these additional form factors.

B.1.1. $\bar{B} \to D \ell \bar{\nu}$ Decay

Within the standard model, where a $(V-A)$ current structure is used, the semileptonic decay rate is defined by Eq. (4.23). With the scalar and tensor hadronic form factors the function $|\mathcal{G}(w)|$ becomes

$$\begin{aligned} |\mathcal{G}^{\mathrm{NP}}(w)|^2 =& c_+^2 \left[h_+(w) - \frac{1-r}{1+r} h_-(w) \right]^2 \\ &+ \frac{r^2 - 2rw + 1}{(1+r)^2} \left[d_+^2 h_T^2(w) - 3 \frac{g_+^2}{w^2-1} h_S^2(w) \right] . \end{aligned} \tag{B.1}$$

In the heavy-quark limit the form factor $h_-(w)$ vanish, whereas the other ones become a single function. With respect to (5.6) one finds

$$|\mathcal{G}^{\rm NP}_{\rm HQL}(w)|^2 = \left\{ c_+^2 + \frac{r^2 - 2rw + 1}{(1+r)^2} \left[d_+^2 - 3\frac{w+1}{w-1} g_+^2 \right] \right\} |\xi(w)|^2 \ , \tag{B.2}$$

where $|\xi(w)|$ is the Isgur-Wise function. Neglecting the scalar and tensor form factors the heavy-quark limit result is in agreement with the one presented in Ref. [198].

B.1.2. $\bar{B} \to D^* \ell \bar{\nu}$ Decay

For the semileptonic $\bar{B} \to D^* \ell \bar{\nu}$ decay the function $\mathcal{F}(w)$ - Eq. (4.15) - becomes

$$\left|\mathcal{F}^{\rm NP}(w)\right|^2 = \frac{c_-^2 |h_{A_1}(w)|^2}{g(w)} \sum_{i=\pm,0} \left|H_i^{\rm NP}(w)\right|^2 \ , \tag{B.3}$$

where the helicity functions containing new physics contributions can be splitted into a transverse decay mode

$$\begin{aligned}
|H_\perp|^2 =& \left|H_+^{\rm NP}(w)\right|^2 + \left|H_-^{\rm NP}(w)\right|^2 \\
=& 2\frac{1 - 2wr_* + r_*^2}{(1-r_*)^2} \left[1 + \frac{c_+^2}{c_-^2} \frac{w-1}{w+1} R_1^2(w) \right] \\
&+ 2\frac{d_+^2}{c_-^2} \left\{ 2\frac{1 - 2wr_* + r_*^2}{(1-r_*)^2} \left[\left| \frac{h_{T_+}(w)}{h_{A_1}(w)} \right|^2 - \frac{w-1}{w+1} \left| \frac{h_{T_-}(w)}{h_{A_1}(w)} \right|^2 \right] \right. \\
&+ \frac{2}{1-r_*} \left[\left| \frac{h_{T_+}(w)}{h_{A_1}(w)} \right|^2 + \frac{1+r_*}{1-r_*} \left(\frac{w-1}{w+1} \right)^2 \left| \frac{h_{T_-}(w)}{h_{A_1}(w)} \right|^2 \right] \\
&\left. + \frac{1+r_*}{1-r_*} \left[\frac{h_{T_+}(w)}{h_{A_1}(w)} - \frac{w-1}{w+1} \frac{h_{T_-}(w)}{h_{A_1}(w)} \right]^2 \right\} \\
&+ \frac{2}{(1-r_*)^2} \frac{d_-^2}{c_-^2} \frac{w-1}{w+1} \left\{ \frac{1 - 2wr_* + r_*^2}{(w^2-1)} \left[\left| \frac{h_{PT_1}}{h_{A_1}(w)} \right|^2 \right. \right. \\
&\qquad \left. + 2w \frac{h_{PT_1}(w) h_{PT_2}(w)}{|h_{A_1}(w)|^2} + \left| \frac{h_{PT_2}(w)}{h_{A_1}(w)} \right|^2 \right] \\
&\left. - \left[r_*^2 \left| \frac{h_{PT_1}(w)}{h_{A_1}(w)} \right|^2 + 2r_* \frac{h_{PT_1}(w) h_{PT_2}(w)}{|h_{A_1}(w)|^2} + \left| \frac{h_{PT_1}(w)}{h_{A_1}(w)} \right|^2 \right] \right\} ,
\end{aligned} \tag{B.4}$$

and a longitudinal one,

$$\begin{aligned}
\left|H_{\parallel}(w)\right|^2 &= \left|H_0^{\mathrm{NP}}(w)\right|^2 \\
&= \left[1+\frac{w-1}{1-r_*}\left(1-R_2(w)\right)\right]^2 \\
&\quad -3\frac{g_-^2}{c_-^2}\left|\frac{h_P(w)}{h_{A_1}(w)}\right|^2\frac{w-1}{w+1}\frac{1-2wr_*+r_*^2}{(1-r_*)^2} \\
&\quad +2\frac{g_-^2}{c_-^2}\frac{1-2wr_*+r_*^2}{(1-r_*)^2}\left\{\frac{w-1}{w+1}\left|\frac{h_{T_-}(w)}{h_{A_1}(w)}\right|^2\right. \\
&\qquad \left.-\left[\left|\frac{h_{T_+}(w)}{h_{A_1}(w)}\right|^2+(w-1)\left|\frac{h_{T'}(w)}{h_{A_1}(w)}\right|^2\right]\right\} \\
&\quad +\frac{d_-^2}{c_-^2}\frac{1-2wr_*+r_*^2}{(1-r_*)^2}\frac{1}{(w+1)^2} \\
&\qquad \times\left[\frac{wh_{PT_1}(w)+h_{PT_2}(w)+(w^2-1)h_{PT_3}(w)}{h_{A_1}(w)}\right]^2 .
\end{aligned} \tag{B.5}$$

Here, $R_1(w)$ and $R_2(w)$ are defined as in Eq. (3.102) and (3.103), respectively. In the heavy-quark limit, one find,

$$\begin{aligned}
\left|H_{\perp}^{\mathrm{HQL}}(w)\right|^2 =& 2\frac{1-2wr_*r_*^2}{(1-r_*)^2}\left[1+\frac{c_+^2}{c_-^2}\frac{w-1}{w+1}\right] \\
&+\frac{2}{(1-r_*)^2}\left[\frac{d_+^2}{c_-^2}\left(2\frac{1-2wr_*+r_*^2}{w+1}+(1-r_*)^2\right)\right. \\
&\left.+\frac{d_-^2}{c_-^2}\frac{w-1}{w+1}\left(2\frac{1-2wr_*+r_*^2}{w-1}-(1+r_*)^2\right)\right], \\
\left|H_{\parallel}^{\mathrm{HQL}}(w)\right|^2 =& 1+\frac{1-2wr_*+r_*^2}{(1-r_*)^2}\left[\frac{d_-^2+2d_+^2-3(w-1)g_-^2}{c_-^2}\right] .
\end{aligned} \tag{B.6}$$

Within the standard model the coefficients $d_\pm$ and $g_\pm$ are suppressed. The results are in agreement with the standard model predictions.

B.2. Isgur-Wise function

The behaviour of the Isgur-Wise function near zero-recoil is determined by the slope $\rho^2 > 0$, $\xi(1)' = -2\rho^2$. As discussed in Chap. 5 the $B \to D^*$ transitions has longitudinal and transverse decay modes. For the slope one finds in both decay modes

$$\begin{aligned}\rho^2_{\perp\mathrm{NP}} &= \frac{-1}{2\mathcal{F}_\perp^{\mathrm{NP,HQL}}(1)}\frac{\partial\mathcal{F}_\perp^{\mathrm{NP,HQL}}(w)}{\partial w}\bigg|_{w=1}, \\ \rho^2_{\parallel\mathrm{NP}} &= \frac{-1}{2\mathcal{F}_\parallel^{\mathrm{NP,HQL}}(1)}\frac{\partial\mathcal{F}_\parallel^{\mathrm{NP,HQL}}(w)}{\partial w}\bigg|_{w=1},\end{aligned} \tag{B.7}$$

with

$$\rho^2_{\perp\mathrm{NP}} = \rho^2_{*\mathrm{NP}} + \frac{1}{2}\left\{\frac{1}{3}\frac{r_*^2+1}{(r_*-1)^2} - \frac{1}{2}\left(\frac{c_+ + m_B(r_*+1)d_+}{c_- + m_B(r_*-1)d_-}\right)^2\right\}, \tag{B.8}$$

$$\rho_{\parallel\mathrm{NP}^2} = \rho^2_{*\mathrm{NP}} + \frac{1}{6}\frac{r_*+1}{(r_*-1)^2} - \frac{r_*}{(r_*-1)^2}\frac{[c_- - m_B(r_*-1)(d_- - 2g_-)]}{c_- + d_- m_B(r_*-1)}. \tag{B.9}$$

C

Time-dependent Angular Distributions of $B_s^0 \to J/\psi \bar{K}^{*0}$ and CP Conjugates

In this appendix the time-dependent angular distributions of $B_s^0 \to J/\psi \bar{K}^{*0}$ and its CP-conjugates are presented. Following Ref. [229], one introduced the following set of trigonometric functions,

$$\begin{aligned}
f_1 &= 2\,\cos^2\psi\,(1-\sin^2\theta\,\cos^2\varphi)\\
f_2 &= \sin^2\psi\,(1-\sin^2\theta\,\sin^2\varphi)\\
f_3 &= \sin^2\psi\,\sin^2\theta\\
f_4 &= \sin^2\psi\,\sin 2\theta\,\sin\varphi\\
f_5 &= (1/\sqrt{2})\,\sin 2\psi\,\sin^2\theta\sin 2\varphi\\
f_6 &= (1/\sqrt{2})\,\sin 2\psi\,\sin 2\theta\,\cos\varphi.
\end{aligned} \tag{C.1}$$

Using the notation $A_f \equiv A(B_s^0 \to (J/\psi \bar{K}^{*0})_f)$ for the unevolved amplitude in (6.8) and $\bar{A}_f$ for its CP conjugate, one finds

$$\begin{aligned}
&\frac{d^3\Gamma[B_s^0(t) \to J/\psi(\to \ell^+\ell^-)\bar{K}^{*0}(\to \pi^+K^-)]}{d\cos\theta\,d\varphi\,d\cos\psi}\\
&= \frac{9}{64\pi}\,[\cosh(\Delta\Gamma_s t/2) + \cos(\Delta M_s t)]\,e^{-\Gamma_s t}\big[f_1|A_0|^2 + f_2|A_\parallel|^2 + f_3|A_\perp|^2\\
&\quad - f_4\Im\{A_\parallel^* A_\perp\} + f_5\Re\{(A_0^* A_\parallel\} + f_6\Im\{(A_0^* A_\perp\}\big]\\
&\frac{d^3\Gamma[\bar{B}_s^0(t) \to J/\psi(\to \ell^+\ell^-)K^{*0}(\to \pi^-K^+)]}{d\cos\theta\,d\varphi\,d\cos\psi}
\end{aligned} \tag{C.2}$$

$$= \frac{9}{64\pi} [\cosh(\Delta\Gamma_s t/2) + \cos(\Delta M_s t)]\, e^{-\Gamma_s t} \big[f_1 |\bar{A}_0|^2 + f_2 |\bar{A}_\parallel|^2 + f_3 |\bar{A}_\perp|^2 + f_4\, \Im\{\bar{A}_\parallel^* \bar{A}_\perp\} + f_5 \Re\{\bar{A}_0^* \bar{A}_\parallel\} - f_6 \Im\{\bar{A}_0^* \bar{A}_\perp\} \big] \tag{C.3}$$

$$\frac{d^3\Gamma[B_s^0(t) \to J/\psi(\to \ell^+\ell^-) K^{*0}(\to \pi^- K^+)]}{d\cos\theta\, d\varphi\, d\cos\psi}$$

$$= \frac{9}{64\pi} [\cosh(\Delta\Gamma_s t/2) - \cos(\Delta M_s t)]\, e^{-\Gamma_s t} \big[f_1 |\bar{A}_0|^2 + f_2 |\bar{A}_\parallel|^2 + f_3 |\bar{A}_\perp|^2 + f_4 \Im\{\bar{A}_\parallel^* \bar{A}_\perp\} + f_5 \Re\{\bar{A}_0^* \bar{A}_\parallel\} - f_6 \Im\{\bar{A}_0^* \bar{A}_\perp\} \big] \tag{C.4}$$

$$\frac{d^3\Gamma[\bar{B}_s(t) \to J/\psi(\to \ell^+\ell^-) \bar{K}^{*0}(\to \pi^+ K^-)]}{d\cos\theta\, d\varphi\, d\cos\psi}$$

$$= \frac{9}{64\pi} [\cosh(\Delta\Gamma_s t/2) - \cos(\Delta M_s t)]\, e^{-\Gamma_s t} \big[f_1 |A_0|^2 + f_2 |A_\parallel|^2 + f_3 |A_\perp|^2 - f_4 \Im\{A_\parallel^* A_\perp\} + f_5 \Re\{A_0^* A_\parallel\} + f_6 \Im\{A_0^* A_\perp\} \big] . \tag{C.5}$$

In the case of $\Delta\Gamma_s \to 0$, one gets

$$\cosh(\Delta\Gamma_s t/2) + \cos(\Delta M_s t) \to 2\cos^2(\Delta M_s t/2) , \tag{C.6}$$

$$\cosh(\Delta\Gamma_s t/2) - \cos(\Delta M_s t) \to 2\sin^2(\Delta M_s t/2) . \tag{C.7}$$

Consequently, the expressions listed above reduce to those given in Ref. [229] for the flavour-specific $B_d \to J/\psi[\to \ell^+\ell^-] K^*[\to K^\pm \pi^\mp]$ modes with the assumption of $|A_f| = |\bar{A}_f|$.

Bibliography

[1] Euclid and T. L. Heath [ed.], *The Thirteen Books of The Elements, Vol. I (Books I - II)*, vol. 2. Dover Publications, New York, 1956.

[2] O. Hagenmaier, *Der Goldene Schnitt*, vol. 3. Heinz Moos Verlag, Heidelberg, 1963.

[3] D. B. Litvin, "The Icosathedral Point Groups," *Acta. Crys.* **A47** (1991) 70.

[4] L. Corbusier, *Der Modulor*, vol. 6. Deutsche Verlags-Anstalt GmbH, Stuttgart, 1995.

[5] J. F. Donoghue *et al.*, "Dynamics of the Standard Model," Cambridge Monographs on Particle Physics, Nuclear Physics and Cosmology (No. 2), pp. 1–540. Cambridge University Press, 1992.

[6] E. Noether, "Invariante Variationsprobleme," *Nachr. Kgl. Ges. Wiss., Math.-Phys. Klasse* (1918) 235. online available: `http://resolver.sub.uni-goettingen.de/purl?PPN252457811_1918`.

[7] C. Quigg, *Gauge Theories of the Strong, Weak, and Electromagnetic Interactions*. The Benjamin/Cummings Publishing Company Inc., 1983.

[8] S. L. Glashow, "Partial symmetries of weak interactions," *Nucl. Phys.* **22** (1961) 579.

[9] S. Weinberg, "A model of leptons," *Phys. Rev. Lett.* **19** (1967) 1264.

[10] A. Salam, "Weak and Electromagnetic Interactions," in *Elementary Particle Theory*, W. Svartholm, ed., p. 367. Almquvist und Wiksell, 1968.

[11] S. Glashow, J. Iliopoulos, and L. Maiani, "Weak Interactions with Lepton-Hadron Symmetry," *Phys. Rev.* **D2** (1970) 1285.

[12] P. Higgs, "Broken symmetries, massless particles and gauge fields," *Phys. Lett.* **12** (1964) 132.

[13] P. Higgs, "Broken Symmetries and the Masses of Gauge Bosons," *Phys. Rev. Lett.* **13** (1964) 508.

[14] F. Englert and R. Brout, "Broken Symmetry and the Mass of Gauge Vector Bosons," *Phys. Rev. Lett.* **13** (1964) 321.

[15] G. Guralnik *et al.*, "Global Conservation Laws and Massless Particles," *Phys. Rev. Lett.* **13** (1964) 585.

[16] "Symmetry Breaking in Biology," in *Cold Spring Harbor Perspectives in Biology*, R. Li and B. Bowerman, eds., vol. 1. Cold Spring Harbor, New York, 2010.

[17] **ATLAS** Collaboration, "Expected Performance of the ATLAS Experiment - Detector, Trigger and Physics," `arXiv:0901.0512`.

[18] **CMS** Collaboration, "CMS Physics Technical Design Report, Volume II: Physics Performance," *J. Phys. G: Nucl. Phys.* **34** (2007) 995.

[19] **LHCb** Collaboration, S. Amato *et al.*, "LHCb: Technical Proposal," *preprint* **CERN-LHCC-98-4, LHCC-P-4** (1998) .

[20] C. Quigg, "Unanswered Questions in the Elektroweak Theory," *Ann. Rev. Nucl. Part. Sci.* **59** (2009) 505, `arXiv:0905.3187`.

[21] J. Ellis, "Beyond the standard model with the LHC," *Nature* **448** (2007) 297.

[22] G. Altarelli, "Particle Physics at the LHC Start," `arXiv:1010.5637`.

[23] A. Buras, "Waiting for Clear Signals of New Physics in B and K Decays," in *Particle Physics and the Universe*, J. Trampetić and J. Wess, eds., vol. 98 of *Springer Proceedings Physics*, p. 315. Springer Berlin Heidelberg, 2005.

[24] R. Fleischer, "Flavour Physics and CP violation: Expecting the LHC," arXiv:0802.2882.

[25] G. Buchalla *et al.*, "B, D and K decays," *Eur. Phys. J.* **C57** (2008) 309, arXiv:0801.1833.

[26] G. Isidori *et al.*, "Flavor Physics Constraints for Physics Beyond the Standard Model," *Ann. Rev. Nucl. Part. Sci.* **60** (2010) 355, arXiv:1002.0900.

[27] G. Perez, "Brief Introduction to Flavor Physics," arXiv:0911.2092.

[28] N. Cabbibo, "Unitary Symmetry and Leptonic Decays," *Phys. Rev. Lett.* **10** (1963) 531.

[29] M. Kobayashi and T. Maskawa, "*CP*-Violation in the Renormalization Theory of Weak Interaction," *Prog. Theo. Phys.* **49** (1973) 652.

[30] **UTfit** Collaboration, M. Bona *et al.*, "The UT*fit* collaboration report on the status of the unitarity triangle beyond the Standard Model I. Model-independent analysis and minimal flavour violation," *JHEP* **03** (2006) 080, arXiv:hep-ph/0509219v.

[31] J. Charles *et al.*, "Status of CKM Matrix and a simple New Physics scenario," *Nucl. Phys. Prog. Suppl.* **185** (2008) 17.

[32] M. E. Peskin and D. V. Schroeder, *An Introduction to Quantum Field Theory*. Westview Press, 1995.

[33] M. Maggiore, *A Modern Introduction to Quantum Field Theory*. Oxford University Press, 2005.

[34] M. Böhm *et al.*, *Gauge Theories of the Strong and Electroweak Interaction*. B. G. Teubner, Leipzig, Wiesbaden, 3 ed., 2001.

[35] P. Langacker, "Introduction to the Standard Model and Eletroweak Physics," arXiv:0901.0241.

[36] S. D. Leo, "Quaternionic Lorentz Group and Dirac Equation," *Found. Phys. Lett.* **14** (2001) 37, arXiv:hep-th/0103129.

[37] G. Dixon, *Division Algebras: Octonions, Quaternions, Complex Numbers and the Algebraic Design of Physics*. Kluwer Academic Publishers, 1994.

[38] P. Lounesto, "Clifford Algebras and Spinor Operators," in *Clifford (Geometric) Algebras*, Baylis, ed., pp. 5–35. 1996.

[39] P. Lounesto, *Clifford Algebras and Spinors*. Cambridge University Press, 1997.

[40] C. Yang and R. Mills, "Conservation of Isotopic Spin and Isotopic Gauge Invariance," *Phys. Rev.* **96** (1954) 191.

[41] Y. Nir, "Flavor Physics and CP Violation," `arXiv:hep-ph/9810520`.

[42] M. Gell-Mann, "Symmetries of Baryons and Mesons," *Phys. Rev.* **125** (1962) 1067.

[43] **Particle Data Group** Collaboration, K. Nakamura *et al.*, "Review of particle physics," *J. Phys.* **G37** (2010) 075021. Online updates: `http://pdg.lbl.gov`.

[44] L. Wolfenstein, "Parametrization of the Kobayashi-Maskawa Matrix," *Phys. Rev. Lett.* **51** (1983) 1945.

[45] A. J. Buras, M. E. Lautenbacher, and G. Ostermaier, "Waiting for the top quark mass, $K^+ \to \pi^+ \nu\bar{\nu}$, $B_s^0 - \bar{B}_s^0$ mixing and CP asymmetries in B decays," *Phys. Rev.* **D50** (1994) 3433, `arXiv:hep-ph/9403384`.

[46] **CKMfitter Group** Collaboration, J. Charles *et al.*, "CP violation and the CKM matrix: assessing the impact of the asymmetric B factories," *Eur. Phys. J.* **C41** (2005) 1, `arXiv:hep-ph/0406184`. Updated results and plots available at: `http://ckmfitter.in2p3.fr`.

[47] M. Ciuchini *et al.*, "2000 CKM triangle analysis: A Critical review with updated experimental inputs and theoretical parameters," *JHEP* **07** (2001) 013, `arXiv:hep-ph/0012308`. Updated results and plots available at: `http://www.utfit.org`.

[48] A. Höcker *et al.*, "A New approach to a global fit of the CKM matrix," *Eur. Phys. J.* **C21** (2001) 225, `arXiv:hep-ph/0104062`.

[49] Chodos *et al.*, "Modern Kaluza-Klein Theories," in *Frontiers in Physics*, T. Appelquist, ed. Addison-Wesley, Menlo Park, CA, 1987.

[50] H. P. Nilles, "Supersymmetry, supergravity and particle physics," *Phys. Rept.* **110** (1984) 1.

[51] G. ′t Hooft and M. Veltman, "One-loop divergences in the theory of gravitation," *Ann. Inst. Henri Poincaré, Sec. A* **20(1)** (1974) 69.

[52] M. Veltman, "Quantum Theory of Gravitation," in *Methods in field theory. Les Houches, Session XXVIII, 1975*, R. Balian and J. Zinn-Justin, eds., pp. 265–327. North Holland Publishing Company, 1976.

[53] J. F. Donoghue, "General relativity as an effective field theory: The leading quantum corrections," *Phys. Rev.* **D50** (1994) 3874, arXiv:gr-qc/9405057.

[54] J. F. Donoghue, "Leading Quantum Correction to the Newtonian Potential," *Phys. Rev. Lett.* **72** (1994) 2996, arXiv:gr-qc/9310024.

[55] R. Barate *et al.*, "Search for the Standard Model Higgs boson at LEP," *Phys. Lett.* **B565** (2003) 61, arXiv:hep-ex/0306033. updates available at http://lepewwg.web.cern.ch/LEPEWWG/.

[56] **CDF and DØ** Collaboration, T. Aaltonen *et al.*, "Combination of Tevatron Searches for the Standard Model Higgs Boson in the W^+W^- Decay Mode," *Phys. Rev. Lett.* **104** (2010) 061802, arXiv:1001.4162.

[57] N. Arkani-Hamed *et al.*, "The hierarchy problem and new dimensions at a millimeter," *Phys. Lett.* **B429** (1998) 263, arXiv:hep-ph/9803315.

[58] G. ′t Hooft, "Naturalness, Chiral Symmetry, and Spontaneous Chiral Symmetry Breaking," in *Recent Developments in Gauge Theories*, ′t Hooft, ed., NATO Science Series B: Physics **59**, pp. 135–157. 1980. M. Veltman, "The Infrared-Ultraviolet Connection," *Act. Phys. Pol.* **B12** (1981) 437.

[59] G. Altarelli, "The Elektroweak Symmetry Breaking Riddle," *Fortschr. Phys.* **1-17** (2010) , arXiv:1003.3180.

[60] S. W. Herb *et al.*, "Obeservation of a dimuon resonance at 9.5 gev in 400-gev proton-nucleus collisions," *Phys. Rev. Lett.* **39** 259.

[61] H. Schröder, "Physics of B mesons," *Rep. Prog. Phys.* **52** (1989) 765.

[62] J. H. Christenson *et al.*, "Evidence for the 2π Decay of the K_2^0 Meson," *Phys. Rev. Lett.* **13** (1964) 138. V. L. Fitch, "The discovery of the charge-conjugation parity asymmetry," *Rev. Mod. Phys.* **53** (1981) 367; *Science* **212** (1981) 989.

J. W. Cronin, "CP symmetry violation - the search for its origin," *Rev. Mod. Phys.* **53** (1981) 373; *Science* **212** (1981) 1221.

[63] **BABAR** Collaboration, B. Aubert *et al.*, "Oberservation of CP Violation in the B^0 Meson System," *Phys. Rev. Lett.* **87** (2001) 091801, `arXiv:hep-ex/0107013`.

[64] **Belle** Collaboration, K. Abe *et al.*, "Observation of Large CP Violation in the Neutral B Meson System," *Phys. Rev. Lett.* **87** (1981) 091802, `arXiv:hep-ex/0107061`.

[65] C. Jarlskog, "Introduction to CP Violation," in *CP Violation*, C. Jarlskog, ed., Adv. Ser. Direct. High Energy Physics - Vol. 3, pp. 3–40. World Scientific, Singapore, 1989.

[66] I. I. Bigi and A. I. Sanda, *CP Violation*. Cambridge University Press, 2000.

[67] J. R. Fry, "CP violation and the standard model," *Rep. Prog. Phys.* **63** (2000) 117.

[68] Fayyazuddin, "CP-Violation in K, B and B_s decays," `arXiv:0907.3285`.

[69] C. Jarlskog, "A Basis Independent Formulation of the Connection Between Quark Mass Matrices, CP Violation and Experiment," *Z. Phys.* **C29** (1985) 491.

[70] C. Jarlskog, "Commutator of the Quark Mass Matrices in the Standard Electroweak Model and a Measure of Maximal CP Nonconservation," *Phys. Rev. Lett.* **55** (1985) 1039.

[71] J. Bernabeu *et al.*, "CP Restrictions on Quarks Mass Matrices," *Phys. Lett.* **B169** (1986) 243.

[72] A. B. Carter and A. I. Sanda, "CP Nonconservation in Cascade Decays of B Mesons," *Phys. Rev. Lett.* **45** (1980) 952.

[73] A. B. Carter and A. I. Sanda, "CP violation in B-meson decays," *Phys. Rev.* **D23** (1981) 1567.

[74] I. I. Bigi and A. I. Sanda, "Notes on the observability of CP violations in B decays," *Nucl. Phys.* **B193** (1981) 85.

[75] I. Dunietz and J. L. Rosner, "Time-dependent CP-violation effects in $B^0 - \bar{B}^0$ systems," *Phys. Rev.* **D34** (1986) 1404.

[76] I. Dunietz, "Rephase Invariance of KM Matrices and CP violation," *Ann. Phys.* **184** (1988) 350.

[77] R. Fleischer, "CP violation and the Role of Electroweak Penguins in Nonleptonic B Decays," *Int. J. Mod. Phys.* **A12** (1997) 2459, arXiv:hep-ph/9612446.

[78] V. F. Weisskopf and E. P. Wigner, "Berechnung der natürlichen Linienbreite auf Grund der Diracschen Lichttheorie," *Z. Phys.* **63** (1930) 54. "Über die natürliche Linienbreite in der Strahlung des harmonischen Oszillators," *Z. Phys.* **65** (1930) 18.

[79] **HFAG** Collaboration, D. Asner *et al.*, "Averages of b-hadron, c-hadron, and τ-lepton Properties," arXiv:1010.1589. Online updates: http://www.slac.stanford.edu/xorg/hfag/.

[80] M. Gronau, "Theory of CP Violation," *Nucl. Phys. Proc. Suppl.* **B65** (1998) 245, arXiv:hep-ph/9705440v1.

[81] R. Fleischer, "Extracting γ from $B_{\mathrm{s(d)}} \to J/\psi K_{\mathrm{s}}$ and $B_{\mathrm{d(s)}} \to D^{+}_{\mathrm{d(s)}} D^{-}_{\mathrm{d(s)}}$," *Eur. Phys. J.* **C10** (1999) 299, arXiv:hep-ph/9903455.

[82] K. G. Wilson and W. Zimmermann, "Operator product expansions and composite field operator in the general framework of quantum field theory," *Commmun. math. Phys.* **24** (1972) 87.

[83] M. Neubert, "Effective Field Theory and Heavy Quark Physics," in *Physics in $D \geq 4$, TASI 2004*, J. Terning *et al.*, eds., Proc. Theoretical Advanced Study Institute in Elementary Particle Physics, p. 149. World Scientific, Singapore, 2006. arXiv:hep-ph/0512222.

[84] A. J. Buras, "Weak Hamiltonian, CP Violation and Rare Decays," in *Probing the Standard Model of Particle Interactions*, R. Gupta *et al.*, eds., vol. I of *Proc. 1997 Les Houches Summer School LXVIII*, p. 281. Elsevier, Amsterdam, 1999. arXiv:hep-ph/9806471.

[85] G. Buchalla *et al.*, "Weak decays beyond leading logarithm," *Rev. Mod. Phys.* **68** (1996) 1125, arXiv:hep-ph/9512380.

[86] J. Virto, "Topics in Hadronic B Decays," arXiv:0712.3367.

[87] R. Fleischer, "Electroweak penguin effects beyond leading logarithms in the B-meson decays $B^- \to K^-\Phi$ and $B^- \to \pi^-\bar{K}^{0*}$," *Z. Phys.* **C62** (1994) 81. "Analysis of penguin-induced B decays of the type $B \to M\Phi(M \in \{\pi, \rho, \dots\})$,"*Phys. Lett.* **B321** (1994) 259, "Search for the angle γ in the electroweak penguin domianted decay $B_s \to \pi^0\Phi$," *Phys. Lett.* **B332** (1994) 419.

[88] R. Fleischer, "CP Violation and the Role of Electroweak Penguins in Nonleptonic B Decays," *Int. J. Mod. Phys.* **A12** (1997) 2459, arXiv:hep-ph/9612446.

[89] T. Mannel, "Effective Field Theories in Flavour Physics," in *Springer Tracts in Modern Physics*, J. Kühne *et al.*, eds., vol. 203, pp. 1–175. Springer-Verlag Berline Heidelberg, 2004.

[90] T. Inami and C. S. Lim, "Effects of Superheavy Quarks and Leptons in Low-Energy Weak Processes $K_L \to \mu\bar{\mu}$, $K^+ \to \pi^+\nu\bar{\nu}$ and $K^0 \leftrightarrow \bar{K}^0$," *Prog. Theor. Phys.* **65** (1981) 297. ibid. **65** (1981) 1772.

[91] G. Buchalla *et al.*, "The anatomy of ϵ'/ϵ in the standard model," *Nucl. Phys.* **B337** (1990) 313.

[92] M. Neubert, "Heavy Quark Symmetries," *Phys. Rep.* **245** (1994) 259.

[93] M. Beneke *et al.*, "QCD factorization for exclusive non-leptonic B-meson decays: general arguments and the case of heavy-light final states," *Nucl. Phys.* **B591** (2000) 313, arXiv:hep-ph/0006124.

[94] J. D. Bjorken, "Topics in B-physics," *Nucl. Phys. Proc. Suppl.* **B11** (1989) 325.

[95] M. Bauer *et al.*, "Exclusive Non-Leptonic Decays of D-, D_s- and B-Mesons," *Z. Phys.* **C34** (1987) 103.

[96] M. Neubert and B. Stech, "Non-Leptonic Weak Decays of B Mesons," in *Heavy Flavours II*, A. J. Buras and M. Lindner, eds., Adv. Ser. Direct. High Energy Physics - Vol. 15, pp. 294–344. World Scientific, Singapore, 1998. arXiv:hep-ph/9705292.

[97] A. Ali and C. Greub, "Analysis of two-body nonleptonic B decays involving light mesons in the standard model," *Phys. Rev.* **D57** (1998) 2996, arXiv:hep-ph/9707251.

[98] A. Ali *et al.*, "Experimental tests of factorization in charmless nonleptonic two-body b decays," *Phys. Rev.* **D58** (1998) 094009, arXiv:hep-ph/9804363.

[99] Y. H. Chen *et al.*, "Charmless hadronic two-body decays of B_u and B_d mesons," *Phys. Rev.* **D60** (1999) 094014, arXiv:hep-ph/9804363.

[100] M. Beneke *et al.*, "QCD Factorization for $B \to \pi\pi$ Decays: Strong Phases and CP Violation in the Heavy Quark Limit," *Phys. Rev. Lett.* **83** (1999) 1914, arXiv:hep-ph/9905312.

[101] M. Beneke *et al.*, "QCD factorization in $B \to \pi K, \pi\pi$ decays and extraction of Wolfenstein parameters," *Nucl. Phys.* **B606** (2001) 245, arXiv:hep-ph/0104110.

[102] M. Beneke and M. Neubert, "QCD factorization for $B \to PP$ and $B \to PV$ decays," *Nucl. Phys.* **B675** (2003) 333, arXiv:hep-ph/0308039.

[103] M. Beneke and S. Jäger, "Spectator scattering at NLO in non-leptonic B decays: Tree amplitudes," *Nucl. Phys.* **B751** (2006) 160, arXiv:hep-ph/0512351.

[104] M. Beneke and S. Jäger, "Spectator scattering at NLO in non-leptonic B decays: Leading penguin amplitudes," *Nucl. Phys.* **B768** (2007) 51, arXiv:hep-ph/0610322.

[105] V. Pilipp, "Hard spectator interactions in $B \to \pi\pi$ at orders α_s^2," *Nucl. Phys.* **B794** (2008) 154, arXiv:0709.3214.

[106] N. Kivel, "Radiative corrections to hard spectator scattering in $B \to \pi\pi$ decays," *JHEP* **05** (2007) 019, arXiv:hep-ph/0608291.

[107] A. Jain *et al.*, "Penguin Loops for Nonleptonic B-decays in the Standard Model: Is there a Penguin Puzzle?," arXiv:0706.3399.

[108] G. Bell, "NNLO vertex corrections in charmless hadronic B decays: Imaginary part," *Nucl. Phys.* **B795** 1, arXiv:0705.3127. "NNLO vertex corrections in

charmless hadronic B decays: Real Part," *Nucl. Phys.* **B822** (2009) 172, arXiv:0902.1915.

[109] M. Beneke *et al.*, "NNLO vertex corrections to non-leptonic B decays: Tree amplitudes," *Nucl. Phys.* **B832** (2010) 109, `arXiv:0911.3655`.

[110] V. M. Braun and I. E. Filyanov, "QCD sum rules in exclusive kinematics and pion wave function," *Z. Phys.* **C44** (1989) 157. ibid. *Sov. J. Nucl. Phys.* **50** (1989) 511. *Yad. Fiz.* **50** (1989) 818.

[111] V. M. Braun and I. E. Filyanov, "Conformal invariance and pion wave functions of nonleading twist," *Z. Phys.* **C48** (1990) . ibid. *Sov. J. Nucl. Phys.* **52** (1990) 126. *Yad. Fiz.* **52** (1990) 199.

[112] M. Beneke and T. Feldmann, "Symmetry-breaking corrections to heavy-to-light b meson form factors at large recoil," *Nucl. Phys.* **B592** (2001) 3, `arXiv:hep-ph/0008255`.

[113] V. L. Chernyak and A. R. Zhitnitsky, "Asymptotic behaviour of exclusive Processes in QCD," *Phys. Rept.* **112** (1984) 173.

[114] P. Ball *et al.*, "Higher twist distribution amplitudes of vector mesons in QCD: Formalism and twist 3 distributions," *Nucl. Phys.* **B529** (1998) 323, `arXiv:hep-ph/9802299`. P. Ball and V. M. Braun,"Higher twist distribution amplitudes of vector mesons in QCD: twist-4 distributions and meson mass corrections," *Nucl. Phys.* **B534** (1999) 201, arXiv:hep-ph/9810475.

[115] A. G. Grozin and M. Neubert, "Asymptotics of heavy-meson form factors," *Phys. Rev.* **D55** (1997) 272.

[116] N. Offen, *B-Zerfallsformfaktoren aus QCD-Summenregeln*. PhD thesis, University of Siegen, 2008. Electronic version available from UB Siegen: http://dokumentix.ub.uni-siegen.de/opus/volltexte/2008/334/.

[117] M. Wirbel *et al.*, "Exclusive Semileptonic Decays of Heavy Mesons," *Z. Phys.* **C29** (1985) 637.

[118] M. Beneke *et al.*, "Branching fractions, polarisation and asymmetries of $B \to VV$ decays," *Nucl. Phys.* **B774** (2007) 64, `arXiv:hep-ph/0612290`.

[119] A. L. Kagan, "Polarization in $B \to VV$ decays," *Phys. Lett.* **B601** (2004) 151, arXiv:hep-ph/0405134.

[120] H. Y. Cheng and C. K. Chuan, "QCD factorization for charmless hadronic B_s decays revisited," *Phys. Rev.* **D80** (2009) , arXiv:0910.5237.

[121] N. Isgur and M. B. Wise, "Weak decays of heavy mesons in the static quark approximation," *Phys. Lett.* **B232** (1989) 113.

[122] N. Isgur and M. B. Wise, "Weak transition form factors between heavy mesons," *Phys. Lett.* **B237** (1990) 527.

[123] E. Eichten and B. Hill, "An effective field theory for the calculation of matrix elements involving heavy quarks," *Phys. Lett.* **B234** (1990) 511. "Static effective field theory: $1/m$ corrections," *Phys. Lett.* **B243** (1990) 427.

[124] B. Grinstein, "The static quark effective theory," *Nucl. Phys.* **B339** (1990) 253.

[125] H. Georgi, "An effective field theory for heavy quarks at low energies," *Phys. Lett.* **B240** (1990) 447.

[126] A. F. Falk *et al.*, "Heavy mesons form factors," *Nucl. Phys.* **B343** (1990) 1.

[127] A. F. Falk *et al.*, "Leading mass corrections to the heavy quark effective theory," *Nucl. Phys.* **B357** (1991) 185.

[128] T. Mannel, "Review of Heavy Quark Effective Theory," arXiv:hep-ph/9611411. "Spin Effects in Heavy Quark Processes," *Act. Phys. Pol.* **29** (1998) 1413.

[129] T. Mannel, "Heavy-quark effective field theory," *Rep. Prog. Phys.* **60** (1997) 1113.

[130] H. Georgi, "Heavy Quark Effective Field Theory," in *Perspectives in the Standard Model, TASI 1991*, C. T. Ellis, R. K. Hill and J. D. Lykken, eds., Proc. Theoretical Advanced Study Institute in Elementary Particle Physics, p. 589. World Scientific, Singapore, 1992. HUTP-91-A039.

[131] B. Grinstein, "An Introduction To Heavy Mesons," arXiv:hep-ph/9508227.

[132] F. Hussain and G. Thompson, "An Introduction to the Heavy Quark Effective Theory," arXiv:hep-ph/9502241.

[133] A. V. Manohar and M. B. Wise, "Heavy Quark Physics," Cambridge Monographs on Particle Physics, Nuclear Physics and Cosmology (No. 10), pp. 1–191. Cambridge University Press, 2000.

[134] A. G. Grozin, "Heavy Quark Effective Theory," in *Springer Tracts in Modern Physics*, J. Kühne *et al.*, eds., vol. 201, pp. 1–213. Springer-Verlag Berline Heidelberg, 2004.

[135] H. Georgi, "$D - \bar{D}$ mixing in heavy quark effective theory," *Phys. Lett.* **B297** (1992) 353, `arXiv:hep-ph/9209291`.

[136] T. M. Yan *et al.*, "Heavy-quark symmetry and chiral dynamics," *Phys. Rev.* **D46** (1992) 1148.

[137] G. Burdmann and J. F. Donoghue, "Union of chiral and heavy quark symmetries," *Phys. Lett.* **B280** (1992) 287.

[138] D. Ebert *et al.*, "Effective meson lagrangian with chiral and heavy quark symmetries from quark flavor dynamics," *Nucl. Phys.* **B434** (1995) 619.

[139] J. M. Flynn and N. Isgur, "Heavy-quark symmetry: ideas and applications," *J. Phys. Nucl. Part. Phys.* **18** (1992) 1627.

[140] A. F. Falk, "Hadrons of arbitrary spin in the heavy-quark effective theory," *Nucl. Phys.* **B378** (1992) 79.

[141] T. Mannel and Z. Ryzak, "Spin symmetry in e^+e^- annihilation into heavy mesons," *Phys. Lett.* **B247** (1990) 412.

[142] H. Georgi, "Comment on heavy baryon weak form factors," *Nucl. Phys.* **B348** (1991) 293.

[143] T. Mannel *et al.*, "Baryons in the heavy quark effective theory," *Nucl. Phys.* **B355** (1991) 38.

[144] N. Isgur and M. B. Wise, "Spectroscopy with Heavy-Quark Symmetry," *Phys. Rev. Lett.* **66** (1991) 1130.

[145] J. G. Körner and G. A. Falk, "Exclusive semi-leptonic decays of bottom mesons in the spectator quark model," *Z. Phys.* **C38** (1988) 511. Erratum: *Z. Phys.* **C41** (1989) 41.

[146] M. Voloshin and M. Shifman, "On Annihilation of Mesons Built from Heavy and Light Quark and and anti-$B^0 \leftrightarrow B^0$ Oscillations," *Yad. Fiz.* **45** (1987) 463. ibid. *Sov. J. Nucl. Phys.* **45** (1987) 292.

[147] M. Voloshin and M. Shifman, "On Production of D and D^* Mesons in B-Meson Decays," *Yad. Fiz.* **47** (1988) 801. ibid. *Sov. J. Nucl. Phys.* **47** (1988) 511.

[148] E. P. Wigner, "Einige Folgerungen aus der Schrödingerschen Theorie für die Termstrukturen," *Z. Phys.* **43** (1927) 624.

[149] C. Eckart, "The Application of Group theory to the Quantum Dynamics of Monatomic Systems," *Rev. Mod. Phys.* **2** (1930) 305.

[150] H. Umezawa, *Quantum Field Theory*. North Holland, Amsterdam, 1956.

[151] G. Preparata and W. I. Weisenberger, "Ultraviolet Divergences in Radiative Corrections to Weak Decays," *Phys. Rev.* **175** (1968) 1965.

[152] H. D. Politzer and M. B. Wise, "Leading logarithms of heavy quark masses in processes with light and heavy quarks," *Phys. Lett.* **B206** (1988) 681.

[153] H. D. Politzer and M. B. Wise, "Effective field theory approach to processes involving both light and heavy field," *Phys. Lett.* **B208** (1988) 504.

[154] G. P. Korchemsky and A. V. Radyushkin, "Renormalization of the Wilson loops beyond the leading order," *Nucl. Phys.* **B283** (1987) 342.

[155] T. Mannel *et al.*, "A derivation of the heavy quark effective langrangian from QCD," *Nucl. Phys.* **B368** (1992) 204.

[156] T. Mannel *et al.*, "Higher Order Power Corrections in Inclusive B Decays," `arXiv:1009.4622`.

[157] S. Turczyk, *Testing the Standard Model with Precision Calculations of Semileptonic B-Decays*. PhD thesis, University of Siegen, 2010.

[158] J. G. Körner and G. A. Schuler, "Exclusive semi-leptonic decays of bottom mesons in the spectator quark model," *Z. Phys.* **C38** (1988) 511. Erratum: *Z. Phys.* **C41** (1989) 690, "Exclusive semileptonic heavy meson decays including lepton mass effects," Z. Phys. **46** (1990) 93.

[159] F. J. Gilman and R. L. Singleton, "Analysis of semileptonic decays of mesons containing heavy quarks," *Phys. Rev.* **D41** (1990) 142.

[160] **BABAR** Collaboration, B. Aubert *et al.*, "Measurements of the $B \to D^*$ form factors using the decay $\bar{B}^0 \to D^{*+} e^- \bar{\nu}_e$," *Phys. Rev.* **D74** (2006) 092004, arXiv:hep-ex/0602023.

[161] M. E. Luke, "Effects of subleading operators in the heavy quark effective theory," *Phys. Lett.* **B252** (1990) 447.

[162] M. Neubert, "Model-independent extraction of V_{cb} from semi-leptonic decays," *Phys. Lett.* **B264** (1991) 455.

[163] M. Okamoto *et al.*, "Semileptonic $D \to \pi/K$ and $B \to \pi/D$ decays in $2+1$ flavor lattice QCD," *Nucl. Phys. Proc. Suppl.* **B140** (2005) 461, arXiv:hep-lat/0409116.

[164] J. A. Bailey *et al.*, "$B \to D^* l \nu$ at zero recoil: an update," arXiv:1011.2166.

[165] M. A. Shifman *et al.*, "QCD and resonance physics. Theoretical foundations," *Nucl. Phys.* **B147** (1979) 385. "QCD and resonance physics. Applications," *Nucl. Phys.* **B147** (1979) 448.

[166] A. V. Radyushkin, "Introduction to QCD Sum Rule Approach," in *Strong interactions at Low and Intermediate Energies*, J. L. Goity, ed., pp. 91–150. World Scientific, Singapore, 2000. arXiv:hep-ph/0101227.

[167] P. Colangelo and A. Khodjamirian, "QCD Sum Rules, A Modern Perspective," in *At the Frontier of Particle Physics – Handbook of QCD, Vol. 3*, M. Shifman, ed., pp. 1495 – 1576. World Scientific, Singapore, 2001. arXiv:hep-ph/0010175.

[168] A. Khodjamirian *et al.*, "B-meson distribution amplitudes form $B \to \pi$ form factor," *Phys. Lett.* **B620** (2005) 52, arXiv:hep-ph/0504091.

[169] A. Khodjamirian *et al.*, "Form factors from light-cone sum rules with B-meson distribution amplitudes," *Phys. Rev.* **D75** (2007) 054013, arXiv:hep-ph/0611193.

[170] S. Faller *et al.*, "$B \to D^{(*)}$ form factors from QCD light-cone sum rules," *Eur. Phys. J.* **C60** (2009) 603, arXiv:0809.0222.

[171] N. S. Craigie and J. Stern, "What can we learn from sum rules for vertex functions in QCD?," *Nucl. Phys.* **B216** (1983) 209. N. S. Craigie *et al.*, "QCD Determination of the $A_1 - \rho - \phi$ System Through Vertex Light-Cone Sum Rules," *Z. Phys.* **C30** (1986) 69.

[172] M. Neubert, "Symmetry breaking corrections to meson decay constants in the heavy-quark effective theory," *Phys. Rev.* **D46** (1992) 1076. "Subleading Isgur-Wise form factors form QCD sum rules," *Phys. Rev.* **D46** (1992) 3914.

[173] P. Ball and R. Zwicky, "New results on $B \to \pi, K, \eta$ decay form factors from light-cone sum rules," *Phys. Rev.* **D71** (2005) 014015, arXiv:hep-ph/0406232.

[174] G. Duplančić *et al.*, "Light-cone sum rules for $B \to \pi$ form factors revisited," *JHEP* **04** (2008) 014, arXiv:0801.1796.

[175] I. I. Balitsky and V. M. Braun, "Evolution equations for QCD string operators," *Nucl. Phys.* **B311** (1989) 541.

[176] H. Kawamura *et al.*, "B-meson light-cone distribution amplitudes in the heavy-quark limit," *Phys. Lett.* **B523** (2001) 111. Erratum: *Nucl. Phys.* **B536** (2002) 344.

[177] V. M. Braun *et al.*, "B-meson distribution amplitude in QCD," *Phys. Rev.* **D69** (2004) 034014, arXiv:hep-ph/0309330.

[178] A. Khodjamirian *et al.*, "Predictions on $B \to \pi \bar{l} \nu_l$, $D \to \pi \bar{l} \nu_l$, and $D \to K \bar{l} \nu_l$ from QCD light-cone sum rules," *Phys. Rev.* **D62** (2000) 114002, arXiv:hep-ph/0001297.

[179] A. A. Penin and M. Steinhauser, "Heavy-light meson decay constant from QCD sum rules in the three-loop approximation," *Phys. Rev.* **D65** (2002) 054006, arXiv:hep-ph/0108110.

[180] S. Narison, "Light and heavy quark masses, Flavour breaking of chiral condensates, Meson weak leptonic decay constants in QCD," arXiv:hep-ph/0202200.

[181] **CLEO** Collaboration, B. I. Eisenstein *et al.*, "Precision measurement of $\mathcal{B}(D^+ \to \mu^+ \nu)$ and the pseudoscalar decay constant f_{D^+}," *Phys. Rev.* **D78** (2008) 052003, arXiv:0806.2112.

[182] A. Khodjamirian *et al.*, "Perturbative QCD correction to the light-cone sum rule for the $B^*\ B\pi$ and $D^*\ D\pi$ couplings," *Phys. Lett.* **B457** (1999) 245, arXiv:hep-ph/9903421.

[183] B. O. Lange and M. Neubert, "Renormalization-Group Evolution of the B-Meson Light-Cone Distribution Amplitude," *Phys. Rev. Lett.* **91** (2003) 102001, arXiv:hep-ph/0303082. S. J. Lee and M. Neubert,"Model-independent properties of the B-meson distribution amplitude ," *Phys. Rev.* **D72**, (2002) 094028, arXiv:hep-ph/0509350.

[184] Caprini *et al.*, "Dispersive bounds on the shape of $\bar{B} \to D^{(*)}\ell\bar{\nu}$ form factors," *Nucl. Phys.* **B530** (1998) 153.

[185] **BABAR** Collaboration, B. Aubert *et al.*, "Measurements of the semileptonic decays $\bar{B} \to D\ell\bar{\nu}$ and $\bar{B} \to D^*\ell\bar{\nu}$ using a global fit to $DX\ell\bar{\nu}$ final states," *Phys. Rev.* **D79** (2009) 012002, arXiv:0809.0828.

[186] **Belle** Collaboration, I. Adachi *et al.*, "Measurement of the form factors of the decay $B^0 \to D^{*-}\ell^+\nu_\ell$ and determination of the CKM matrix element $|V_{cb}|$," arXiv:0810.1657.

[187] C. Bernard *et al.*, "$\bar{B} \to D^*\ell\bar{\nu}$ form factor at zero recoil from three-flavor lattice QCD: A model independent determination of $|V_{cb}|$," *Phys. Rev.* **D79** (2009) 014506, arXiv:0808.2519.

[188] **BABAR** Collaboration, B. Aubert *et al.*, "Determination of the form factors for the decay $B^0 \to D^{*-}l^+\nu_l$ and the CKM matrix element V_{cb}," *Phys. Rev.* **D77** (2008) 032002, arXiv:0705.4008.

[189] **Belle** Collaboration, W. Dungel, "Measurement of the form factors of the decay $B^0 \to D^{*-}\ell^+\nu_\ell$ and determination of the CKM matrix element $|V_{cb}|$," arXiv:1010.5620.

[190] C. Bernard *et al.*, "$\bar{B} \to D^*\ell\bar{\nu}$ form factor at zero recoil from three-flavor lattice QCD: A model independent determination of $|V_{cb}|$," *Phys. Rev.* **D79** (2009) 014506, arXiv:0808.2519.

[191] **BABAR** Collaboration, B. Aubert *et al.*, "Measurement of $|V_{cb}|$ and the Form-Factor Slope in $\bar{B} \to D\ell\bar{\nu}_\ell$ Decays in Events Tagged by a Fully

Reconstructed B Meson," *Phys. Rev. Lett.* **104** (2010) 011802, arXiv:0904.4063.

[192] R. Feger *et al.*, "Limit in Right-Handed Admixture to the Weak $b \to c$ Current from Semileptonic Decays," arXiv:1003.4022.

[193] R. Lebed and M. Suzuki, "Current Algebra and the Ademollo-Gatto theorem in spin-flavor symmetry of heavy quarks," *Phys. Rev.* **D44** (1991) 829.

[194] B. Dassinger *et al.*, "Testing the left-handedness of $b \to c$ transition," *Phys. Rev.* **D75** (2007) 095007, arXiv:hep-ph/0701054.

[195] M. Ademollo and R. Gatto, "Nonrenormalization Theorem for the Strangeness-Violating Vector Currents," *Phys. Rev. Lett.* **13** (1964) 264.

[196] W. Buchmüller and D. Wyler, "Effective lagrangian analysis of new interactions and flavour conservation," *Nucl. Phys.* **B268** (1986) 621.

[197] B. Dassinger *et al.*, "Complete Michel parameter analysis of the inclusive semileptonic $b \to c$ transition," *Phys. Rev.* **D79** (2009) 075015, arXiv:0803.3561.

[198] M. Neubert, "Model-independent extraction of V_{cb} from semi-leptonic decays," *Phys. Lett.* **B264** (1991) 455.

[199] G. D'Ambrosio *et al.*, "Minimal flavour violation: an effective field theory approach," *Nucl. Phys.* **B645** (2002) 155, arXiv:hep-ph/0207036.

[200] B. Dassinger *et al.*, "Limits on New Physics from exclusive $B \to D^{(*)}\ell\nu$ Decays," *SI-HEP-2010-06* (2010) . [in preparation].

[201] T. Muta, "Foundations of Quantum Chromodynamics," in *World Scientific Lecture Notes in Physics*, vol. 57, pp. 1–409. World Scientific, Singapore, 2000.

[202] G. t'Hooft and M. Veltman, "Regularization and renormalization of gauge fields," *Nucl. Phys.* **B44** (1972) 189. G. t'Hooft, "Dimensional regularization and the renormalization group," *Nucl. Phys.* **B61** (1973) 455, C. G. Bollini and J. J. Giambiagi,"Lowest order "divergent" graphs in ν-dimensional space," *Phys. Lett.* **B40** (1972) 566, "Dimensional Renormalization: The number of Dimensions as a Regularizing Parameter," *Nuovo Cimento* **B12** (1972) 20.

[203] W. A. Bardeen *et al.*, "Deep-inelastic scattering beyond the leading order in asymptotically free gauge theories," *Phys. Rev.* **D18** 3998.
A. J. Buras,"Asymptotic freedom in deep inelastic processes in the leading order and beyond," *Rev. Mod. Phys.* **52** (1980) 199.

[204] D. J. Gross, "Applications of the Renormalization Group to High-energy Physics," in *Methods in field theory. Les Houches, Session XXVIII, 1975*, R. Balian and J. Zinn-Justin, eds., pp. 141–250. North Holland Publishing Company, 1976.

[205] M. Chanowitz *et al.*, "The axial current in dimensional regularization," *Nucl. Phys.* **B159** (1979) 225.

[206] J. H. Kühn and M. Steinhauser, "Determination of α_s and heavy-quark masses from recent measurements of $R(s)$," *Nucl. Phys.* **B619** (2001) 588, `arXiv:hep-ph/0109084`.

[207] A. Czarnecki, "Two-Loop QCD Corrections to $b \to c$ Transitions at Zero Recoil," *Phys. Rev. Lett.* **76** (1996) 4124, `arXiv:hep-ph/9603261`.

[208] P. Gambino *et al.*, "$B \to D^*$ at Zero Recoil Revisted," `arXiv:1004.2859`.

[209] R. Fleischer, "CP violation in the B system and relations to $K \to \pi\nu\bar{\nu}$ decays," *Phys. Rep.* **370** (2002) 537, `arXiv:hep-ph/0207108`. M. Battaglia,"The CKM Matrix and the Unitary Triangle," `arXiv:hep-ph/0207108`.

[210] M. Jung and T. Mannel, "General analysis of U-spin breaking in B decays," *Phys. Rev.* **D80** (2009) 116002, `arXiv:0907.0117`.

[211] M. J. Savage and M. B. Wise, "SU(3) predictions for nonleptonic B-meson decays," *Phys. Rev.* **D39** (1989) 3346. Erratum: *Phys. Rev.* **D40** (1989) 3127.

[212] M. Gronau *et al.*, "Decays of B mesons to two light pseudoscalars," *Phys. Rev.* **D50** (1994) 4529, `arXiv:hep-ph/9404283`.

[213] A. S. Dighe *et al.*, "Amplitude relations for B decays involving η and η'," *Phys. Lett.* **B367** (1996) 357, `arXiv:hep-ph/9509428`. Erratum: *Phys. Lett.* **B377** (1996) 325.

[214] M. Gronau, "U-spin symmetry in charmless B decays," *Phys. Lett.* **B492** (2000) 297, `arXiv:hep-ph/0008292`.

[215] M. Gronau and J. L. Rosner, "U-spin symmetry in doubly Cabibbo-suppressed charmed meson decays," *Phys. Lett.* **B500** (2001) 247, arXiv:hep-ph/0010237.

[216] M. Gronau and J. L. Rosner, "I-spin, U-spin, and penguin dominance in $B \to KK\bar{K}$," *Phys. Lett.* **B564** (2004) 90, arXiv:hep-ph/0304178.

[217] M. Gronau *et al.*, "Weak coupling phase from decays of charged B mesons to πK and $\pi\pi$," *Phys. Rev. Lett.* **73** (1994) 21, arXiv:hep-ph/9404282.

[218] A. J. Buras and R. Fleischer, "Limitations in measuring the angle β by using $SU(3)$ relations for B-meson decay-amplitudes," *Phys. Lett.* **B341** (1995) 379, arXiv:hep-ph/9409244.

[219] A. J. Buras and R. Fleischer, "A general analysis of γ determinations form $B \to \pi K$ decays," *Eur. Phys. J.* **C11** (1999) 93, arXiv:hep-ph/9810260.

[220] A. Soni and D. A. Suprun, "Determination of γ from charmless $B \to M_1 M_2$ decays using U-spin," *Phys. Rev.* **D75** (2007) 054006, arXiv:hep-ph/0609089.

[221] P. Ball and R. Fleischer, "Probing New Physics through B Mixing: Status, Benchmarks and Prospects," *Eur. Phys. J.* **C48** (2006) 413, arXiv:hep-ph/0604249.

[222] D. London and R. D. Peccei, "Penguin effects in hadronic B asymmetries," *Phys. Lett.* **B223** (1989) 257.

[223] B. Grinstein, "Critical reanalysis of CP asymmetries in B^0 decays to CP eigenstates," *Phys. Lett.* **B229** (1989) 280.

[224] M. Gronau, "CP Violation in Neutral-B Decays to CP Eigentates," *Phys. Rev. Lett.* **63** (1989) 1451.

[225] K. Anikeev *et al.*, "B Physics at the Tevatron: Run II and Beyond," arXiv:hep-ph/0201071.

[226] S. Faller *et al.*, "The golden modes $B^0 \to J/\psi K_{S,L}$ in the era of precision flavor physics," *Phys. Rev.* **D79** (2009) 014030, arXiv:0809.0842.

[227] S. Faller *et al.*, "Precision physics with $B_s^0 \to J/\psi\phi$ at the LHC: The quest for new physics," *Phys. Rev.* **D79** (2009) 014005, arXiv:0810.4248.

[228] J. L. Rosner, "Determination of pseudoscalar-charmed-meson decay constants from B-meson decays," *Phys. Rev.* **D42** (1990) 3732.

[229] A. S. Dighe *et al.*, "Extracting CKM phases $B_s - \bar{B}_s$ mixing parameters from angular distributions of non-leptonic B decays," *Eur. Phys. J.* **C6** (1999) 647, arXiv:hep-ph/9804253.

[230] **Belle** Collaboration, Y. Liu *et al.*, "Search for $B^0 \to J/\psi\phi$ decays," *Phys. Rev.* **D78** (2008) 011106, arXiv:0805.3225.

[231] I. Dunietz *et al.*, "In pursuit of new physics with B_s decays," *Phys. Rev.* **D63** (2001) 114015, arXiv:hep-ph/0012219.

[232] **DØ** Collaboration, "Measurement of the Flavor Oscillation Frequency of B_s^0 Mesons at DØ," *DØnote* **5474-conf** . [http://www-d0.fnal.gov/].

[233] **CDF** Collaboration, A. Abulencia *et al.*, "Observation of $B_s^0 - \bar{B}_s^0$ Oscillations," *Phys. Rev. Lett.* **97** (2006) 242003, arXiv:hep-ex/0609040.

[234] **HPQCD** Collaboration, E. Dalgic *et al.*, "$B_s^0 - \bar{B}_s^0$ mixing parameters from unquenched lattice QCD," *Phys. Rev.* **D76** (2007) 011501(R), arXiv:hep-lat/0610104.

[235] **HPQCD** Collaboration, J. Shigemitsu *et al.*, "Recent results on b mixing and decay constants form hpqcd," *PoS* **Lat2009** (2009) 251, arXiv:0910.4131. [http://pos.sissa.it/].

[236] CDF/DØ $\Delta\Gamma_s$, β_s Combination Working Group, "Combination of DØ and CDF Results on $\Delta\Gamma_s$ and the CP-Violating Phase $\beta_s^{J/\psi\phi}$," *DØ note* **5928-conf** (2009) . [http://www-d0.fnal.gov/].

[237] **BABAR** Collaboration, B. Aubert *et al.*, "Measurement of time-dependent CP asymmetry in $B^0 \to c\bar{c}K^{(*)0}$ decays," *Phys. Rev.* **D79** (2009) 072009, arXiv:0902.1708.

[238] **Belle** Collaboration, K. F. Chen *et al.*, "Observation of Time-Dependent CP Violation in $B^0 \to \eta' K^0$ Decays and Improved Measurements of CP

Asymmetries in $B^0 \to \varphi K^0$, $K^0_S K^0_S K^0_S$ and $B^0 \to J/\psi K^0$ Decays," *Phys. Rev. Lett.* **98** (2007) 031802, arXiv:hep-ex/0608039.

[239] A. J. Buras and L. Silvestrini, "Non-leptonic two-body B decays beyond factorization," *Nucl. Phys.* **B569** (2000) 3, arXiv:hep-ph/9812392.

[240] M. Jung, *Non-leptonic B Meson Decays as a Probe of New Physics*. PhD thesis, University of Siegen, 2009. Electronic version available from UB Siegen: http://dokumentix.ub.uni-siegen.de/opus/volltexte/2009/392/.

[241] **BABAR** Collaboration, B. Aubert *et al.*, "Evidence for CP Violation in $B^0 \to J/\psi\pi^0$ Decays," *Phys. Rev. Lett.* **101** (2008) 021801, arXiv:0804.0896.

[242] **Belle** Collaboration, S. E. Lee *et al.*, "Improved measurement of time-dependent CP violation in $B^0 \to J/\psi\pi^0$ decays," *Phys. Rev.* **D77** (2008) 071101(R), arXiv:0708.0304.

[243] D. Duplančić and B. Melić, "B, $B_s \to K$ form factors: An update of light-cone sum rule results," *Phys. Rev.* **D78** (2008) 054105, arXiv:0805.4170.

[244] D. Becirevic and A. B. Kaidalov, "Comment on the heavy $\to$ light form factors," *Phys. Lett.* **B478** (2000) 417, arXiv:hep-ph/9904490.

[245] M. Gronau and J. L. Rosner, "B decays dominated by $\omega - \phi$ mixing," *Phys. Lett.* **B666** (2008) 185, arXiv:0806.3584.

[246] R. Fleischer, "$B_{s,d} \to \pi\pi, \pi K, KK$: status and prospects," *Eur. Phys. J.* **C52** (2007) 267, arXiv:0705.1121.

[247] A. Khodjamirian *et al.*, "Kaon distribution ampltiude from QCD sum rules," *Phys. Rev.* **D70** (2004) 094002, arXiv:hep-ph/0407226.

[248] M. Gronau and J. L. Rosner, "Doubly CKM-suppressed corrections to CP asymmetries in $B^0 \to J/\psi K^0$," *Phys. Lett.* **B672** (2009) 349, arXiv:0812.4796.